Charles University in Prague
Faculty of Science

Program of Study: Organic Chemistry

Mgr. Miroslav Kašpar

Syntéza steroidních modulátorů pro receptory žlučových kyselin

Synthesis of Steroidal Modulators for Bile Acid Receptors

Ph.D. Thesis

Supervisor: RNDr. Eva Kudová, Ph.D.

Institute of Organic Chemistry and Biochemistry,

Academy of Sciences of the Czech Republic, v.v.i.

Prague 2024

Declaration

Prohlašuji, že jsem závěrečnou práci zpracoval samostatně a že jsem uvedl všechny použité informační zdroje a literaturu. Tato práce ani její podstatná část nebyla předložena k získání jiného nebo stejného akademického titulu.

I declare that I have prepared the Thesis independently and that I have listed all the information sources and literature. Neither this Thesis nor any substantial part has been submitted for another or the same academic degree.

V Praze, 1.1.2024 …..

Miroslav Kašpar

"All that we do, all that we are, begins and ends with ourselves."

Arno Victor Dorian

Acknowledgment

I unexpectedly discovered that I enjoy mentoring students, and when the time comes, this may become my primary motivation. Tom, what we have experienced cannot be repeated (at least, I hope so). My friend, I wish you nothing but the best in both your private and professional life. Lada, you are one of the smartest, most charismatic, and motivated students I've been privileged to teach. So, when things go south, breathe in, breathe out, and believe in yourself. Remember, you got this. Both of you do. I am in no doubt that you will make your dreams come true.

Notably, despite being competitive, there is such a friendly atmosphere among the groups at IOCB. People celebrate each other's success, and I have never had anyone refuse to give me advice, help me with experiments, or lend me something. So, I routinely go into the surrounding labs with my synthetic problems these days. I don't think it's common or should be taken for granted. Therefore, I am grateful to the IOCB management, especially two directors, Doc. Zdeněk Hostomský, and Prof. Jan Konvalinka. My thanks also go to the rest of the IOCB population. You are the Institute, not only the iron and concrete around. I very much hope that IOCB will be able to inspire other scientific organizations and our little country will be among the centers of scientific excellence. There are just too many brilliant minds around Czechia to pass this opportunity. So, let's create an environment where great minds can connect rather than disconnect.

Many people helped me directly, shaped my ideas through consultations, or motivated me to keep going. I dare not to rank their importance. Instead, here is an exhaustive list of their names alphabetically.

Adam Jaroš, Adam Sklenář, Adéla Šimková, Adriana Struminská, Alena Karnošová, Alexander Kasal, Anna Hruzíková, Anna Kubíčková, Anna Poryvai, Aneta Miklošinová, Anita Kiss, Artem Chayka, Attila Palágyi, Bára Doksanská, Bart Kieftenbelt, Bedřich Formánek, Blanka Collis, Blanka Klepetářová, Charlotte O'Brien, Dagmar Hybšová, David Kodr, David Tichý, Dragan Ćosić, Ema Chaloupecká, Emanuela Jahn, Filip Skřiček, Florian Chevrier, Giammarco Liuni, Hynek Mácha, Irena G. Stará, Isabel Sanchez Gay, Jakub Brož, Jakub Doležal, Jakub Sivek, Jakub Šoukal, Jakub Štoček, Jan Dohnálek, Jan Skácel, Jan Voldřich, Jaromír Vyhnanovský, Jaromír Zahrádka, Jaroslav Kurfürst, Jiří Neradil, Jiří Rybáček, Josef Cvačka, Josef Šulc, Joshua Smith, Karolína Vaňková, Katarína Markušová, Kateřina Pokorná, Kateřina Radilová, Kateřina Šolcová, Kristýna Jelínková, Kryštof Škach, Luca Julianna Tóth, Lucie Čechová Mužíková, Lucie Holá, Lucie Svobodová, Lukáš Cudlman, Lukáš Janecký, Marek Jaroš, Marianne Fleuti, Marijo Čičak, Marina Morozovová, Markéta Penkerová, Martin Hadzima, Martin Hubálek, Martin Jakubec, Martin Žáček, Michael Franc, Michaela Sedláčková, Michal Česnek, Michal Rahm, Milan Dejmek, Miloš Buděšínský, Miloslav Polášek, Miroslava Šedinová, Miroslava Štejfová, Norbert Baris, Oldřich Hudeček, Ondřej Flaška, Ondřej Hillmich, Ondřej Pačes, Ondřej Štěpánek, Ondřej Ticháček, Pavel Kraina, Pavel Majer, Pavel Šácha, Petr Beier, Radek Pohl, Rafael Navrátil, Róbert Reiberger, Seiya Asai, Šimon Pospíšil, Svatava Voltrová, Terezie Páníková, Timotej Strmeň, Tomáš Bartl, Tomáš Belloň, Tomáš Lášek, Tomáš Mašek, Tomáš Slanina, Ullrich Jahn, Václav Chmela, Veronika Vetýšková, Viktor Klančík, Vladimír Vrkoslav, Vojta Havlíček, Vojta Kapras, Zlatko Janeba, and Žofie Ćosić.

The following sentiments are deeply personalized and intended for my relatives, family, and loved ones. There is no other official place to express my gratitude. You have made me who I am: My successes are your merits.

To an unknown night-shift from Thomayer Hospital, who brought a newborn boy back to life on October 29, 1992. To my angel PaedDr. Iveta Heyrovská, words cannot express how I am grateful. Therefore, let me express myself by living my life to the best of my ability and offering a helping hand to those in need, just as you offered yours.

Not everyone who has accompanied me through life has been as lucky as I have. But despite that, you have always supported me unconditionally, and I appreciate you sincerely. The saying goes that it's darkest before dawn. But the greatest darkness is within ourselves. It's like a dark forest in the night when the clouds cover the stars. We all wander in those lands from time to time, and sometimes, you feel lost, consumed by the void. But even the darkest night ends, the clouds part, and the sun comes out. You step out of the forest, sit in the blooming meadow, and watch the sunrise. The warmth will spread across your chest, and you realize you're in the right place at the right time. And once the time comes to face the horrors again, you will accept the darkness as part of your journey rather than its end. Because not all those who wander are lost, and as long as I draw breath, you will not walk alone.

Brother, Sister, and Péťo, I'm glad I have you, that we have each other. Babičko a Dědečku, Vy víte, že bez vašeho jídla bych nikdy neměl energii dokončit den. A taky víte že bez poskytnutí klidného studijního místa bych nedokočil ani školu. Pamatujete co jste mi řekli na magisterské promoce? Já ano. Je to 5 let. To to uteklo. Mom, I'll never forget all that you've done for me, and I'll always be there for you. I love you. We don't get to choose our family, but I couldn't have picked any better. I know you'd be proud, Dad.

Here we are, now it's evident that all my life adventures begin and end with you. Meeting you 15 years ago completely transformed me for the better. I deeply value our relationship, our ability to settle things down, our journey toward a common goal, and our ability to seek solutions rather than excuses. Together, we are stronger than the sum of our parts. I believe our greatest strength lies in the fact that, despite our differing opinions, we have a deep connection. You always present me with a fresh perspective, and you not only complete the mosaic of my persona, but you hold it all together. I can't imagine anyone else for midnight discussions about the shape of molecular orbitals, how to correctly fillet Atlantic bluefin tuna, the redefinition of SI units in 2019, or the size difference between miniature and kaninchen dachshunds. Those precious moments, fleeting and unrepeatable, transcend time, and I will forever guard them within my heart. They are my everything. *You* are my everything.

It's an autumn evening. Light rays flood through my lab window, filling the room with an orange glow. Dejvice, I know I will miss your beautiful sights. As the day draws to a close, so does my five-year journey. Filled with joy, I write these last lines to acknowledge my mentors, colleagues, friends, and loved ones.

In pursuit of science, my ultimate motivation has always been to make our world a better place one day. However, you have already made my world a better place today.

Děkuji Vám.

Abstract

The Thesis comprises three major projects. The first project is concerned with the creation of a pregnane compound library that can be used to explore the structure-activity relationship with the TGR5 and FXR receptors. The project draws structural inspiration from Sato's work and involves the compound characterization, digitization, computational methods, and biochemical analysis of a historic group collection of steroids. The second project focuses on the synthesis of modified bile acids using Grignard, Wittig, cross-coupling, or cycloaddition reactions. The synthesized compounds were tested for their TGR5 and FXR activity, leading to the discovery of (*E*)-7-ethylidene-3α-hydroxy-5β-cholan-24-oic acid (75), which is known to be the only bile acid with TGR5/FXR dual action. In the last part of the Thesis, 16 oxidizing agents were tested on 5 substrates for their selectivity in oxidizing axial or equatorial hydroxyl groups.

Souhrn

Disertační práce je rozdělena na tři projekty. První projekt se zabývá tvorbou knihovny sloučenin steroidních pregnanů, která byla použita k strukturně-aktivitní studii s receptory TGR5 a FXR. Projekt čerpá inspiraci z práce Satoa a zahrnuje charakterizaci sloučenin, digitalizaci, výpočetní metody a biochemickou analýzu historické kolekce steroidů. Druhý projekt se zaměřuje na syntézu analogů žlučových kyselin pomocí Grignardových, Wittigových, cross-coupling nebo cykloadičních reakcí. Syntetizované sloučeniny byly testovány na na receptorech TGR5 a FXR, což vedlo k objevu kyseliny (*E*)-7-ethyliden-3α-hydroxy-5β-cholan-24-ové (75), která je zatím jedinná žlučová kyselina s dvojitým účinkem na TGR5/FXR. V poslední části práce bylo na 5 substrátech testováno 16 oxidačních činidel pro jejich selektivitu v schopnosti oxidace axiálních nebo ekvatoriálních hydroxylových skupin. Výsledky ukazují, že u molekul obsahující obě hydroxylové skupiny jsou pro oxidaci ekvatoriálních hydroxylů optimální činidla na bázi nitroxidových radikálů, zatímco činidla Stevens nebo Dess−Martin jsou lepší pro oxidaci axiálních hydoxylů.

1   INTRODUCTION

1.1   STEROIDS, A BRIEF HISTORY

Arnold Adolph Berthold can be considered a pioneer in steroid chemistry. In his work from 1839,[1] he described the different dimorphism in castrated and uncastrated roosters. The reason was unknown up to the 1920s when steroids were discovered. The first isolated and characterized steroid hormone was estrone (Butenandt, 1929),[2-4] which was awarded the Nobel prize (co-awarded with Leopold Ružička, 1939).[5, 6] The discovery of estrone was followed by progesterone (multiple groups, 1934),[7-13] testosterone (multiple groups, 1935),[14-16] cortisone (Kendall and Reichstein, 1936),[17-19] for which, they shared Nobel prize (co-awarded with Philip S. Hench, 1950), and aldosterone (Reichstein, 1953).[20-22]

1.2   NOMENCLATURE OF STEROIDS

According to the 1989 IUPAC[23] definition, steroids are:

"Compounds possessing the skeleton of cyclopenta[a]phenantrene or a skeleton derived therefrom by one or more bond scissions or ring expansions or contractions."

The document proposes standard steroid ring letters and numbering (**Figure 1**). As some of its recommendations (especially how to draw stereocenters in 3D six-membered systems) are in contrast with newer 2006 IUPAC[24] documentation, this Thesis uses the 1989 IUPAC nomenclature exclusively for naming new steroid compounds and 2006 IUPAC recommendations for the representation of 3D structures.

In steroid nomenclature, it is common to use absolute stereodescriptors alpha (α) and beta (β) rather than R and S. The convention is that substituents below the steroid's plane are labeled with a hashed bond (⸲⸲⸲⸲) and named alpha, while substituents above the plane are marked with a wedged bond (➤), and named beta.[25] Those stereodescriptors are relevant only if the tetracyclic steroid system's exact orientation is agreed upon → ABCD. Therefore, the tetracyclic steroid system must be drawn, as shown in **Figure 1.**

Because the vast majority of natural steroids related to human metabolisms, such as corticosteroids, anabolic steroids, sex hormones, and bile acids, share the exact stereochemistry at chiral centers C8, C9, C10, C13, C14, C17, and C20, it is common not to draw those. Other stereocenters, including C5, must be explicitly marked in the name and structure. For instance, consider cholane, a triterpene that naturally can exist either as 5α-cholane or 5β-cholane.

Although not all stereocenters are usually marked in steroid drawings, the author deliberately includes the full stereochemistry in all illustrations to prevent any ambiguity.
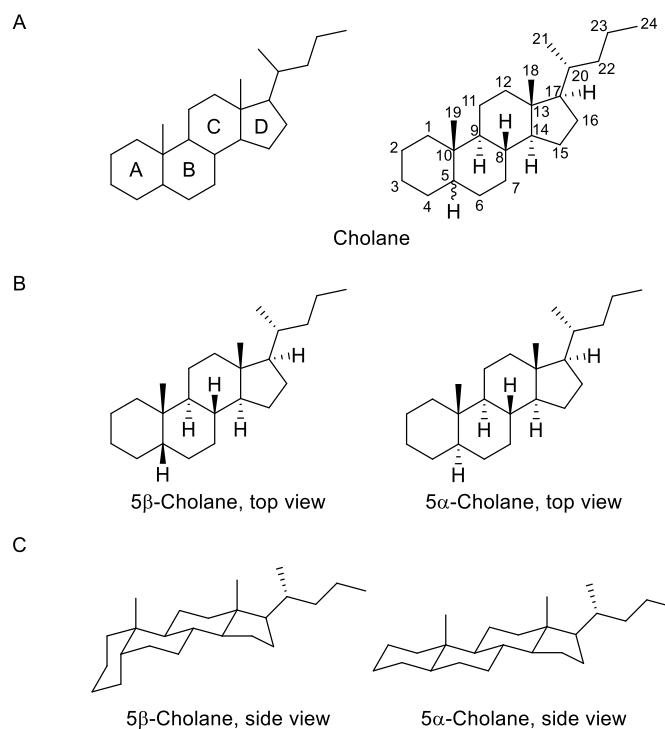
Figure 1. A – Cholane with ring letters and steroid ring numbering, **B** – 5β-cholane and 5α-cholane top view, **C** – 5β-cholane and 5α-cholane side view.

1.3 PHYSICAL PROPERTIES OF BILE ACIDS

Bile acids are small molecules (< 500 Da) with a 5β-cholane skeleton, which, when dissolved in water, aggregate together into micelles or tiny clumps.[26] This is caused by the presence of hydroxyl groups at positions C3, C7, and C12, as well as methyl groups at C18 and C19.[27] The hydrophilic hydroxyl groups are oriented toward the α-side, and the hydrophobic methyl groups are oriented toward the β-side. This makes the hydrophilic α-face concave and the hydrophobic β-face convex.[28] This unique molecule shape gives the bile acids their amphiphilic properties.
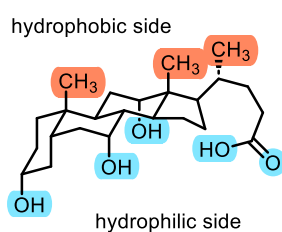
Figure 2. Cholic acid with polar and non-polar sides marked.

1.4 BILE ACIDS METABOLISM

In the 1940s, Bloch et al.,[29] confirmed that bile acids are products of cholesterol metabolism. The dogs in the experiment received an intravenous dose of deuterium-labeled cholesterol. The blood, urine, and feces samples were analyzed and contained a significantly elevated concentration of deuterated bile acids against the control.

Cholesterol metabolism primarily involves the conversion of cholesterol into bile acids, which occurs through two pathways. The major pathway is called classical, and the minor pathway is called alternative (**Figure 3**). The central enzyme is cholesterol-7-alpha-hydroxylase (CYP7A1). It

introduces the 7-hydroxy group in position C7. Moreover, hydroxylation at C7 is a rate-limiting step of the classical pathway. The importance of CYP7A1 in mice was demonstrated in the 1990s by Ishibashi et al.[30] A fetus of *CYP7A1* gene knockout mice developed symptoms of oily coat, low weight, and neurological problems. Approximately 85% of *CYP7A1* deficient mice died within the first 18 days of life. Interestingly, most deaths could be prevented by adding vitamins and cholic acid to the water of nursing mothers. The authors proposed that after three weeks of age, *CYP7B1* is expressed. Remarkably, the next generations of mice showed high survivability of pups (> 65%, in > 10 generations). This was maintained even in the absence of dietary vitamin and bile acids supplementation.[31]

In humans, neonatal CYP7A1 deficiency is survivable but associated with increased low-density lipoprotein (LDL) cholesterol levels, decreased bile acid excretion, hypertriglyceridemia, and premature gallstone disease.[32-34]
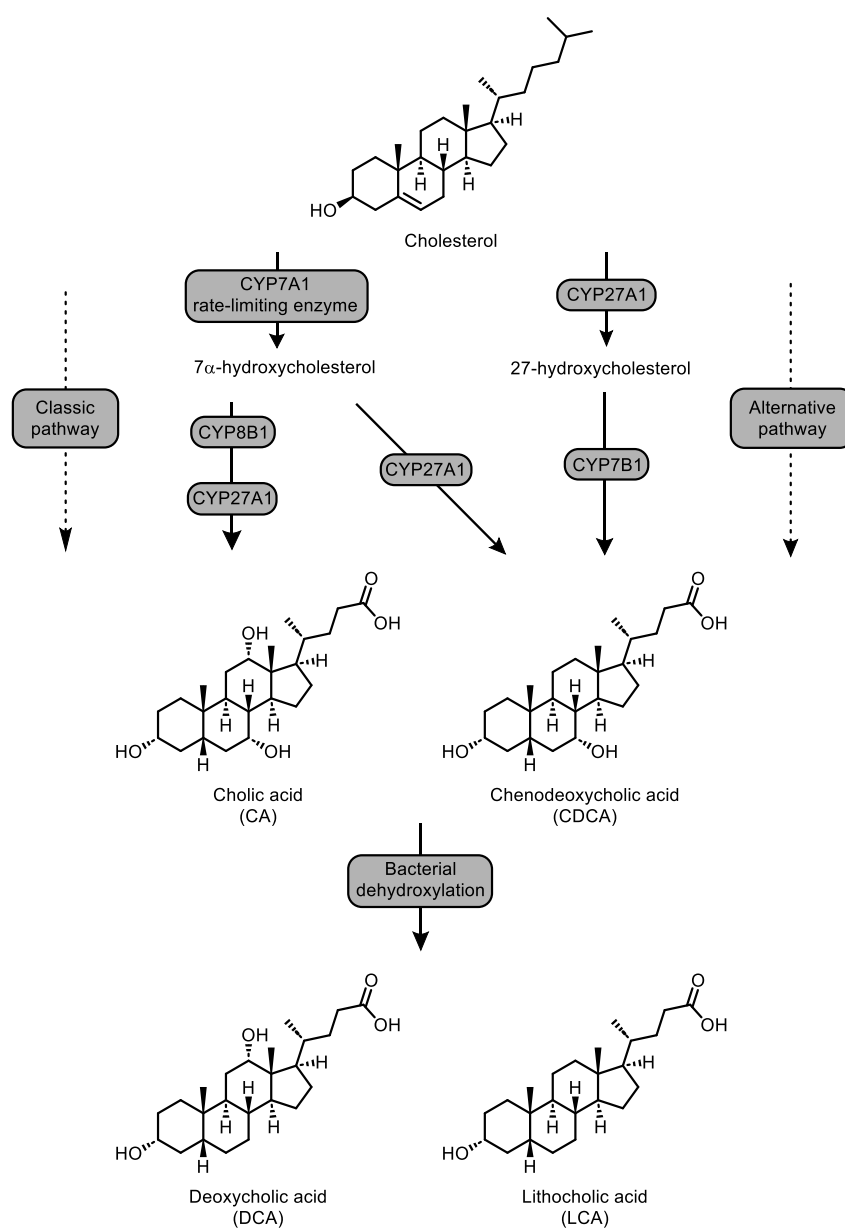
Figure 3. Bile acids metabolism. Cholesterol-7-alpha-hydroxylase (CYP7A1), sterol-12-alpha-hydroxylase (CYP8B1), sterol-27-hydroxylase (CYP27A1), 25-hydroxycholesterol 7-alpha-hydroxylase (CYP7B1). Adopted and modified.[35, 36]

Catabolism of cholesterol in the liver yields primary bile acids – cholic acid (CA) and chenodeoxycholic acid (CDCA), which are conjugated with amino acids glycine or taurine. Conjugates are then transported and stored in a gallbladder. Upon food intake, conjugates are released into the duodenum to digest fat or fat-soluble vitamins. In the intestine, gut microflora deconjugate and dehydroxylate the bile acids to form secondary bile acids - deoxycholic acid (DCA) and lithocholic acid (LCA). Around 200–600 mg of bile acids are excreted daily via feces. This accounts for approximately 5% of daily turnover and is compensated by *de novo* synthesis from cholesterol. The remaining 95% is reabsorbed by active transport into intestinal erythrocytes and taken to hepatocytes via the portal vein. Bile can be recycled up to twelve times per day between hepatocytes and erythrocytes. This cycle is called enterohepatic circulation.[37-39]
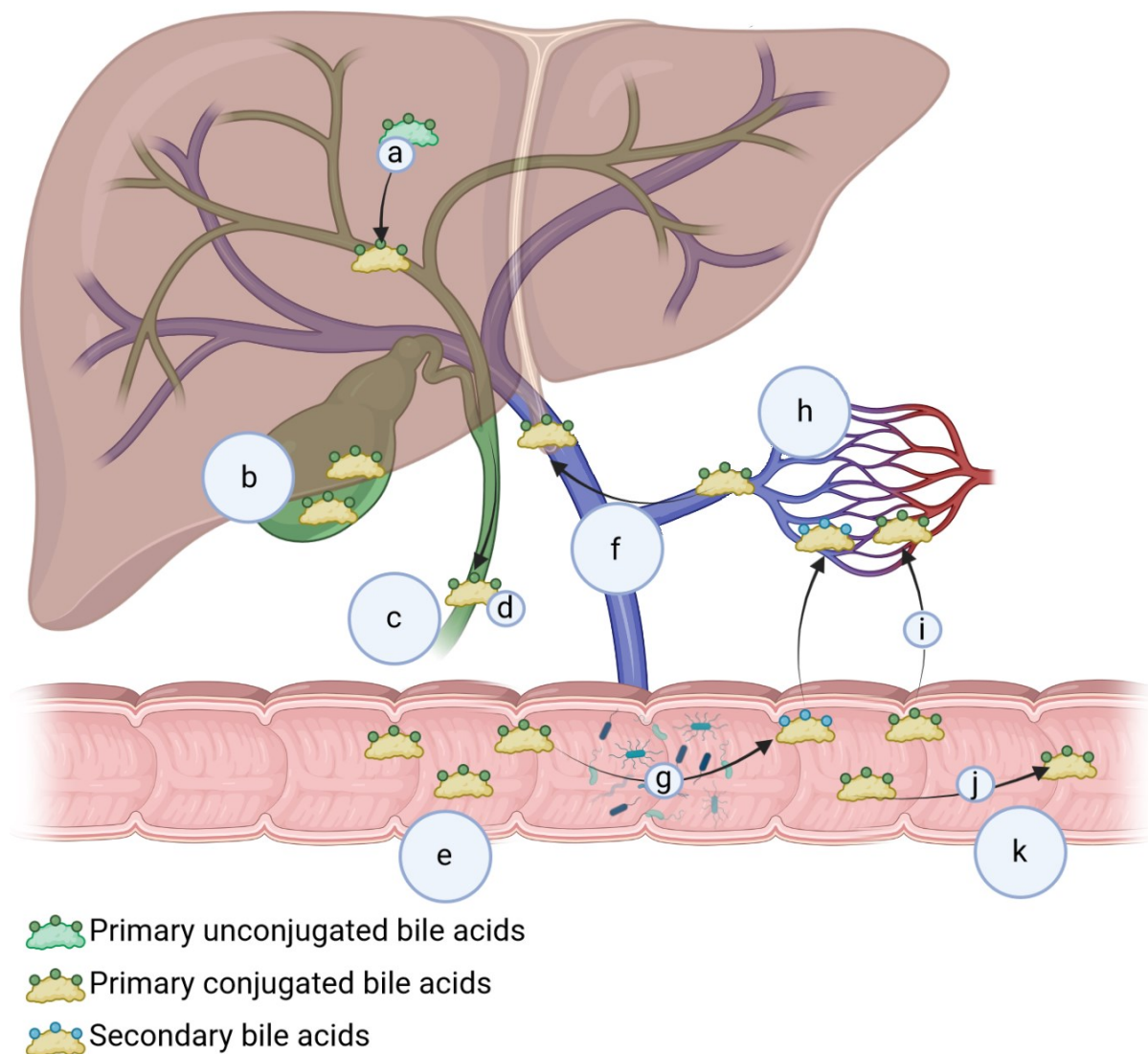
Figure 4. Schematic illustration of bile acids enterohepatic circulation, a – conjugation of primary bile acids, CDCA and CA, to their taurine and glycol conjugates, b – storage of conjugates in the gallbladder, c – bile duct, d – excretion of bile conjugates, e – duodenum, f – portal hepatic vein, g – gut microsome is responsible bile acid deoxygenation, consequently producing secondary bile acids – DCA and LCA, h – capillary bed, i – reabsorption of bile acid content, j – bile acid content excretion, which is approximately 200–500 mg daily, k – ileum. The picture was drawn in BioRender app[40] and is based on a medical textbook.[41]

1.5 BILE ACIDS AS SIGNALING MOLECULES

Bile acids were thought to aid in nutrient absorption because of their amphiphilic nature.[42-45] However, at high concentrations, bile acids are inflammatory, causing damage to the liver, intestines, and other tissues.[46] Moreover, bile acids and gut microorganisms are in an intricate relationship. When these systems fail, such as during biliary obstruction, the consequences are bacteria overgrowing or gut epithelial damage.[47] Also, an increase in the concentration of bile acids in the colon causes inhibition of bacterial growth, changing the microbiome.[48] Therefore, there must be a regulation mechanism to control the homeostasis of bile acids. It was shown[49-51] that bile acids themselves can regulate their biosynthesis and serve as signaling molecules. There are several membranes and nuclear receptors collectively known as bile acid receptors (BARs). The most important BARs are the farnesoid x receptor (FXR) and Takeda G-protein coupled receptor (TGR5). Because this work aims to discover ligands for these two particular receptors without off-targeting other BARs, mainly FXR and TGR5 are discussed.

1.6 FARNESOID X RECEPTOR

FXR is a ligand-activated transcription factor that belongs to the nuclear receptor family.[52] It was first identified in 1995 as a farnesol-activated receptor, hence the name Farnesoid.[53] Four years later, three groups independently identified FXR as a natural bile acid receptor.[49-51] In humans, it is encoded on chromosome 12 in the *NR1H4* gene, encoding 476 amino acids.[54] There are currently 85 crystal structures published in the protein data bank (PDB) related to FXR.[55-75]

FXR consists of five domains.[76] The N-terminal domain, the DNA binding domain (DBD), the hinge region, the ligand-binding domain (LBD), and the C-terminal domain (**Figure 5**). The DBD recognizes a specific DNA sequence called a responsive element (RE) and binds the receptor to this site. The DBD contains two zinc fingers that provide the protein's orientation to the large DNA groove and the formation of dimer complexes typical of nuclear receptors. A hinge region connects the DBD and LBD, providing some flexibility to the receptor.[77] In the LBD domain, the ligand interacts with the receptor and is the most critical for drug design and relevant to this work. When an agonist binds, the LBD adopts an active conformation that can interact with the coactivator and induce transcription of the targeted DNA sequence. In contrast, the LBD does not adopt active conformation when the antagonist binds, and the coactivator cannot interact and induce transcription. Antagonists block active sites for natural agonists, inhibiting the function of the receptor.
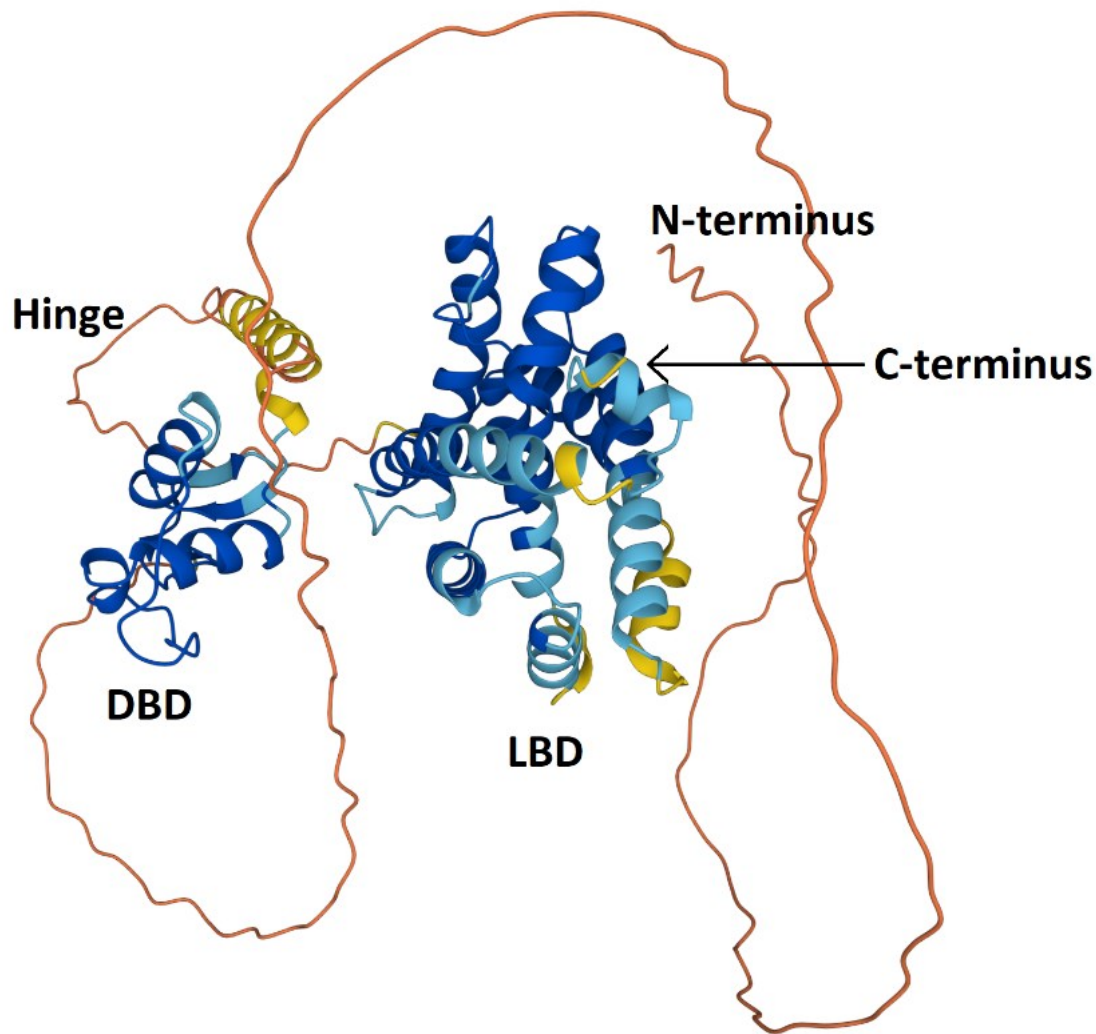
Figure 5. The tertiary structure of FXR as predicted by AlphaFold.[78, 79] DBD – DNA binding domain, LBD – ligand-binding domain. AlphaFold produces a predicted local distance difference test (pLDDT) with values between 0 and 100. This represents a per-residue confidence score. Some regions below 50 pLDDT may be unstructured in isolation. Deep blue – Very high (pLDDT > 90), light blue – confident (90 > pLDDT > 70), yellow – low (70 > pLDDT > 50), orange – very low (pLDDT < 50).

The activation of FXR causes a negative feedback loop in bile acid biosynthesis. For example, when the FXR is activated, the small heterodimer partner (*SHP*) gene is expressed. The SHP protein causes the hydrolysis of another nuclear receptor (Liver Receptor Homolog-1, LRH-1). The LRH-1 regulates the expression of the *CYP7A1* gene. Thus, an increase in bile acid concentration in hepatocytes inhibits the production of CYP7A1, a rate-limiting enzyme for bile acid biosynthesis.

Moreover, FXR is involved in the regulation of expression of many other genes, most notably sterol 12-alpha-hydroxylase (*CYP8B1*),[80] bile salt export pump (*BSEP*),[81] organic solute and steroid transporter (*OST alpha, OST beta*),[82] solute carrier family 10 member 2 (*ABST*),[83] and fibroblast growth factor 19 (*FGF19*).[84] Through regulation of the genes mentioned above, FXR plays a role not only in bile acids metabolism but is also responsible for the metabolism of high-density lipoprotein (HDL), LDL, triacyl glycerides, glucose homeostasis,[85] and even plays a role in colorectal cancer[86-88] and hepatocellular carcinoma.[89-91] Full role of FXR in systemic metabolism is summarized in **Table 1**. The FXR is therefore considered a promising target for the treatment of cholestasis, a disorder of the

mechanism of bile production and excretion that is a significant contributor to the development of primary biliary cholangitis (PBC), autoimmune liver disease, and nonalcoholic steatohepatitis (NASH), progressive deposition of triacyl glycerides in the liver. These diseases progressively lead to cirrhosis and in the final stage, liver transplantation is the only possible therapy today.[85, 92, 93]

Table 1. The role of FXR in systemic metabolism. Adopted and modified.[94]

Organ	Affected functions	Related indications	Ref.
Liver	Bile acid metabolism	Cholestasis	95, 96
	Lipid metabolism	NASH/NAFLD	97-99
	Glucose metabolism	Liver injury and fibrosis	100-102
	Fibrosis	Alcohol-associated liver disease	103, 104
	Inflammation	Drug-induced liver injury	105
		Liver regeneration	106
Intestine	Bile acid transport	Inflammatory bowel disease	107
	Inflammation	Obesity and insulin resistance	108-110
	Glucose homeostasis	NAFLD	111
	Antibacterial activity	Mucosal injury	112
Kidney	Bile acid transport	Diabetic nephrotoxicity	113
	Lipid metabolism	Ischemia-reperfusion damage	114
	Fibrosis	Renal fibrosis	115
White adipose tissues	Adipogenesis Insulin sensitivity	Obesity and insulin resistance	115-117
Pancreas	Lipid metabolism	Acute pancreatitis	118
	B Cell function	Pancreatic lipid toxicity	119
Cardiovascular system	Lipid metabolism	Atherosclerosis	120
FXR – Farnesoid X receptor, NAFLD – Nonalcoholic fatty liver disease, NASH – Nonalcoholic steatohepatitis.			

1.7 LIGANDS OF FXR

The first known FXR ligand was farnesol. However, farnesol activates FXR in supraphysiological concentration. In 1999, conjugated and unconjugated bile acids were identified[49-51] as ligands that can activate FXR in physiological concentrations (ca 10 μM). The order of potency of bile acids is CDCA > LCA = DCA > CA. Ursodeoxycholic acid (UDCA) and muricholic acid (MCA) do not activate FXR.

The ligand binding pocket's interior, which faces the α side of the steroid, is relatively lipophilic thanks to Ile-122, Leu-287, Leu-348, and Ile-352. A more hydrophilic region is located on the other side of the cavity with His-208, Tyr-361, Tyr-369, and Ser-332. Those four amino acids form polar interactions with C3-OH and C7-OH groups. The bile acid acidic side chain is stabilized by ionic interaction with ARG_{331} (**Figure 6**). According to the PubChem database,[121-123] in total 9447 unique compounds were tested, from which 559 are steroids, and 233 are bile acids derivatives. The published data allowed us to propose a pharmacophore for the active compound as follows: the hydroxyl group at C3 is likely not crucial for the biological activity as 3-deoxy-CDCA demonstrates a 6-fold higher affinity than CDCA.[124] Moreover, several 3-deoxy derivatives have lower affinity than their 3-hydroxy counterpart.[125] Next, the 7α-hydroxy group might be pivotal for activating the receptor, as 7β-hydroxy epimers are generally inactive (derivatives of UDCA).[126-128] Finally, modifications of the side chain at position C17 (e.g., alcohol, amine, amide, sulfonate, carbamate, sulfonamide, thiocarbamate, glycine, or taurine conjugates) demonstrated high tolerability towards the biological activity.[124, 125, 129, 130] In contrast, side-chain shortening decreased the affinity for FXR.[124]

In 2002, Pellicciari et al.,[131] investigated a variety of bile acid-related compounds that had been produced previously in their laboratory. Compound 6α-methyl-chenodeoxycholic acid was found to be a more potent FXR agonist than CDCA. This discovery encouraged them to create CDCA analogs with increasing bulkiness of C6 substituents (ethyl, propyl, butyl). Compound 6α-ethyl-chenodeoxycholic acid was identified as the most potent one, and it was given the trivial name

obeticholic acid (OCA). In 2016, the Food and Drug Administration (FDA) approved OCA as therapy for PBC for adults with an inadequate response to UDCA.[132] Unfortunately, the FDA discovered 25 incidences of significant liver damage resulting in hepatic decompensation or liver failure in patients taking OCA. As a result of that, due to the risk of severe liver injury, the FDA announced a restriction on the use of OCA for patients with advanced cirrhosis.[133]
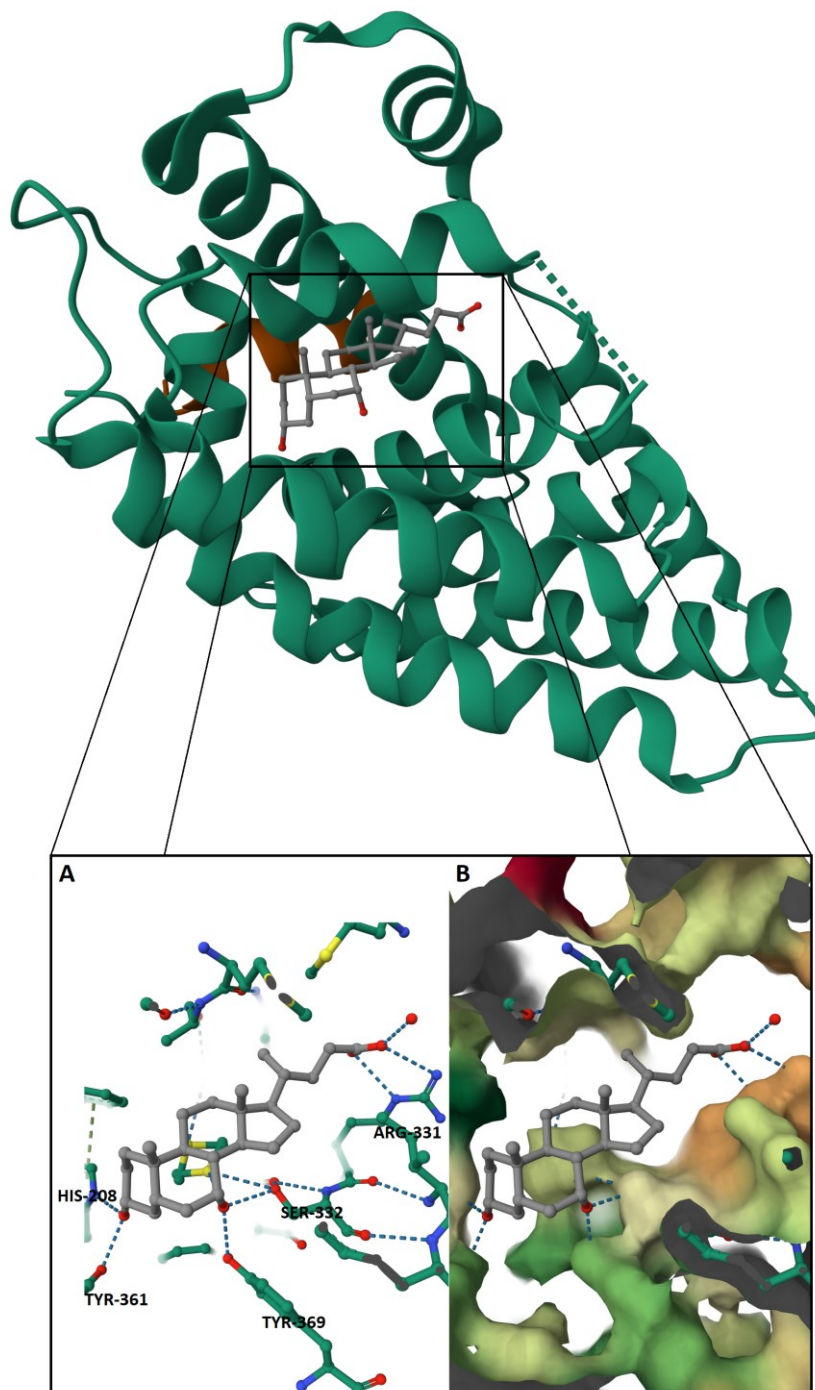
Figure 6. Crystal structure of FXR with CDCA (PDB: 6HL1).[66] **A**: Blue – CDCA, green – FXR residue within 5Å distance, white – polar interactions. **B**: Gaussian protein surface, with a visible lipophilic cavity in the bottom part of the picture, green – lipophilic region, red – hydrophilic region. Visualized and edited.[134, 135] Lipophilic residues Ile-122, Leu-287, Leu-348, and Ile-352 that form Van der Waals interactions with C18 and C19 methyl groups were omitted for clarity.

According to the literature, thousands of nonsteroidal analogs have already been prepared with combinatorial chemistry. The most prominent steroidal and nonsteroidal compounds are summarized in **Table 2** and **Figure 7**. Unfortunately, neither of them has yet been approved by the FDA.

Table 2. The clinical pipeline of the most prominent FXR ligands. Adopted and modified.[94, 136]

Agent	Targeted diseases	Status	Analyzed subjects or animal models	Ref.
FXR agonists				
Steroid compounds				
CDCA	Cerebrotendinous xanthomatosis	Phase III	Adult and pediatric patients with Cerebrotendinous xanthomatosis (n = 12)	[137]
OCA (INT-747)	PBC	FDA-approved (OCALIVA)	Adults with an inadequate response to UDCA (OCA is used in combination with UDCA) or adults unable to tolerate UDCA (OCA is used as monotherapy)	[131, 138]
	NASH	Phase III	Adults with definite NASH (NAFLD activity score ≥ 4, and fibrosis stages F2 or F3; n = 2,480)	[139]
EDP-305	NASH	Phase II	Subjects with liver-biopsy-proven NASH (n = 336)	[140-142]
Non-steroid compounds				
GW4064	Cholestatic liver damage	Preclinical	Bile duct-ligated adult male rats	[143-145]
Tropifexor	NASH	Phase II (completed)	Adults with histological evidence of the presence of NASH (n = 351)	[146, 147]
	PBC	Phase II (completed)	Adults with diagnosed PBC (n = 61)	[148]
Fexaramine	Insulin resistance	Preclinical	High-fat diet-fed C57Bl/6 mice	[149-151]
Turofexorate isopropyl	NASH	Preclinical	Methionine-deficient and choline-deficient diet-fed C57Bl/6 mice	[60, 150, 152]
Nidufexor	NASH and diabetic nephropathy	Phase II	Adults with NASH (n = 122) and adults with diabetic nephropathy (n = 116)	[153-155]
PX20606	Imbalance in bile acid synthesis	Phase III (completed)	Healthy male adults (n = 54)	[156, 157]
Cilofexor	Non-cirrhotic NASH	Phase II (completed)	Adults with non-cirrhotic NASH (n = 140)	[158-160]
FXR antagonists				
UDCA*	PBC	FDA-approved	Patients with PBC	[161-164]
GβMCA*	NAFLD	Preclinical	High-fat diet-fed wild-type and intestine-specific Fxr-null mice	[165]
GUDCA*	Insulin resistance	Preclinical	High-fat diet-fed wild-type and intestine-specific FXR-null mice	[109, 166-168]
Guggulsterone	Chronic Hepatitis C	Withdrawn	Male patients infected by HCV genotype 1, with anti-HCV antibodies, non-responders to at least one first line of therapy (n = 15)	[169]

CDCA – Chenodeoxycholic acid, FXR – Farnesoid X receptor, GβMCA – Glycine-β-muricholic acid, GUDCA – Glycoursodeoxycholic acid, NAFLD – Nonalcoholic fatty liver disease, NASH – Nonalcoholic steatohepatitis, OCA – Obeticholic acid; PBC – Primary biliary cholangitis, UDCA – Ursodeoxycholic acid, FDA – Food and Drug Administration, HCV – Hepatitis C virus. *Literature is inconclusive whenever those are FXR antagonists.
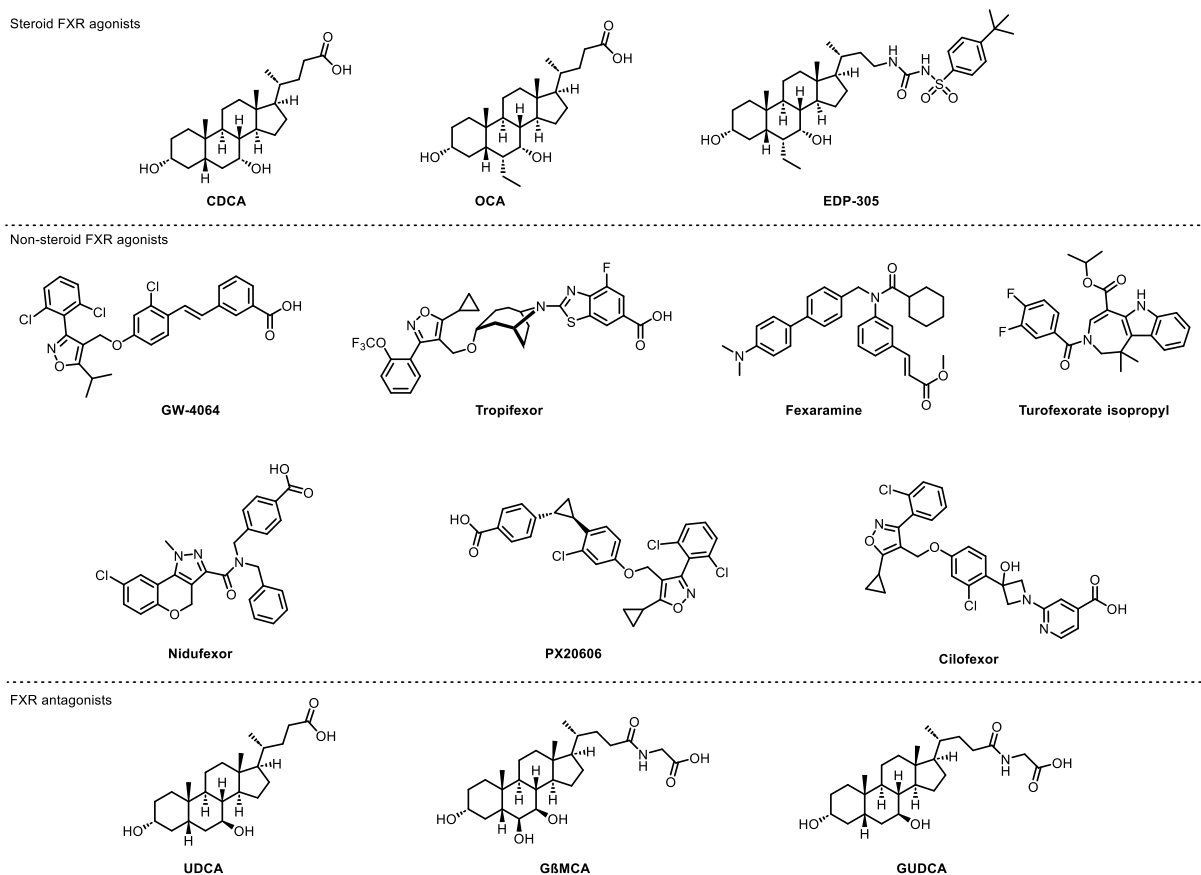
Figure 7. Structures of the most prominent FXR ligands. CDCA – Chenodeoxycholic acid, OCA – Obeticholic acid, UDCA – Ursodeoxycholic acid, GβMCA – Glycine-β-muricholic acid, GUDCA – Glycoursodeoxycholic acid.

1.8   TAKEDA G-PROTEIN COUPLED RECEPTOR

Takeda G-Protein coupled receptor (TGR5), also known as G protein-coupled bile acid receptor 1 (GPBAR1), G-protein coupled receptor 19 (GPCR19) or membrane-type bile acid receptor (M-BAR), is a membrane protein which was identified in 2002.[170, 171] In humans, it is encoded on chromosome 2 in *GPBAR1* gene, encoding 330 amino acids. TGR5 is mostly expressed in the small intestine, stomach, liver, lung, placenta, and spleen.[172, 173]

The receptor structure was unknown until 2020 when the cryogenic electron microscopy (cryo-EM) structure was published in Nature.[174] This opened the possibility for rational ligand design and computer simulation methods. TGR5 consists of seven transmembrane helixes. The ligand binding pocket is located on the extracellular side of the membrane (**Figure 8**). Upon ligand binding to this region, a variety of pathways can be activated. This allows a cell to react to outside stimuli.[175] For example, activation of TGR5 stimulates cyclic adenosine monophosphate (cAMP) synthesis, a well-known second-messenger,[176] regulates the function of cAMP-dependent protein kinases.[177] Those kinases then regulate glycogen, sugar, and lipid metabolism. Moreover, TGR5 is involved in nuclear factor-κB (NF-κB), protein kinase B (AKT), and extracellular signal-regulated kinases (ERK) cell signaling pathways.[178] Consequently, modulation of TGR5 is considered a promising target for the treatment of type 2 diabetes mellitus and other metabolic or digestive diseases.[179-190]
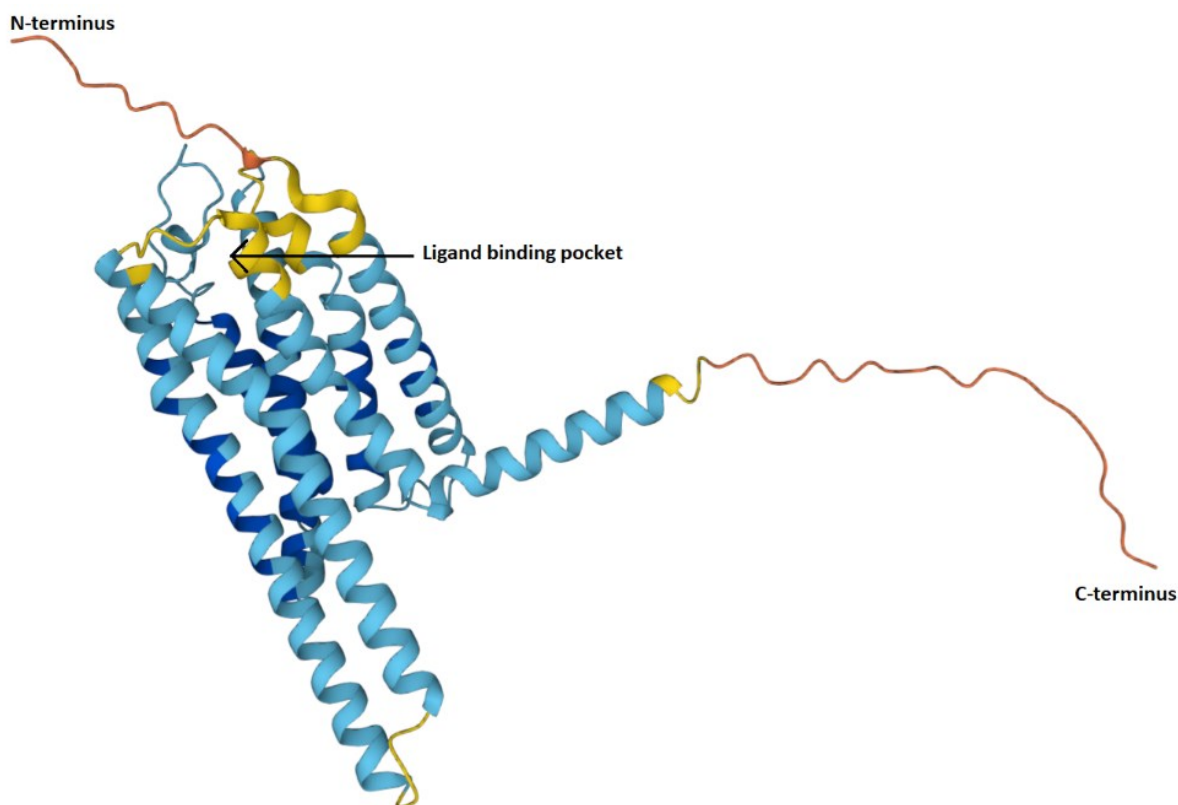
Figure 8. The tertiary structure of TGR5, as predicted by AlphaFold.[78, 79] AlphaFold, produces a predicted local distance difference test (pLDDT) with values between 0 and 100. This represents a per-residue confidence score. Some regions below 50 pLDDT may be unstructured in isolation. Deep blue – Very high (pLDDT > 90), light blue – confident (90 > pLDDT > 70), yellow – low (70 > pLDDT > 50), very low (pLDDT < 50).

1.9 LIGANDS OF TGR5

Bile acids are natural ligands for TGR5 with the order of their potency LCA > DCA > CDCA > CA. The potency of bile acids is further increased upon conjugation with taurine. UDCA and HDCA do not activate the receptor, and MCA affords only weak activation.[191]

The interior of the ligand binding pocket is more open as compared to FXR. Phe-161 and Leu-74 are facing the α side of the bile acid, while Tyr-240 and Ser-247 are providing polar interactions with C3-OH and C7-OH, respectively. The bile acid acidic side chain is not stabilized by any amino acid interaction but is sticking out of the transmembrane protein part into the extracellular space (**Figure 9**). According to the PubChem database,[121-123] in total 866 compounds were tested, from which 258 are steroids and 188 are bile acids derivatives. The published data allowed us to propose a pharmacophore for the active compound as follows: position C3 is critical for TGR5 activation. The C3 deoxygenation, inversion to 3β-OH, or substitution with an acetoxy or sulfate moiety completely diminishes the activity.[191] The 7α-hydroxy group is probably not important because 7-deoxy modification (LCA) is more active than its 7α-hydroxy counterpart (CDCA). It should be noted that some substitution on C7 might be beneficial since 7α-methoxy derivatives are more active than 3-deoxo ones.[192] Finally, modifications of the side chain at position C17 (e.g., alcohol, amide, tetrazole, nitrile, isoxazole, sulfonamide, sulfonate, carbamate, ureate, 1,3,4-oxadiazolate, amine, glycine or taurine conjugates) demonstrate high tolerability towards the biological activity.[125, 192-195] Shortening of the bile acid side chain decreases ligand activity on TGR5.[191]
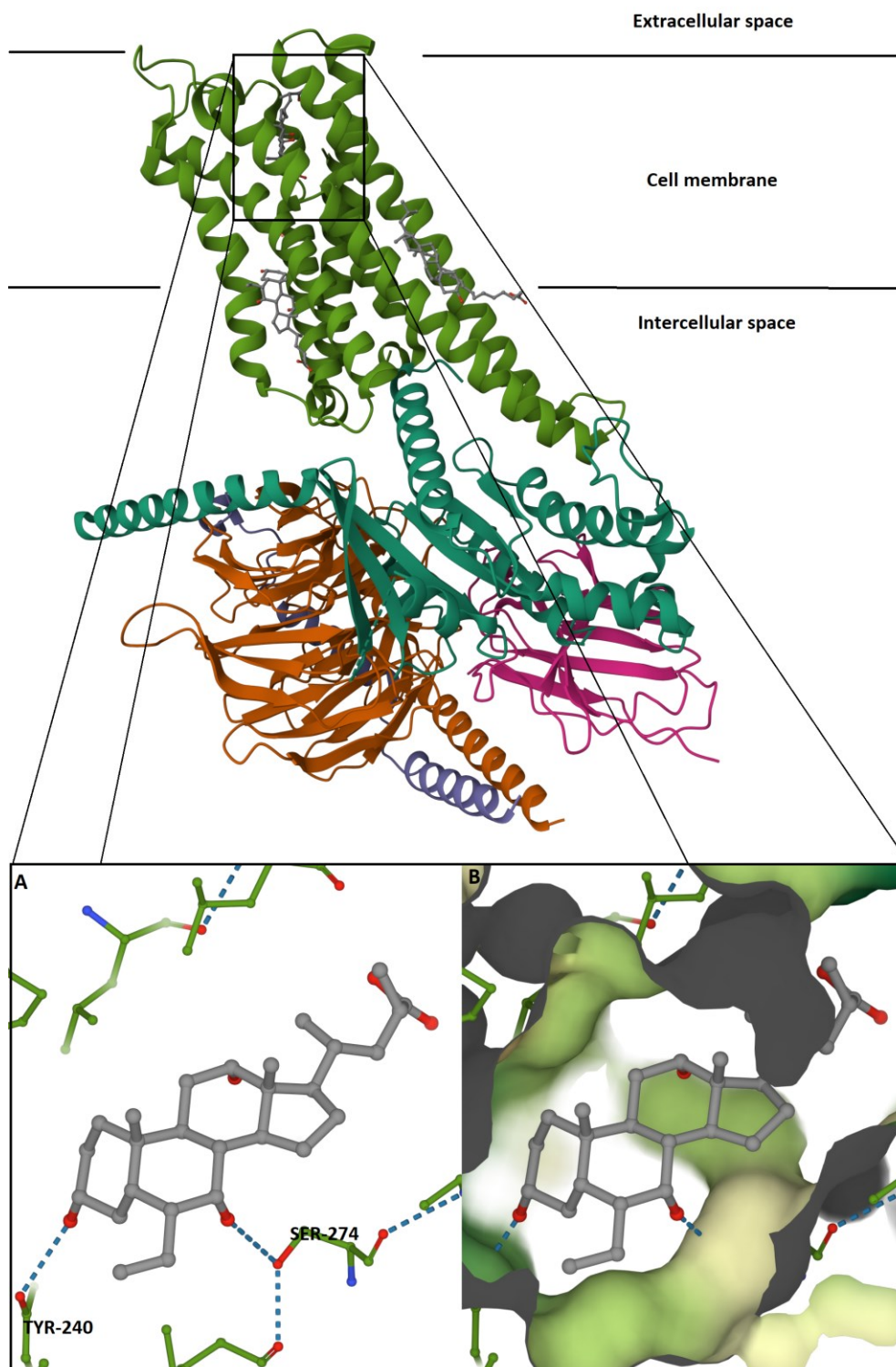
Figure 9. Cryo-EM structure of TGR5 with INT-777 (PDB: 7CFN).[174] **A**: Black – INT-777, green – FXR residue within 5Å distance, blue – polar interactions. **B**: Gaussian protein surface with a visible lipophilic cavity in the bottom part of the picture, green – lipophilic region, red – hydrophilic region. Visualized and edited.[134, 135] Lipophilic residues Phe-161 and Leu-74 were omitted for clarity.

In general, TGR5 is a more promiscuous receptor than FXR, and therefore, it can be activated by a wider range of hydrophobic compounds, including steroid hormones or neurosteroids, for example, pregnanediol.[185, 191, 196] Structures of selected TGR5 ligands are summarized in **Figure 10**. The most prominent TGR5 agonist, compound INT-777, was shown to be effective in reducing hepatic steatosis

and obesity in obese rats,[197] however, there wasn't any clinical follow-up. Non-steroid TGR5 agonists were discovered with high-throughput screening of heterocyclic molecules. Compounds TC-G-1005 and SB-756050 were identified as selective TGR5 agonists,[198-200] and the latter with follow-up clinical trials.[201] Even though no adverse effects were observed for compound SB-756050, the results of the clinical trials were inconclusive, and the high variability of study outcomes prevented further clinical development.[202] Only thirty-four TGR5 antagonists have been identified, such as SBI-115. Compound SBI-115 has been shown to reduce polycystic liver disease hepatogenesis.[203]

Figure 10. Structures of selected TGR5 ligands. LCA – lithocholic acid, TGR5 – Takeda G protein-coupled Receptor 5.

2   AIMS OF THE WORK

2.1   PROJECT 1. PREPARATION OF PREGNANE LIBRARY

The goal was to create a library of steroid compounds derived from the pregnane skeleton and evaluate their TGR5 and FXR activity. Based on the published data described above, we have chosen the pregnane skeleton for screening. The pregnane skeleton offers structural variability in A/B rings, namely 5α, 5β, Δ^4, and Δ^5 modifications. This project aimed to use a departmental steroid compounds library of approximately 2000 samples (1200 unique) and select, characterize, and purify (if needed) those that comply with proposed structural requirements.

2.2   PROJECT 2. SYNTHESIS OF C7 MODIFIED BILE ACIDS

The second project of the Thesis aimed to modify CDCA and OCA at position C7. This particular modification was selected based on the crystal structure analysis that demonstrated a lipophilic cavity in the FXR that was in close vicinity to the C7 hydroxyl group. TGR5 structure was not considered since TGR5 tertiary structure was unknown at the time.

2.3   PROJECT 3. OXIDATION OF AXIAL AND EQUATORIAL HYDROXY GROUPS

Propose and design a methodological study describing the selectivity of oxidizing agents toward axial and equatorial hydroxyl groups. The synthesis of C7-modified bile acids within Project 2 required synthetically distinguishing the reactivities of C3 and C7 hydroxyl groups. Therefore, a study targeting the selectivity of oxidizing agents was performed.

3 PREPARATION OF PREGNANE LIBRARY

3.1 RESULTS AND DISCUSSION

The pregnane motif was selected for further characterization of TGR5 receptor requirements. This selection was inspired by Sato's work,[191] where (20S)-5β-pregnan-3α,20-diol, 5α-pregnandione, and progesterone showed the highest activity on TGR5 from tested steroid hormones.

COMPOUND SELECTION

There are approximately 2,000 vials with steroid compounds in the group deposit, making up 1,200 unique molecules. The deposit was created in the late 1960s and was not in electronic form.

The first task was to create a software database in which structures could be filtered and associated with their experimental data. The Microsoft Access database software with the associated Structured Query Language (SQL) using Visual Basic for Applications (VBA) programming language was used. This setup allows the creation of a graphical interface in a drag-drop manner and the integration of ChemDraw structures directly into the database. In brief, SQL commands are used to insert and retrieve data from the database. Next, NMR spectra, elemental analysis, or chromatograms are stored in separate folders, and they can be accessed with a VBA code. Finally, a custom RDKit[204, 205] Python script was created to populate the database with molecular properties, such as molecular weight, exact mass, SMILES, or inchi. This is convenient because it enables additional database functionalities, such as advanced sorting or structure search. A schematic overview of the created database software is shown bellow (**Figure 11**).
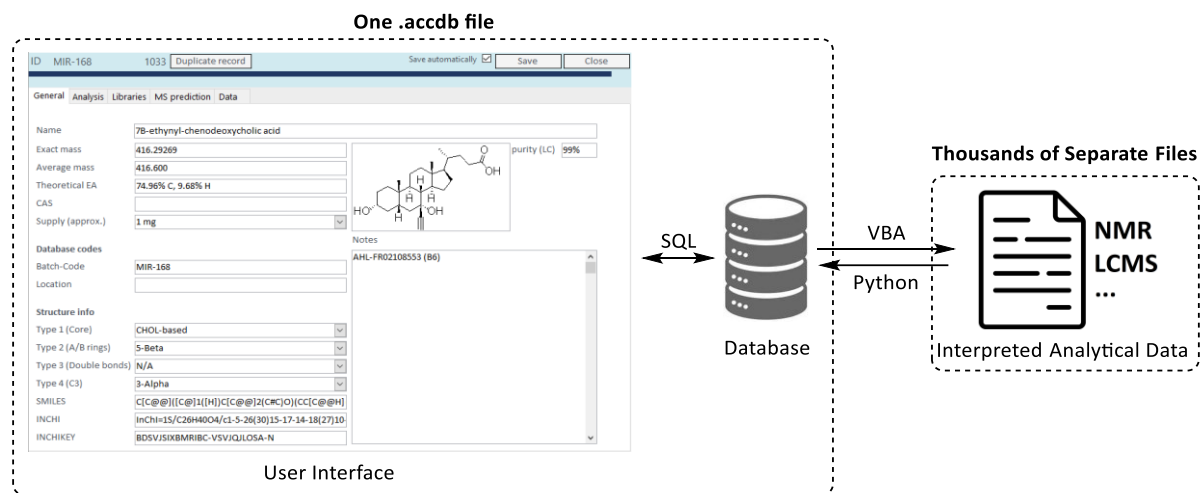
Figure 11. Schematic structure of constructed software tool to organize compounds. accdb – Microsoft's Access database, SQL – Structured Query Language, VBA – Visual Basic for Applications.

All 2000 vials and their labels were visually checked, drawn in ChemDraw, and uploaded into the database.

Chemical Analysis

Compounds that satisfied our structure-related selection criteria were tested on LC-MS for their purity. With a wide variety of structures in our library, it was not possible to use only one analytical HPLC method for all compounds. Therefore, multiple columns (C4, C8, C18), solvent systems (methanol,

isopropanol, acetonitrile), and additives (formic acid, trifluoroacetic acid, ammonium formate) were used to evaluate the purity of compounds.

Compounds with chromatographic purity $\geq 95.0\%$ were further characterized by ^{1}H NMR followed by the Attached Proton Test (APT). NMR signals were partially assigned with the help of Correlation Spectroscopy (COSY), Heteronuclear Single Quantum Coherence (HSQC), and Heteronuclear Multiple Bond Correlation (HMBC) techniques. First, the C18 and C19 methyl groups were assigned in proton and carbon NMR. As all pregnane structures are substituted in position C17, shared HMBC interactions between H18 ↔ C17 and H21 ↔ C17 allowed the assignment of position C17. Next, the assignment of C18 and C19 carbons allowed us to assign C1, C5, C9, C10, C12, C13, and C14 carbons through HMBC. As the intensities of HMBC cross peaks correlate with coupling constants[206] the shorter interactions of $^2J_{H,C}$ are usually stronger than $^3J_{H,C}$ interactions. Moreover, the quaternary carbons usually give low signals in APT. Consequently, the above-mentioned facts allowed the assignment of C10 and C13 quaternary carbons. The $^3J_{H,C}$ interactions follow Karplus[207] equation, and therefore, whenever the dihedral angle is close to 90 degrees, the coupling is very close to zero. As a result, missing cross peak is not evidence that carbon-proton are far apart. Taken together, this is the main advantage of using methyl groups for assignment because free rotation between C10-C19 and C13-C18 allows us to observe all cross peaks near C18 and C19 methyl groups.
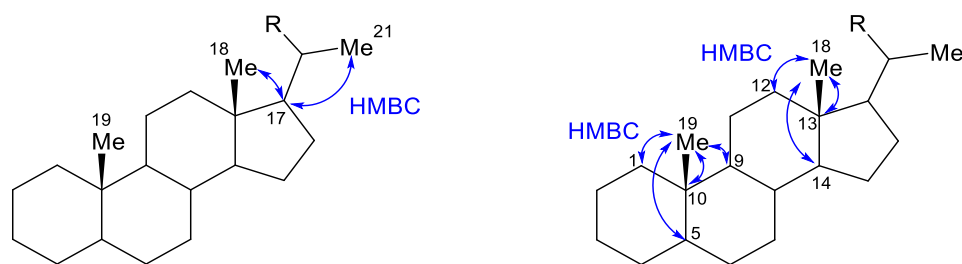
R = usually polar groups: =O, -OH etc.

Figure 12. Selected HMBC interactions are crucial for determining the structure of steroids using NMR techniques.

This process yielded 46 compounds, which were clustered into four groups of 5α-, 5β-, Δ^4-, and Δ^5-steroids and are summarized in **Figure 13**.

Figure 13. List of the selected compounds from our library that passed the purity and structure requirements.

Compound **31** is discussed as a representative example of the analytical process. First, the purity of **31** was analyzed by HPLC-MS with acetonitrile/water gradient on the C18 column (*HPLC Method B, section 6.1*). The LC-MS analysis (**Figure 14**) showed only one peak on both detectors and correct *m/z*. Compound **31** was, therefore, suitable for the NMR analysis.
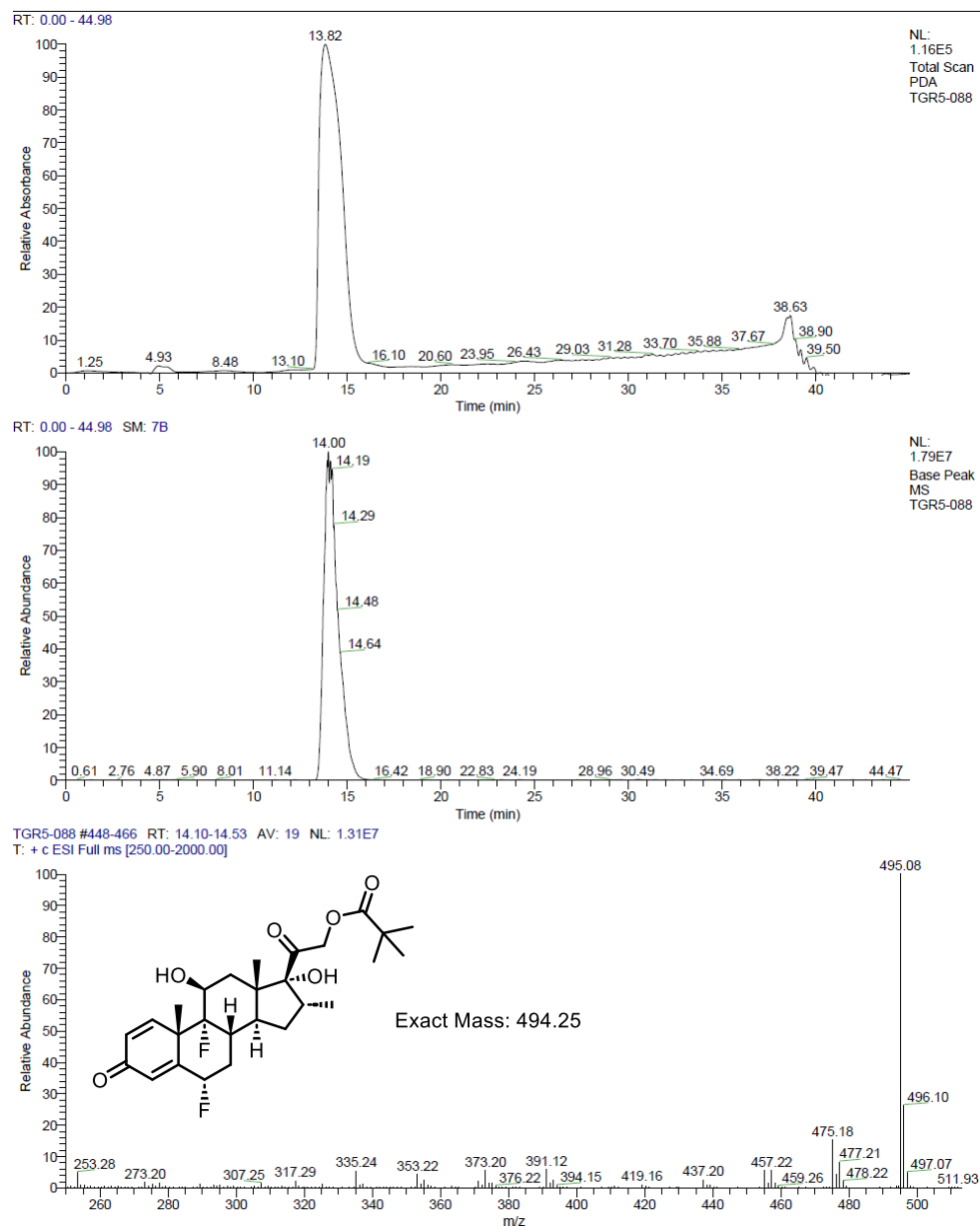
Figure 14. Representative HPLC chromatogram of compound **31**.

As illustrated in **Figure 15**, compound **31** has a good separation of signals in ^{1}H and APT spectra, which allows an assignment of the whole molecule. For example, methyl groups C18 and C19 can be distinguished by cross-peak interactions of H18-C12, H18-C14, H18-C17, H19-C1, H19-C5, and H19-C9 (**Figure 15**).

29
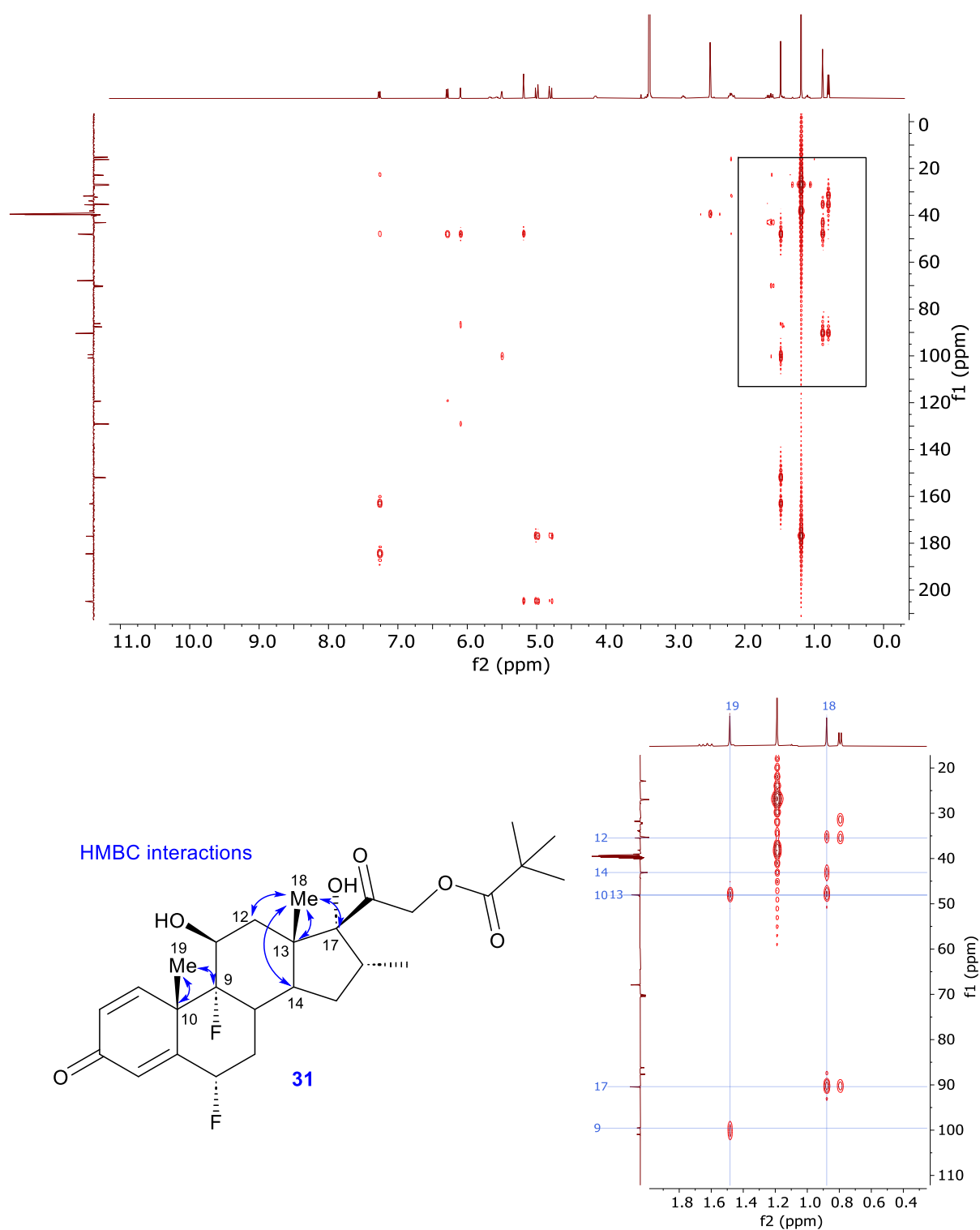
Figure 15. HMBC analysis of **31**. Top – full HMBC spectrum, bottom – the key $^2J_{H,C}$, and $^3J_{H,C}$ interactions and their cross peaks are highlighted in blue. Only key HMBC interactions are shown for clarity.

Other compounds were analyzed analogously, and their analytical data are summarized in the *Experimental section 6.3*.

BIOLOGICAL EVALUATION

The LanthaScreen assay was performed in collaboration with the group of Dr. Helena Mertlíková-Kaiserová by Dr. Jaroslav Kozák. The TGR5 luciferase assay was performed in collaboration with the Faculty of Pharmacy in Hradec Králové, Charles University, in the group of Prof. Petr Pávek by Dr. Alžběta Štefela.

Figure 16. A: Interaction of ligands with human FXR in TR-FRET FXR Coactivator Assay. Commercially available LanthaScreen™ Assay Kit in 384 plate formats (Thermo Fischer Scientific, MA, USA, PV4833) was used according to the manufacturer, along with Bravo automated liquid handling platform (Agilent, CA, USA). Compounds were tested against DMSO and GW-4064 (activity = 100%) as negative and positive controls, respectively. **B**: Effects of C7-modified CDCA derivatives on the human TGR5. HepG2 cells were co-transfected 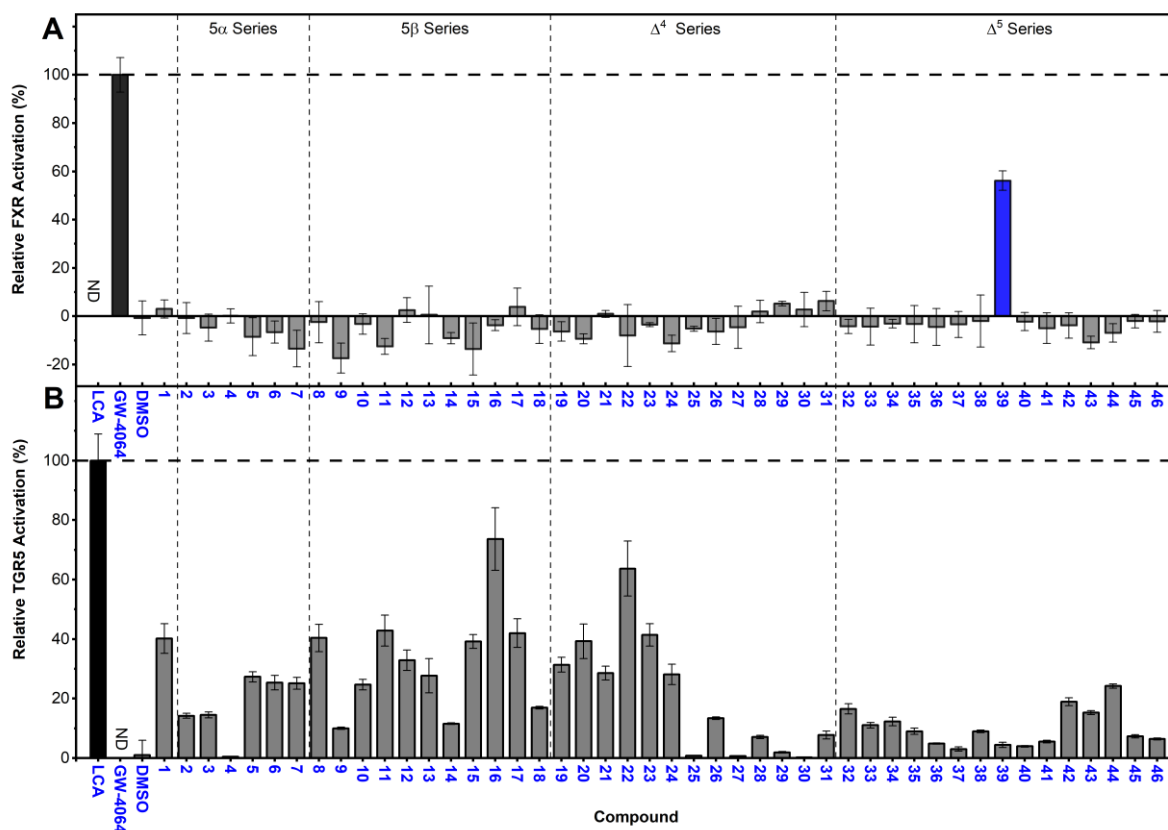with a CRE containing luciferase reporter plasmid and a TGR5 expression vector. Cells were treated with indicated compounds at 10 μM concentrations for 5 hours. Compounds were tested against DMSO and LCA (activity = 100%) as negative and positive controls, respectively. CRE – cAMP response element, DMSO – dimethyl sulfoxide, FXR – Farnesoid X receptor, LCA – lithocholic acid, GW-4064 – 3-(2,6-dichlorophenyl)-4-(3'-carboxy-2-chlorostilben-4-yl)oxymethyl-5-isopropylisoxazole, TGR5 – Takeda G protein-coupled Receptor 5, TR-FRET – Time-resolved fluorescence energy transfer. Each measurement is an arithmetic mean from three independent experiments (n = 3), with standard deviation marked as error bars. Vehicle (0.1% DMSO) was used as a solvent in all samples, including control samples. Created in OriginPro.[208] All relevant experimental and calculated compound properties are summarized in the *Appendix*.

Structure-activity relationship (SAR) was done in the StarDrop™ application.[209] The SAR analysis was done for both FXR and TGR5 independently.

Structure-Activity Relationship, FXR

Unfortunately, our FXR dataset contains only one active compound (**39**). This prevented us from using more sophisticated methods for SAR analysis. For example, machine learning, which heavily depends on the data's diversity.[210] For this reason, we focus the discussion only on **39**.

Compound **39** exhibited partial activity on FXR (RLU = 0.56 ± 0.04) as compared to GW-4064. We hypothesize that the C2' carboxylic group can mimic the C24 side chain of bile acids, which serve as natural ligands for FXR. We supported this hypothesis by demonstrating the binding mode through docking (for docking protocols see *Experimental, section 6.1*). Compound **39**'s carboxylic group C2' interacts with the basic amino acids Arg-331 and His-294. Additionally, the methyl groups C18 and C19 forms interactions with Leu-287, Leu-348, and Met-280. Lastly, the C20 carbonyl group engages in hydrogen bonding with Tyr-361. Other carboxylic acids (**25**, **40**–**44**) were inactive, presumably due to their longer linker between the carboxylic acid and the rest of the molecule, and therefore too far away to establish polar interactions with basic amino acids Arg-331 and His-294.
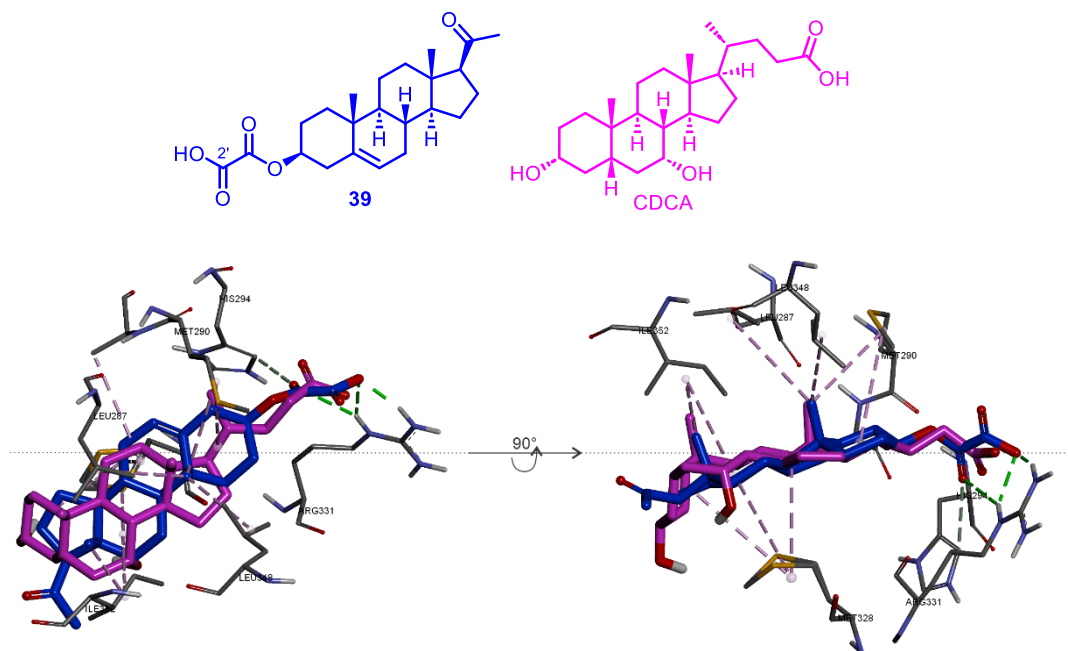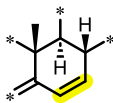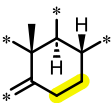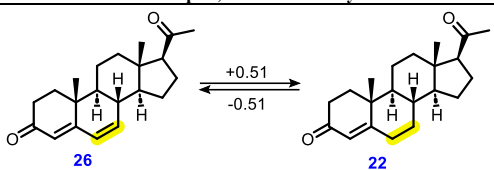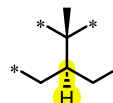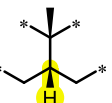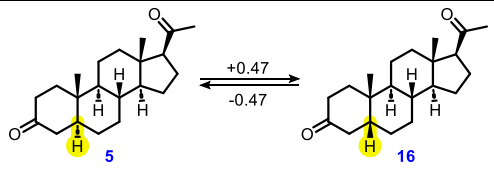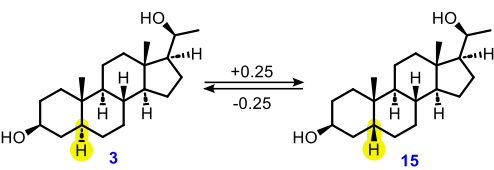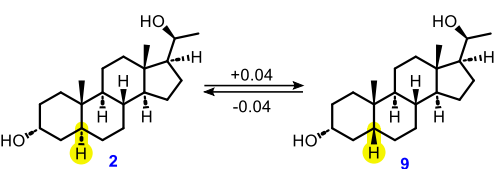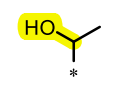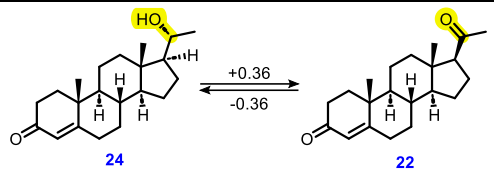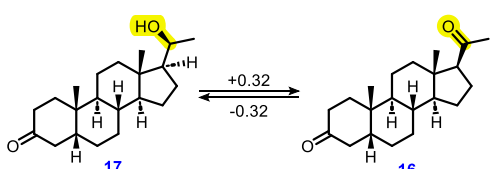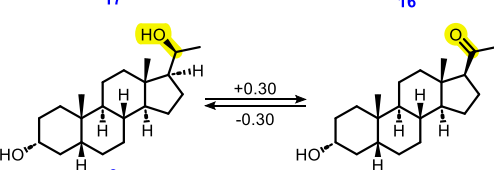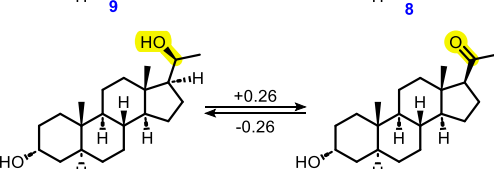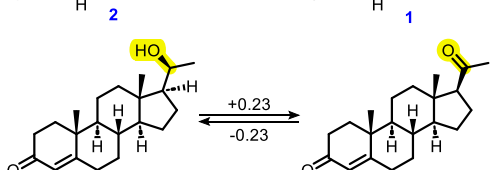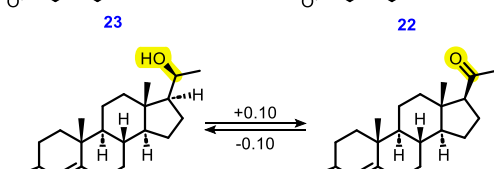
Figure 17. Ligand **39** and CDCA position within LBD of FXR (PDB: 6HL1).[66] Pose of **39** was calculated, while the position of CDCA is from the crystal structure.[66] CDCA – chenodeoxycholic acid, FXR – Farnesoid X receptor, LBD – ligand-binding domain, PDB – Protein Data Bank. Ligands: **39** carbon backbone – blue, CDCA carbon backbone – magenta, red – oxygen, white – hydrogen. Amino acids: black – carbon, yellow – sulfur, blue – nitrogen, red – oxygen, white – hydrogen. Only residues within 5Å distance are shown. Non-exchangeable hydrogens and Tyr-361 were omitted for clarity. Calculated with AutoDock vina,[211] visualized in Discovery studio,[212] and edited in CorelDraw.[213]

Structure-Activity Relationship, TGR5

Compounds **1**–**46** were clustered into pairs based on their structure similarity. This allowed us to pinpoint which modification on the steroid core has a positive or negative effect. The most important structural features are summarized in **Table 3.**

Table 3. Compound pairs based on structural similarity. The three most important transformations for TGR5 activity are shown with specific examples.

Transformation	Examples, ΔTGR5 Activity

To examine this hypothesis and further explore chemical space for possible ligands, we used in-silico compound library enumeration. First, we used our experimentally measured compounds **1**–**46** activities to train the Q*uantitative structure-activity relationship model* (*QSAR_TGR5*). After training, the model predicts the activity of novel compounds toward TGR5. The protocol for model training, as well as model performance, are in *Appendix*. The ten most active compounds towards TGR5 were selected as seeds. The enumeration algorithm generates new compound ideas by applying chemical transformations to our seed compounds. This results in all possible compounds that could be made from the initial ten molecules within three transformation steps. Each step consists of 30096 possible transformations. This would (in ideal case) generate over 10^{12} compounds, too much for our hardware to handle. Therefore, the activity of each compound was predicted with the *QSAR_TGR5* model, and only the 200 best compounds were selected from each generation for further transformations. To mitigate selection bias, the 200 molecules were selected based on *QSAR_TGR5* predicted activity and structural diversity with weights 85:15, respectively. This yielded 600 non-unique compounds. The seed compounds were added as well for comparison. The 610 compounds dataset was stripped of duplicates and scored with computationally expensive *Non-central nervous system orally taken drugs scoring function* (*NCNSOTD*, see *Appendix*). The purpose of scoring is to consider other important parameters such as solubility, metabolic stability, or partition coefficient. The entire process is shown graphically below (**Figure 18**).
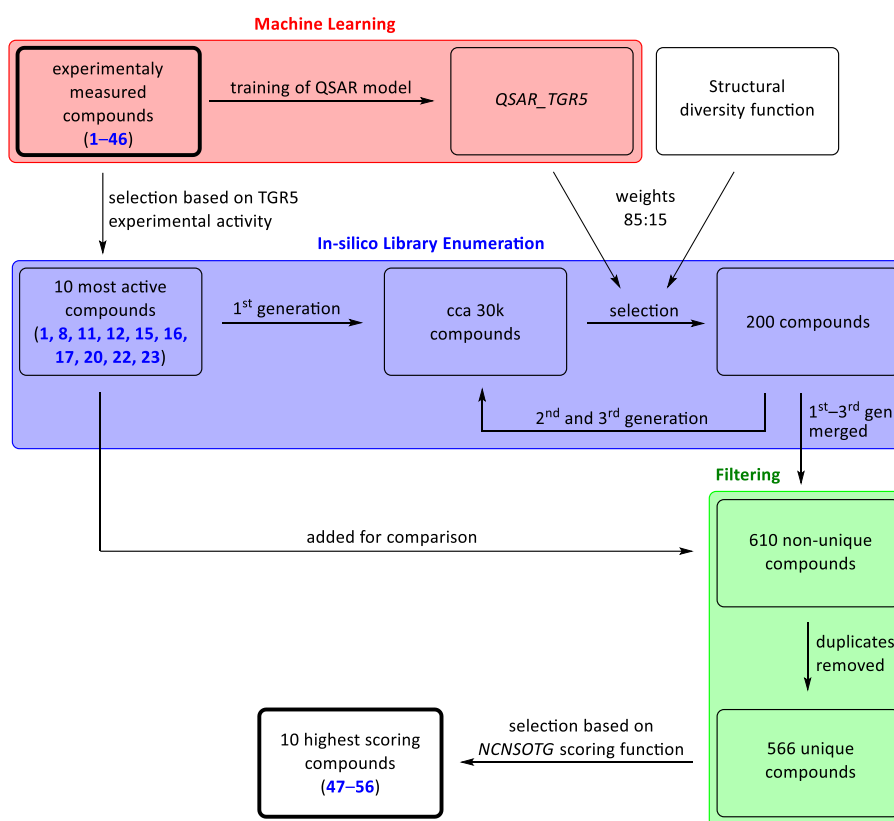
Figure 18. Schematic representation of TGR5 drug discovery process. NCNSOTD – Non-central nervous system orally taken drugs scoring function, QSAR – Quantitative structure–activity relationship.

The initial ten seed compounds and the ten highest-scoring predicted compounds are compared below (**Figure 19**).
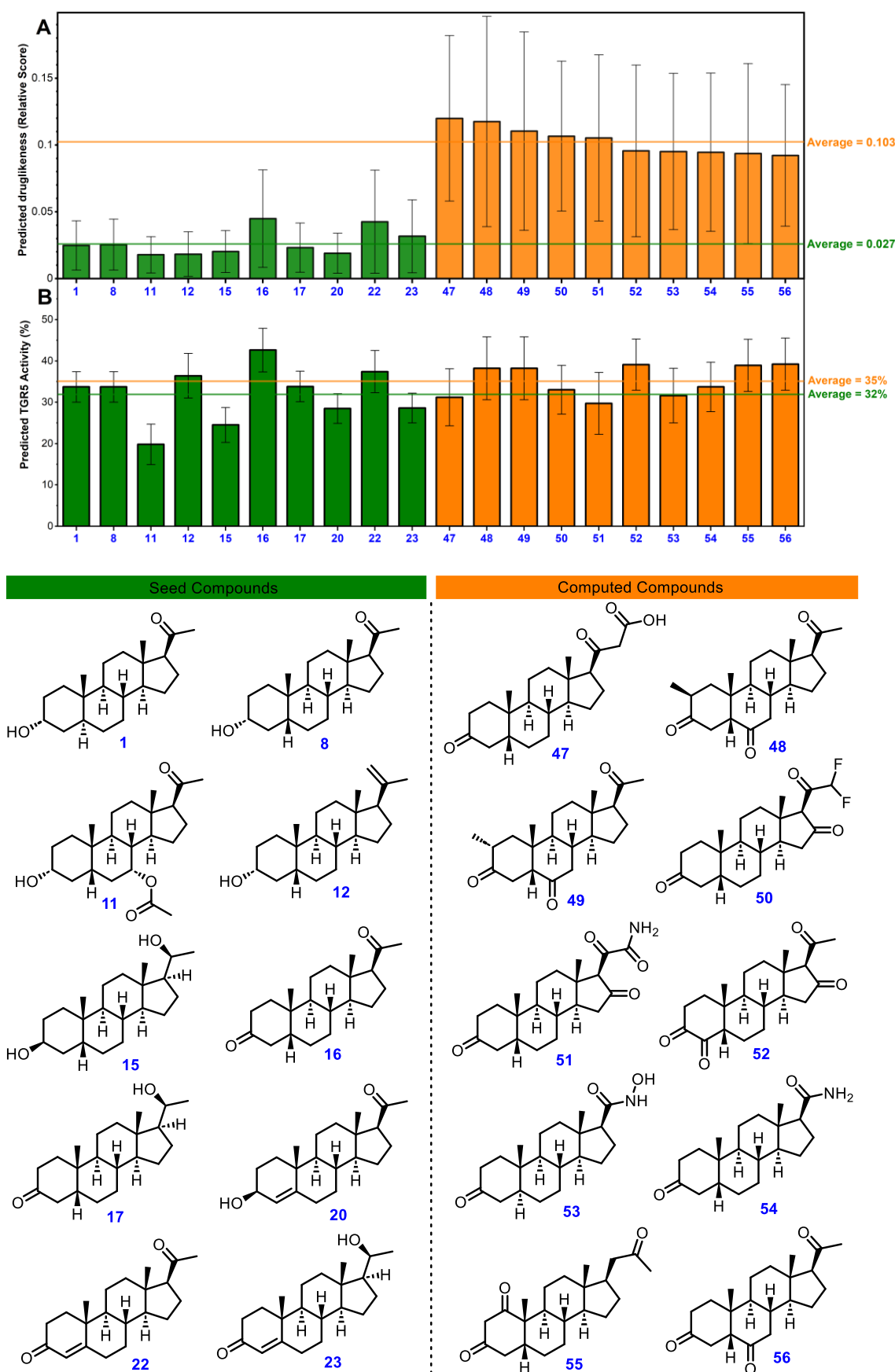
Figure 19. Predicted activities and scores toward TGR5. RLU – Relative luminescence unit, TGR5 – Takeda G protein-coupled receptor 5, NCNSOTD – Non-central nervous system orally taken drugs scoring function.

35

The *cis* A/B rings junction stands out as the most critical structural feature. This motif is consistently observed in both experimental and predicted molecules (**Figure 19**). Such a trend aligns with expectations, as natural TGR5 ligands – bile acids share this structural characteristic. Our predictive model shows a strong preference for oxo substitution at positions C3 and C20. Indeed, in the experimental dataset, the hydroxy group at C20 was usually inferior to the oxo group (**Table 3**). Concerning the C3 position, our experimental results demonstrated that both hydrogen bond acceptors and donors are viable (**Figure 19**).

As shown by calculations, six out of ten predicted ligands exhibit alterations in the C17 side chain. This suggests that the C17 position is a promising target for modification. Additionally, our model occasionally introduces extra oxo groups at positions C1, C4, C6, or C16. Such additions are likely intended to enhance solubility, which ranks as the second most critical factor in the *NCNSOTD* function.

3.2 CONCLUSION

None of the tested molecules showed better activity for FXR or TGR5 than the positive controls. Only notable compounds are **39** (FXR activation, 56% ± 4%) and **16** (TGR5 activation, 74% ± 11%). From our experimental data, we trained the artificial intelligence (AI) predictive model *QSAR_TGR5*. The model can predict the TGR5 activity of novel steroid ligands. We used the model to select suitable molecules from a large pool (> 10^{12} possibilities) of in-silico-generated compound ideas. Selected compounds were further scored for other important drug properties (logP, solubility, etc.) and ranked. The highest rank in-silico and experimental compounds were compared to propose general requirements for TGR5 agonists. Unfortunately, we were not able to train a complimentary AI model (*QSAR_FXR*) due to a lack of data diversity. Based on our results, we propose a general structure of TGR5 agonist (**Figure 20**).
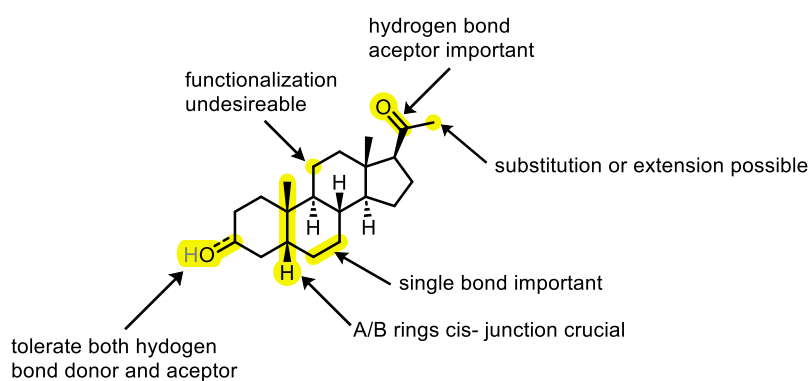
Figure 20. The proposed general structure of TGR5 agonist. Critical structural features on the steroid core are highlighted.

Outcomes

- An electronic compound database, designed for internal group use, was developed by a student who learned coding by himself.

- A still-growing library of endogenous and synthetic steroids with confirmed purity and structure.

- Rigorous analytical work significantly enhanced the students' expertise, particularly in developing LC-MS methods and interpreting 2D NMR spectra.

37

4   SYNTHESIS OF C7-MODIFIED BILE ACIDS

4.1   RESULTS AND DISCUSSION

SYNTHESIS

Position C7 was modified due to the presence of a nearby lipophilic cavity in FXR (**Figure 6**). Furthermore, modifying position C7 is easily achievable when using CDCA as the starting material. The TGR5 binding pocket was not considered for ligand design since the TGR5 structure was unknown at the time. CDCA was chosen as the starting material for synthesis due to its commercial availability and low cost (1 USD/gram ≈ 0.4 USD/mmol). Synthetic protocols for C6 alkylation of CDCA were previously developed in our laboratory and are mentioned only briefly.
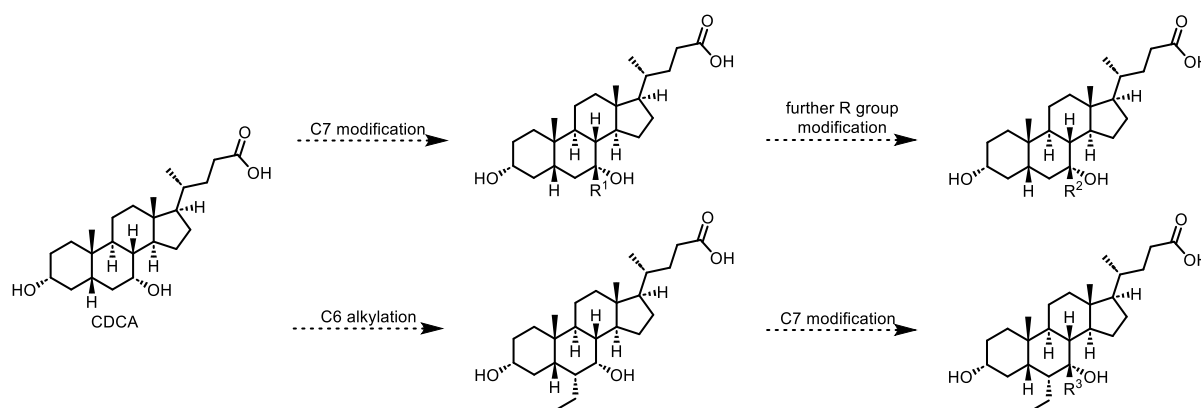
Scheme 1. Synthetic strategy for C7 modified bile acids.

Grignard Addition on C7 Carbonyl Group

7-Ketolithocholic acid (**61**) was synthesized from CDCA in three steps (**Scheme 2**). The synthetic process began with the esterification of CDCA, which was successfully achieved with either diazomethane or Fischer esterification, both yielding quantitatively compound **57**. However, it should be noted that diazomethane is a toxic and explosive reagent. Therefore, for safety reasons, we preferred Fischer esterification. The introduction of the ester moiety aimed to facilitate purification after the oxidation step. The good regioselectivity of the oxidation step is determined by the different reactivities of the equatorial C3 and axial C7 hydroxy groups. This topic is discussed in more detail in *section 5.1*. The ester **59** was hydrolyzed with an aqueous methanolic NaOH solution to yield free acid **61**. This step was necessary because the carbanionic nature of Grignard and Wittig reagents in the following reactions is incompatible with the ester moiety.
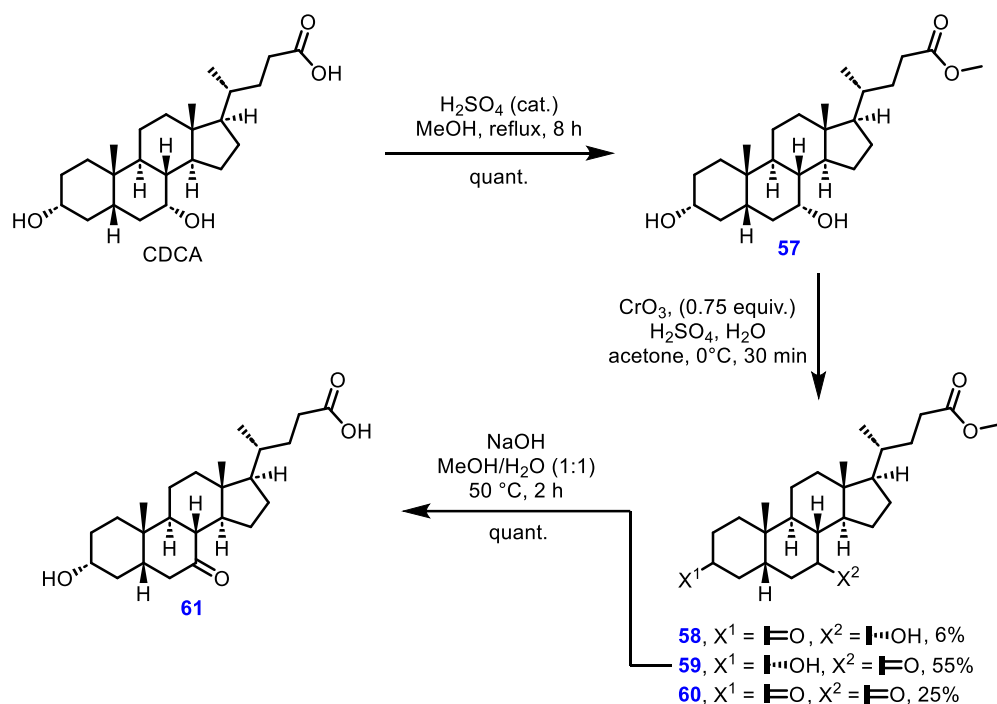
Scheme 2. Preparation of **61**, a starting material for the synthesis of 7-oxo-modified bile acids.

To synthesize C7 alkylated compounds **62–74**, we used Grignard reagents (**Scheme 3**). In most cases (**Scheme 3**, *entry 1–10*), we obtained enough material for structure evaluation and biochemistry assays after the first batch. For that reason, even low yield reactions were not optimized. Reaction with bulky nucleophiles (**Scheme 3**, *entry 11–13*) failed, even after extended reaction time.
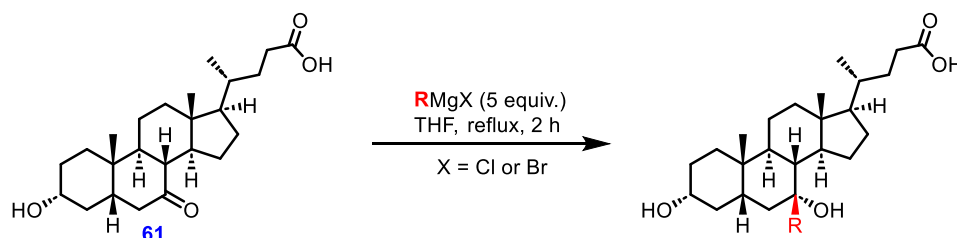
Entry	1	2	3	4	5	6	7	8	9	10	11	12	13
Compound	62	63	64	65	66	67	68	69	70	71	72	73	74
R	methyl	ethyl	vinyl	ethynyl	propyl	allyl	isopropyl	cyclopropyl	pent-4-en	nonyl	*sec*-butyl	*tert*-butyl	phenyl
Yield (%)[a]	29	47	51	63	36	40	36	33	34	35	n/a[b]	n/a[b]	n/a[b]

Scheme 3. Synthesis of C7-alkylated ligands. [a]Isolated yield after 2 hours of reflux. [b]Only side products were identified in the mixture after 48 hours of reflux.

Grignard reagents are not only strong nucleophiles but also strong bases. The reaction substrate is a free carboxylic acid, therefore the first and fastest reaction is acid-base proton exchange. The first exchange is with carboxylic proton and the second with alcoholic one. Given that, an excess of Grignard reagent (5 equiv.) was used in all cases. The resulting bile magnesium halide salt was poorly soluble in organic solvents and precipitated. Fortunately, with vigorous mixing and reflux, all reactions (including **Scheme 3**, *entry 11–13*) achieved full conversion, but harsh reaction conditions

led to the formation of side products in all cases. The identified side reactions were the reduction of the ketone to alcohol (**Scheme 3**, *entry 2, 5, 7, 9, 10, 11, 12*) and the addition on carboxylate (all cases). The reduction was likely to be achieved by the hydride transfer from the β-carbon of the Grignard reagent to the carbonyl carbon via a cyclic six-membered transition state.[214] The addition to carbon C24 occurred even though the carboxylate is a very poor electrophile. Other possible side reactions are aldol condensations or single electron transfer-induced radical reactions,[215] but we didn't observe any of those. Observed side products are depicted below (**Figure 21**).
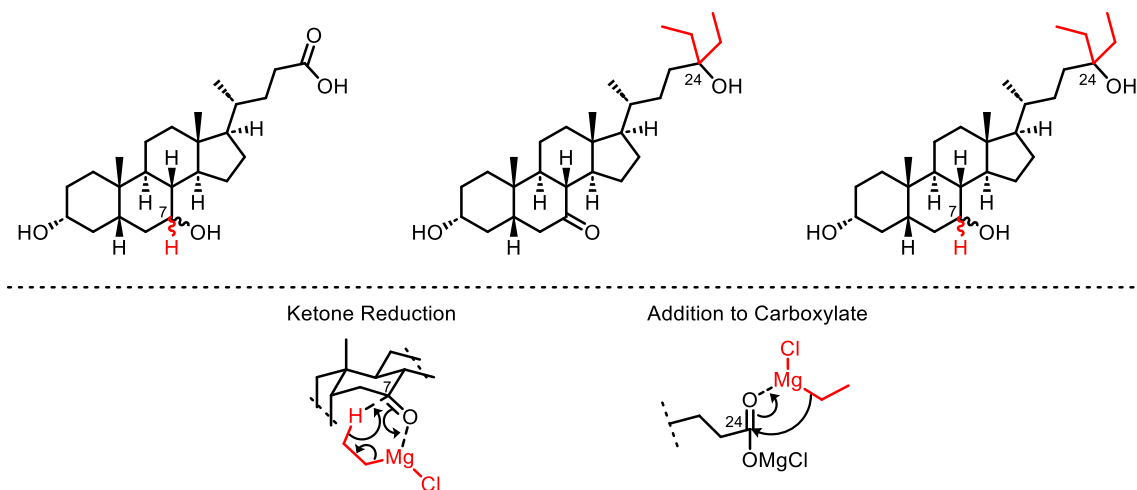
Figure 21. Observed side product after Grignard reaction with the proposed mechanism of formation. Only reaction with ethyl magnesium chloride is shown in each example.

The alkyl addition to ketone proceeded stereoselectively, and only one diastereoisomer was obtained. This diastereoselectivity in alkylation of 7-oxobile acids was first observed by Une et al.[216]

> *"The predominant formation of the 7β-alkylated epimer seems to be reasonable probably because the bending of ring A shields the α-side, and the Grignard reagent predominantly approaches to 7-keto group from the β-side.*
>
> *...*
>
> *The β-orientation of the newly introduced 7-alkyl groups of 7-Et-CDA and 7-Pr-CDA was tentatively assigned by PMR*[*]*. The chemical shifts of 19-CH$_3$ of 7-Et-CDA and 7-Pr-CDA, which are at δ 0.94 and δ 0.92, respectively, are almost the same as that (δ 0.97) of 19-CH$_3$ of 7-Me-CDA but different from that (δ 1.09) of 19-CH$_3$ of 7-methyl-ursodeoxycholic acid[†]. This result strongly suggests that the orientation of C7 alkyl groups in these compounds is the same as that of 7-Me-CDA[‡]."*

The authors relied solely on comparison of ^{1}H chemical shifts with similar compounds for assigment of absolute configuration at C7. However, we should take into consideration that at the end of the 1980s, 2D NMR techniques were not yet widespread. Therefore, we used ROESY and X-ray to assign the absolute configuration on C7. Unfortunately, we were able to conclusively assign only **63**, **64**, and **68**. All of them have **R** substituent in the equatorial position. Due to this, the configuration on C7 for

---

[*] proton magnetic resonance
[†] 7β-hydroxy-7α-methyl-5β-cholan-24-oic acid
[‡] 7α-hydroxy-7β-methyl-5β-cholan-24-oic acid

the **62**, **65**, **66**, **67**, **69**, **70**, and **71** was considered the same. This agrees with the chemist's intuition: Nucleophile attacks from the less hindered β-side and thermodynamically more stable equatorial adduct is formed (see **Figure 22**).
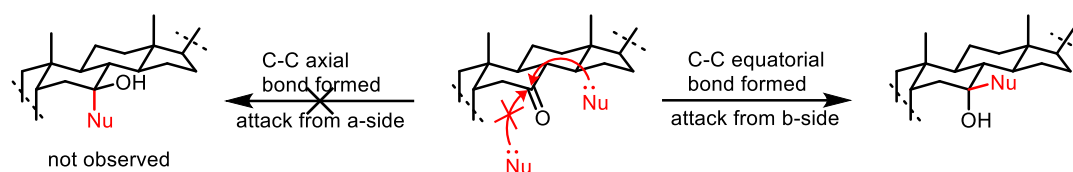
Figure 22. The rationale for observed diastereoselectivity of Grignard reagent addition on C7 carbonyl double bond within compound **61**.

Absolute Configuration on C7 for Compound **63**

Unfortunately, the ROESY spectra of **63** did not exhibit clear resonance correlations between the ethyl substituent and the steroid skeleton. Therefore, the structure was confirmed by the catalytic hydrogenation on palladium in ethanol of **64** that afforded a compound with an identical ^{1}H and ^{13}C NMR spectrum to that of **63**.
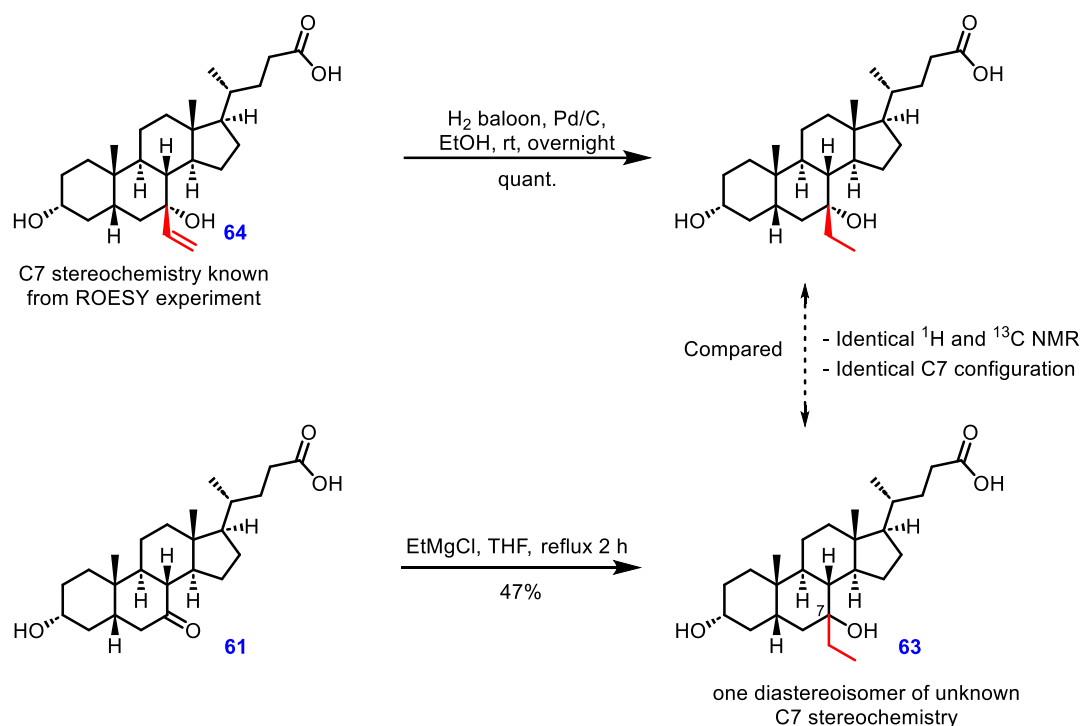
Scheme 4. Hydrogenation of **64** to compound **63** served as proof of C7 stereochemistry after EtMgCl addition.

Absolute Configuration on C7 for Compound 64

In the ROESY spectrum, the olefinic H1' proton exhibited cross-peaks with axial hydrogens H6β and H8, which confirmed that the vinyl substituent was equatorial (7β). (**Figure 23**)
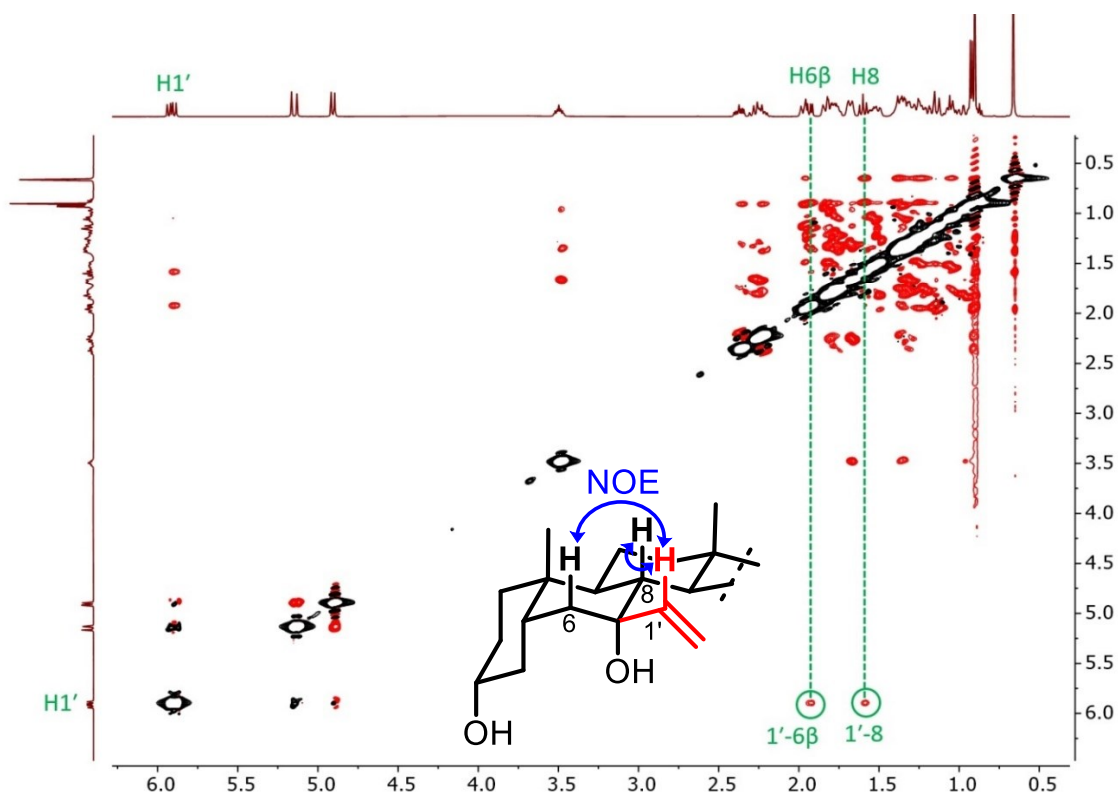
Figure 23. ROESY spectrum of 64, showing H1'-H6β and H1'-H8 contacts.

Absolute Configuration on C7 for Compound 68

Compound **68** was crystalized from the mixture of DCM and MeOH (100:1). Dichloromethane was chosen because it is a nonpolar-aprotic solvent. This forced **68** to aggregate through the formation of hydrogen bonds. Because **68** was only slightly soluble in dichloromethane, methanol was added to formulate a true solution. Under crystallization conditions, **68** formed a dimer, where polar-protic groups were pointing inward, and nonpolar-aprotic groups were pointing outwards (**Figure 24**). This arrangement maximizes lipophilic molecule/solvent surface and demonstrates amphiphilic properties, which are typical for bile acids.
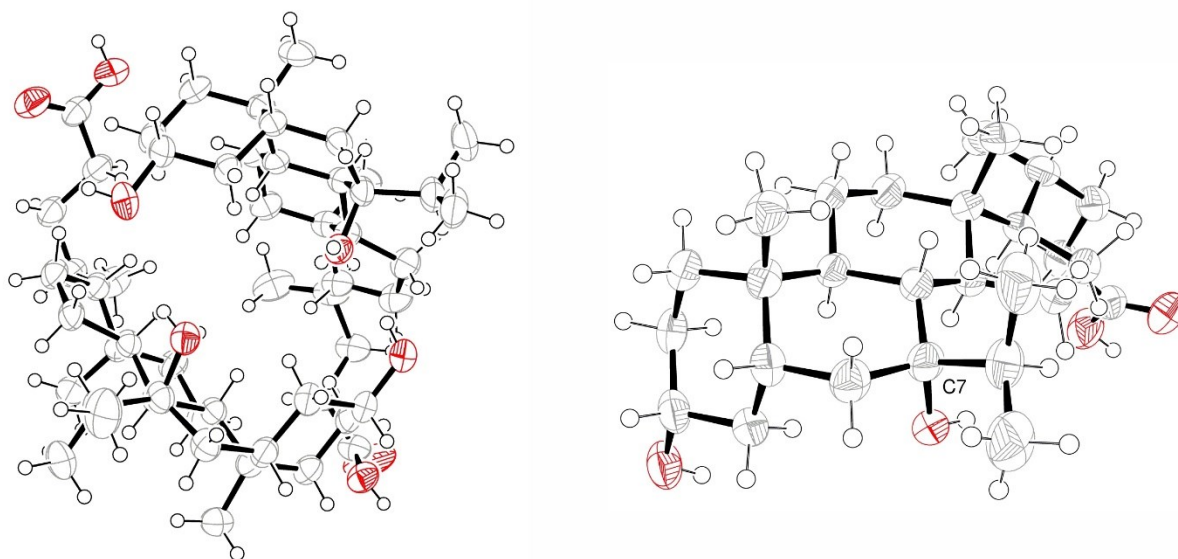
Figure 24. ORTEP[217] representations of the X-ray structure of **68** displacement ellipsoids are shown with 50% probability. Dimer (left) and mono structure (right) confirmed the equatorial position of the isopropyl group.

Wittig Reaction with C7 Carbonyl Group

(*E*)-7-Ethylidene derivative (**75**) was prepared by the Wittig reaction from corresponding carbonyl using ethyltriphenylphosphonium bromide (**Scheme 5**). The conditions were inspired by Poša et al.,[218] where authors attempted Wittig reaction on 3α,12α-dihydroxy-7-oxo-5β-cholan-24-oic acid and obtained exclusively *E*-isomer in 8.2% yield. Like Poša et al., we also obtained only *E*-isomer in a comparable 3% yield. The reaction was not optimized, as 6 mg obtained under these reaction conditions was sufficient for biological assays.
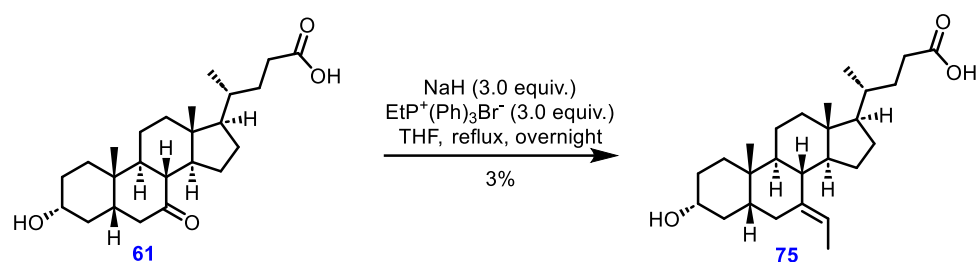
Scheme 5. Wittig reaction. Inspired by Poša et al.[218]

Double bond isomerism was confirmed by ROESY NMR, exhibiting NOE contacts of the H1' olefinic proton with protons H14 and H15 (**Figure 25**).
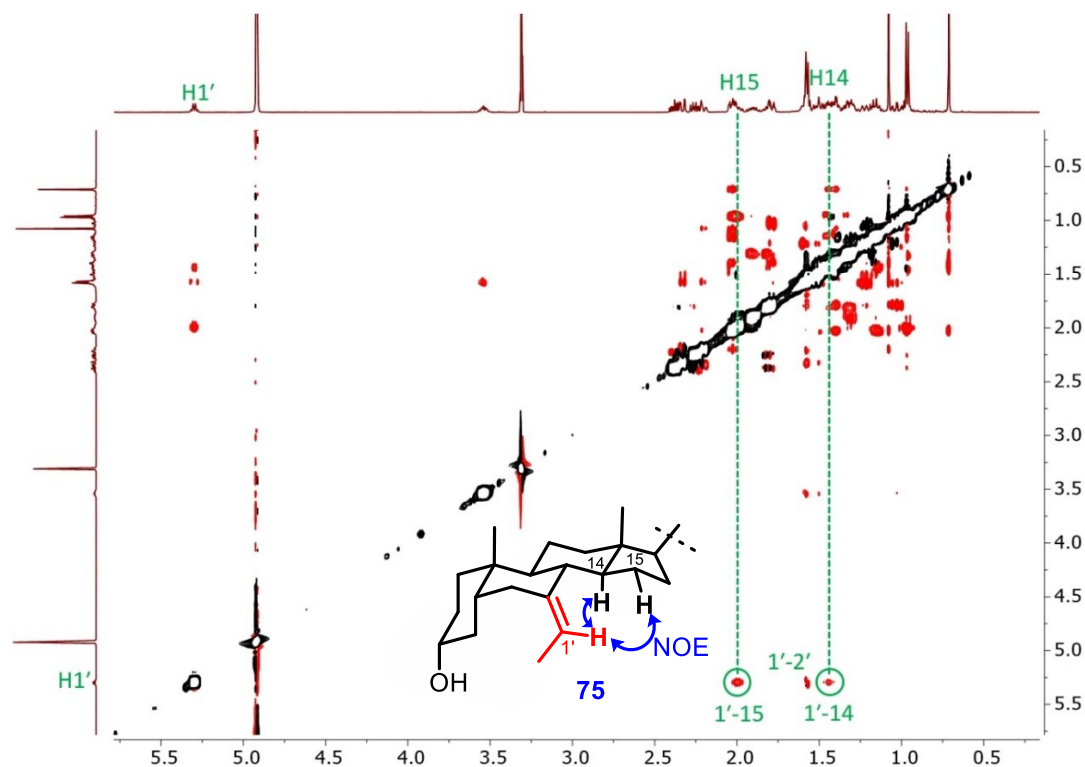
Figure 25. ROESY spectrum of **75**. The double bond stereochemistry was confirmed by H1'-H15 and H1'-H14 NOE interactions.

44

Further Modification of C7 Substituents

Compound **65** was selected for further modifications, as terminal alkyne offers the possibility of cross-coupling reactions and cycloaddition reactions. For the cross-coupling, we used an established Sonogashira reaction with a Pd/Cu catalytic cycle and iodobenzene as the coupling partner.
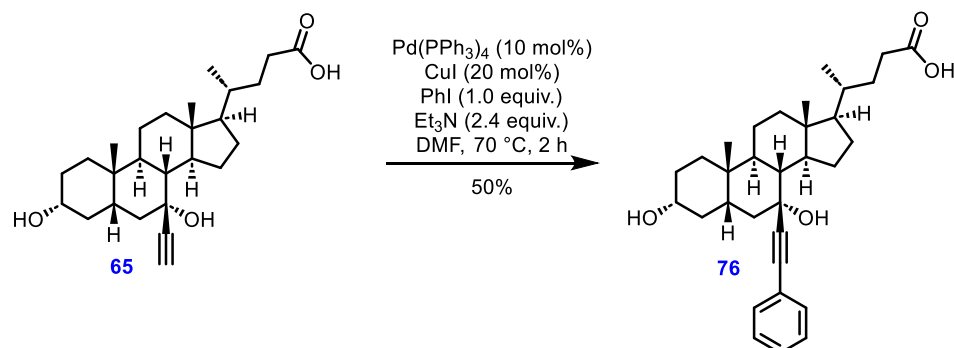
Scheme 6. Sonogashira reaction.

For click reaction, we used the perfluoroazide that was developed at our Institute in Dr. Beier's group.[219] Based on their recommendation, we used $C_2F_5N_3$, which is more stable and easier to prepare than other perfluoro azides. Perfluoro azides cannot be prepared as conventional azides by SN2 displacement of the leaving group because fluoride atoms shield the α-carbon atom.

The method developed in Dr. Beier's lab consists of deprotonation of **77** by *n*-BuLi, which generates **78**. The reaction is quenched with N_3^+ electrophilic reagent (tosyl azide). The resulting **79** is co-distilled with THF and condensed in cryotrap.
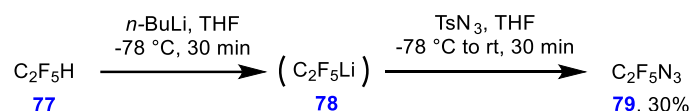
Scheme 7. Preparation of $C_2F_5N_3$ as developed by Dr. Beier's group and published by Dr. Blastik et al.[220]

Tetrahydrofuran solution of **79** was stored in a tightly closed screw-cap vial under an inert atmosphere of argon gas, and we did not observe any concentration decline after 5-day storage in the fridge. Moreover, Dr. Blastik[220] noted that the THF solution of **79** was thermally stable (no sign of decomposition at 150 °C after 80 minutes in a sealed tube). The concentration of $C_2F_5N_3$ was determined by ^{19}F NMR with PhCF$_3$ as the internal standard prior to the click reaction.
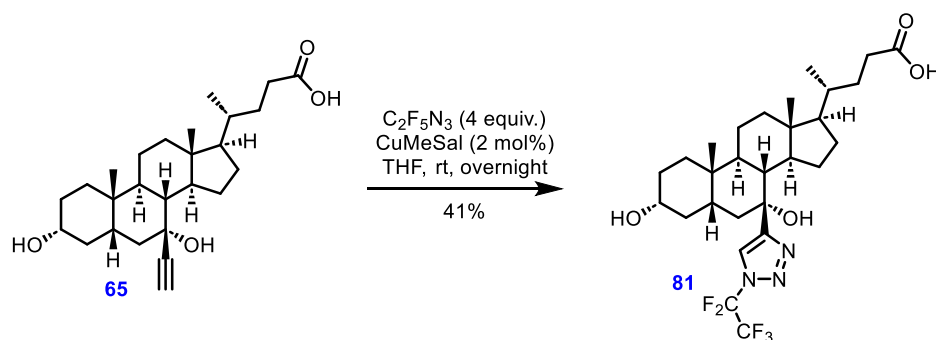
Scheme 8. Copper(I)-catalyzed azide-alkyne cycloaddition (CuAAC).

Preparation of C6 Substituted Bile Acids

Ethyl substituent was introduced in position C6 according to D'Amore et al.[221] The sequence starts with 7-oxo-lithocholic acid's methyl ester (59) that is converted to a silyl enol ether (82). The resulting silyl enol ether acts as a nucleophile in a Mukaiyama aldol condensation, producing aldol and eventually an enone. Compound 86 was prepared with Grignard reagent. Starting material 85 was prepared from 59 in 4 steps.
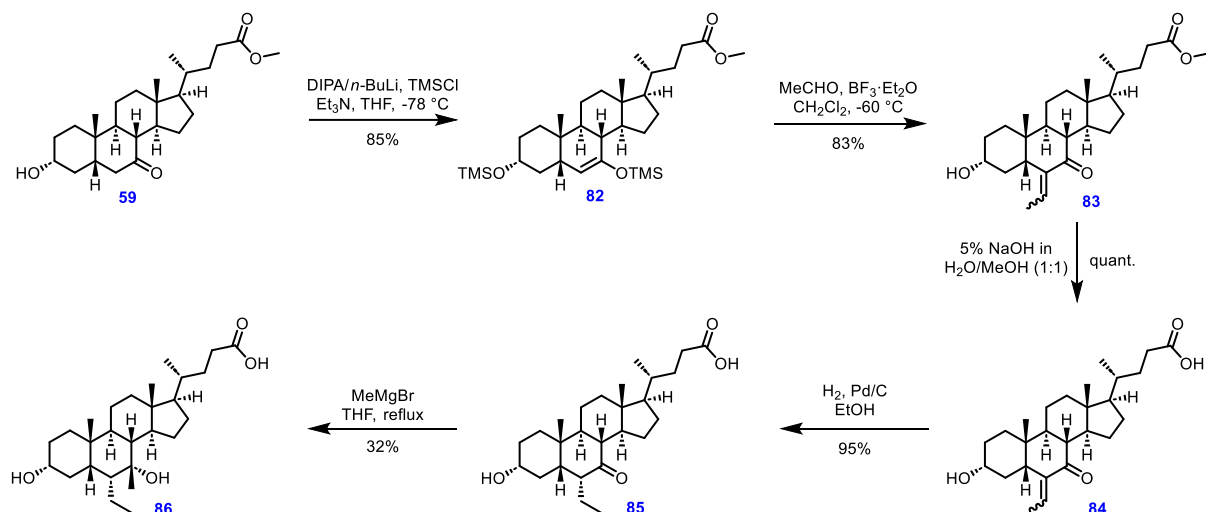
Scheme 9. Preparation of 86 from 59 by 5-step sequence. The first three reactions were inspired by D'Amore et al.[221] and were already optimized in our lab prior to this work. Their stereochemical, mechanistic, and optimization aspects are discussed elsewhere.[222]

BIOLOGICAL EVALUATION

Assays were performed in collaboration with the Faculty of Pharmacy in Hradec Králové, Charles University, in the group of Prof. Petr Pávek by Dr. Alžběta Štefela, as described.[223]

To assess the combined effect on FXR and TGR5, we employed luciferase gene reporter assays using human hepatocyte-derived HepG2 cells. We evaluated a total of 14 compounds for their ability to activate both FXR and TGR5. The results of these assays, along with the structures of all synthesized compounds, are summarized in **Figure 26** and **Figure 27**, respectively.
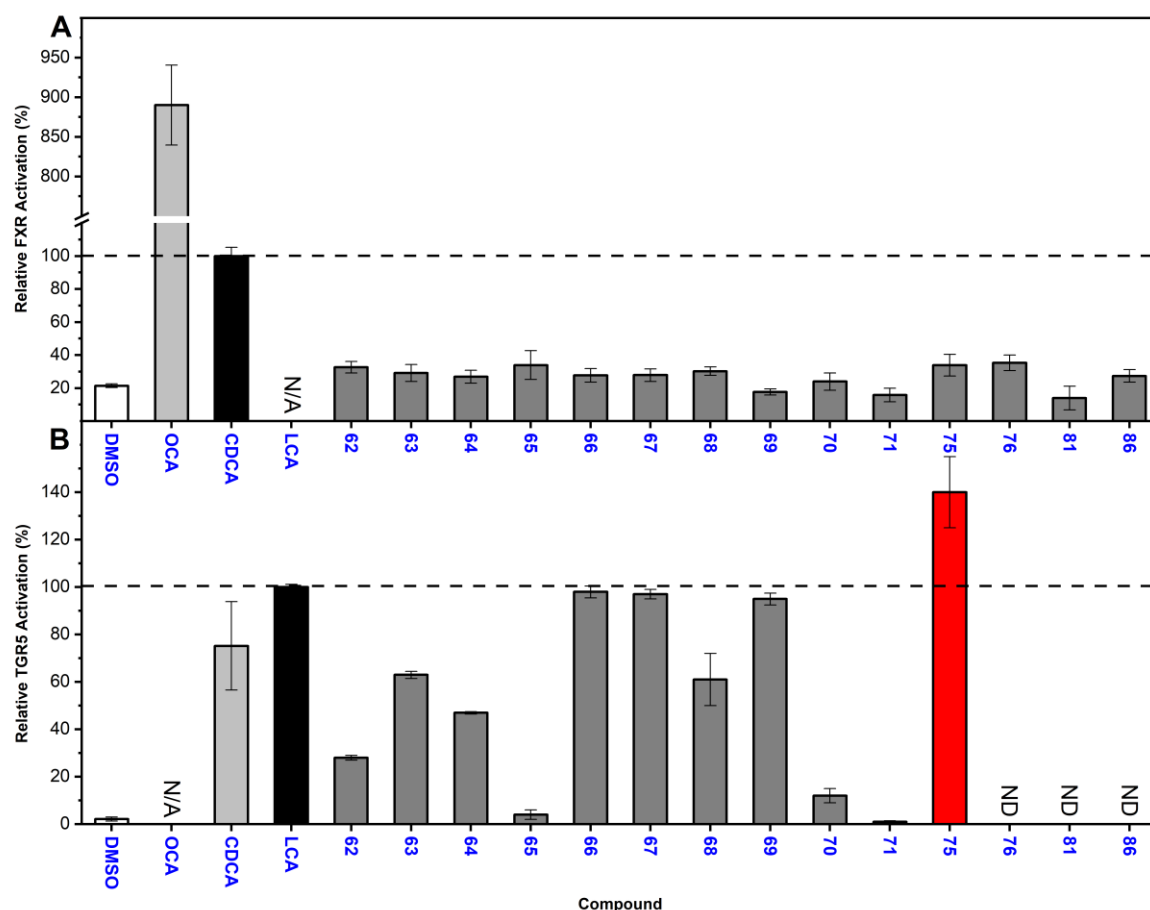
Figure 26. A: Interaction of C7-modified CDCA derivatives with human FXR in luciferase reporter gene assay. HepG2 cells were co-transfected with the luciferase FXRE-luc construct and with expression vectors. Then, the cells were treated with tested compounds at 10 μM concentration for 24 hours. Data were normalized to Renilla luciferase activity and are expressed relative to the activity of 10 μM CDCA (set as 100% activation). **B:** Effects of C7-modified CDCA derivatives on the human TGR5. HepG2 cells were co-transfected with a CRE containing luciferase reporter plasmid and a TGR5 expression vector. Cells were treated with tested compounds at 10 μM concentration for 5 hours. The efficacy of tested compounds to activate CRE-luc was compared to the activity of 10 μM LCA (set as 100% activation). All values are presented as the means ± SD of three independent experiments performed in biological triplicates (n = 3). Vehicle (0.1% DMSO) was used as a solvent in all samples, including control samples.

Compound	62	63	64	65	66	67	68	69	70	71	76	81
R												
	methyl	ethyl	vinyl	ethynyl	propyl	allyl	isopropyl	cyclopropyl	pent-4-en	nonyl	phenylethynyl	*
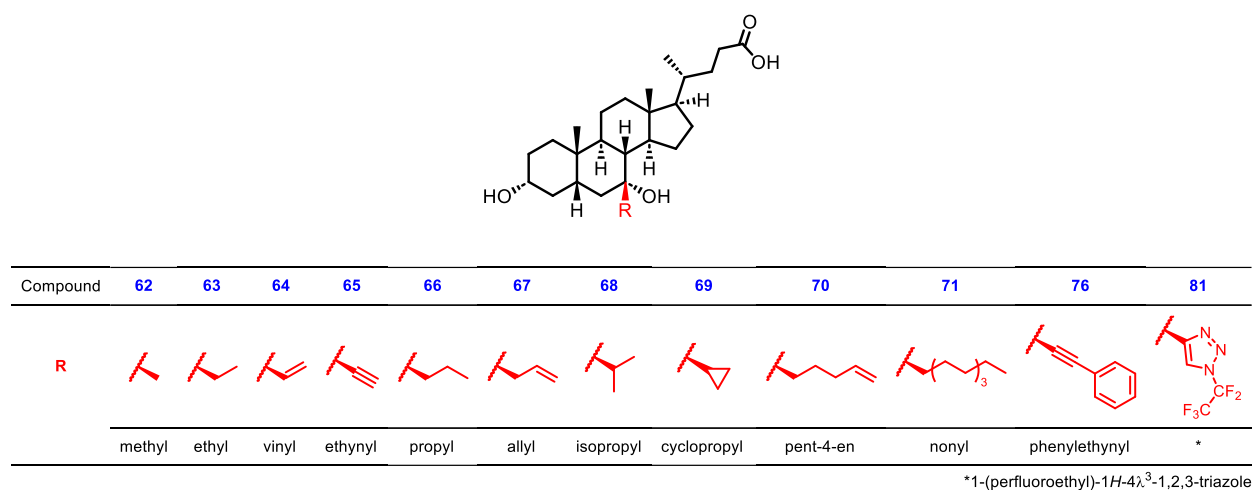
*1-(perfluoroethyl)-1H-4λ^3-1,2,3-triazole
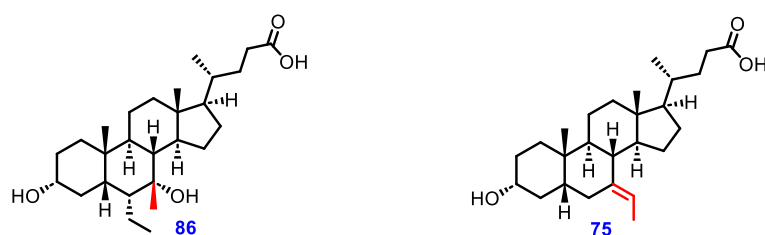
Figure 27. Compounds generated in this study.

Structure-Activity Relationship for FXR

Our results showed that all derivatives lost the ability to activate FXR at a concentration of 10 µM (**Figure 26**, **A**). Moreover, the introduction of cyclopropyl (**69**) and nonyl (**71**) moieties resulted in significant inhibition of the basal activation of FXR.[§]

This prompted us to investigate compounds with antagonistic activity. To achieve this, we treated HepG2 cells with known FXR agonists, the semisynthetic bile acid OCA (1 µM), the nonsteroidal ligand GW4064 (1 µM), and the endogenous bile acid CDCA (20 µM), together with the tested compounds. Our results (**Figure 28**) showed antagonistic behavior. The FXR-antagonizing capacity was enhanced with a longer alkyl chain, with the propyl (**66**) derivative showing lower activity compared to the branched isopropyl (**68**) and cyclopropyl (**69**) analogs. However, substituents longer than C5 (**70**, **71**) impaired cell viability at higher concentrations. This effect was probably due to the increased compound lipophilicity. Other compounds showed no effect on cellular viability, with IC$_{50}$ values above 100 µM (for toxicity data, see *Appendix*).

[§]Only data for OCA are shown in this Thesis; the rest are published[229] as supplementary information.
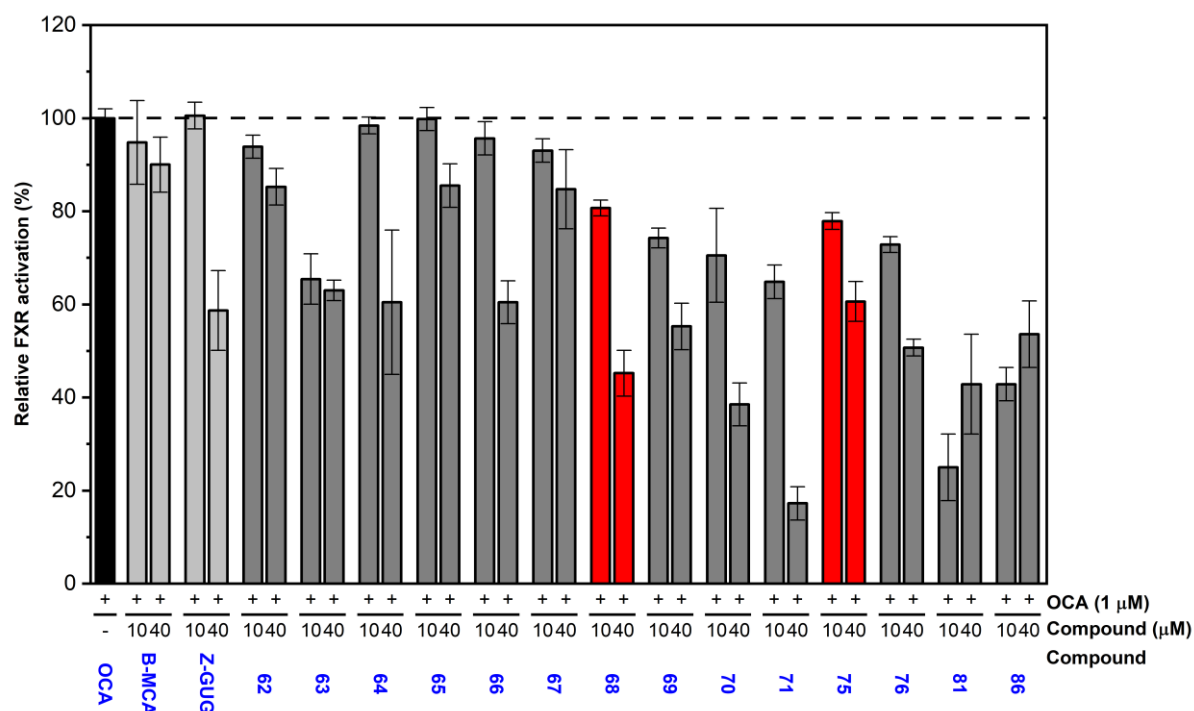
Figure 28. Interaction of target compounds with human FXR in luciferase reporter gene assays. HepG2 cells were transiently cotransfected with the luciferase FXRE-luc construct and with expression reporter vectors. Cells were treated with indicated concentrations for 24 hours with 1 μM OCA as an FXR agonist. Tβ-MCAand Z-GUG were used as known FXR antagonists. Data were normalized to Renilla luciferase activity and are expressed relative to 1 μM OCA (100%). *Toxic effect on cells.

Structure-Activity Relationship for TGR5

We tested compounds (10 μM) and compared their ability to activate a CRE-luc construct to LCA (10 μM), a known TGR5 agonist (**Figure 26**, **B**). Only ethylidene derivative (**75**) significantly increased CRE-luc activation. Propyl (**66**), allyl (**67**), and cyclopropyl (**69**) derivatives showed comparable activity to LCA. Other compounds did not activate the receptor significantly at 10 μM concentrations.

Figure 29 shows a hydrophilic pocket created by Phe-161, Leu-166, Val-170, Leu-244, Ser-247, and Val-248. Ligands with alkyl substituents at the C7 position may fit into the pocket more tightly. The C7 alkylation also affects the hydrogen bond formation with Ser-270. Ligands with two-carbon substituents on C7 only form one hydrogen bond interaction between the C3 hydroxyl and Tyr-240, as the Ser-270 hydroxyl is too far away. The C7 two-carbon substituent drags the ligand towards the hydrophobic pocket cleft for hydrophobic interactions. However, compounds with three-carbon substituents are wide enough to reach both the hydrophobic pocket cleft with its C7 substituent and the polar Tyr-240 and Ser-270 groups with its C3 hydroxyl. LCA, which lacks a C7 alkyl substituent, is not strongly attracted towards the hydrophobic pocket cleft. Instead, it prefers to form hydrogen bonds with both Tyr-240 and Ser-270.
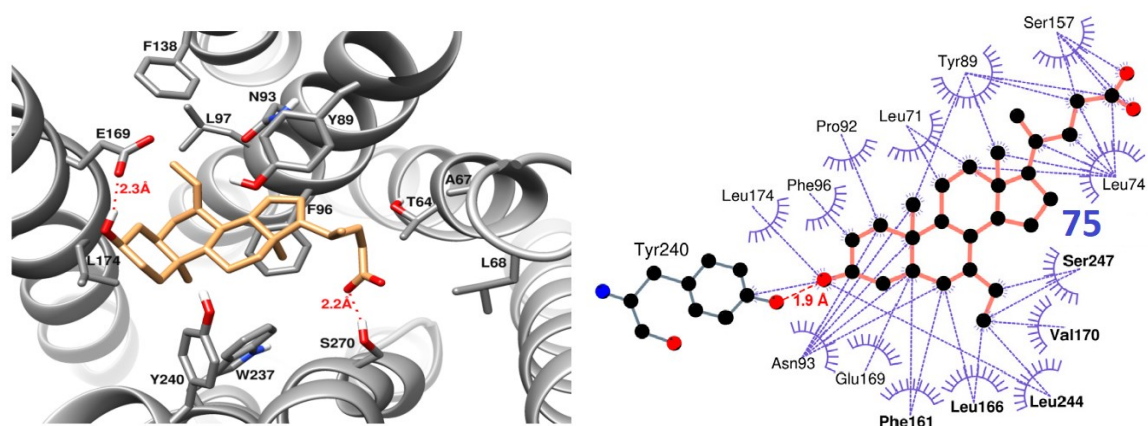
Figure 29. Interactions of **75** with the ligand binding pocket of TGR5. Left – detail of the TGR5 LBD with docked **75**. Docking was carried out using AutoDock Vina 1.1.2. software. Right – a 2D representation of molecular interactions between **75** and TGR5 LBD as generated in LigPlot+. The dashed line in red represents the hydrogen bond between the C3 substituent of **75** and Tyr-240. Only compound **75** showed clarity. Adopted and modified.[223]

Biological Profile of 75

To determine the specificity of **75**, we tested its interaction with a variety of nuclear receptors that interact with BAs or regulate metabolic processes: vitamin D receptor (VDR), pregnane X receptor (PXR), constitutive androstane receptor (CAR), peroxisome proliferator-activated receptors α, γ, β/δ (PPAR α, γ, β/δ), glucocorticoid receptor (GR), liver X receptor α, β (LXR α, β) and thyroid receptor (TRα). We found that **75** did not activate any of these nuclear receptors. Furthermore, **75** demonstrated superior TGR5 activation in dose-response, with the EC_{50} value being about two orders of magnitude lower than LCA activity (26 ± 6 nM vs. 1.54 ± 0.4 μM, respectively). For dose-response and receptor specificity data, see *Appendix*.

4.2   CONCLUSION

We introduced (*E*)-7-ethylidene-3α-hydroxy-5β-cholan-24-oic acid (**75**, **Figure 30**), which is the first bile acid derivative with a unique TGR5/FXR dual effect to the best of our knowledge. With the increasing prevalence of metabolic disorders in the Western population, the dual potency of **75** as an FXR antagonist and TGR5 agonist presents a promising synergistic pharmacological intervention and therapeutic application.
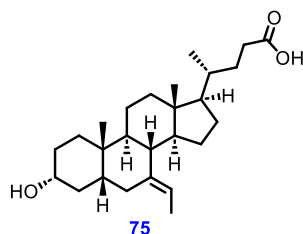
Figure 30. (*E*)-7-Ethylidene-3α-hydroxy-5β-cholan-24-oic acid, our most successful compound.

Outcomes

- Discovery of (*E*)-7-ethylidene-3α-hydroxy-5β-cholan-24-oic acid (**75**), first know steroid ligand with dual FXR/TGR5 mode of action.

- Publication in Frontiers in Pharmacology.[223]

5 OXIDATION OF AXIAL AND EQUATORIAL HYDROXY GROUPS

5.1 RESULTS AND DISCUSSION

One of the most significant reactions in a chemist's toolkit is the oxidation of alcohols to aldehydes or ketones. The different reactivities between axial and equatorial alcohols were already known in the 1950s.[224-228] Many oxidation methods have since been devised, including approaches with high selectivity. For example, chromium(VI) complexes cause quicker oxidation of the axial hydroxy groups due to the cleavage of the chromate ester intermediate, which releases a 1,3-diaxial strain in the rate-limiting step.[229] Another example is the preferential oxidation of hindered alcohols using trifluoroacetic acid anhydride-activated DMSO[230, 231] or the recent publication by Mikhael et al.[232] on selective equatorial alcohol oxidation using *N*-Ligated λ^3-Iodanes. While general reactivities and limits of most oxidants are well understood,[233, 234] to the best of our knowledge, there was no literature to compare typical oxidizing reagents for their preference to oxidize axial or equatorial alcohol.

For discussion purposes, we rated the "effectiveness" of chemical reactions by two parameters: the axial/equatorial selectivity factor (A/E_f, **eq. 1**) and the efficiency factor (Ef_f, **eq. 2**).

$$A/E_f = \frac{n_{aop}}{n_{eop}} \qquad \textbf{(eq. 1)}$$

$$Ef_f = \frac{n_{aop} + n_{eop}}{n_{sm} + n_{aop} + n_{eop} + n_i} \qquad \textbf{(eq. 2)}$$

Where n_{sm} is the amount of starting material, n_{aop} is the amount of axial oxidation product, n_{ep} is the amount of equatorial oxidation product, and n_i is the total amount of other observed products (usually dioxo compound). Amounts are determined experimentally after quenching, as either relative concentrations from HPLC analysis or gravimetrically after isolation. In the case of reactions where we did not observe any n_{aop} or n_{eop} we used our HPLC detection threshold of 1% in the calculation to avoid division by zero.

We examined a total of 16 most common oxidants used for the oxidation of secondary alcohols. First, we screened the oxidants with methyl chenodeoxycholate (**57**). In total, 93 reactions were performed. To better understand oxidant behavior, we used increasing amounts of oxidant from sub-stoichiometric (0.25 equiv.) to excess (3.0 equiv.), with exceptions in the case of Fétizon and Oppenauer oxidations as both of them are commonly done with an excess of the reagent.[234, 235] Please note that the amount of oxidizing reagent was calculated as molar equivalents, not the oxidation equivalents. For example, the chromium(VI)-type reagent can accept up to 3 electrons as it can be reduced to chromium(III). Thus, in this study, 1.0 equivalent chromium(VI) reagent can oxidize up to 1.5 equivalent of the substrate.

To speed throughput, the relative composition of most reaction mixtures was determined with the analytical HPLC against external calibration curves of authentic standards **57**–**60**. The standards were isolated from Jones oxidation and purified to virtual 100% HPLC purity and combustion CHN analysis error ≤ 0.2% (for analytics, see *Appendix*).

Selected representative reactions were repeated on a 2.5 mmol scale with different substrates: methyl chenodeoxycholate (**57**), *cis*- and *trans*-4-*tert*-butylcyclohexanol (**87** and **88**), methyl deoxycholate (**90**), and 5α-cholestane-2α,3α-diol (**94**). Products were separated and weighted. This study aimed to

validate the developed analytical HPLC method and demonstrate reaction repeatability, scalability, and robustness. The project map is graphically depicted below (**Figure 31**).

The reactions were carried out on a 0.5 mmol or 2.5 mmol scale, in 5 mL or 25 mL of solvent, respectively, to maintain the concentration of a substrate comparable (0.1 M). The remaining conditions (e.g., temperature, reaction time, etc.) were defined with respect to common practice.[234]
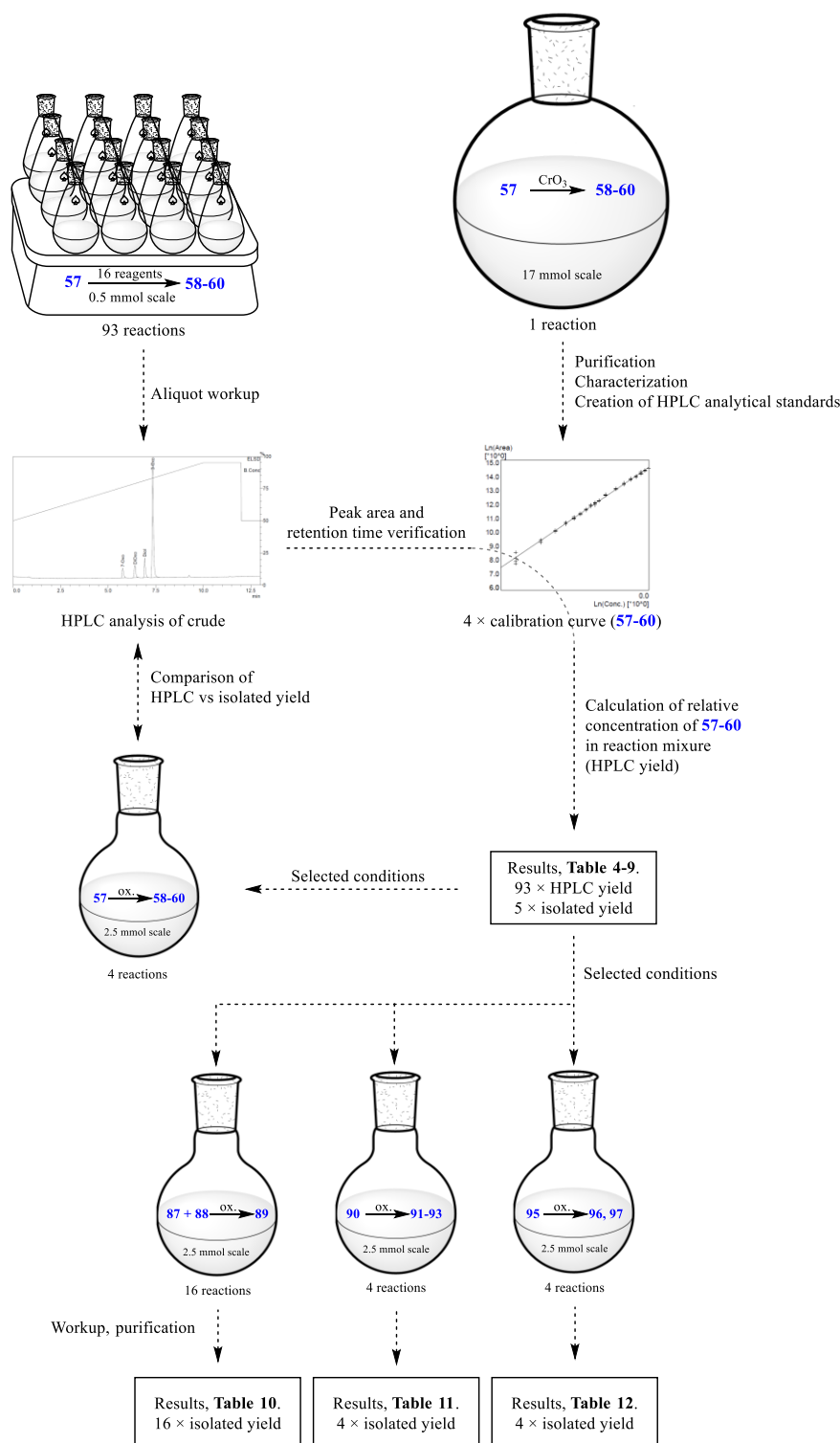
Figure 31. The project map. The main backbone was the oxidation of methyl chenodeoxycholate (**57**). Results were further evaluated on different substrates (**87**, **88**, **90**, and **94**). In total, 16 oxidants, 5 substrates, and 6 reaction variations were evaluated, totaling 122 reactions.

53
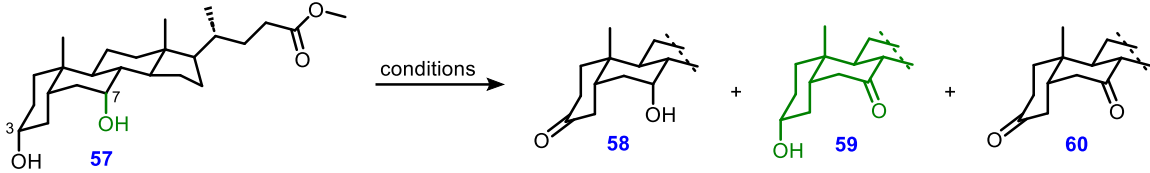
OXIDATION OF METHYL CHENODEOXYCHOLATE

Methyl chenodeoxycholate (**57**) was selected as the main substrate because it bears both axial (C7) and equatorial (C3) hydroxyl groups on its skeleton.

Chromium-Based Reagents (Table 4)

Chromium-based reagents are known to oxidize axial alcohols faster.[228] Indeed, we observed a clear preference for oxidation of the axial hydroxyl group in all three cases. For example, 0.75 equiv. of Jones reagent[236] provided the product of axial oxidation (**59**) in 56% yield and the product of the equatorial oxidation (**58**) in 9% yield (*entry 3*) or A/E_f = 6.2:1. This reaction was scaled up by a factor of 34, without loss of selectivity, and with isolated yields comparable to HPLC yields. Pyridinium dichromate (*entry 7–12*) also gave the best result in 0.75 equiv., where we achieved A/E_f = 10.3:1, E_{ff} = 0.65 (*entry 8*). Pyridinium chlorochromate (*entry 13–18*) gave the best results with 1.0 equiv. (*entry 16*), where we observed improved selectivity compared with the Jones reagent but lower yield.

Table 4. Chromium-based reagents.

Entry	Name reaction	Conditions	Yield (%)[b]				Effectiveness	
			57	58	59	60	A/E_f	E_{ff}
1		CrO$_3$ (0.25 equiv.)	56	17	21	6	1.2:1	0.38
2		CrO$_3$ (0.50 equiv.)	27	18	42	14	2.3:1	0.59
3		CrO$_3$ (0.75 equiv.)	2 (8)[c]	9 (6)[c]	56 (55)[c]	33 (25)[c]	6.2:1	0.65
4	Jones	CrO$_3$ (1.0 equiv.)	ND	ND	33	67	33:1	0.33
5		CrO$_3$ (2.0 equiv.)	ND	ND	ND	100	1:1	< 0.02
6		CrO$_3$ (3.0 equiv.)	ND	ND	ND	100	1:1	< 0.02
7		PDC (0.25 equiv.)	58	13	25	4	1.9:1	0.38
8		PDC (0.50 equiv.)	29	16	41	14	2.6:1	0.57
9	Corey–Schmidt	PDC (0.75 equiv.)	4	4	41	51	10.3:1	0.45
10		PDC (1.0 equiv.)	ND	ND	25	75	25:1	0.25
11		PDC (2.0 equiv.)	ND	ND	ND	100	1:1	< 0.02
12		PDC (3.0 equiv.)	ND	ND	ND	100	1:1	< 0.02
13		PCC (0.25 equiv.)	68	9	22	ND	2.4:1	0.31
14		PCC (0.50 equiv.)	45	12	38	5	3.2:1	0.50
15	Corey–Suggs	PCC (0.75 equiv.)	27	14	48	10	3.4:1	0.63
16		PCC (1.0 equiv.)	ND	4	44	52	11:1	0.48
17		PCC (2.0 equiv.)	ND	ND	19	81	19:1	0.20
18		PCC (3.0 equiv.)	ND	ND	ND	100	1:1	< 0.02

[a]Only limiting reagents for each reaction are listed. The rest of the reaction conditions were as follows. Jones: aq. H$_2$SO$_4$, acetone, 0 °C, 30 min. Corey–Schmidt: 3Å sieves, DCM, rt, 16 hours. Corey–Suggs: DCM, rt, 16 hours. [b]The ratio of products **57–60** was determined by HPLC with ELSD detection and represents the relative composition of **57–60** in the reaction mixture. All reactions were performed on a 0.5 mmol scale unless mentioned otherwise. [c]Isolated yield from 17 mmol scale reaction is reported in parentheses. In the case of reactions where no product was detected (ND), we calculated as if 1% was present. Green – most effective conditions for axial oxidation.

Dimethyl Sulfoxide-Based Reagents (Table 5)

The most popular Swern oxidation showed only a slight preference for equatorial alcohol A/E_f = 10.3:1, E_{ff} = 0.65 (*entry 3*), when the limiting reagent was used in the sub-stochiometric amount 0.75 equiv. This oxidation is nevertheless very mild and with 2 equiv. of (COCl)$_2$, proceeded smoothly to complete oxidation of both hydroxy groups to yield dioxo derivative **60** quantitatively (*entry 5*). The steric selectivity of Omura–Sharma–Swern modification was discussed in the original publication by Huang et al.[230] Authors defined the TFAA/DMSO oxidations as superior for oxidation of sterically hindered alcohols. In particular, the more hindered the hydroxyl group is, the higher yield of carbonyl can be obtained.[230] However, under the comparable conditions (*entry 7–12*), we didn't observe any selectivity towards the more hindered axial C7 hydroxyl group over the more accessible

equatorial C3 hydroxyl group (*entry 7–12*). Moreover, the Omura–Sharma–Swern was most unpredictable, with A/E_f = 1.2:1 (*entry 8 and 9*) to opposite selectivity with A/E_f = 1:2.5 (*entry 11*). The selectivity of sulfur trioxide pyridine complex (SO$_3$·pyridine) was observed and noted in the original publication[237], Parikh et al. wrote:

> *"While 11α-hydroxyprogesterone was oxidized to 11-ketoprogesterone (isolated in 70% yield), the corresponding 11β epimer was virtually inert."*

This matches our observations. In neither case, we have observed **59**, the product of axial oxidation. Instead, we observed a 70% yield of **58,** as well as a 30% yield of **60**, the product of oxidation of both axial and equatorial alcohols (*entry 18*).

Table 5. Dimethyl sulfoxide-based reagents.
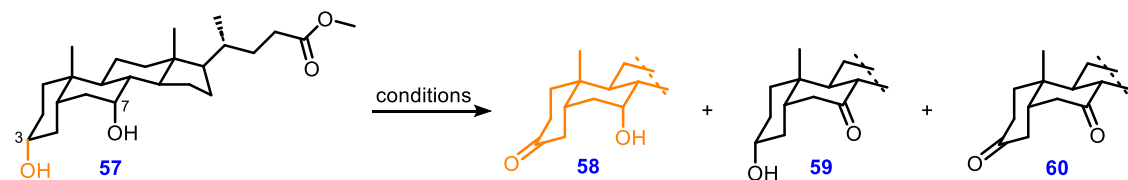
Entry	Name reaction	Conditions[a]	Yield (%)[b]				Effectiveness	
			57	**58**	**59**	**60**	*A/E_f*	*E_{ff}*
1		(COCl)$_2$ (0.25 equiv.), DMSO (0.50 equiv.)	73	18	9	ND	1:2	0.27
2		(COCl)$_2$ (0.50 equiv.), DMSO (1.0 equiv.)	28	20	48	4	2.4:1	0.68
3	Swern	(COCl)$_2$ (0.75 equiv.), DMSO (1.5 equiv.)	12	17	56	16	3.3:1	0.72
4		(COCl)$_2$ (1.0 equiv.), DMSO (2.0 equiv.)	5	14	37	44	2.6:1	0.51
5		(COCl)$_2$ (2.0 equiv.), DMSO (4.0 equiv.)	ND	ND	ND	100	1:1	< 0.02
6		(COCl)$_2$ (3.0 equiv.), DMSO (6.0 equiv.)	ND	ND	ND	100	1:1	< 0.02
7		TFAA (0.25 equiv.), DMSO (0.5 equiv.)	85	8	7	ND	1:1.1	0.15
8		TFAA (0.50 equiv.), DMSO (1.0 equiv.)	71	11	12	7	1.1:1	0.23
9	Omura–Sharma–	TFAA (0.75 equiv.), DMSO (1.5 equiv.)	61	12	14	12	1.2:1	0.26
10	Swern	TFAA (1.0 equiv.), DMSO (2.0 equiv.)	53	17	20	9	1.2:1	0.37
11		TFAA (2.0 equiv.), DMSO (4.0 equiv.)	11	12	8	69	1:1.5	0.20
12		TFAA (3.0 equiv.), DMSO (6.0 equiv.)	ND	7	5	87	1:1.4	0.12
13		SO$_3$·pyridine (0.25 equiv.)	100	ND	ND	ND	1:1	0.02
14		SO$_3$·pyridine (0.50 equiv.)	91	9	ND	ND	1:9	0.10
15	Parikh–Doering	SO$_3$·pyridine (0.75 equiv.)	87	13	ND	ND	1:13	0.14
16		SO$_3$·pyridine (1.0 equiv.)	73	27	ND	ND	1:27	0.27
17		SO$_3$·pyridine (2.0 equiv.)	32	68	ND	ND	1:68	0.68
18		SO$_3$·pyridine (3.0 equiv.)	ND	70	ND	30	1:70	0.70

[a]Only limiting reagents for each reaction are listed. The rest of the reaction conditions were as follows. Swern: Et$_3$N (7 equiv.), DCM, -60 °C to rt, 16 hours. Omura–Sharma–Swern: Et$_3$N (7 equiv.), DCM, -60 °C to rt, overnight. Parikh–Doering: Et$_3$N (7 equiv.), DCM/DMSO (1:1), 0 °C, overnight. [b]The ratio of products **57–60** was determined by HPLC against authentic standards and represents the relative composition of **57–60** in the reaction mixture. All reactions were performed on a 0.5 mmol scale. In the case of reactions where no product was detected (ND), we calculated as if 1% was present. Green – most effective conditions for axial oxidation, orange – most effective conditions for equatorial oxidation.

Nitroxide Radical-Based Reagents (Table 6)

Oxidants based on nitroxide radicals are known to be sensitive toward steric factors. For example, 2,2,6,6-tetramethylpiperidin-1-yl)oxyl (TEMPO) can be used to oxidize primary alcohols in the presence of secondary ones.[238] In our study, TEMPO oxidations were highly selective towards the less hindered equatorial hydroxyl. For example, the Anelli protocol[239] (*entry 5*) using TEMPO (2 mol%) and NaOCl (2 equivalents)/NaBr (10 mol%) as the re-oxidant afforded 91% of compound **58** and only 9% of the overoxidation product **60**. Next, the Piancatelli–Margarita protocol[240] (*entry 12*) employing bis(acetoxy)iodobenzene (BAIB, 3 equivalents) as re-oxidant afforded exclusively product **58**. To confirm this remarkable selectivity, we scaled-up the Piancatelli–Margarita protocol (from 0.2 g/0.5 mmol substrate to 1 g/2.5 mmol), and after the column chromatography, **58** was isolated in an almost quantitative yield (95%). We also examined a recent method developed in the Jahn group.[241] Authors used TEMPO in conjunction with boron trifluoride-ether complex (BF$_3$·Et$_2$O) as pre-catalysts and *tert*-butyl nitrite (*t*BuONO) as a stoichiometric oxidant (*entry 13–18*). In our hands, we unfortunately failed to achieve the full conversion even after the extension of reaction time up to 12 hours. A mixture of starting material **57** and desired product **58** was obtained in all cases (best case: *entry 18, A/E$_f$ = 1:69, Ef$_f$ = 0.69*).

Table 6. Nitroxide radical-based reagents.

Entry	Name reaction	Conditions[a]	Yield (%)[b]				Effectiveness	
			57	**58**	**59**	**60**	*A/E$_f$*	*Ef$_f$*
1		NaOCl (0.25 equiv.)	93	7	ND	ND	1:7	0.08
2		NaOCl (0.50 equiv.)	76	18	6	ND	1:3	0.24
3	Anelli	NaOCl (0.75 equiv.)	67	29	5	ND	1:5.8	0.33
4		NaOCl (1.0 equiv.)	36	54	4	5	1:13.5	0.59
5		NaOCl (2.0 equiv.)	ND (0)[c]	91 (82)[c]	ND (0)[c]	9 (12)[c]	1:91	0.90
6		NaOCl (3.0 equiv.)	ND	85	ND	15	1:85	0.84
7		BAIB (0.25 equiv.)	88	12	ND	ND	1:12	0.13
8		BAIB (0.50 equiv.)	64	36	ND	ND	1:36	0.36
9	Piancatelli–Margarita	BAIB (0.75 equiv.)	51	49	ND	ND	1:49	0.49
10		BAIB (1.0 equiv.)	36	64	ND	ND	1:64	0.64
11		BAIB (2.0 equiv.)	10	90	ND	ND	1:90	0.89
12		BAIB (3.0 equiv.)	ND (0)[c]	100 (95)[c]	ND (0)[c]	ND (0)[c]	1:100	0.98
13		tBuONO (0.25 equiv.)	94	6	ND	ND	1:6	0.07
14		tBuONO (0.50 equiv.)	84	16	ND	ND	1:16	0.17
15	Jahn–Holan[d]	tBuONO (0.75 equiv.)	67	33	ND	ND	1:33	0.33
16		tBuONO (1.0 equiv.)	52	48	ND	ND	1:48	0.48
17		tBuONO (2.0 equiv.)	42	50	8	ND	1:6.3	0.57
18		tBuONO (3.0 equiv.)	31	69	ND	ND	1:69	0.69

[a]Only limiting reagents for each reaction are listed. The rest of the reaction conditions were as follows. Anelli: TEMPO (2 mol%), NaBr (10 mol%), DCM/H$_2$O, (4:1), 0 °C to rt, 4 hours. Piancatelli–Margarita: TEMPO (10 mol%), DCM, 0 °C to rt, 4 hours. Jahn–Holan: TEMPO (5 + 5 mol%), BF$_3$·Et$_2$O (5 mol%), DCM, reflux, 3 hours. [b]The ratio of products **57**–**60** was determined by HPLC with ELSD detection and represents the relative composition of **57**–**60** in the reaction mixture. All reactions were performed on a 0.5 mmol scale unless mentioned otherwise. [c]Isolated yield from 2.5 mmol scale reaction is reported in parentheses. [d]All Jahn–Holan oxidations were also analyzed after 12 hours. No improvement in the conversion was identified. In the case of reactions where no product was detected (ND), we calculated as if 1% was present. Orange – most effective conditions for equatorial oxidation.

Hypervalent Iodine-Based Reagents (Table 7)

o-Iodoxybenzoic acid (IBX)[242] and Dess–Martin periodinane (DMP)[243] both showed remarkable selectivity towards oxidation of the axial hydroxy group. The IBX was the most selective axial hydroxyl oxidant in our study, as we haven't observed any **58**, the product of equatorial oxidation in any case (best case: *entry 5*, A/E_f = 58:1, Ef_f = 0.61). However, no reaction with IBX proceeded to full conversion, even when an excess of oxidant was used (3 equiv.). We believe it is due to limited IBX solubility dichloromethane.[244] This limitation was addressed by Dr. Dess and Dr. Martin, which led to the discovery of DMP.[243] Dess–Martin periodinane was superior for oxidation of axial alcohols (best case: *entry 10*, A/E_f = 14.6:1, Ef_f = 0.78). To confirm this selectivity, the Dess–Martin protocol was scaled-up (from 0.2 g/0.5 mmol substrate to 1 g/2.5 mmol), and after column chromatography, **58** and **59** were isolated in an 8% and 73% yield, respectively.

Table 7. Hypervalent iodine-based reagents.
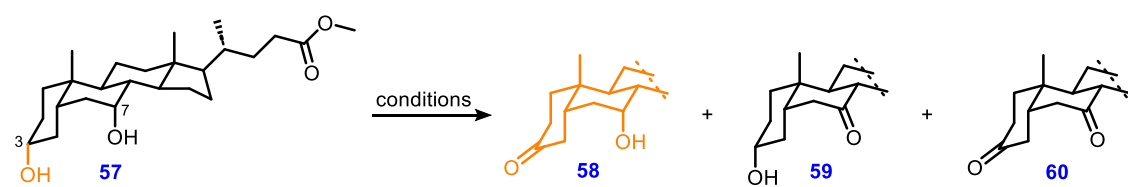
Entry	Name reaction	Conditions[a]	Yield (%)[b]				Effectiveness	
			57	**58**	**59**	**60**	A/E_f	Ef_f
1		IBX (0.25 equiv.)	89	ND	11	ND	11:1	0.12
2		IBX (0.50 equiv.)	77	ND	23	ND	23:1	0.24
3	*o*-Iodoxybenzoic acid	IBX (0.75 equiv.)	66	ND	34	ND	34:1	0.34
4		IBX (1.0 equiv.)	51	ND	49	ND	49:1	0.49
5		IBX (2.0 equiv.)	37	ND	58	ND	58:1	0.61
6		IBX (3.0 equiv.)	37	ND	54	3	54:1	0.58
7		DMP (0.25 equiv.)	75	ND	25	ND	25:1	0.25
8		DMP (0.50 equiv.)	50	4	44	2	11:1	0.48
9	Dess–Martin	DMP (0.75 equiv.)	20	4	69	6	17.3:1	0.74
10		DMP (1.0 equiv.)	12 (8)[c]	5 (8)[c]	73 (73)[c]	10 (7)[c]	14.6:1	0.78
11		DMP (2.0 equiv.)	ND	ND	20	80	20:1	0.21
12		DMP (3.0 equiv.)	ND	ND	ND	100	1:1	< 0.02

[a]Only limiting reagents for each reaction are listed. The rest of the reaction conditions were as follows. *o*-Iodoxybenzoic acid: DCM, rt, 24 hours. Dess–Martin: DCM, rt, 24 hours. [b]The ratio of products **57**–**60** was determined by HPLC with ELSD detection and represents the relative composition of 1-4 in the reaction mixture. All reactions were performed on a 0.5 mmol scale unless mentioned otherwise. [c]Isolated yield from 2.5 mmol scale reaction is reported in parentheses. In the case of reactions where no product was detected (ND), we calculated as if 1% was present. Green – most effective conditions for axial oxidation.

Ruthenium-Based Reagents (Table 8)

Ruthenium tetroxide is a very strong oxidant able to oxidize various functional groups.[245] It is so reactive that it reacts violently with the ignitable organic solvents.[246] Therefore, our solvent selection was limited to biphasic CCl_4/H_2O or $CHCl_3/H_2O$. First, we have used the in situ generated RuO_4 from the $NaIO_4/RuO_2$ mixture (*entry 1–6*). This energetic oxidant resulted in low selectivity with a weak preference for oxidation of equatorial alcohol (best case: *entry 3*, A/E_f = 1:3.3, Ef_f = 0.64). The milder conditions of Ley oxidation (tetrapropylammonium perruthenate/*N*-methyl morpholine-*N*-oxide) gave an improved ratio of compounds **58** and **59** as demonstrated in *entry 12*, A/E_f = 1:6.4, Ef_f = 0.59.

Table 8. Ruthenium-based reagents.

Entry	Name reaction	Conditions [a]	Yield (%)[b]				Effectiveness	
			57	**58**	**59**	**60**	A/E_f	Ef_f
1		NaIO$_4$ (0.25 equiv.)	60	26	10	3	1:2.6	0.36
2		NaIO$_4$ (0.50 equiv.)	49	30	14	7	1:2.1	0.44
3	Catalytic RuO$_4$	NaIO$_4$ (0.75 equiv.)	18	49	15	18	1:3.3	0.64
4		NaIO$_4$ (1.0 equiv.)	9	43	18	31	1:2.4	0.60
5		NaIO$_4$ (2.0 equiv.)	ND	37	ND	63	1:37	0.37
6		NaIO$_4$ (3.0 equiv.)	ND	44	5	51	1:8.8	0.49
7		NMO (0.25 equiv.)	76	15	6	3	1:2.5	0.21
8		NMO (0.50 equiv.)	67	20	7	6	1:2.9	0.27
9	Ley	NMO (0.75 equiv.)	58	27	10	6	1:2.7	0.37
10		NMO (1.0 equiv.)	51	34	8	7	1:4.3	0.42
11		NMO (2.0 equiv.)	26	48	8	18	1:6	0.56
12		NMO (3.0 equiv.)	24	51	8	17	1:6.4	0.59

[a]Only limiting reagents for each reaction are listed. The rest of the reaction conditions were as follows. Catalytic RuO$_4$: RuO$_2$·H$_2$O (5 mol %), CCl$_4$/H$_2$O (1:1), rt, overnight. Ley: TPAP (5 mol %), 3Å sieves, DCM, rt, overnight. [b]The ratio of products **57-60** was determined by HPLC with ELSD detection and represents the relative composition of **57-60** in the reaction mixture. All reactions were performed on a 0.5 mmol scale. In the case of reactions where no product was detected (ND), we calculated as if 1% was present. Orange – most effective conditions for equatorial oxidation.

Other Reagents (Table 9)

First, the conditions of Fétizon oxidation were tested (*entry 1–3*). As the reaction of silver carbonate (Ag$_2$CO$_3$) proceeds on the surface of Celite, both the reacting hydroxy group and hydrogen must be accessible from the surface.[235] Consequently, in our study, the equatorial hydroxy group was supposed to be more reactive. Indeed, Fétizon oxidation (*entry 2*) was very selective, providing 72% of equatorial oxidation product – **58**. However, only 72% conversion was achieved, even though 5 equiv. of Ag$_2$CO$_3$/Celite were used, and the reaction time was extended up to 48 hours of reflux in benzene. Next, the conditions of Oppenauer (*entry 4–9*) oxidation were tested. The hydride transfer reactions with aluminum isopropoxide Al(OiPr)$_3$ catalysis is a very mild method, utilizing cyclohexanone or *N*-methyl-4-piperidinone as a hydride acceptor. Both cyclohexanone and *N*-methyl-4-piperidinone possess similar oxidation potential, while the latter is easier to remove by washing with aqueous acid.[247] The protocol utilizing 25 equiv. of cyclohexanone and 1 equiv. of Al(OiPr)$_3$ (*entry 5*) afforded preferential oxidation of the equatorial hydroxyl group, yielding 82% of **58**. Similarly, the selective oxidation of the equatorial hydroxyl group was achieved with *N*-methyl-4-piperidinone (*entry 7–9*). However, the HPLC chromatograms demonstrated peak broadening, including tailing and shoulder peaks, suggesting the formation of side products that limited the interpretation of the spectra. Finally, the conditions of Steven's oxidation were tested (*entry 10–15*). Sodium hypochlorite (NaOCl) for the oxidation of steroids is a convenient method for large-scale synthesis. Indeed, this method is used for industrial production[248, 249] of 7-ketolithocholic acid. Protocol with 1 equiv. of NaOCl (*entry 13*), gave 75% of **59**. To confirm this result, the reaction was scaled-up (from 0.2 g/0.5 mmol substrate to 1 g/2.5 mmol) and after the column chromatography **58** and **59** and were isolated in a 3% and 70% yield, respectively.

Table 9. Other reagents.

Entry	Name reaction	Conditions [a]	Yield (%)[b]				Effectiveness	
			57	58	59	60	A/E$_f$	Ef$_f$
1		Ag$_2$CO$_3$/celite (1 equiv.)	58	42	ND	ND	1:42	0.42
2	Fétizon	Ag$_2$CO$_3$/celite (5 equiv.)	28	72	ND	ND	1:72	0.72
3		Ag$_2$CO$_3$/celite (10 equiv.)	47	53	ND	ND	1:53	0.53
4		Cyclohexanone (5 equiv.)	32	38	16	14	1:2.4	0.54
5		Cyclohexanone (25 equiv.)	6	82	3	9	1:27.3	0.85
6	Oppenauer[c]	Cyclohexanone (50 equiv.)	5	86	5	4	1:17.2	0.91
7		*N*-Methyl-4-piperidinone (5 equiv.)	23	62	7	8	1:8.9	0.69
8		*N*-Methyl-4-piperidinone (50 equiv.)	69	31	ND	ND	1:31	0.31
9		*N*-Methyl-4-piperidinone (100 equiv.)	78	22	ND	ND	1:22	0.23
10		NaOCl (0.25 equiv.)	79	ND	21	ND	21:1	0.22
11		NaOCl (0.50 equiv.)	58	ND	42	ND	42:1	0.42
12	Steven's	NaOCl (0.75 equiv.)	36	5	60	ND	12:1	0.64
13		NaOCl (1.0 equiv.)	19 (15)[d]	6 (3)[d]	75 (70)[d]	ND (2)[d]	12.5:1	0.81
14		NaOCl (2.0 equiv.)	ND	ND	48	52	48:1	0.48
15		NaOCl (3.0 equiv.)	ND	ND	ND	100	1:1	< 0.02

[a]Only limiting reagents for each reaction are listed. The rest of the reaction conditions were as follows. Fétizon: benzene, reflux, 48 hours. Oppenauer: Al(OiPr)$_3$ (1 equiv.), toluene, reflux, 16 hours. Steven's: AcOH, rt, 6 hours. [b]The ratio of products **57–60** was determined by HPLC with ELSD detection and represents the relative composition of **57–60** in the reaction mixture. All reactions were performed on a 0.5 mmol scale unless mentioned otherwise. [c]All Oppenauer reactions with cyclohexanone were also analyzed after 48 hours. Peak broadening in HPLC chromatograms, including tailing and shoulder peaks, suggests the formation of side products, limiting the chromatograms' interpretation. [d]Isolated yield from 2.5 mmol scale reaction is reported in parentheses. In the case of reactions where no product was detected (ND), we calculated as if 1% was present. Green – most effective conditions for axial oxidation, orange – most effective conditions for equatorial oxidation.

OXIDATION OF 4-*TERT*-BUTYLCYCLOHEXANOL

The selectivity could be significantly affected by the steric influence of the adjacent six-membered rings of the steroidal skeleton. Therefore, we have subsequently evaluated the selectivity of oxidizing reagents on a 1:1 mixture of *cis-* and *trans*-4-*tert*-butylcyclohexanol. First, the commercially available *tert*-butylcyclohexanol (mixture *cis/trans*, 1:2.4) was subjected to column chromatography on silica gel, followed by crystallization of each isomer. Next, a 1:1 mixture of **87** and **88** was prepared, and their ratio was validated by the integration of proton peaks on C1 carbon in the ^{1}H NMR spectra.
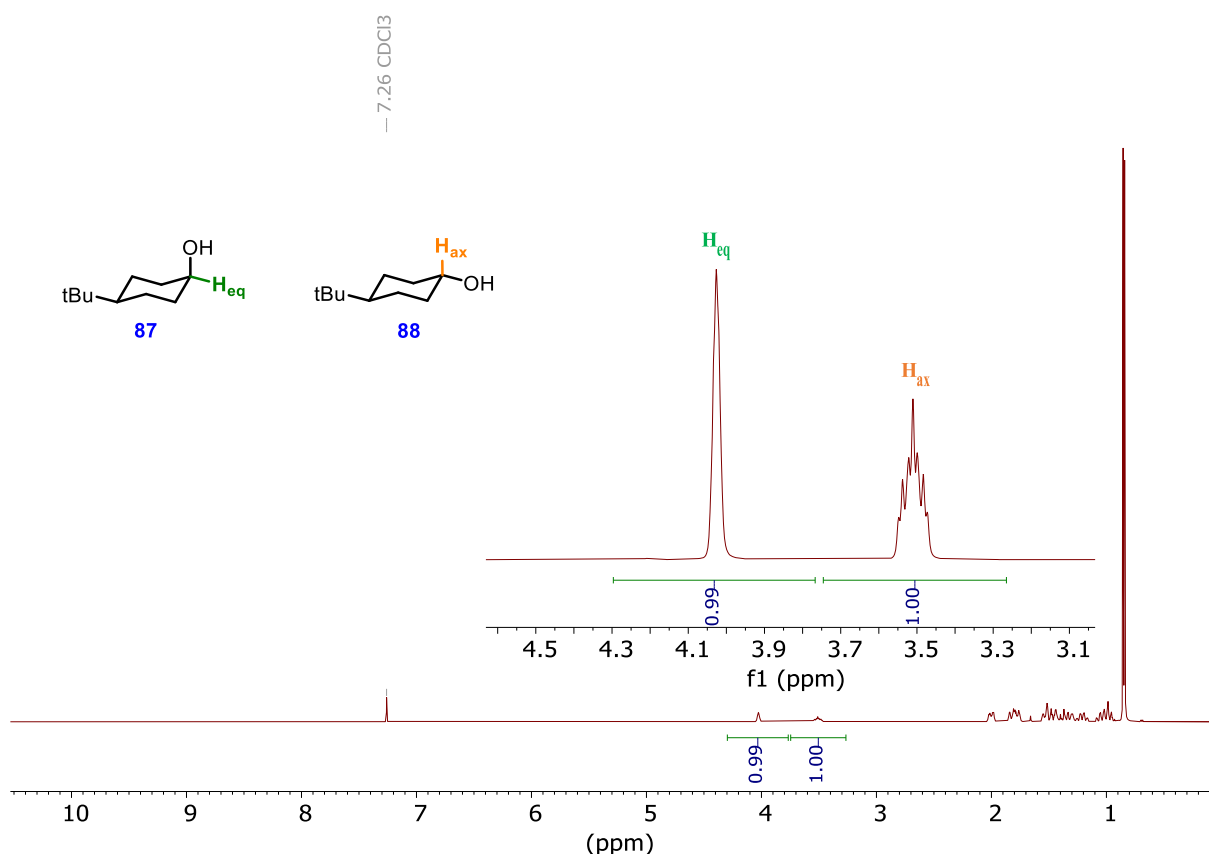
Figure 32. ^{1}H NMR spectra of 1:1 mixture of **87** and **88**.

The prepared mixture of **87** and **88** (1:1) was oxidized under various conditions. It is crucial to prevent the reaction from reaching full conversion. This imperative arises from the fact that both **87** and **88**, upon oxidation, yield the identical product, compound **89**. We achieved that by using a sub-stoichiometric amount of the oxidizing reagent, except for Oppenauer and Fétizon oxidations that require an excess of the reagent. Then, the recovered unreacted **87**, **88** and yield of prepared **89** describe the reagent preference for axial or equatorial alcohol. (**Table 10**). Because **87** and **88** lack chromophores and are too volatile to be detected by ELSD, we used isolated yields in all cases.

Table 10. Selectivity of common oxidizing reagents on oxidation of *cis*- and *trans*-4-*tert*-butylcyclohexanol

mixture cis/trans, 1:1

Entry	Name reaction	Conditions[a]	Yield (%)[b]			Effectiveness	
			87	**88**	**89**	A/E_f[c]	Ef_f
Chromium-based reagents							
1	Jones	CrO_3 (0.5 equiv.), aq. H_2SO_4, acetone, 0 °C, 30 min	4	32	62	2.6:1	0.65
2	Corey–Schmidt	PDC (0.5 equiv.), 3Å sieves, DCM, rt, 16 h	11	17	62	1.2:1	0.80
3	Corey–Suggs	PCC (0.5 equiv.), DCM, rt, 16 h	16	31	46	1.8:1	0.57
Dimethyl sulfoxide-based reagents							
4	Swern	$(COCl)_2$ (0.5 equiv.), DMSO (1.0 equiv.), Et_3N (7 equiv.), DCM, -60 °C to rt, 16 h	32	36	27	1.3:1	0.34
5	Omura–Sharma–Swern	TFAA (0.5 equiv.), DMSO (1.0 equiv.), Et_3N (7 equiv.), DCM, -60 °C to rt, overnight	34	36	26	1.1:1	0.31
6a	Parikh–Doering	SO_3·pyridine (0.5 equiv.), Et_3N (3.5 equiv.), DCM/DMSO (1:1), 0 °C to rt, 8 h	45	36	13	n/a[d]	
6b	Parikh–Doering	SO_3·pyridine (1.0 equiv.), Et_3N (3.5 equiv.), DCM/DMSO (1:1), 0 °C to rt, 8 h	36	17	41	1:2.4	0.50
Nitroxide radical-based reagents							
7	Anelli	NaOCl (0.5 equiv.), TEMPO (2 mol%), NaBr (10 mol%), DCM/H_2O, (4:1), 0 °C, 4 h	36	23	40	1:1.9	0.41
8	Piancatelli–Margarita	BAIB (0.5 equiv.), TEMPO (5 mol%), DCM, 0 °C to rt, 4 h	24	25	47	1:1	0.53
9	Jahn–Holan	tBuONO (0.5 equiv.), TEMPO (5 + 5 mol%), BF_3·Et_2O (5 mol%), DCM, reflux °C, 3 h	20	40	38	2.0:1	0.41
Hypervalent iodine-based reagents							
10	*o*-Iodoxybenzoic acid	IBX (0.5 equiv.), DMSO, rt, 24 h	26	31	34	1.3:1	0.47
11	Dess–Martin	DMP (0.5 equiv.), DCM, rt, 24 h	22	37	39	2.2:1	0.42
Ruthenium-based reagents							
12	Catalytic RuO_4	$NaIO_4$ (0.5 equiv.), RuO_2·H_2O (2.5 mol%), CCl_4/H_2O (1:1), rt, overnight	16	12	69	1:1.1	0.74
13	Ley	NMO (0.5 equiv.), TPAP (2.5 mol%), 3Å sieves, DCM, rt, overnight	31	30	36	1:1	0.40
Other reagents							
14	Fétizon	Ag_2CO_3/celite (2.5 equiv.), benzene, reflux, 48 h	36	43	13	2.8:1	0.23
15	Oppenauer	Cyclohexanone (12.5 equiv.), $Al(OiPr)_3$ (0.5 equiv.), toluene, reflux, 16 h	8	16	36	n/a[e]	
16	Steven's	NaOCl (0.5 equiv.), AcOH, rt, 6 h	31	43	24	2.7:1	0.27

[a]All reactions were performed on a 2.5 mmol scale (1.25 mmol of **87** and 1.25 mmol of **88**). [b]Isolated yields. [c]Axial/equatorial ratio represents preferential reactivity of **87** or **88** towards oxidation. It was calculated as a ratio of converted **87** and **88** that was determined from the isolated yields described in the table. [d]Reaction conversion was too low to calculate effectiveness reliably. [e]Due to the formation of unknown impurities during the Oppenauer oxidation, the effectiveness could not be reliably calculated. Green – most effective conditions for axial oxidation, orange – most effective conditions for equatorial oxidation.
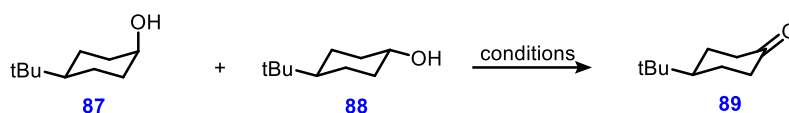
Chromium-Based Reagents (Table 10, Entry 1–3)

Similar to the steroid system, the Jones oxidation (*entry 1*) of 4-*tert*-butylcyclohexanol exhibited selectivity toward the axial hydroxyl group and also showed a high reaction conversion. Indeed, the A/E_f was 2.6:1. Similar trend was also demonstrated for the Corey−Suggs oxidation (*entry 3*), which afforded A/E_f = 1.8:1. The lowest selectivity was exhibited by the Corey− Schmidt oxidation (*entry 2*), with A/E_f = 1.2:1.

Dimethyl Sulfoxide-Based Reagents (Table 10, Entry 4–6)

The conditions of Swern oxidation demonstrated low selectivity toward the axial hydroxy group, affording A/E_f = 1.3:1 (*entry 4*). This result agrees with the Swern oxidation of steroid **57**. The Omura−Sharma−Swern oxidation with TFAA as a DMSO activator demonstrated no selectivity, with A/E_f = 1.1:1 (*entry 5*). This agrees with data from oxidation on steroid **57**, where we also did not observe any selectivity. The Parikh−Doering oxidation with 0.5 equiv. of the SO_3-py complex (*entry 6a*) only afforded 13% conversion, which did not allow us to calculate A/E_f and Ef_f ratios reliably. Therefore, the reaction was performed with 1 equiv. of the SO_3-py complex (*entry 6b*). The reaction demonstrated significant selectivity toward the equatorial hydroxyl group, with A/E_f = 1:2.4 and Ef_f = 0.5. This result was the most prominent selectivity achieved for 4-*tert*-butylcyclohexanol in our study.

Nitroxide Radical-Based Reagents (Table 10, Entry 7–9)

The NaOCl/TEMPO Anelli protocol (*entry 7*) produced the desired selectivity in the equatorial hydroxyl oxidation with an A/E_f = 1:1.9 and an Ef_f = 0.41, consistent with the oxidation of **57**. In contrast, the TEMPO/BAIB-mediated oxidation of 4-*tert*-butylcyclohexanol did not maintain the high selectivity observed in the equatorial hydroxyl oxidation of **57**. Instead, the reaction resulted in a complete lack of selectivity with A/E_f = 1:1 and Ef_f = 0.53 (*entry 8*). Interestingly, the Jahn-Holan selectivity towards the axial hydroxyl group in 4-*tert*-butylcyclohexanol with (A/Ef = 2:1) was different from the results of the previous experiment on **57** (see **Table 6**, *entry 18*). However, this outcome is consistent with the original Holan paper,[241] where the authors also tested 4-*tert*-butylcyclohexanol in substrate-scope.

Hypervalent Iodine-Based Reagents (Table 10, Entry 10 and 11)

The oxidation with IBX (*entry 10*) demonstrated a low selectivity toward the axial hydroxyl group, with A/E_f = 1.3:1. The Dess−Martin oxidizing reagent, similar to the oxidation of steroid **57**, exhibited selectivity toward the oxidation of the axial hydroxyl with A/E_f = 2.1:1 (*entry 11*).

Ruthenium-Based Reagents (Table 10, Entry 12 and 13)

No selectivity was identified for the oxidation with ruthenium-based reagents. RuO_4 generated in situ from a $NaIO_4/RuO_2$ mixture and TPAP/NMO oxidants gave A/E_f ratios of 1:1.1 and 1:1, respectively.
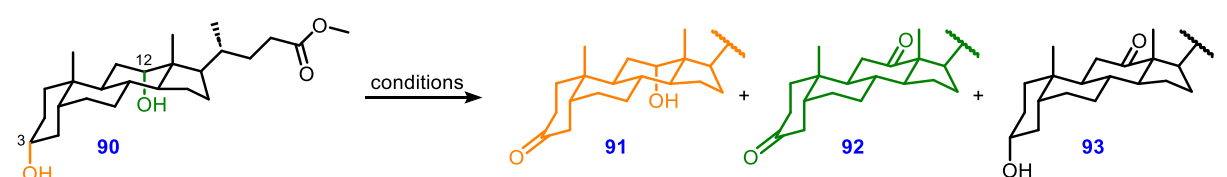
Other Reagents (Table 10, Entry 14–16)

The Fétizon oxidation (*entry 14*) demonstrated a higher reactivity for the axial hydroxyl group of **87,** with A/E_f = 2.8:1, which is in contrast to the higher reactivity of the equatorial hydroxyl group on steroid **57** (for explanation, see *section 5.2)* It should be noted that the reaction's conversion was low compared to those of other reactions. The conditions of Oppenauer oxidation (*entry 15*) could not be reliably described, as unknown impurities formed under the tested reaction conditions even after repeated experiments. Finally, we evaluated the protocol of Stevens oxidation (*entry 16*). We observed a clear preference for axial alcohol A/E_f = 2.7:1, which agrees with results obtained for the oxidation of steroid **57** (see **Table 9**, *entry 10−15*).

OXIDATION OF METHYL DEOXYCHOLATE

The high selectivity of TEMPO oxidation towards the equatorial hydroxyl group and Dess–Martin or Steven's oxidation towards the axial hydroxyl group was further evaluated on methyl deoxycholate (**90**) that bears the equatorial group at position C3 and the axial group at position C12. Similarly, as the oxidation of compound **57**, the high selectivity of TEMPO oxidation towards the equatorial hydroxyl group and Dess–Martin or Steven's oxidation towards the axial hydroxyl group was demonstrated. The results are summarized below (**Table 11**). In brief, the Anelli protocol afforded 82% of compound **91**, and the Piancatelli–Margarita afforded 87% of compound **91**. In contrast, the Dess-Martin oxidation afforded 85% of compound **92**, and the Steven's oxidation afforded 73% of compound **92**. All of those results are consistent with previous observations (see **Table 4 − Table 10**).

Table 11. Selectivity of oxidizing reagents on oxidation of methyl deoxycholate

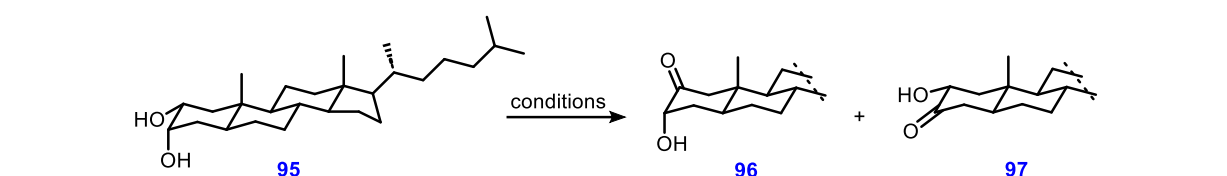| Entry | Name reaction | Conditions[a] | Yield (%)[b] | | | | Effectiveness | |
			90	91	92	93	A/E$_f$	Ef$_f$
1	Anelli	NaOCl (2.0 equiv.), TEMPO (2 mol%), NaBr (10 mol%), DCM/H$_2$O, (4:1), 0 °C, 4	5	82	2	6	1:41	0.88
2	Piancatelli–	BAIB (3.0 equiv.), TEMPO (5 mol%), DCM, 0 °C to rt, 4 h	2	87	1	2	1:87	0.96
3	Dess–Martin	DMP (1.0 equiv.), DCM, rt, 24 h	4	1	85	9	85:1	0.87
4	Steven's	NaOCl (1.0 equiv.), AcOH, rt, 6 h	3	14	73	5	5.2:1	0.92

[a]All reactions were performed on a 2.5 mmol scale. [b]Isolated yields. Green – most effective conditions for axial oxidation, orange – most effective conditions for equatorial oxidation.

OXIDATION OF 5α-CHOLESTANE-2α,3α-DIOL

Finally, the conditions of TEMPO oxidation, Dess–Martin oxidation, and Steven's oxidation were tested on 5α-cholestane-2α,3α-diol (**94**). According to the literature, the selective oxidation[250, 251] of 1,2-diol is challenging. Unfortunately, we did not observe any reasonable selectivity on our model 1,2-diol system. The results are summarized below (**Table 12**).

Table 12. Selectivity of oxidizing reagents on oxidation of 5α-cholestane-2α,3α-diol (**94**)

| Entry | Name reaction | Conditions[a] | Yield (%)[b] | | | Effectiveness | |
			95	96	97	A/E$_f$	Ef$_f$
1	Anelli	NaOCl (2.0 equiv.), TEMPO (2 mol%), NaBr (10 mol%), DCM/DMSO/H$_2$O (10:1:2), 0 °C, 4 h	22	21	19	1:1.1	0.40
2	Piancatelli–Margarita	BAIB (3.0 equiv.), TEMPO (5 mol%), DCM/DMSO (10:1), 0 °C to rt, 4 h	10	25	22	1:1.1	0.47
3	Dess–Martin	DMP (1.0 equiv.), DCM/DMSO (10:1), rt, 24 h	30	21	23	1.1:1	0.44
4	Steven's	NaOCl (1.0 equiv.), AcOH, rt, 6 h	23	24	25	1:1	0.49

[a]All reactions were performed on a 2.5 mmol scale. [b]Isolated yields. Compound 5α-cholestan-2,3-dione was isolated in an inseparable mixture with additional non-polar compounds and, therefore, is not included in the table.

63

5.2 MECHANISTIC EXPLANATION

Dess–Martin Periodinane

The proposed mechanistic explanation is depicted in **Figure 33**. We propose that the dissociation of intermediate **A** is a slower step than a nucleophile attack at the iodine atom. Consequently, the axial hydroxyl group would react faster since the *syn*-axial strain is released in the rate-limiting step. This phenomenon is particularly known for chromium-based reagents[228, 252]. It should be noted, however, that authors also suggest the steric hindrance is a simplified explanation and notify the crucial role of the solvent.[253] The proposed mechanism would be subject to first-order kinetics. This is consistent with the observed behavior of hypervalent iodine species.[254]
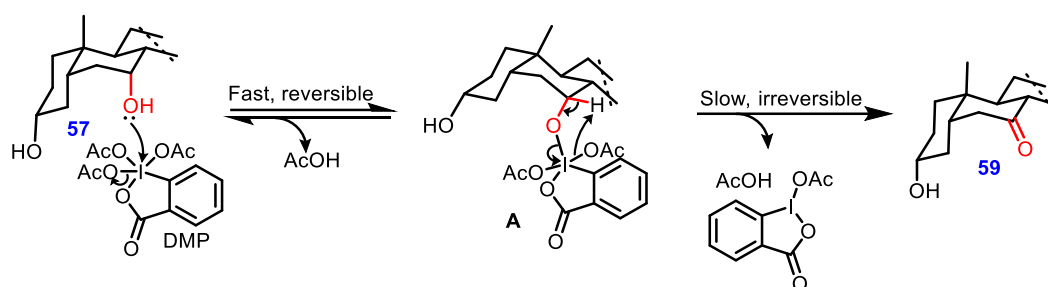
Figure 33. The proposed rationale for observed Dess–Martin periodinane selectivity.

Sodium Hypochlorite

Similarly, to DMP or Cr(IV) oxidants, the initial nucleophilic attack is reversible and fast compared to the irreversible dissociation of the stable chloride anion. As water is present in the reaction mixture in a significant excess, compared to the amount of intermediate **A**, the reaction is proposed to follow pseudo-first-order kinetics (**Figure 34**). This hypothesis is supported by other researchers who also observed the pseudo-first-order kinetics behavior of hypochlorite in redox reactions.[255-257]
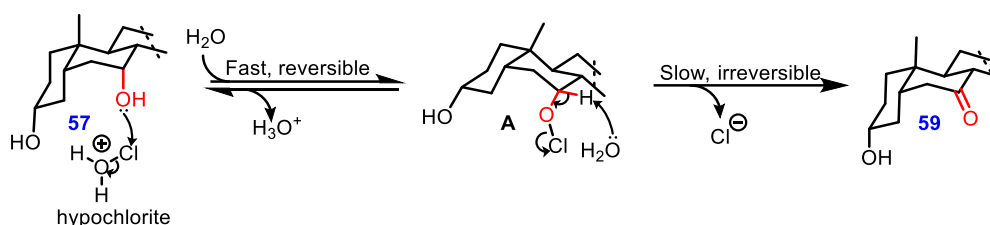
Figure 34. Proposed rationale for observed sodium hypochlorite selectivity.

TEMPO

The proposed mechanistic explanation is summarized in the catalytic cycle (**Scheme 10**). The presence of bulky methyl substituent groups in the nitroxide vicinity of the TEMPO reagent determines the rate-limiting step. Therefore, hydroxyl's ability to attack electrophilic nitrogen in tempoxonium ion **A** dictates selectivity. The decomposition of intermediate **B** to **C** is fast enough not to influence overall reaction kinetics. The initial attack on tempoxonium is more favorable with equatorial hydroxyl, which is less hindered and, therefore, more nucleophilic than the axial one. The proposed mechanism would be subject to second-order kinetics.
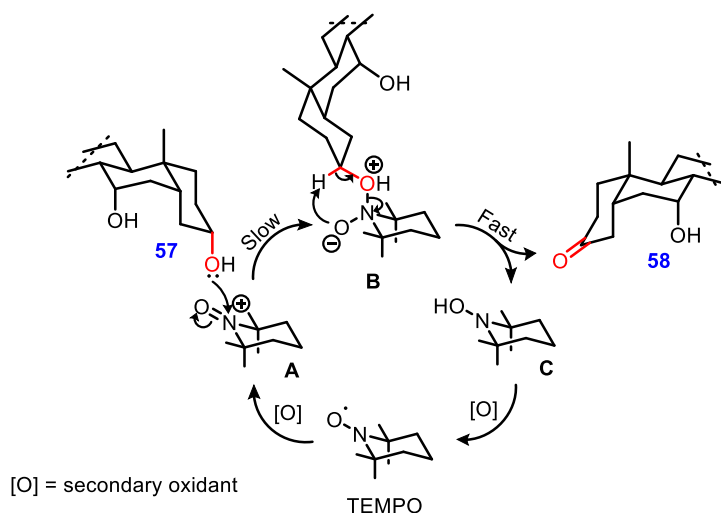
Scheme 10. Proposed rationale for observed TEMPO selectivity.

It is worth mentioning that Jahn-Holan modification (TEMPO/tBuONO) did not obey this selectivity in the case of 4-*tert*-butylcyclohexanol (compare **Table 6**, *entry 18* with **Table 10** *entry 9*). The Jahn-Holan protocol, unlike other TEMPO oxidations, uses reflux. We hypothesize that this particular reaction is rather controlled by thermodynamics and a more complex mechanism is present.

Fétizon

The Fétizon reagent provided opposite selectivity when used on steroid **57** and *trans*-4-*tert*-butylcyclohexanol **87:88** A/E_f = 1:72 vs A/E_f = 2.8:1 respectively (compare **Table 9**, *entry 2* with **Table 10**, *entry 14*). Ag$_2$CO$_3$/Celite oxidation is a heterogeneous reaction and takes place on the surface of the reagent. The accessibility of α-proton dictates the reaction kinetics.[235] In molecule **57**, the C3 axial α-proton is more accessible than on the 4-*tert*-butylcyclohexanol because of the adjacent B, C rings and C18 C19 methyl groups. (**Figure 35**).
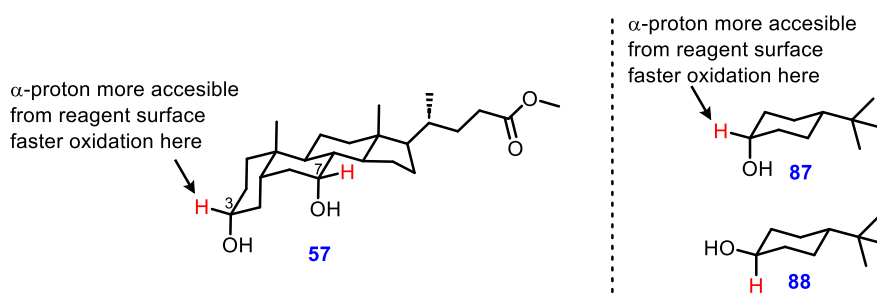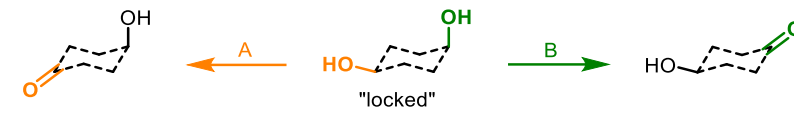
Figure 35. The explanation for different results in Fétizon oxidation.

5.3 CONCLUSION

In this work, we assessed the selectivity toward axial and equatorial hydroxyl groups for the 16 popular oxidizing reagents. Reagents were tested in various concentrations on 5 different substrates: methyl chenodeoxycholate, methyl deoxycholate, 5α-cholestane-2α,3α-diol, *cis*-4-*tert*-butylcyclohexanol, and *trans*-4-*tert*-butylcyclohexanol. Our findings are summarized below (**Table 13**).

Table 13. Recommended reagents for required transformation.

Required reaction	Recommended Reagent	Name Reaction
A	TEMPO/NaOCl	Anelli
	TEMPO/BAIB	Piancatelli–Margarita
B	PCC	Corey–Suggs
	Dess–Martin	Dess–Martin
	NaOCl	Stevens

We recommend TEMPO/NaOCl or TEMPO/BAIB for selective oxidation of equatorial alcohols and Dess-Martin, NaOCl, and PCC for selective oxidation of axial alcohols. The limitations are that the two hydroxyl groups mustn't be adjacent next to each other (1,2-diol), as we didn't observe any selectivity in the oxidation of 5α-cholestane-2α,3α-diol. Moreover, the cyclohexane moiety must be "locked" to prevent ring flip.

Outcomes

- Protocols for selective oxidation of axial or equatorial alcohols without the use of protecting groups.

- Publication in the Journal of Organic Chemistry.[258]

6 EXPERIMENTAL

6.1 GENERAL METHODS

Chemicals

Chenodeoxycholic acid and deoxycholic acid were purchased from a commercial supplier (CDCA: Carbosynth, UK, no. FC096751801, DCA: TCI Chemicals, JP, no. C0315).

Compounds for *Project 1* were either purchased from commercial vendors or obtained from existing group deposits. The chromatographic purity of all final compounds was > 95%. Their analytical data are presented in *Experimental, section 6.3.*

The concentration of sodium hypochlorite (NaOCl) in bleach solution was determined prior to use with indirect iodometry titration.[259] Water content in dimethyl sulfoxide was determined prior to each reaction with Karl Fischer titration. Reaction solvents were distilled prior to use: dichloromethane from phosphorous pentoxide, benzene, tetrahydrofuran, and toluene from Na/benzophenone, methanol by distillation over iodine-activated magnesium. Washing of final crystals was done with HPLC grade *n*-pentane, which was distilled from CaH pellets and stored over activated 3Å sieves. *o*-Iodoxybenzoic acid was prepared according to Frigerio protocol.[260] Jones reagent (2.67 M) was prepared as described in the literature.[261] Pentafluoroethane and trifluorotoluene were generous gifts from Dr. Beier's lab. All other commercial reagents and solvents were used without purification.

Instrumentation

Reactions were conducted in a round bottom flask, or a screw-cap vial equipped with a teflon-coated magnetic stirring bar. The laboratory was kept at a constant 23 °C and at ≈40% relative humidity. For solvent evaporation, a rotatory evaporator with a water bath set to 50 °C, and tap-water cooling was used. Reactions were followed by TLC or with the HPLC-MS system Nexera LC-40 (Shimadzu, Japan).

Melting points were determined with a micro melting point apparatus (Hund/Wetzlar, Germany) and were uncorrected. For elemental analysis, PE 2400 Series II CHNS/O Analyzer (Perkin Elmer, MA, USA) was used, with microbalance MX5 (Mettler Toledo, Switzerland). For measurement of optical rotation, AUTOPOL IV (Rudolph Research Analytical, NJ, USA) was used, all samples were measured at 20 °C, at a given concentration c [g · 100 mL^{-1}] in a given solvent at 589 nm, values are represented as $[\alpha]_D$ [10^{-1} · deg · cm^2 · g^{-1}].

Routine NMR experiments (^{1}H, ^{13}C APT, ^{1}H-^{1}H COSY, ^{1}H-^{13}C HSQC, and ^{1}H-^{13}C HMBC) were measured with a Bruker AVANCE III™ 400 and/or a Bruker ASCEND III™ 400 both operating at 400 MHz for ^{1}H and 100.6 MHz for ^{13}C. Advanced NMR experiments (^{1}H-^{1}H ROESY) were measured and interpreted by Dr. Dračínský on a Bruker Avance III™ HD 500 and/or a JEOL ECZ500 spectrometer, both operating at 500 MHz for ^{1}H and 125.7 MHz for ^{13}C. All chemical shifts (δ) are given in parts per million (ppm) relative to residual solvent peak: δ chloroform-d$_1$ = singlet 7.26 ppm (^{1}H, CHCl$_3$) and triplet 77.16 ppm (^{13}C, CDCl$_3$), δ methanol-d$_4$ = pentet 3.31 ppm (^{1}H, CHD$_2$OD) and septet 49.00 ppm (^{13}C, CD$_3$OD), δ dimethyl sulfoxide-d$_6$ = pentet 2.50 ppm (^{1}H, CHD$_2$S(O)CD$_3$) and septet 39.52 ppm (^{13}C, (CD$_3$)$_2$SO). Coupling constants (*J*) are given in Hz, and splitting patterns are abbreviated: brs = broad singlet, s = singlet, d = doublet, t = triplet, q = quartet, p = pentet, dd =

doublet of doublets, dt = doublet of triplets, ddt = doublet of doublets of triplets, m = multiplet (denotes complex pattern). All ^{13}C NMR spectra are [1]H-broadband decoupled. For compounds insoluble in pure deuterated solvent, a mixture of deuterated solvents has been used. In such a case, the specific solvent ratio is given, and the solvent used for referencing is marked with asterisk (*). The assignment of ^{1}H and ^{13}C signals was based on a combination of 1D, 2D NMR experiments and spectra comparison with known compounds. The aliphatic region's 1H spectra of steroid compounds are usually very complex (especially around 1–2 ppm). In such cases, only selected peaks with good spectral separation are reported. The HRMS spectra were recorded with LTQ Orbitrap XL (Thermo Fischer Scientific, MA, USA) in ESI mode. Thin-layer chromatography (TLC) was performed on silica gel (Merck, 60 μm) and visualized with either UV 254 nm or phosphomolybdic acid/ethanol stain with gentle heating. Analytical samples were dried in a pre-heated vacuum oven (50 °C/0.25 kPa) for at least 8 hours. X-ray crystallographic analyses were performed by Dr. Blanka Klepetářová on an Xcalibur PX single-crystal X-ray diffractometer (Oxford Diffraction, United Kingdom) at the University of Chemistry and Technology, Prague. Crystallographic data are summarized in the *Appendix.*

For preparative HPLC and preparative flash chromatography, puriFlash 5.250 instrument (Interchim, France) with neutral bare-silica gel (Phenomenex 5 μm for preparative HPLC, and Merck 40–63 μm or Interchim 20 μm for flash) and an ELS detector was used. For semi-preparative chromatography, HPLC system 33x (Gilson, USA) equipped with an ELS detector with bare-silica gel column (Sigma Aldrich, Supelco 5 μm) was used. All chromatography gradient elutions were linear and solvent ratios are always reported as the volume/volume (v/v).

Non-expensive computations were performed locally on a desktop PC with a 64-bit Windows 10 operating system, 6-core Intel i7-8700 CPU 3.20 GHz, with 16 GB of RAM. More expensive quantum mechanical-based calculations were performed on our institutional computation infrastructure.

Software Tools

A custom compound database was created in Microsoft Access within the Microsoft Office Professional Plus 2019 suite. Raw NMR data (free induction decay) were processed, visualized, and interpreted in Mnova asoftware[262] (multiple versions). AutoDock v4.2.6 and AutoDock Vina v1.2.0 algorithms were used along with Molecular Graphic Laboratory (MGL) Tools v1.5.6. Those are open-access software for academic use under the Scripps Institute Apache license.[211, 263-265] For file conversion Chemdraw v20.0, Chem3D v20.0, and OpenBabel v2.4.1 were used. Python scripts were written with PyCharm v20.2 IDE. To visualize and review the docking results, the standalone application Discovery Studio v21.1.0.20298 or web-based NGL Viewer® was used.[134, 135, 212] QSAR models training and final compound scoring were done in the StarDrop™ application.[209]

The author of this Thesis is aware of the importance of transparency and fairness in the use of AI tools. This Thesis adheres to the recommendation of the dean's college for the fair use of artificial intelligence.[266] Thesis was proofed by Grammarly (Pro) for Microsoft Office v6.8.261. Grammarly is a commercial grammar correction tool that uses the generative pre-trained transformer (GPT-4)[267] natural language processing model and is recommended by Charles University's central library.[268] The software was set to follow the American English convention with a focus on an expert audience and a scientific writing tone. Moreover, Grammarly was used to cross-check this thesis for plagiarism

against a database of 16 billion web pages and ProQuest[269] (Clarivate family) articles database without any positive hits. The reference list was created in the EndNote v20.4.1 desktop application[270] with the provided kaspam@natur.cuni.cz account. The references are formatted according to the ASC style.[271]

Ligand Preparation for Docking

Ligands were drawn in Chemdraw and imported to Chem3D, where structures were minimized with the MM2 algorithm and exported as ".mol2" files. Implicit hydrogens were added, as well as a charge appropriate to pH 7.4, and structures were converted to ".pdbqt" format via OpenBabel.

Docking of Ligands into FXR

The crystal structure of FXR with bound NCoA-2 peptide and CDCA was downloaded from the PDB database (6HL1). This particular structure was selected because it offered the best resolution from all available (1.60 Å) and is co-crystalized with CDCA, which is structurally close to our ligands. NcoA-2 peptide, CDCA, and water molecules were deleted from the structure. Hydrogens and Kollman's charges were added via MGL software. AutoDock4 parameters: A grid box for docking was selected in the LBD cavity for endogenous ligand CDCA. With coordinates x: 11.47, y: -12.74, and z: 12.55 pt. as the centroid of the grid map. Box was selected $25 \times 25 \times 25$ pt. with 1.0 Å spacing. Pose parameters were selected as follows: a number of individuals in the population: 70, generations: $2.7 \cdot 10^4$, energy evaluations: $2.5 \cdot 10^6$, dockings: 40. All other parameters were left default. AutoDock Vina parameters: exhaustiveness 25, grid box was selected to be identical as above, and all other parameters were left default. Final data were processed through a custom Python script, which extracted the lowest binding energies for each ligand. With these settings, calculations took around 2 minutes per ligand, and the control CDCA molecule showed a similar pose as in the experimental crystal structure.

Docking of Ligands into TGR5

The cryo-EM structure of the INT-777-bound TGR5 complex was downloaded from the PDB database (7CFN). All heteroatoms (INT-777, cholesterol, palmitic acid, and water) were deleted from the structure, and hydrogens and Kollman charges were added via MGL software. Autodock4 parameters: A grid box for docking was selected in the cavity where the INT-777 was located, with coordinates x: 95.8, y: 123.0, and z: 115.8 pt. as the centroid of the grid map. Box was selected $20 \times 20 \times 20$ pt. with 1.0 Å spacing. Pose parameters were selected as follows: the number of individuals in the population: 70, generations: $2.7 \cdot 10^4$, energy evaluations: $2.5 \cdot 10^6$, dockings: 40, and all other parameters were left default. AutoDock Vina parameters: exhaustiveness 20, grid box was selected to be identical as above, and all other parameters were left default. Final data were processed through a custom Python script, which extracted the lowest binding energies for each ligand. With this setting, calculations took around 2 minutes per ligand, and the control INT-777 molecule showed a similar pose as in the experimental crystal structure.

HPLC Method A

Analysis was carried out on an HPLC system 33x (Gilson, USA) equipped with an ELS detector. Solvent A was DCM/AcOH (1000:1), and solvent B was MeOH/AcOH (1000:1). Analysis was performed in isocratic mode with 5% of solvent B, and flow rate 1.0 mL/min, column: Supelco, bare-silica LC-SI 5 μm, 150 × 4.6 mm. The sample was prepared by dissolving the material (1 mg) in DCM (1 mL) and then sonicated for 5 minutes. The injection volume was usually 20 μL.

HPLC Method B

Analysis was carried out on HPLC-MS system LCQ Advantage (Thermo Fisher Scientific, MA, USA) equipped with PDA and MS detector. Ions were detected in ESI or APCI positive or negative ion mode, with *m/z* range from 250 to 2000 Da. Solvent A was water/acetonitrile (98:2), and solvent B was acetonitrile/isopropanol/water (95:3:2), with 5 mM ammonium formate in both. Gradient setup: 0–25–30–30.1–45 min, 50–100–100–50–50% of solvent B and flow rate 150 µL/min, column: Phenomenex, C18, Discovery® 5 µm, 250 × 4.6 mm. The sample was prepared by dissolving the material (1 mg) in solution A/B (1:3, 1 mL) and then sonicated for 5 min. The injection volume was usually 10 µL.

HPLC Method C

Analysis was carried out on the HPLC-MS system Nexera LC-40 (Shimadzu, Japan) equipped with PDA, ELS, and MS detectors. Ions were detected in positive DUIS (ESI/APCI) ion mode, with an *m/z* range from 250 to 1000 Da. Solvent A was water/methanol/formic acid (950:50:1), and solvent B was acetonitrile. Analysis was performed in isocratic mode with 50% of solvent B and flow rate 0.6 mL/min, column: Shim-pack Scepter, C8-120, 1.9 µm, 100 × 2.1 mm (Shimadzu). The sample was prepared by dissolving the material (1 mg) in methanol (1 mL) and then sonicated for 5 min. The injection volume was usually 0.5 µL.

HPLC Method D

The aliquot (usually 50 µL) from the reaction mixture was quenched with a solution of cold MeOH/water (4 °C, 1:4, 0.5 mL) and then extracted into DCM (2 × 0.75 mL). The organic phase was dried over $MgSO_4$ and filtered through a pad of cotton. The organic solvents were evaporated by nitrogen blowndown to obtain 0.3–3 mg of crude material, which was usually colorless film or thick oil. Sample was further redissolved in HPLC-MS grade MeOH (1.5 mL), briefly sonicated (1 min), filtered through PTFE filter (0.25 µm) into the HPLC screw vial (1.5 mL), and analyzed on HPLC system as follows: solvent A was water/acetone/formic acid (950:50:1) and solvent B was acetone/water/formic acid (950:50:1). Gradient setup: 0–10–12–12.1–13 min, 50–95–95–50–50% of solvent B and flow rate 0.35 mL/min, column: C18 Shimadzu XR–ODS III, 2.2 µm, 150 × 2.0 mm. Sample injection volume varied from 0.5–5 µL, based on the amount of crude material obtained after the workup.

HPLC Method E

Analysis was carried out on HPLC-MS system LCQ Advantage (Thermo Fisher Scientific, MA, USA) equipped with PDA and MS detector. Ions were detected in ESI or APCI positive or negative ion mode, with *m/z* range from 250 to 2000 Da. Solvent A was water/acetonitrile (98:2), and solvent B was acetonitrile/isopropanol/water (95:3:2), with 5 mM ammonium formate in both. Gradient setup: 0–25–30–30.1–45 min, 50–100–100–50–50% of solvent B and flow rate 150 µL/min, column: Phenomenex, C4, Jupiter® 5 µm, 250 × 4.6 mm. The sample was prepared by dissolving the material (1 mg) in solution A/B (1:3, 1 mL) and then sonicated for 5 min. The injection volume was usually 10 µL.

General Procedure for Grignard Reaction
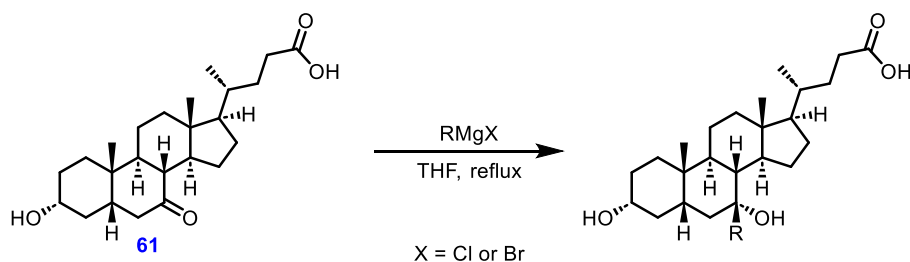
A three-neck round bottom flask (250 mL), equipped with a magnetic stirring bar, was heat gun dried, evacuated, backfilled with nitrogen, and charged with appropriate Grignard reagent (5 equiv., 6.4 mmol) and dry THF (75 mL). To this, a solution of 3α-hydroxy-7-oxo-5β-cholan-24-oic acid (**61**, 1.28 mmol, 500 mg, in 10 mL dry THF) was added dropwise at room temperature through septa under counterflow of nitrogen. Upon addition, a cloud-like precipitate formed. The solution was then vigorously stirred and heated to reflux. The progress of the reaction was monitored by TLC. After full conversion (usually 2 hours), the reaction mixture was acidified to pH 2 (aq. 1 M HCl) and extracted with EtOAc (3 × 75 mL). The combined organic extracts were washed with water (50 mL) and brine (50 mL), dried over Na_2SO_4, and the solvents were evaporated. The crude product was purified by column chromatography on silica gel (MeOH/DCM, 2:98 to 5:95), followed by purification on semi-preparative HPLC (column: Luna® 5 µm bare-silica 250 × 21.2 mm, isocratic: MeOH/DCM, 3:97, 15 mL/min, injected: in DCM, or THF - if insoluble in DCM).

6.2 OXIDATION OF AXIAL AND EQUATORIAL HYDROXY GROUPS

Jones Oxidation (Table 4, Entry 1–6)
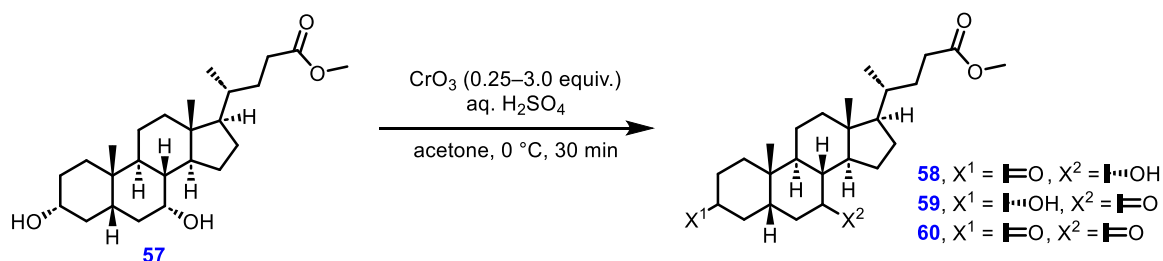
Methyl chenodeoxycholate (**57**, 200 mg, 0.49 mmol) was dissolved in acetone (5 mL), and the solution was cooled to 0 °C in the ice bath. Jones reagent (0.25, 0.50, 0.75, 1.0, 2.0, or 3.0 equiv.) was added dropwise with Hamilton syringe. The reaction mixture was stirred for 30 minutes. Then, the aliquot (50 µL) from each reaction mixture was analyzed according to the *HPLC Method D,* and results are summarized in **Table 4**, *entry 1–6.*

Corey–Schmidt Oxidation (Table 4, Entry 7–12)
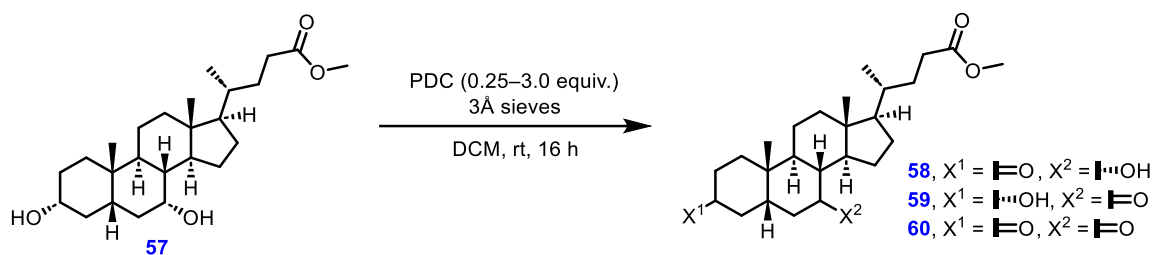
Methyl chenodeoxycholate (**57**, 200 mg, 0.49 mmol) and activated molecular sieves (3Å, finely grounded, 500 mg) were suspended in dry DCM (5 mL) under a nitrogen atmosphere. Pyridinium dichromate (0.25, 0.50, 0.75, 1.0, 2.0, or 3.0 equiv.) was added in one portion, and the reaction mixture was stirred at room temperature for 16 hours. Then, the aliquot (50 µL) from each reaction mixture was analyzed according to the *HPLC Method D,* and results are summarized in **Table 4**, *entry 7–12.*

Corey–Suggs Oxidation (Table 4, Entry 13–18)
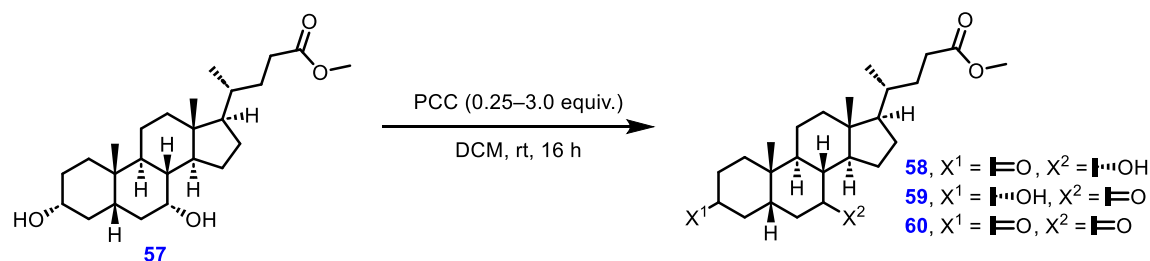
Methyl chenodeoxycholate (**57**, 200 mg, 0.49 mmol) was dissolved in dry DCM (5 mL) under an inert atmosphere. Pyridinium chlorochromate (0.25, 0.50, 0.75, 1.0, 2.0, or 3.0 equiv.) was added in one portion, and the reaction mixture was stirred at room temperature for 16 hours. Then, the aliquot (50 µL) from each reaction mixture was analyzed according to the *HPLC Method D* and results are summarized in **Table 4**, *entry 13–18.*

Swern Oxidation (Table 5, Entry 1–6)
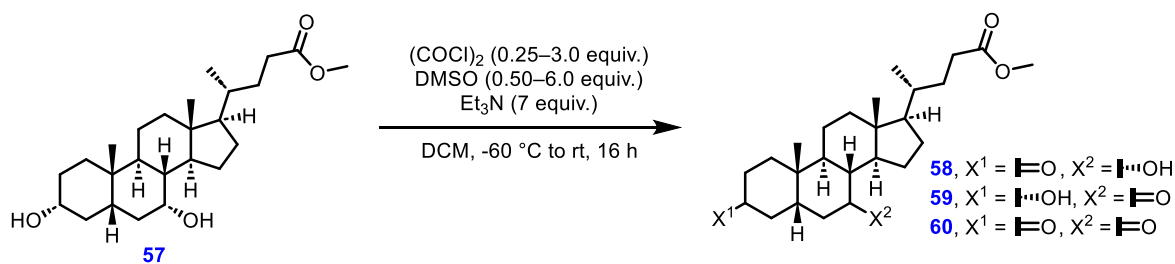
Dimethyl sulfoxide (0.50, 1.0, 1.5, 2.0, 4.0, or 6.0 equiv., 27 ppm of water) was dissolved in dry DCM (4 mL) under a nitrogen atmosphere. Then, the mixture was cooled to -60 °C in the ethanol/dry ice bath. Oxalyl chloride (0.25, 0.50, 0.75, 1.0, 2.0 or 3.0 equiv., 1.0 M solution in DCM) was added in one portion, and the reaction mixture was stirred at -60 °C for 10 minutes. To this mixture, methyl chenodeoxycholate (**57**, 200 mg, 0.49 mmol, dissolved in 1 mL of dry DCM) was added dropwise, and the reaction mixture was stirred at -40 °C for 15 minutes. Then, triethylamine (7 equiv., 3.43 mmol, 478 µL) was added in one portion, and the reaction mixture was allowed to slowly attain room

72

temperature, followed by stirring for 16 hours. Then, the aliquot (50 µL) from each reaction was analyzed according to the *HPLC Method D,* and results are summarized in **Table 5**, *entry 1–6.*
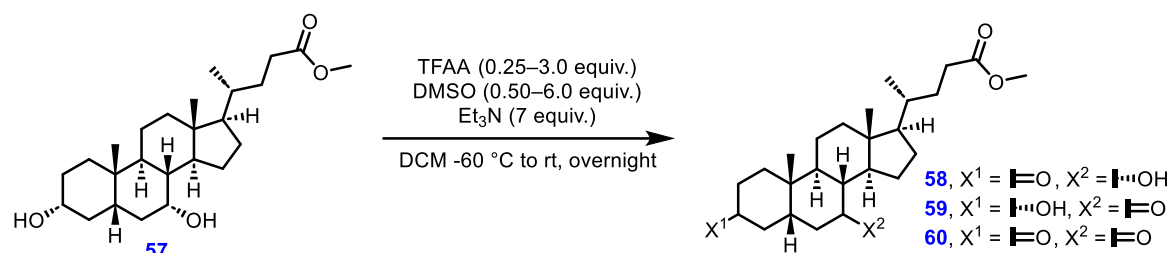
### Omura–Sharma–Swern Oxidation (Table 5, Entry 7–12)

Dimethyl sulfoxide (0.50, 1.0, 1.5, 2.0, 4.0 or 6.0 equiv., 35 ppm of water) was dissolved in dry DCM (4 mL) under an inert atmosphere at -60 °C in the ethanol/dry ice bath. To this mixture, trifluoroacetic anhydride (0.25, 0.50, 0.75, 1.0, 2.0, or 3.0 equiv. respectively) was added in one portion, and the reaction mixture was stirred at -60 °C for an additional 15 minutes. Then, methyl chenodeoxycholate (**57**, 200 mg, 0.49 mmol, dissolved in 1 mL of dry DCM) was added dropwise, and the reaction mixture was stirred at -40 °C for 2 hours. Triethylamine (7 equiv., 3.43 mmol, 0.48 mL) was added in one portion, and the reaction mixture was allowed to attain room temperature overnight. Then, the aliquot (50 µL) from each reaction mixture was analyzed according to the *HPLC Method D,* and results are summarized in **Table 5**, *entry 7–12.*

Parikh–Doering Oxidation (Table 5, Entry 13–18)
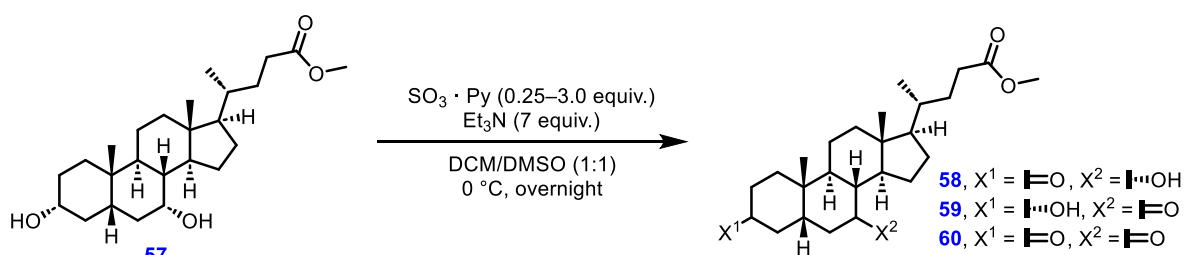
Methyl chenodeoxycholate (**57**, 200 mg, 0.49 mmol) and triethylamine (7 equiv., 3.43 mmol, 478 µL) were dissolved in dry DCM/DMSO (5 mL, 1:1, DMSO with 48 ppm of water) under inert atmosphere. The mixture was cooled to 0 °C in the ice bath. Then, pyridine sulfur trioxide complex (0.25, 0.50, 0.75, 1.0, 2.0, or 3.0 equiv.) was added in one portion, and the reaction mixture was allowed to attain room temperature. After overnight stirring, an aliquot (50 µL) of each reaction mixture was analyzed according to the *HPLC Method D,* and results are summarized in **Table 5**, *entry 13–18.*

Anelli Oxidation (Table 6, Entry 7–12)
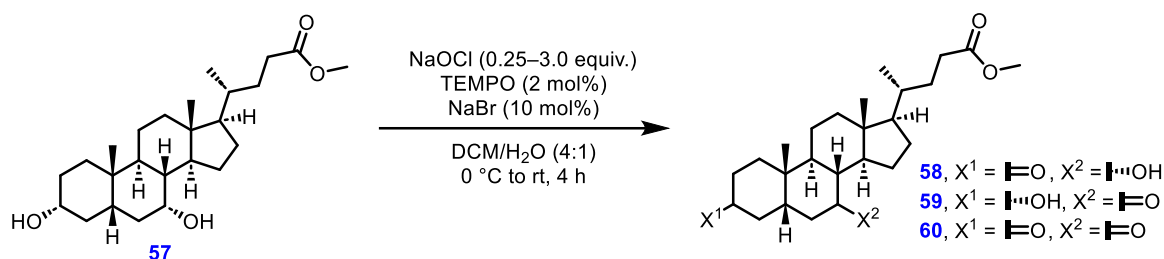
Methyl chenodeoxycholate (**57**, 200 mg, 0.49 mmol), NaBr (0.1 equiv., 0.05 mmol, 6 mg), and TEMPO (0.02 equiv., 0.01 mmol, 2 mg) were dissolved in a mixture of DCM/H$_2$O (5 mL, 4:1) under an inert atmosphere at 0 °C. To the vigorously stirred reaction mixture, sodium hypochlorite (NaOCl, 3.5% w/w aq. solution, 0.25, 0.50, 0.75, 1.0, 2.0, or 3.0 equiv.) was added in small portions. The reaction mixture was allowed to attain room temperature, followed by stirring for another 3 hours. Then, an aliquot (50 µL) of each reaction mixture was analyzed according to the *HPLC Method D,* and results are summarized in **Table 6**, *entry 7–12.*

Piancatelli–Margarita Oxidation (Table 6, Entry 7–12)

Methyl chenodeoxycholate (**57**, 200 mg, 0.49 mmol), BAIB (0.25, 0.50, 0.75, 1.0, 2.0 or 3.0 equiv.), and TEMPO (0.1 equiv., 0.05 mmol, 8 mg) were dissolved in DCM (5 mL) under inert atmosphere at 0 °C. The reaction mixture was allowed to attain room temperature. After stirring for 3 hours at room temperature, the aliquot (50 µL) of each reaction mixture was analyzed according to the *HPLC Method D,* and results are summarized in **Table 6**, *entry 7–12.*

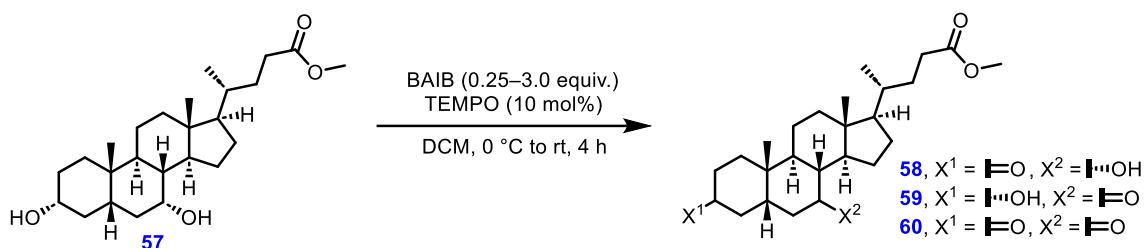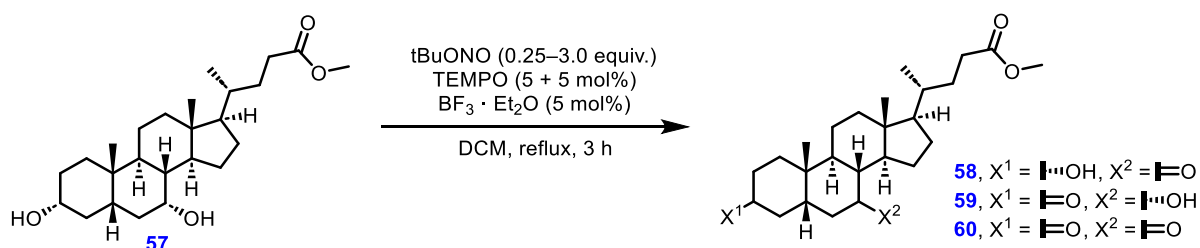**Jahn–Holan Oxidation (Table 6, Entry 13–18)**

Methyl chenodeoxycholate (**57**, 200 mg, 0.49 mmol) was dissolved in dry DCM (5 mL) under an inert atmosphere. Then, boron trifluoride etherate (0.05 equiv., 0.02 mmol, 3 µL) and *tert*-butyl nitrite (0.25, 0.50, 0.75, 1.0, 2.0 or 3.0 equiv.) were added in one portion and the reaction mixture was heated to 35 °C. Next, a solution of TEMPO (0.05 equiv., 3 mg, in 0.2 mL DCM) was added. After 1 hour of stirring, another portion of TEMPO (0.05 equiv., 3 mg, in 0.2 mL DCM) was added, and the reaction mixture was stirred at 35 °C. Then, the aliquot (50 µL) from each reaction was obtained after 2 and 12

hours and analyzed according to the *HPLC Method D,* and results are summarized in **Table 6**, *entry 13–18.*

o-Iodoxybenzoic Acid Oxidation (Table 7, Entry 1–6)
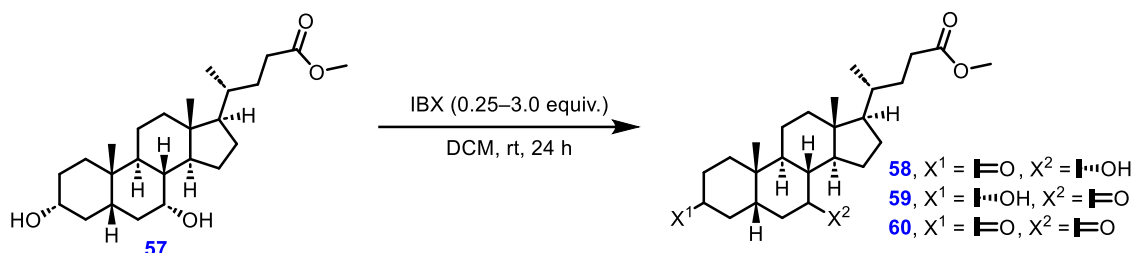
CAUTION: IBX was reported to be explosive when heated over 200 °C or upon impact.[272] Organic or oxidizable inorganic impurities may lower this temperature. IBX can be stored at room temperature for an excess of six months with no significant degradation, provided light is excluded from the container.

Methyl chenodeoxycholate (**57**, 200 mg, 0.49 mmol) was dissolved in dry DCM (5 mL) under an inert atmosphere. Then, *o*-iodoxybenzoic acid (0.25, 0.50, 0.75, 1.0, 2.0, or 3.0 equiv.) was added in one portion, and the reaction mixture was stirred for 24 hours at room temperature. Then, the aliquot (50 µL) from each reaction mixture was analyzed according to the *HPLC Method D,* and results are summarized in **Table 7**, *entry 1–6.*

Dess–Martin Oxidation (Table 7, Entry 7–12)
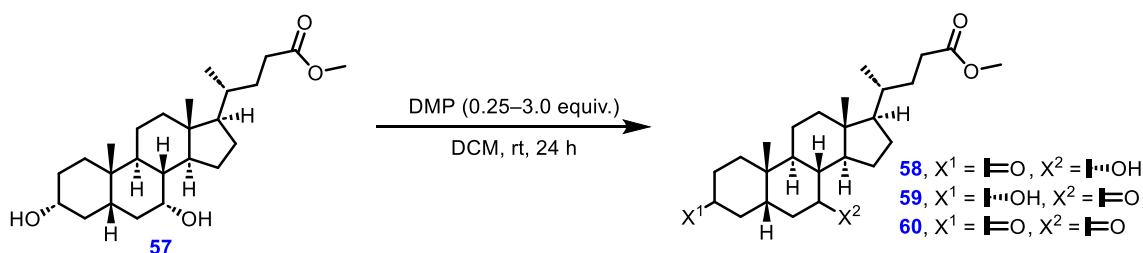
Dess–Martin periodinane was added in one portion (0.25, 0.50, 0.75, 1.0, 2.0, or 3.0 equiv.) to a solution of methyl chenodeoxycholate (**57**, 200 mg, 0.49 mmol) in DCM (5 mL). After stirring for 24 hours at room temperature, the aliquot (50 µL) from each reaction mixture was analyzed according to the *HPLC Method D,* and results are summarized in **Table 7**, *entry 7–12.*

Catalytic RuO₄ Oxidation (Table 8, Entry 1–6)
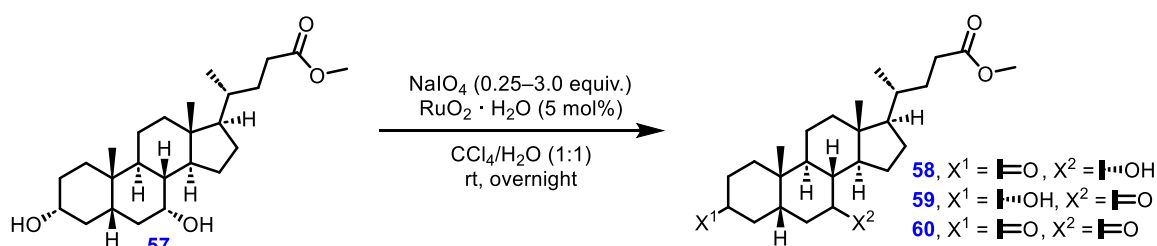
Methyl chenodeoxycholate (**57**, 200 mg, 0.49 mmol) and sodium periodate (0.25, 0.50, 0.75, 1.0, 2.0 or 3.0 equiv.) were dissolved in CCl_4/H_2O (5 mL, 1:1). To each reaction vessel, ruthenium(IV) oxide hydrate (0.05 equiv., 0.02 mmol, 3 mg) was added in one portion and the reaction mixture was stirred

under an inert atmosphere at room temperature overnight. Then, the aliquot (50 µL of the organic layer) from each reaction mixture was analyzed according to the *HPLC method D,* and results are summarized in **Table 8**, *entry 1–6.*

Ley Oxidation (Table 8, Entry 7–12)

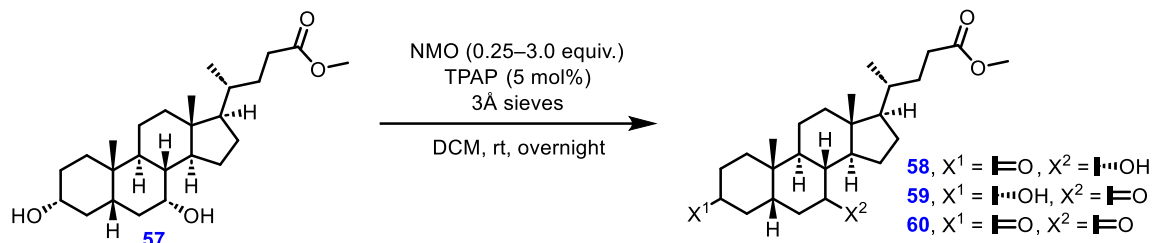N-Methylmorpholine N-oxide (0.25, 0.50, 0.75, 1.0, 2.0 or 3.0 equiv.) and activated molecular sieves (3Å, grounded, 100 mg) were added to a solution of methyl chenodeoxycholate (**57**, 200 mg, 0.49 mmol) in dry DCM (5 mL) under an inert atmosphere. Then, to each reaction vessel, tetrapropylammonium perruthenate (0.05 equiv., 0.02 mmol, 7 mg) was added in one portion, and the reaction mixture was stirred under an inert atmosphere at room temperature overnight. Then, the aliquot (50 µL) from each reaction mixture was analyzed according to the *HPLC Method D,* and results are summarized in **Table 8**, *entry 7–12.*

Fétizon Oxidation (Table 9, Entry 1–3)
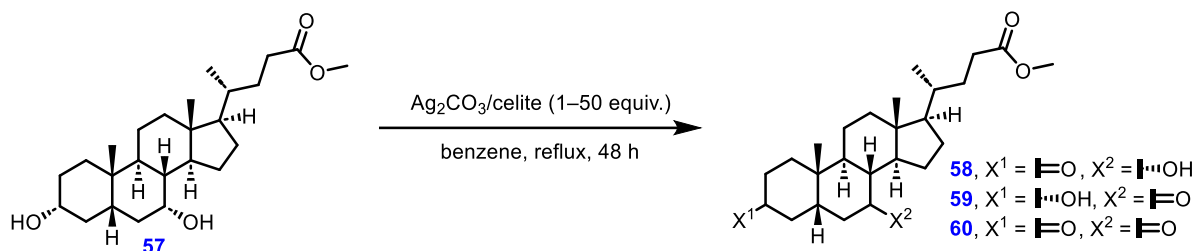
Silver carbonate on Celite (50% w/w loading, 1, 5, or 10 equiv.) was added in one portion (50% w/w loading) to a solution of methyl chenodeoxycholate (**57**, 200 mg, 0.49 mmol) in dry benzene (5 mL) under an inert atmosphere. The reaction mixture was refluxed for 48 hours. Then, the aliquot (50 µL) from each reaction mixture was analyzed according to the *HPLC Method D,* and results are summarized in **Table 9**, *entry 1–3.*

Oppenauer Oxidation with Cyclohexanone (Table 9, Entry 4–6)
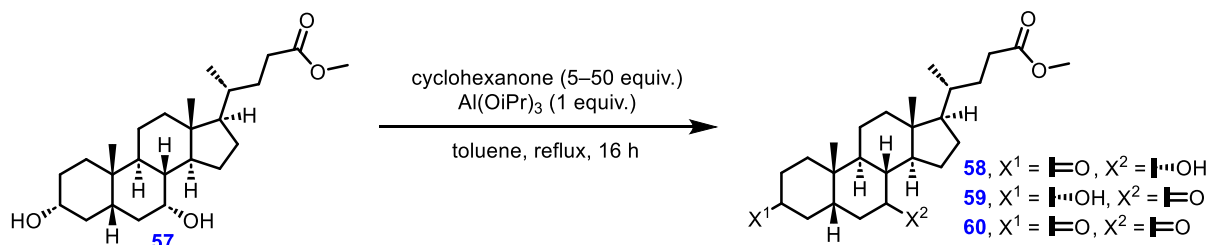
Methyl chenodeoxycholate (**57**, 200 mg, 0.49 mmol) and cyclohexanone (5, 25, or 50 equiv.) were dissolved in dry toluene (5 mL) under an inert atmosphere. Aluminum isopropoxide (1 equiv., 0.49 mmol, 100 mg) was added in one portion, and the reaction mixture was stirred under reflux. After

16 and 48 h, the aliquot (50 µL) from each reaction mixture was analyzed according to the *HPLC Method D,* and results are summarized in **Table 9**, *entry 4–6.*

Oppenauer Oxidation with *N*-Methyl-4-piperidinone (Table 9, Entry 7–9)

58, $X^1 = $ O, $X^2 = $ OH
59, $X^1 = $ OH, $X^2 = $ O
60, $X^1 = $ O, $X^2 = $ O
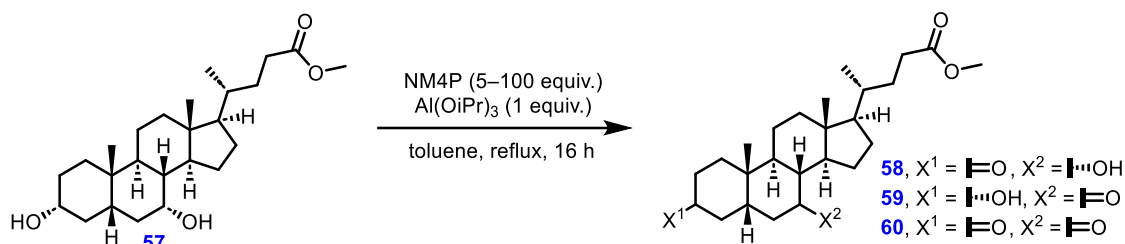
Methyl chenodeoxycholate (**57**, 200 mg, 0.49 mmol) and *N*-methyl-4-piperidinone (5, 50, or 100 equiv.) were dissolved in dry toluene (5 mL) under an inert atmosphere. Aluminum isopropoxide (1 equiv., 100 mg, 0.49 mmol) was added in one portion to each reaction vessel, and the reaction mixture was refluxed. After 16 and 48 h, an aliquot (50 µL) of each reaction mixture was analyzed according to the *HPLC Method D,* following the acidic quenching with an aqueous solution of hydrochloric acid (2 M, 500 µL). Results are summarized in **Table 9**, *entry 7–9.*

Steven's Oxidation (Table 9, Entry 10–15)

58, $X^1 = $ O, $X^2 = $ OH
59, $X^1 = $ OH, $X^2 = $ O
60, $X^1 = $ O, $X^2 = $ O

Methyl chenodeoxycholate (**57**, 200 mg, 0.49 mmol) was dissolved in glacial acetic acid (5 mL), and a solution of sodium hypochlorite (3.2% w/w aq. solution, 0.25, 0.50, 0.75, 1.0, 2.0 or 3.0 equiv.) was added in small portions. The reaction mixture was stirred at room temperature for 6 hours. Then, an aliquot (50 µL) of each reaction mixture was analyzed according to the *HPLC Method D,* and results are summarized in **Table 9**, *entry 10–15.*
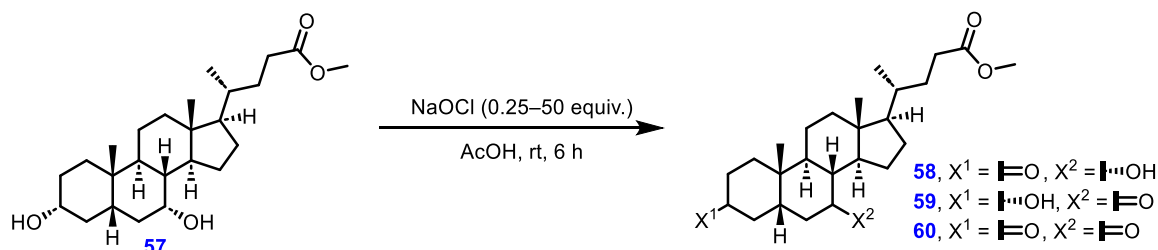
Jones Oxidation (Table 10, Entry 1)
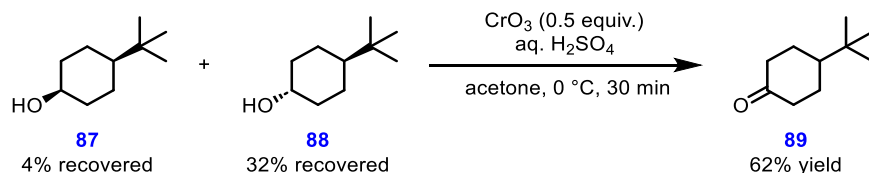
87
4% recovered

88
32% recovered

89
62% yield

A mixture of **87** and **88** (1:1 ^{1}H NMR, 390 mg, 2.5 mmol) was dissolved in acetone (25 mL), and a solution was cooled to 0 °C with an ice bath. Jones reagent was added in portions (2.67 M solution, 0.5 equiv., 1.25 mmol, total 0.47 mL). After 30 minutes of stirring, the reaction mixture was neutralized with a saturated solution of aqueous NaHCO$_3$. Then, water was added (25 mL), and the products were extracted with DCM (3 × 25 mL). The organic solvent was dried with MgSO$_4$ and evaporated with silica gel (2.5 g). The dry load of crude material was purified by flash chromatography on a silica gel. The elution with a gradient of Et$_2$O in PE (5% to 50% over 30 column

volumes) afforded compound **87** (17 mg, 4%), compound **88** (126 mg, 32%) and compound **89** (238 mg, 62%).

Corey–Schmidt Oxidation (Table 10, Entry 2)

A mixture of **87** and **88** (1:1 ^{1}H NMR, 390 mg, 2.5 mmol) and activated molecular sieves (3Å, finely grounded, 500 mg) were suspended in dry DCM (25 mL) under an inert atmosphere. Pyridinium dichromate (0.5 equiv., 470 mg, 1.25 mmol) was added, and the reaction mixture was stirred overnight at room temperature. After 16 hours, silica gel (2.5 g) was added to the reaction mixture, and the organic solvent was evaporated. The dry load of crude material was purified by flash chromatography on a silica gel. The elution with a gradient of Et$_2$O in PE (5% to 50% over 30 column volumes) afforded compound **87** (42 mg, 11%), compound **88** (86 mg, 17%), and compound **89** (240 mg, 62%).
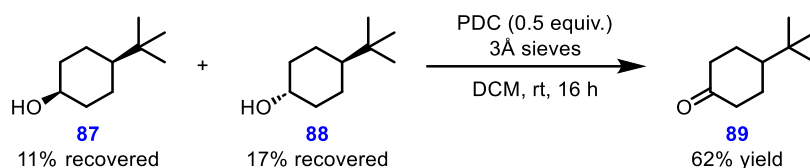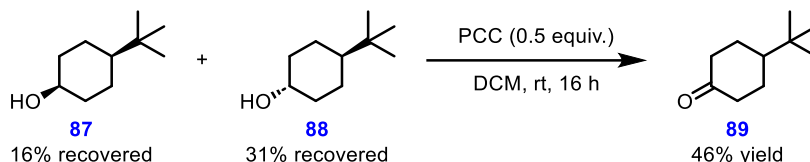
Corey–Suggs Oxidation (Table 10, Entry 3)

A mixture of **87** and **88** (1:1 ^{1}H NMR, 390 mg, 2.5 mmol) was dissolved in dry DCM (25 mL) under an inert atmosphere. Pyridinium chlorochromate (0.5 equiv., 269 mg, 1.25 mmol) was added. After 16 hours of stirring at room temperature, silica gel (2.5 g) was added to the reaction mixture, and the organic solvent was evaporated. The dry load of crude material was purified by flash chromatography on a silica gel. The elution with a gradient of Et$_2$O in PE (5% to 50% over 30 column volumes) afforded compound **87** (64 mg, 16%), compound **88** (123 mg, 31%), and compound **89** (178 mg, 46%).

Swern Reaction Oxidation (Table 10, Entry 4)
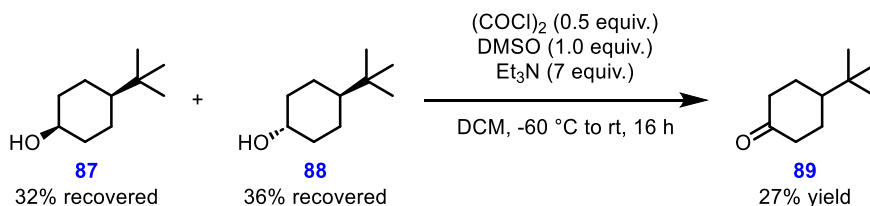
Dimethyl sulfoxide (1.0 equiv., 2.5 mmol, 177 µL, 90 ppm of water) was dissolved in dry DCM (20 mL) under an inert atmosphere. Then, the mixture of solvents was cooled to -60 °C in the ethanol/dry ice bath. Oxalyl chloride (1.0 M solution in DCM, 0.5 equiv., 1.25 mmol, 1.25 mL) was added in one portion, and the reaction mixture was stirred at -60 °C for 10 minutes. To this, a mixture of **87** and **88** (1:1 ^{1}H NMR, 390 mg, 2.5 mmol, dissolved in 5 mL of dry DCM) was added dropwise, and the reaction mixture was stirred at -40 °C for 15 minutes. Then, triethylamine (7 equiv., 17.5 mmol, 2.4 mL) was added in one portion, and the reaction mixture was allowed to slowly attain room

temperature, followed by stirring for 16 hours. The reaction was diluted with DCM (50 mL), washed with water (2 × 25 mL), brine (25 mL), and dried over Na_2SO_4. Silica gel (2.5 g) was added to the organic fraction, and solvents were evaporated. The dry load of crude material was purified by flash chromatography on a silica gel. The elution with a gradient of Et_2O in PE (5% to 50% over 30 column volumes) afforded compound **87** (125 mg, 32%), compound **88** (140 mg, 36%), and compound **89** (105 mg, 27%).

Omura–Sharma–Swern Oxidation (Table 10, Entry 5)

TFAA (0.5 equiv.)
DMSO (1.0 equiv.)
Et_3N (7 equiv.)
DCM, -60 °C to rt, overnight

87 34% recovered   **88** 36% recovered   **89** 26% yield

Dimethyl sulfoxide (1.0 equiv., 2.5 mmol, 177 µL, 90 ppm of water) was dissolved in dry DCM (20 mL) under an inert atmosphere at -60 °C in the ethanol/dry ice bath. To this mixture, trifluoroacetic anhydride (0.50 equiv., 1.25 mmol, 174 µL) was added in one portion, and the reaction mixture was stirred at -60 °C for an additional 15 minutes. To this, a mixture of **87** and **88** (1:1 ^{1}H NMR, 390 mg, 2.5 mmol, dissolved in 5 mL of dry DCM) was added dropwise, and the reaction mixture was stirred at -40 °C for 2 hours. Triethylamine (7 equiv., 17.5 mmol, 2.4 mL) was added in one portion, and the reaction mixture was allowed to attain room temperature overnight. The reaction was diluted with DCM (50 mL), washed with water (2 × 25 mL), brine (25 mL), and dried over Na_2SO_4. Silica gel (2.5 g) was added to the organic fraction, and solvents were evaporated. The dry load of crude material was purified by flash chromatography on a silica gel. The elution with a gradient of Et_2O in PE (5% to 50% over 30 column volumes) afforded compound **87** (131 mg, 34%), compound **88** (141 mg, 36%), and compound **89** (101 mg, 26%).
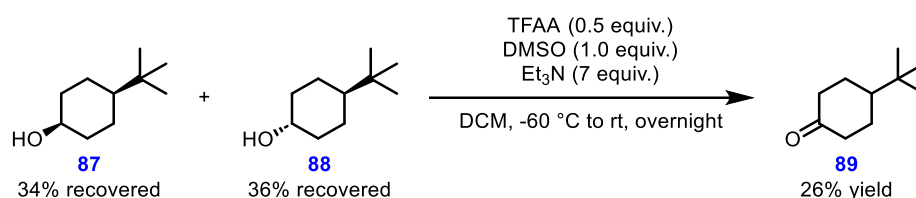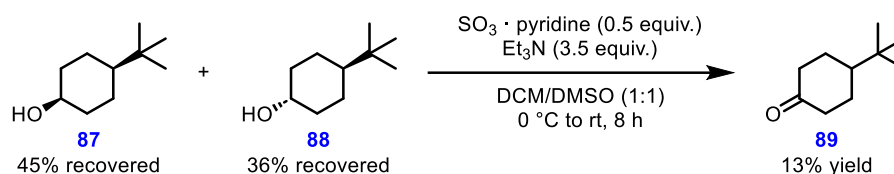
Parikh–Doering Oxidation (Table 10, Entry 6a)

$SO_3 \cdot$ pyridine (0.5 equiv.)
Et_3N (3.5 equiv.)
DCM/DMSO (1:1)
0 °C to rt, 8 h

87 45% recovered   **88** 36% recovered   **89** 13% yield

Pyridine sulfur trioxide complex (0.5 equiv., 1.25 mmol, 200 mg) was added into a solution of **87** and **88** (1:1 ^{1}H NMR, 390 mg, 2.5 mmol) in triethylamine (3.5 equiv., 8.75 mmol, 1.2 mL) and dry DCM/DMSO (25 mL, 1:1) at 0 °C under an inert atmosphere. The reaction mixture was allowed to attain room temperature. After 8 hours of stirring, water was added (25 mL) to quench the reaction. The products were extracted with DCM (3 × 25 mL), combined organic fractions were washed with water (2 × 25 mL), brine (25 mL), and dried over Na_2SO_4. Silica gel (2.5 g) was added to the organic fraction, and solvents were evaporated. The dry load of crude material was purified by flash chromatography on a silica gel. The elution with a gradient of Et_2O in PE (5% to 50% over 30 column volumes) afforded compound **87** (175 mg, 45%), compound **88** (142 mg, 36%), and compound **89** (52 mg, 13%).

Parikh–Doering Oxidation (Table 10, Entry 6b)
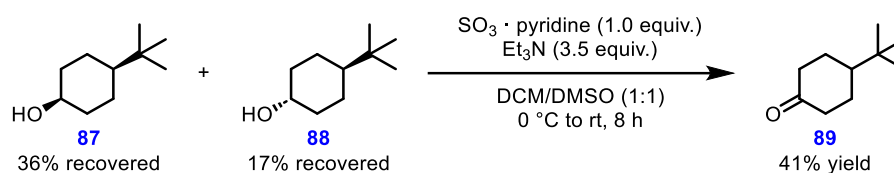
The reaction was performed in the same manner as *Parikh–Doering oxidation, entry 6a* but with 1 equivalent of pyridine sulfur trioxide complex (1.0 equiv., 2.5 mmol, 400 mg). Compound **87** (142 mg, 36%), compound **88** (68 mg, 17%), and compound **89** (159 mg, 41%) were isolated.

Anelli Oxidation (Table 10, Entry 7)
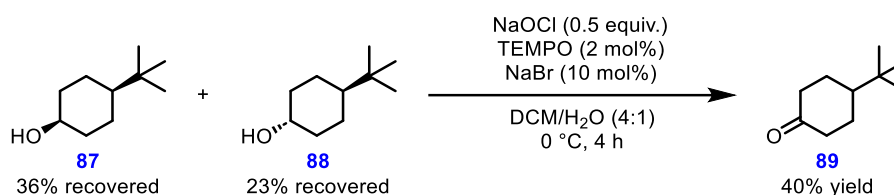
A mixture of **87** and (1:1 ^{1}H NMR, 390 mg, 2.5 mmol), NaBr (0.1 equiv., 0.25 mmol, 26 mg), and TEMPO (0.02 equiv., 8 mg, 0.05 mmol) were dissolved in a mixture of DCM/H$_2$O (25 mL, 4:1) at 0 °C. To a vigorously stirred solution, sodium hypochlorite (2.8% w/w aq. solution, 0.5 equiv., 1.25 mmol, 3.0 mL) was added in small portions. The reaction mixture was allowed to attain room temperature. After 3 hours of stirring, the organic phase was separated, and the water phase was washed with DCM (2 × 25 mL). The combined organic fractions were dried with MgSO$_4$. Silica gel (2.5 g) was added to the organic fraction, and solvents were evaporated. The dry load of crude material was purified by flash chromatography on a silica gel. The elution with a gradient of Et$_2$O in PE (5% to 50% over 30 column volumes) afforded compound **87** (140 mg, 36%), compound **88** (91 mg, 23%) and compound **89** (154 mg, 40%).

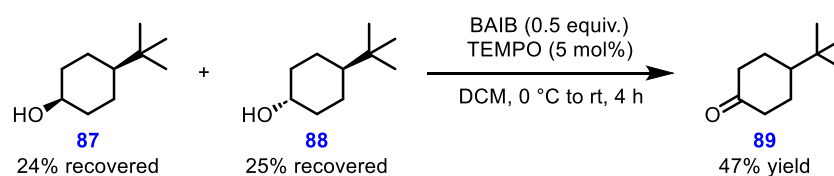**Piancatelli–Margarita Oxidation (Table 10, Entry 8)**

A mixture of **87** and **88** (1:1 ^{1}H NMR, 390 mg, 2.5 mmol), BAIB (0.5 equiv., 411 mg, 1.25 mmol), and TEMPO (0.1 equiv., 39 mg, 0.25 mmol) were dissolved in DCM (25 mL). The reaction mixture was stirred at 0 °C under an inert atmosphere. The reaction mixture was allowed to attain room temperature. After 3 hours of stirring, water was added (25 mL), and the organic phase was separated. Then, the water phase was washed with DCM (2 × 25 mL). The combined organic fractions were dried with MgSO$_4$. Silica gel (2.5 g) was added to the organic fraction, and solvents were evaporated. The dry load of crude material was purified by flash chromatography on a silica gel. The elution with a gradient of Et$_2$O in PE (5% to 50% over 30 column volumes) afforded compound **87** (95 mg, 24%), compound **88** (97 mg, 25%), and compound **89** (182 mg, 47%).

Jahn–Holan Oxidation (Table 10, Entry 9)
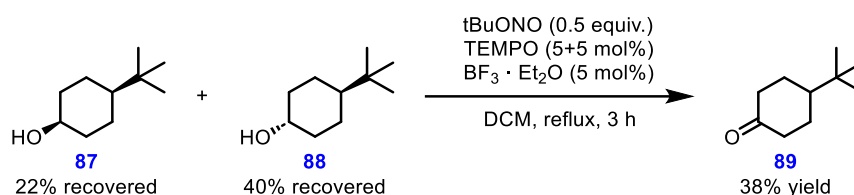
87
22% recovered

88
40% recovered

tBuONO (0.5 equiv.)
TEMPO (5+5 mol%)
$BF_3 \cdot Et_2O$ (5 mol%)

DCM, reflux, 3 h

89
38% yield

A mixture of **87** and **88** (1:1 ^{1}H NMR, 390 mg, 2.5 mmol) was dissolved in dry DCM (25 mL) under an inert atmosphere. Then, boron trifluoride etherate (0.05 equiv., 0.13 mmol, 17 µL) and *tert*-butyl nitrite (0.5 equiv., 1.25 mmol, 165 µL) were added in one portion, and the reaction mixture was heated to 35 °C. Next, a solution of TEMPO (0.05 equiv., 20 mg, 0.13 mmol, in 0.2 mL DCM) was added. After 1 hour of stirring, another portion of TEMPO (0.05 equiv., 20 mg, 0.13 mmol, in 0.2 mL DCM) was added, and the reaction mixture was stirred at 35 °C for 3 hours. Then, water was added (25 mL), the organic phase was separated, and the water phase was washed with DCM (2 × 25 mL). The combined organic fractions were dried with MgSO$_4$. Silica gel (2.5 g) was added to the organic fraction, and solvents were evaporated. The dry load of crude material was purified by flash chromatography on a silica gel. The elution with a gradient of Et$_2$O in PE (5% to 50% over 30 column volumes) afforded compound **87** (77 mg, 22%), compound **88** (158 mg, 40%), and compound **89** (146 mg, 38%).

o-Iodoxybenzoic Acid Oxidation (Table 10, Entry 10)

87
33% recovered

88
44% recovered

IBX (0.5 equiv.)

DMSO, rt, 24 h

89
14% yield
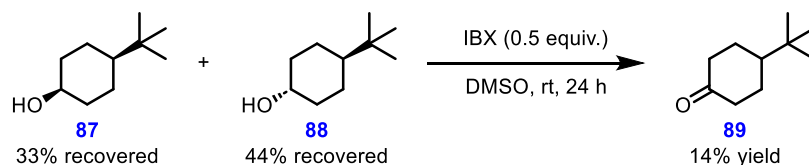
o-Iodoxybenzoic acid (0.5 equiv., 350 mg, 1.25 mmol) was added into a solution of **87** and **88** (1:1 ^{1}H NMR, 390 mg, 2.5 mmol) in dry DCM (25 mL) under an inert atmosphere. The reaction mixture was stirred at room temperature. After 24 hours, DCM (100 mL) was added, and the organic fraction was washed with water (3 × 50 mL), brine (50 mL), and dried over Na$_2$SO$_4$. Silica gel (2.5 g) was added to the organic fraction, and solvents were evaporated. The dry load of crude material was purified by flash chromatography on a silica gel. The elution with a gradient of Et$_2$O in PE (5% to 50% over 30 column volumes) afforded compound **87** (130 mg, 33%), compound **88** (170 mg, 44%), and compound **89** (53 mg, 14%).
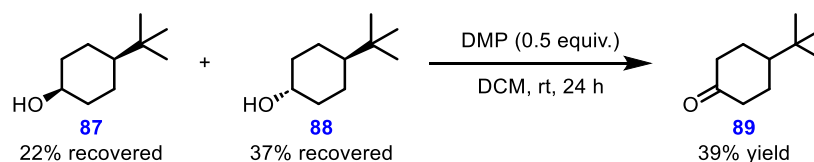
Dess–Martin Oxidation (Table 10, Entry 11)

87
22% recovered

88
37% recovered

DMP (0.5 equiv.)

DCM, rt, 24 h

89
39% yield

Dess–Martin periodinane was added in (0.5 equiv., 530 mg, 1.25 mmol) a solution of **87** and **88** (1:1 ^{1}H NMR, 390 mg, 2.5 mmol) in DCM (25 mL). After stirring at room temperature for 24 hours, silica gel (2.5 g) was added to the reaction mixture, and solvents were evaporated. The dry load of crude material was purified by flash chromatography on a silica gel. The elution with a gradient of Et$_2$O in

PE (linear gradient 5% to 50% over 30 column volumes) afforded compound **87** (86 mg, 22%), compound **88** (144 mg, 37%), and compound **89** (150 mg, 39%).

Catalytic RuO$_4$ Oxidation (Table 10, Entry 12)
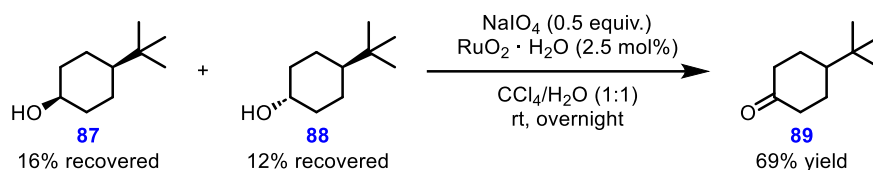
Ruthenium(IV) oxide hydrate (2.5 mol%, 9 mg, 0.06 mmol) was added into a solution of **87** and **88** (1:1 ^{1}H NMR, 390 mg, 2.5 mmol), and sodium periodate (0.5 equiv., 267 mg, 1.25 mmol) in CCl$_4$/H$_2$O (25 mL, 1:1) under an inert atmosphere. After 12 hours of stirring, the organic phase was separated and dried over Na$_2$SO$_4$. Silica gel (2.5 g) was added to the organic phase, and solvents were evaporated. The dry load of crude material was purified by flash chromatography on a silica gel. The elution with a gradient of Et$_2$O in PE (5% to 50% over 30 column volumes) afforded compound **87** (61 mg, 16%), compound **88** (47 mg, 12%), and compound **89** (265 mg, 69%).

Ley Oxidation (Table 10, Entry 13)

N-Methylmorpholine *N*-oxide (0.5 equiv., 146 mg, 1.25 mmol) and activated molecular sieves (3Å, grounded, 200 mg) were added into a solution of **87** and **88** (1:1 ^{1}H NMR, 390 mg, 2.5 mmol) in dry DCM (25 mL) under an inert atmosphere. Then, tetrapropylammonium perruthenate (2.5 mol%, 22 mg, 0.06 mmol) was added in one portion, and the reaction mixture was stirred at room temperature overnight. Silica gel (2.5 g) was added to the organic phase, and solvents were evaporated. The dry load of crude material was purified by flash chromatography on a silica gel. The elution with a gradient of Et$_2$O in PE (5% to 50% over 30 column volumes) afforded compound **87** (120 mg, 31%), compound **88** (118 mg, 30%), and compound **89** (140 mg, 36%).

Fétizon Oxidation (Table 10, Entry 14)

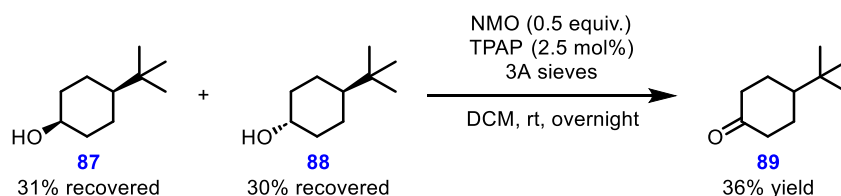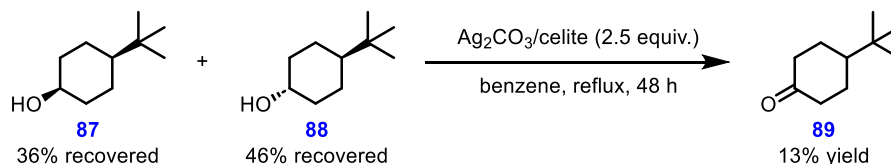Silver carbonate on Celite (50% w/w loading, 2.5 equiv., 3.45 g, 6.25 mmol) was added into a solution of **87** and **88** (1:1 ^{1}H NMR, 390 mg, 2.5 mmol) in dry benzene (25 mL) under an inert atmosphere. The reaction mixture was refluxed for 48 hours. Then, it was filtered through a short column of Celite (approx. 5 g) and washed with DCM (3 × 50 mL). Silica gel (2.5 g) was added to the organic phase, and solvents were evaporated. The dry load of crude material was purified by flash chromatography on a silica gel. The elution with a gradient of Et$_2$O in PE (5% to 50% over 30 column volumes) afforded compound **87** (140 mg, 36%), compound **88** (181 mg, 46%), and compound **89** (52 mg, 13%).

Oppenauer Oxidation with Cyclohexanone (Table 10, Entry 15)
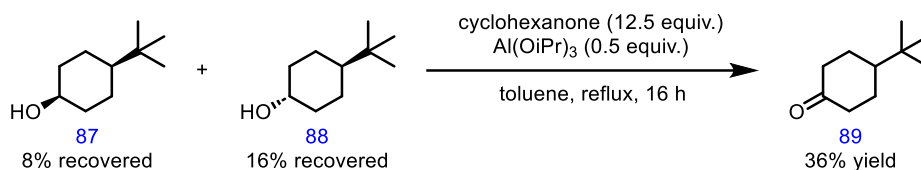
Aluminum isopropoxide (1 equiv., 511 mg, 2.5 mmol) was added into a solution of **87** and **88** (1:1 ^{1}H NMR, 390 mg, 2.5 mmol), and cyclohexanone (12.5 equiv., 31.25 mmol, 3.2 mL) in dry toluene (25 mL) under an inert atmosphere. After stirring for 16 hours under reflux, a solution of aqueous hydrochloric acid (2M, 25 mL) was added, and the reaction mixture was extracted with DCM (3 × 50 mL). The combined organic fractions were washed with brine (25 mL) and dried over Na_2SO_4. Silica gel (2.5 g) was added to the organic phase, and solvents were evaporated. The dry load of crude material was purified by flash chromatography on a silica gel. The elution with a gradient of Et_2O in PE (5% to 50% over 30 column volumes) afforded compound **87** (31 mg, 8%), compound **88** (62 mg, 16%), and compound **89** (140 mg, 36%).

Steven's Oxidation (Table 10, Entry 16)
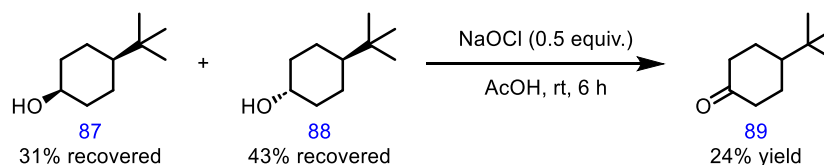
A solution of sodium hypochlorite (2.8% w/w aq. solution, 0.5 equiv., 1.25 mmol, 3.0 mL) was added in small portions into a solution of **87** and **88** (1:1 ^{1}H NMR, 390 mg, 2.5 mmol) in glacial acetic acid (25 mL). The reaction was stirred at room temperature for 6 hours. Then, it was neutralized with a saturated solution of aqueous $NaHCO_3$ and extracted with DCM (3 × 50 mL). Combined organic fractions were washed with water (50 mL), brine (50 mL), and dried over Na_2SO_4. Silica gel (2.5 g) was added to the organic phase, and solvents were evaporated. The dry load of crude material was purified by flash chromatography on a silica gel. The elution with a gradient of Et_2O in PE (5% to 50% over 30 column volumes) afforded compound **87** (121 mg, 31%), compound **88** (167 mg, 43%), and compound **89** (91 mg, 24%).

Anelli Oxidation (Table 11, Entry 1)
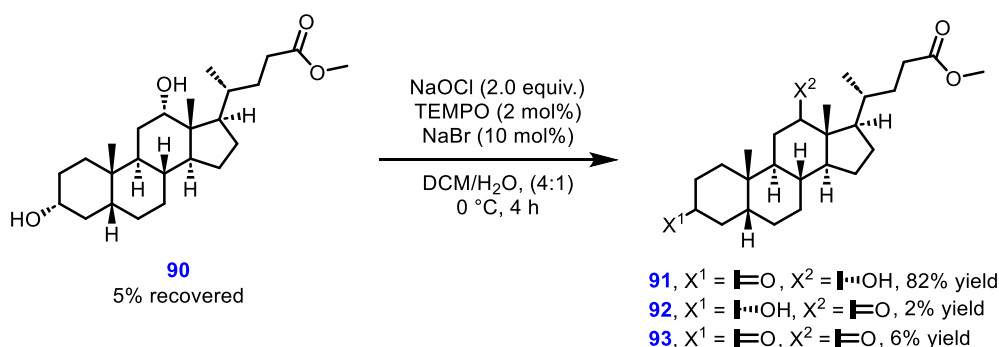
Methyl deoxycholate (**90**, 1.0 g, 2.5 mmol), NaBr (0.1 equiv., 0.25 mmol, 26 mg), and TEMPO (0.02 equiv., 8 mg, 0.05 mmol) were dissolved in a mixture of DCM/H$_2$O (25 mL, 4:1) at 0 °C. To a vigorously stirred solution, sodium hypochlorite (2.8% w/w aq. solution, 1.0 equiv., 2.5 mmol, 6.0

mL) was added in small portions. The reaction mixture was allowed to attain room temperature. After 3 hours of stirring, the organic phase was separated, and the water phase was washed with DCM (2 × 25 mL). The combined organic fractions were dried with $MgSO_4$. Silica gel (2.5 g) was added to the organic fraction, and solvents were evaporated. The dry load of crude material was purified by flash chromatography on a silica gel. Elution with a gradient of EtOAc in PE (5% to 50% over 35 column volumes) afforded compound **90** (52 mg, 5%), compound **91** (824 mg, 82%), compound **92** (21 mg, 2%), and compound **93** (60 mg, 6%).

Piancatelli–Margarita Oxidation (Table 11, Entry 2)

90
2% recovered

91, X^1 = O, X^2 = OH, 87% yield
92, X^1 = OH, X^2 = O, 1% yield
93, X^1 = O, X^2 = O, 2% yield

Methyl deoxycholate (**90**, 1.0 g, 2.5 mmol), BAIB (3.0 equiv., 2.47 g, 7.5 mmol), and TEMPO (0.05 equiv., 20 mg, 0.125 mmol) were dissolved in DCM (25 mL). The reaction mixture was stirred at 0 °C under an inert atmosphere. The reaction mixture was allowed to attain room temperature. After 3 hours of stirring, water was added (25 mL), and the organic phase was separated. Then, the water phase was washed with DCM (2 × 25 mL). The combined organic fractions were dried with $MgSO_4$. Silica gel (2.5 g) was added to the organic fraction, and solvents were evaporated. The dry load of crude material was purified by flash chromatography on a silica gel. Elution with a gradient of EtOAc in PE (5% to 50% over 35 column volumes) afforded compound **90** (20 mg, 2%), compound **91** (868 mg, 87%), compound **92** (12 mg, 1%), and compound **93** (15 mg, 2%).

Dess–Martin Oxidation (Table 11, Entry 3)

90
4% recovered

91, X^1 = O, X^2 = OH, 1% yield
92, X^1 = OH, X^2 = O, 85% yield
93, X^1 = O, X^2 = O, 9% yield

Dess–Martin periodinane (1.0 equiv., 1.06 g, 2.5 mmol) was added to a solution of methyl deoxycholate (**90**, 1.0 g, 2.5 mmol) in DCM (25 mL). After stirring at room temperature for 24 hours, silica gel (2.5 g) was added to the reaction mixture, and solvents were evaporated. The dry load of crude material was purified by flash chromatography on a silica gel. Elution with a gradient of EtOAc in PE (5% to 50% over 35 column volumes) afforded compound **90** (42 mg, 4%), compound **91** (8 mg, 1%), compound **92** (853 mg, 85%), and compound **93** (91 mg, 9%).

Steven's Oxidation (Table 11, Entry 4)

90
3% recovered

NaOCl (1.0 equiv.)

AcOH, rt, 6 h

91, $X^1 = $ O, $X^2 = $ OH, 14% yield
92, $X^1 = $ OH, $X^2 = $ O, 73% yield
93, $X^1 = $ O, $X^2 = $ O, 5% yield

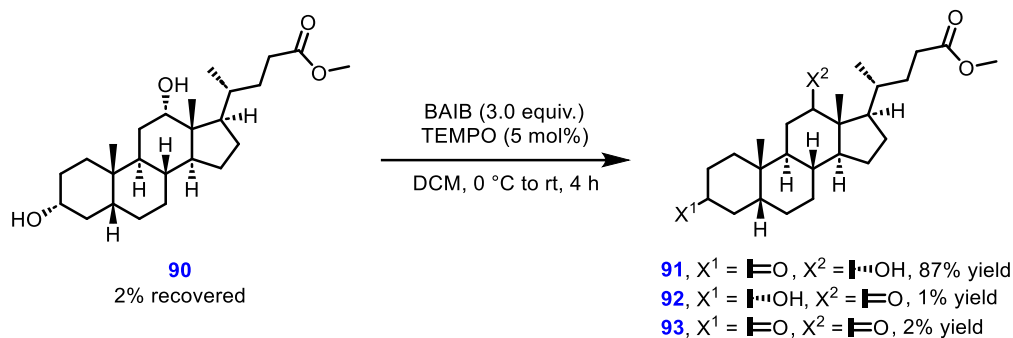A solution of sodium hypochlorite (2.8% w/w aq. solution, 1.0 equiv., 2.5 mmol, 6.0 mL) was added in small portions into a solution of methyl deoxycholate (**90**, 1.0 g, 2.5 mmol), in glacial acetic acid (25 mL). The reaction was stirred at room temperature for 6 hours. Then, it was neutralized with a saturated solution of aqueous NaHCO₃ and extracted with DCM (3 × 50 mL). Combined organic fractions were washed with water (50 mL), brine (50 mL), and dried over Na₂SO₄. Silica gel (2.5 g) was added to the organic phase, and solvents were evaporated. The dry load of crude material was purified by flash chromatography on a silica gel. Elution with a gradient of EtOAc in PE (5% to 50% over 35 column volumes) afforded compound **90** (31 mg, 3%), compound **91** (142 mg, 14%), compound **92** (733 mg, 73%), and compound **93** (51 mg, 5%).

Anelli Oxidation (Table 12, Entry 1)

94
22% recovered

NaOCl (2.0 equiv.)
TEMPO (2 mol%)
NaBr (10 mol%)

DCM/DMSO/H₂O (10:1:2)
0 °C, 4 h

95, $X^1 = $ O, $X^2 = $ OH, 21% yield
96, $X^1 = $ OH, $X^2 = $ O, 19% yield
97, $X^1 = $ O, $X^2 = $ O, not isolated

5α-Cholestane-2α,3α-diol (**94**, 1.0 g, 2.5 mmol), NaBr (0.1 equiv., 0.25 mmol, 26 mg), and TEMPO (0.02 equiv., 8 mg, 0.05 mmol) were dissolved in a mixture of DCM/H₂O (25 mL, 4:1) at 0 °C. To a vigorously stirred solution, sodium hy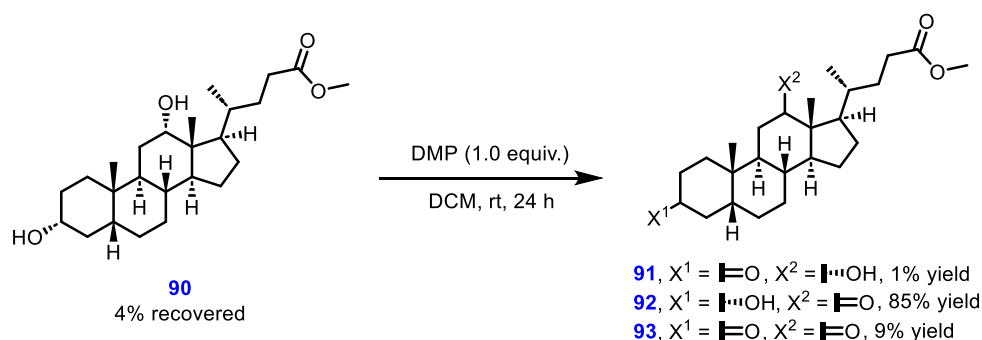pochlorite (2.8% w/w aq. solution, 1.0 equiv., 2.5 mmol, 6.0 mL) was added in small portions. After full reagent addition, the reaction mixture was allowed to attain room temperature. After 3 hours of stirring, the organic phase was separated, the water phase was washed with DCM (2 × 25 mL), and the combined organic fractions were dried over MgSO₄. After filtration, silica gel (2.5 g) was added to the liquor, and solvents were evaporated. The dry load of crude material was purified by flash chromatography on a silica gel. Elution with a gradient of EtOAc in PE (5% to 50% over 35 column volumes) afforded compound **94** (22 mg, 22%), compound **95** (21 mg, 21%), and compound **96** (19 mg, 19%), and an inseparable mixture of oily non-polar products (9 mg).

Piancatelli–Margarita Oxidation (Table 12, Entry 2)

94
10% recovered

BAIB (3.0 equiv.)
TEMPO (5 mol%)

DCM/DMSO (10:1)
0 °C to rt, 4 h

95, $X^1 = $ O, $X^2 = $ OH, 25% yield
96, $X^1 = $ OH, $X^2 = $ O, 22% yield
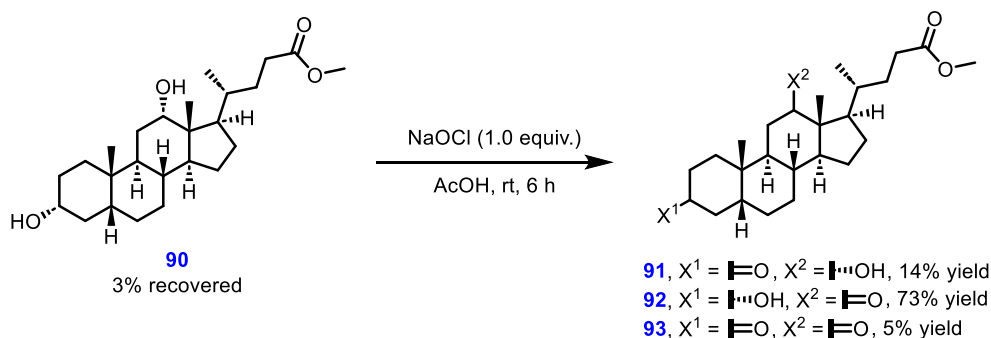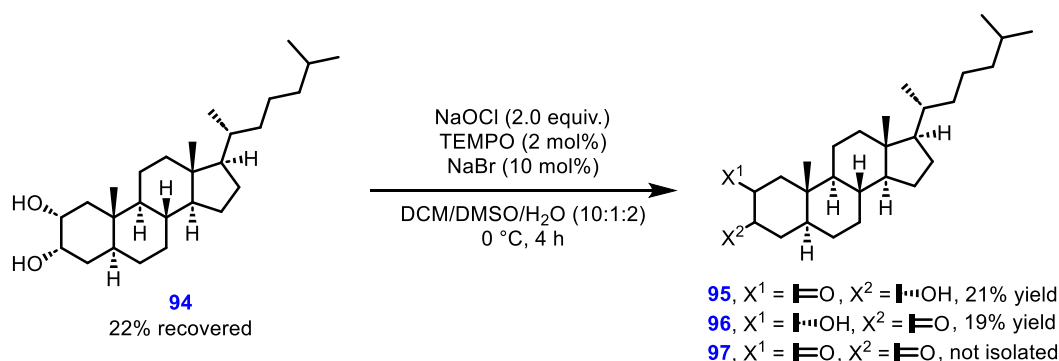**97**, $X^1 = $ O, $X^2 = $ O, not isolated

5α-Cholestane-2α,3α-diol (**94**, 1.0 g, 2.5 mmol), BAIB (3.0 equiv., 2.47 g, 7.5 mmol), and TEMPO (0.05 equiv., 20 mg, 0.125 mmol) were dissolved in DCM/DMSO (25 mL, 10:1). The reaction mixture was stirred at 0 °C under an inert atmosphere. The reaction mixture was allowed to attain room temperature. After 3 hours of stirring, water was added (25 mL), and the organic phase was separated. Then, the water phase was washed with DCM (2 × 25 mL). The combined organic fractions were dried with MgSO₄. Silica gel (2.5 g) was added to the organic fraction, and solvents were evaporated. The dry load of crude material was purified by flash chromatography on a silica gel. Elution with a gradient of EtOAc in PE (5% to 50% over 35 column volumes) afforded compound **94** (10 mg, 10%), compound **95** (25 mg, 25%), and compound **96** (22 mg, 22%) and an inseparable mixture of oily non-polar products (15 mg).

Dess–Martin Oxidation (Table 12, Entry 3)

94
30% recovered

DMP (1.0 equiv.)

DCM/DMSO (10:1)
rt, 24 h

95, $X^1 = $ O, $X^2 = $ OH, 21% yield
96, $X^1 = $ OH, $X^2 = $ O, 23% yield
97, $X^1 = $ O, $X^2 = $ O, not isolated
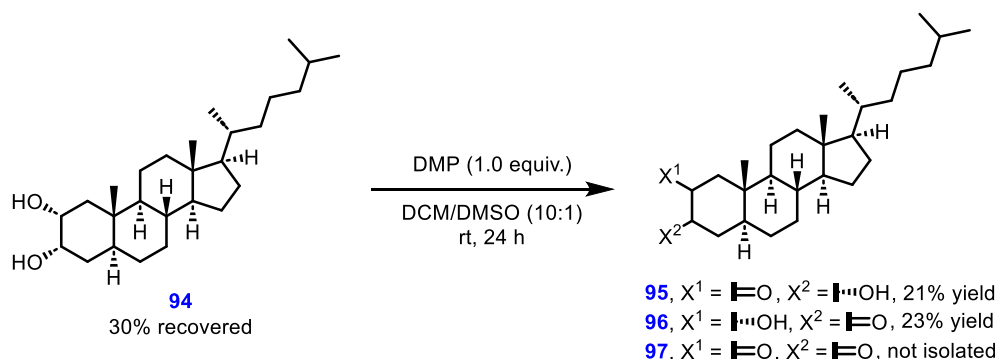
Dess–Martin periodinane (1.0 equiv., 1.06 g, 2.5 mmol) was added in a solution of 5α-cholestane-2α,3α-diol (**94**, 1.0 g, 2.5 mmol), in DCM/DMSO (25 mL, 10:1). After stirring at room temperature for 24 hours, silica gel (2.5 g) was added into the reaction mixture and solvents were evaporated. The dry load of crude material was purified by flash chromatography on a silica gel. Elution with a gradient of EtOAc in PE (5% to 50% over 35 column volumes) afforded compound **94** (30 mg, 30%), compound **95** (21 mg, 21%), and compound **96** (23 mg, 23%) and an inseparable mixture of oily non-polar products (21 mg).
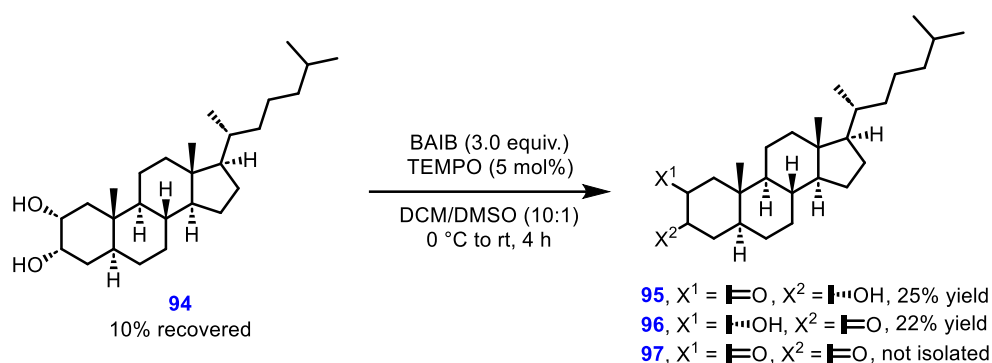
Steven's Oxidation (Table 12, Entry 4)

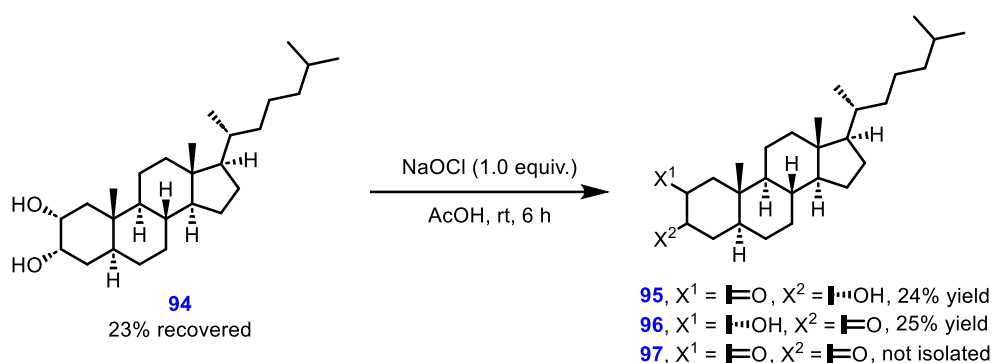A solution of sodium hypochlorite (2.8% w/w aq. solution, 1.0 equiv., 2.5 mmol, 6.0 mL) was added in small portions into a solution of 5α-cholestane-2α,3α-diol (**94**, 1.0 g, 2.5 mmol), in glacial acetic acid (25 mL). The reaction was stirred at room temperature for 6 hours. Then, it was neutralized with a saturated solution of aqueous $NaHCO_3$ and extracted with DCM (3 × 50 mL). Combined organic fractions were washed with water (50 mL), brine (50 mL), and dried over Na_2SO_4. Silica gel (2.5 g) was added to the organic phase, and solvents were evaporated. The dry load of crude material was purified by flash chromatography on a silica gel. Elution with a gradient of EtOAc in PE (5% to 50% over 35 column volumes) afforded compound **94** (23 mg, 23%), compound **95** (24 mg, 24%), and compound **96** (25 mg, 25%) and an inseparable mixture of oily non-polar products (18 mg).
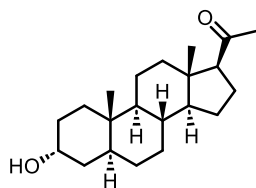
6.3 COMPOUND SYNTHESIS AND ANALYTICAL DATA

3α-Hydroxy-5α-pregnan-20-one (1)

Compound **1** was taken from the group deposit, with the appearance of fine white powder. Selected ^{1}H NMR (401 MHz, CDCl$_3$): δ 4.04 (t, J = 2.7 Hz, 1H, H-3), 2.52 (t, J = 8.9 Hz, 1H, H-17), 2.10 (s, 3H, H-21), 0.77 (s, 3H, H-19), 0.60 (s, 3H, H-18). ^{13}C NMR (101 MHz, CDCl$_3$): δ 209.9 (C20), 66.7 (C3), 64.0, 56.9, 54.3, 44.4, 39.2, 39.2, 36.3, 36.0, 35.6, 32.3, 32.1, 31.7, 29.1, 28.6, 24.5, 22.9, 20.9, 13.6 (C18), 11.3 (C19). The NMR analysis is consistent with the previous report.[273] LRMS (APCI pos): m/z 301.0 (100%, [M-H$_2$O+H]$^+$), 318.9 (60%, [M+H]$^+$). Purity 98.9% (*HPLC Method B*, t_R = 19.99 min).

(20S)-5α-Pregnan-3α,20-diol (2)
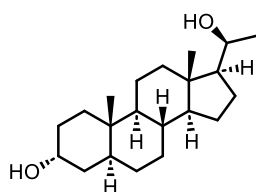
Compound **2** was purchased from Steraloids (Newport, RI, USA, cat. P1950-000, Batch L1844). LRMS (DUIS pos): m/z 285.2 (100%, [M-2H$_2$O+H]$^+$), 303.2 (5%, [M-H$_2$O+H]$^+$). Purity 97.3% (*HPLC Method C*, t_R = 3.35 min).

(20S)-5α-Pregnan-3β,20-diol (3)

Compound **3** as purchased from Steraloids (Newport, RI, USA, cat. P2050-000, Batch L1286). LRMS (DUIS pos): m/z 285.3 (100%, [M-2H$_2$O+H]$^+$), 303.2 (15%, [M-H$_2$O+H]$^+$), 344.2 (5%, [M+Na]$^+$). Purity 99.9% (*HPLC Method C*, t_R = 2.30 min).

(20R)-5α-Pregnan-3β,6β,20-triol (4)
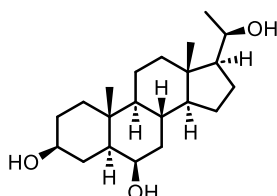
Compound **4** was taken from the group deposit, with the appearance of fine white powder. Selected ^{1}H NMR (401 MHz, CDCl$_3$/CD$_3$OD*/(CD$_3$)$_2$SO, 1:1:1): δ 3.57 (q, J = 2.8 Hz, 1H, H-6), 3.48 (dq, J = 11.7, 5.9 Hz, 1H, H-20), 3.38 (tt, J = 10.6, 4.8 Hz, 1H, H-3), 0.98 (dd, J = 6.1, 1.0 Hz, 3H, H-21), 0.91 (d, J = 2.8 Hz, 3H, H-19), 0.66 (s, 3H, H-18). ^{13}C NMR (101 MHz, CDCl$_3$/CD$_3$OD*/(CD$_3$)$_2$SO, 1:1:1): δ 69.0 (C3), 68.8 (C6), 67.3 (C20), 56.5, 54.2, 52.8, 46.1, 40.9, 38.1, 37.0, 34.3, 34.2, 33.8, 29.9, 28.7, 24.1, 23.0, 22.2 (C21), 19.2, 14.1 (C19), 10.8 (C18). LRMS (APCI pos): m/z 283.1 (60%, [M-3H$_2$O+H]$^+$), 301.3 (100%, [M-2H$_2$O+H]$^+$), 319.0 (35%, [M-H$_2$O+H]$^+$). Purity 99.9% (*HPLC Method B*, t_R = 8.60 min).

*Chemical shift reference solvent.

5α-Pregnan-3,20-dione (5)
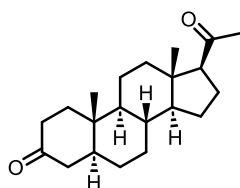
Compound **5** was taken from the group deposit, with the appearance of fine white powder. Selected ^{1}H NMR (401 MHz, CDCl$_3$): δ 2.52 (t, *J* = 9.0 Hz, 1H, H-17), 2.11 (s, 3H, H-21), 1.01 (s, 3H, H-19), 0.63 (s, 3H, H-18). ^{13}C NMR (101 MHz, CDCl$_3$): δ 212.0 (C3), 209.7 (C20), 63.9, 56.6, 53.8, 46.8, 44.8, 44.3, 39.1, 38.7, 38.3, 35.8, 35.5, 31.8, 31.7, 29.0, 24.6, 23.0, 21.6, 13.6, 11.6. The NMR analysis is consistent with the previous report.[274] LRMS (APCI pos): *m/z* 317.1 (100%, [M+H]$^+$). Purity 97.0% (*HPLC Method B*, t$_R$ = 19.57 min).
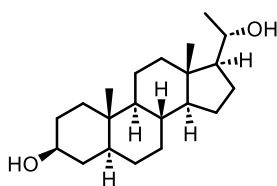
21-Hydroxy-5α-pregnan-3,20-dione (6)
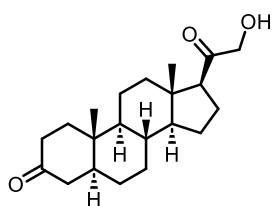
Compound **6** was taken from the group deposit, with the appearance of fine white powder. Selected ^{1}H NMR (500 MHz, CDCl$_3$*/CD$_3$OD, 1:1): δ 3.88 (d, *J* = 18.7 Hz, 1H, H$_a$-21), 3.81 (d, *J* = 18.7 Hz, 1H, H$_b$-21), 2.18 (t, *J* = 8.8 Hz, 1H, H-17), 0.47 (s, 3H, H-19), 0.30 (s, 3H, H-18). ^{13}C NMR (126 MHz, CDCl$_3$/CD$_3$OD, 1:1): δ 212.6 (C3), 210.8 (C20), 69.1 (C21), 59.0, 56.7, 54.0, 44.8, 42.4, 38.7, 35.7, 35.5, 35.2, 35.0, 31.9, 28.3, 28.2, 24.4, 22.8, 21.1, 13.3 (C19), 11.3 (C18). The NMR analysis is consistent with the previous report.[275] LRMS (ESI pos): *m/z* 333.2 (100%, [M+H]$^+$). Purity 99.5% (*HPLC Method B*, t$_R$ = 18.04 min).

*Chemical shift reference solvent.

5α-Androst-1-en-17-one (7)
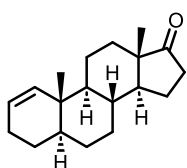
Compound **7** was taken from the group deposit, with the appearance of fine white powder. Selected ^{1}H NMR (401 MHz, CDCl$_3$): δ 5.66–5.52 (m, 2H, H-1 and H-2), 2.44 (ddd, *J* = 19.1, 9.0, 1.1 Hz, 1H, H$_a$-16), 2.06 (dt, *J* = 19.0, 9.0 Hz, 1H, H$_b$-16), 0.87 (d, *J* = 0.5 Hz, 3H, H-19), 0.78 (d, *J* = 0.7 Hz, 3H, H-18). ^{13}C NMR (101 MHz, CDCl$_3$): δ 221.6 (C17), 125.92 and 125.88 (C1 and C2), 54.3, 51.6, 47.9, 41.6, 39.8, 36.0, 35.3, 34.9, 31.7, 30.8, 30.4, 28.6, 21.9, 20.3, 13.9 (C18), 11.8 (C19). The NMR analysis is consistent with the previous report.[276] LRMS (APCI pos): *m/z* 255.1 (90%, [M-H$_2$O+H]$^+$), 273.0 (100%, [M+H]$^+$). Purity 96.8% (*HPLC Method B*, t$_R$ = 26.38 min).

3α-Hydroxy-5β-pregnan-20-one (8)
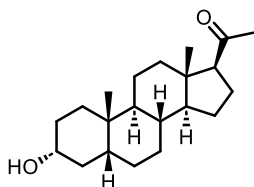
Compound **8** was taken from the group deposit, with the appearance of fine white powder. Selected ^{1}H NMR (401 MHz, CDCl$_3$): δ 3.64 (tt, *J* = 11.0, 4.7 Hz, 1H, H-3), 2.53 (t, *J* = 8.9 Hz, 1H, H-17), 2.11 (s, 3H, H-21), 0.92 (s, 3H, H-19), 0.59 (s, 3H, H-18). ^{13}C NMR (101 MHz, CDCl$_3$): δ 209.9 (C20), 71.9 (C3), 64.0, 56.9, 44.5, 42.1, 40.6, 39.4, 36.5, 36.0, 35.5, 34.8, 31.7, 30.6, 27.2, 26.5, 24.6, 23.5 (C19), 23.0, 21.0, 13.6 (C18). The NMR analysis is consistent with the previous report.[277] LRMS (APCI pos): *m/z* 301.1 (100%, [M-H$_2$O+H]$^+$), 319.0 (15%, [M+H]$^+$). Purity 99.9% (*HPLC Method B*, t$_R$ = 18.28 min).

(20*S*)-5β-Pregnan-3α,20-diol (9)
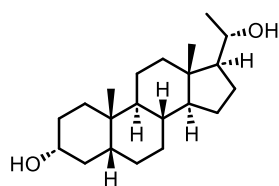
Compound **9** was taken from the group deposit, with the appearance of fine white powder. Selected ^{1}H NMR (401 MHz, CD$_3$OD): δ 3.63–3.49 (m, 2H, H-20 and H-3), 1.19 (d, *J* = 6.2 Hz, 3H, H-21), 0.93 (s, 3H, H-19), 0.65 (s, 3H, H-18). ^{13}C NMR (101 MHz, CD$_3$OD): δ 72.2 (C3), 70.9 (C20), 59.6 (C17), 57.6, 43.3, 42.8 (C13), 41.7, 40.4, 36.9, 36.7, 36.3, 35.5 (C10), 31.0, 28.2, 27.5, 27.3, 25.0, 23.94 (C19), 23.90 (C21), 21.5, 12.9 (C18). LRMS (DUIS pos): *m/z* 285.3 (100%, [M-2H$_2$O+H]$^+$), 303.2 (15%, [M-H$_2$O+H]$^+$). Purity 99.9% (*HPLC Method C*, t$_R$ = 3.18 min).

(20*R*)-20-Hydroxy-5β-pregnan-3α-yl Acetate (10)
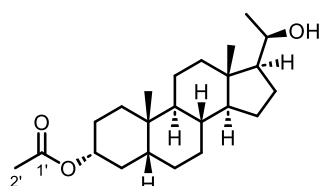
Compound **10** was taken from the group deposit, with the appearance of fine white powder. Selected ^{1}H NMR (401 MHz, CDCl$_3$): δ 4.72 (tt, *J* = 11.4, 4.8 Hz, 1H, H-3), 3.72 (dq, *J* = 9.8, 5.7 Hz, 1H, H-20), 2.03 (s, 3H, H-2'), 1.13 (d, *J* = 6.1 Hz, 3H, H-21), 0.93 (s, 3H, H-19), 0.73 (s, 3H, H-18). ^{13}C NMR (101 MHz, CDCl$_3$): δ 170.7 (C1'), 74.4 (C3), 70.6 (C20), 58.7, 56.0, 42.6, 41.9, 40.5, 40.3, 35.7, 35.1, 34.7, 32.3, 27.0, 26.7, 26.4, 25.7, 24.5, 23.6, 23.4, 21.5, 20.7, 12.6 (C18). The NMR analysis is consistent with the previous report.[278] LRMS (APCI pos): *m/z* 285.1 (100%, [M-AcOH-H$_2$O+H]$^+$), 344.9 (30%, [M-H$_2$O+H]$^+$). Purity 99.9% (*HPLC Method B*, t$_R$ = 25.43 min).

3α-Hydroxy-5β-pregnan-20-one-7α-yl Acetate (11)
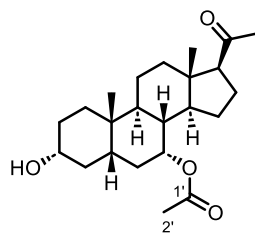
Compound **11** was taken from the group deposit, with the appearance of fine white powder. Selected ^{1}H NMR (401 MHz, CDCl$_3$): δ 4.89 (q, *J* = 3.2 Hz, 1H, H-7), 3.58–3.44 (m, 1H, H-3), 2.55 (t, *J* = 9.3 Hz, 1H, H-17), 2.12 (s, 3H, H-2'), 2.05 (s, 3H, H-21), 0.92 (s, 3H, H-19), 0.60 (s, 3H, H-18). ^{13}C NMR (101 MHz, CDCl$_3$): δ 209.5 (C20), 170.6 (C1'), 71.8 (C7), 71.4 (C3), 63.7, 50.8, 44.4, 41.2, 39.0, 38.7, 38.1, 35.3, 34.9, 34.3, 31.7, 31.5, 30.7, 23.9, 23.0, 22.8, 21.7, 20.8, 13.2 (C18). LRMS (APCI pos): *m/z* 299.1 (100%, [M-AcOH-H]$^+$), 316.9 (45%, [M-AcOH+H]$^+$). Purity 95.6% (*HPLC Method B*, t$_R$ = 11.91 min).

3α-Hydroxy-20-methylene-5β-pregnane (12)

Compound **12** was taken from the group deposit, with the appearance of fine white powder. Selected ^{1}H NMR (401 MHz, CDCl$_3$): δ 4.84 (brs, 1H, H$_a$-1'), 4.70 (brs, 1H, H$_b$-1'), 3.63 (tt, *J* = 11.1, 4.7 Hz, 1H, H-3), 2.03 (t, *J* = 9.1 Hz, 1H, H-17), 1.75 (s, 3H, H-21), 0.92 (s, 3H, H-19), 0.55 (s, 3H, H-18). ^{13}C NMR (101 MHz, CDCl$_3$): δ 145.9 (C20), 110.8 (C1'), 72.0 (C3), 57.5, 56.5, 43.6, 42.3, 40.8, 39.2, 36.6, 36.4, 35.5, 34.8, 30.7, 27.3, 26.6, 25.6, 24.8, 24.4, 23.5 (C19), 21.0, 13.0 (C18). The NMR analysis is consistent with the previous report.[279] LRMS (APCI pos): *m/z* 299.1 (100%, [M-H$_2$O+H]$^+$). Purity 99.9% (*HPLC Method B*, t$_R$ = 17.60 min).

(20*R*)-5β-Pregnan-3β,20-diol (13)

Compound **13** was purchased from Steraloids (Newport, RI, USA, cat. P6140-000, Batch L746 LRMS (DUIS pos): *m/z* 285.3 (100%, [M-2H$_2$O+H]$^+$), 303.3 (15%, [M-H$_2$O+H]$^+$). Purity 99.9% (*HPLC Method C*, t$_R$ = 3.65 min).

(20*S*)-20-Hydroxy-5β-pregnan-3β-yl Acetate (14)

Compound **14** was taken from the group deposit, with the appearance of fine white powder. Selected ^{1}H NMR (401 MHz, CDCl$_3$): δ 4.72 (tt, *J* = 11.4, 4.8 Hz, 1H, H-3), 3.69 (dq, *J* = 8.4, 6.2 Hz, 1H, H-20), 2.03 (s, 3H, H, H-2'), 1.22 (d, *J* = 6.2 Hz, 3H, H-21), 0.93 (s, 3H, H-19), 0.64 (s, 3H, H-18). ^{13}C NMR (100 MHz, CDCl$_3$): δ 169.7 (C1'), 71.1 (C3), 69.0 (C20), 58.6, 56.3, 43.6, 40.6, 39.2, 39.2, 35.8, 35.0, 34.6, 32.3, 27.7, 27.3, 27.0, 26.2, 25.3, 23.6, 22.9, 21.6, 21.5, 14.0 (C18). LRMS (APCI pos): *m/z* 285.1 (100%, [M-AcOH-H$_2$O+H]$^+$), 344.9 (20%, [M-H$_2$O+H]$^+$). Purity 95.8% (*HPLC Method B*, t$_R$ = 24.78 min).

(20*S*)-5β-Pregnan-3β,20-diol (15)

Compound **15** was purchased from Steraloids (Newport, RI, USA, cat. P6100-000, Batch 8230). LRMS (DUIS pos): *m/z* 285.3 (100%, [M-2H$_2$O+H]$^+$), 303.3 (10%, [M-H$_2$O+H]$^+$), 343.3 (10%, [M+Na]$^+$). Purity 99.1% (*HPLC Method C*, t$_R$ = 2.60 min).
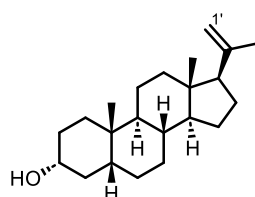
5β-Pregnan-3,20-dione (16)
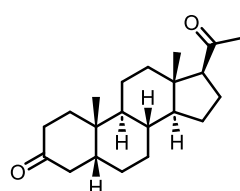
Compound **16** was taken from the group deposit, with the appearance of fine white powder. Selected ^{1}H NMR (401 MHz, CDCl$_3$): δ 2.12 (s, 3H, H-21), 1.02 (s, 3H, H-19), 0.63 (s, 3H, H-18). ^{13}C NMR (101 MHz, CDCl$_3$): δ 213.2 (C3), 209.6 (C20), 63.9, 56.8, 44.4, 44.3, 42.4, 40.9, 39.2, 37.3, 37.1, 35.7, 35.1, 31.7, 26.6, 25.9, 24.5, 23.0, 22.8, 21.3, 13.6. The NMR analysis is consistent with the previous report.[274] LRMS (APCI pos): *m/z* 317.0 (100%, [M+H]$^+$). Purity 99.0% (*HPLC Method B*, t$_R$ = 18.78 min).

(20*S*)-20-Hydroxy-5β-pregnan-3-one (17)

Compound **17** was purchased from Steraloids (Newport, RI, USA, cat. P8210-000, Batch L1437). LRMS (DUIS pos): *m/z* 283.2 (50%, [M-2H$_2$O+H]$^+$), 301.3 (100%, [M-H$_2$O+H]$^+$), 319.3 (65%, [M+H]$^+$), 360.3 (65%, [M+ACN+H]$^+$). Purity 99.9% (*HPLC Method C*, t$_R$ = 3.40 min).

16α,17α-Epoxy-5β-androst-3α-ol (18)
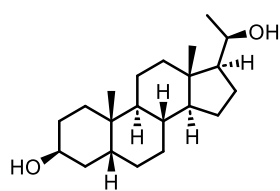
Compound **18** was taken from the group deposit, with the appearance of fine white powder. Selected ^{1}H NMR (401 MHz, CDCl$_3$): δ 3.60 (tt, *J* = 10.7, 4.6 Hz, 1H, H-3), 3.33 (dt, *J* = 3.1, 1.1 Hz, 1H, H-16), 3.08 (d, *J* = 3.0 Hz, 1H, H-17), 0.93 (s, 3H, H-19), 0.71 (s, 3H, H-18). ^{13}C NMR (101 MHz, CDCl$_3$): δ

91

71.9 (C3), 62.4 (C17), 54.0 (C16), 44.3, 42.2, 41.2, 40.8, 36.7, 35.6, 34.9, 34.1, 32.8, 30.7, 27.5, 27.2, 26.5, 23.4 (C19), 20.6, 15.7 (C18). LRMS (APCI pos): m/z 255.2 (25%, M-2H$_2$O+H$^+$), 273.0 (100%, [M-H$_2$O+H]$^+$), 290.9 (2%, [M+H]$^+$), 313.6 (20%, [M+Na]$^+$). Purity 99.9% (*HPLC Method B*, t_R = 16.64 min).

3α-Hydroxypregn-4-en-20-one (19)
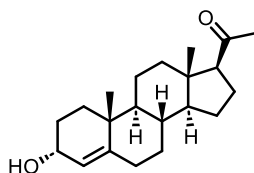
Compound **19** was purchased from Steraloids (Newport, RI, USA, cat. Q3510-000, Batch B1615). LRMS (DUIS pos): m/z 281.2 (100%, [M-2H$_2$O+H]$^+$), 299.2 (10%, [M-H$_2$O+H]$^+$), 615.5 (10%, [2M-H$_2$O+H]$^+$). Purity 99.9% (*HPLC Method C*, t_R = 3.18 min).

3β-Hydroxypregn-4-en-20-one (20)
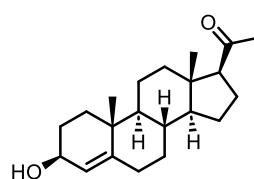
Compound **20** was purchased from Steraloids (Newport, RI, USA, cat. Q3540-000, Batch B0683). LRMS (DUIS pos): m/z 281.2 (10%, [M-2H$_2$O+H]$^+$), 299.2 (100%, [M-H$_2$O+H]$^+$), 317.2 (15%, [M+H]$^+$). Purity 99.9% (*HPLC Method C*, t_R = 2.95 min).

(20S)-Pregn-4-en-3β,20-diol (21)
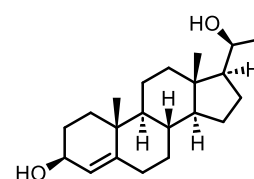
Compound **21** as purchased from Steraloids (Newport, RI, USA, cat. Q1460-000, Batch L1039). LRMS (DUIS pos): m/z 283.3 (100%, [M-2H$_2$O+H]$^+$), 301.3 (50%, [M-H$_2$O+H]$^+$). Purity 99.9% (*HPLC Method C*, t_R = 2.12 min).

Pregn-4-ene-3,20-dione (22), (Progesterone)
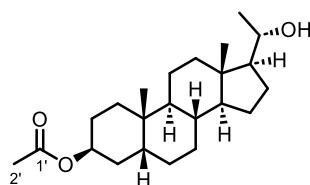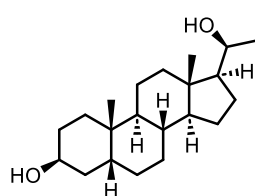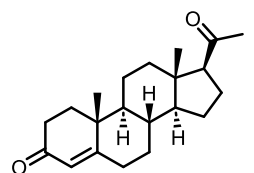
Compound **22** was taken from the group deposit, with the appearance of fine white powder. Selected ^{1}H NMR (401 MHz, CDCl$_3$): δ 5.73 (s, 1H, H-4), 2.53 (t, *J* = 9.0 Hz, 3H, H-17), 2.12 (s, 3H, H-21), 1.18 (d, 3H, H-19), 0.66 (s, 3H, H-18). ^{13}C NMR (101 MHz, CDCl$_3$): δ 209.4 (C20), 199.6 (C3), 171.1 (C5), 124.1 (C4), 63.6, 56.2, 53.8, 44.1, 38.8, 38.7, 35.9, 35.7, 34.1, 32.9, 32.0, 31.6, 24.5, 23.0, 21.1, 17.5, 13.5. The NMR analysis is consistent with the previous report.[280] LRMS (ESI pos): m/z 315.2 (100%, [M+H]$^+$), 356.3 (10%, [M+ACN+H]$^+$). Purity 99.9% (*HPLC Method B*, t_R = 22.57 min).

(20S)-20-Hydroxypregn-4-en-3-one (23)
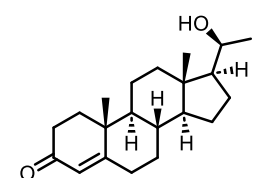
Compound **23** was purchased from Steraloids (Newport, RI, USA, cat. P3600-000, Batch L1739). LRMS (DUIS pos): m/z 317.2 (100%, [M+H]$^+$), 358.2 (5%, [M+ACN+H]$^+$). Purity 99.8% (*HPLC Method C*, t_R = 2.30 min).

(20*R*)-20-Hydroxypregn-4-en-3-one (24)
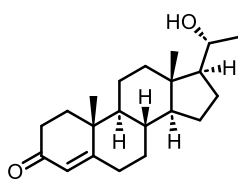
Compound **24** was purchased from Steraloids (Newport, RI, USA, cat. Q3630-000, Batch B2202). LRMS (DUIS pos): *m/z* 317.2 (100%, $[M-2H_2O+H]^+$), 358.3 (10%, $[M+ACN+H]^+$), 633.5 (15%, $[2M+H]^+$). Purity 99.4% (*HPLC Method C*, t_R = 2.93 min).
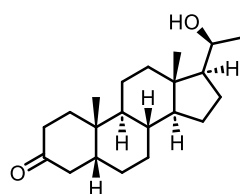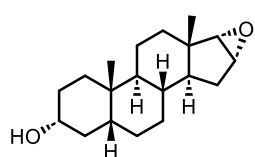
3-(O-(2'-Carboxyethoxy)oxime)-17β-hydroxyandrost-4-ene (25)
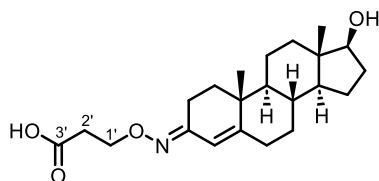
Compound **25** was taken from the group deposit, with the appearance of fine white powder. Selected ^{1}H NMR (401 MHz, CDCl$_3$): δ 6.34 (d, *J* = 1.7 Hz, 1H, H-4), 4.29 (t, *J* = 6.0 Hz, 2H, H-1'), 3.64 (t, *J* = 8.5 Hz, 1H, H-17), 2.77 (t, *J* = 5.9 Hz, 2H, H-2'), 1.10 (s, 3H, H-19), 0.77 (s, 3H, H-18). ^{13}C NMR (101 MHz, CDCl$_3$): δ 175.3 (C3'), 161.2 (C5), 154.4 (C3), 110.9 (C4), 81.9 (C1'), 68.4, 54.2, 50.7, 43.0, 39.2, 36.6, 36.2, 35.9, 35.6, 33.1, 32.1, 30.6, 24.7, 23.5, 20.9, 18.2 (C19), 11.2 (C18). The NMR analysis is consistent with the previous report.[281] LRMS (ESI neg): *m/z* 374.2 (100%, $[M-H]^-$), 302.4 (40%, $[M-CH_2CH_2COOH]^-$). Purity 99.9% (*HPLC Method E*, t_R = 7.30 min).

Pregna-4,6-dien-3,20-dione (26)
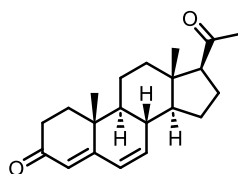
Compound **26** was purchased from Steraloids (Newport, RI, USA, cat. P0950-000, Batch B1326). LRMS (DUIS pos): *m/z* 313.2 (100%, $[M+H]^+$). Purity 99.9% (*HPLC Method C*, t_R = 2.37 min).

17α,21-Dihydroxypregna-1,4-dien-3,11,20-trione (27), (Prednisone)
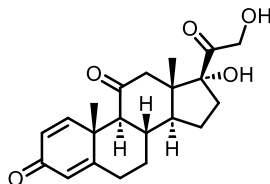
Compound **27** was taken from the group deposit, with the appearance of fine white powder. Selected ^{1}H NMR (401 MHz, CDCl$_3$/CD$_3$OD*, 1:1): δ 7.70 (d, *J* = 10.3 Hz, 1H, H-1), 6.17 (dd, *J* = 10.2, 1.5 Hz, 1H, H-2), 6.06 (s, 1H, H-4), 4.58 (d, *J* = 19.7 Hz, 1H, H$_a$-21), 4.17 (d, *J* = 19.6 Hz, 1H, H$_b$-21), 2.87 (d, *J* = 12.3 Hz, 1H, H-9), 1.41 (s, 3H, H-19), 0.61 (s, 3H, H-18). ^{13}C NMR (101 MHz, CDCl$_3$/CD$_3$OD*, 1:1): δ 212.1 (C20), 210.3 (C11), 187.5 (C3), 168.7 (C5), 156.8 (C1), 127.4 (C2), 124.3 (C4), 87.9 (C17), 67.2 (C21), 60.3, 51.6 (C13), 50.2, 49.7 (C9), 42.9 (C10), 36.5, 34.6, 33.9, 32.5, 23.5, 18.9 (C19), 15.8 (C18). The NMR analysis is consistent with the previous report.[282] LRMS (ESI pos): *m/z* 359.1 (100%, $[M+H]^+$), 341.2 (20%, $[M-H_2O+H]^+$). Purity 96.9% (*HPLC Method B*, t_R = 6.51 min).

*Chemical shift reference solvent.

17α,21-Dihydroxypregna-4-en-3,20-dione (28)
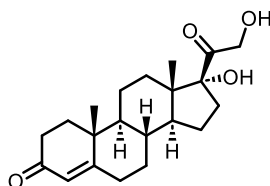
Compound **28** was taken from the group deposit, with the appearance of fine white powder. Selected ^{1}H NMR (500 MHz, CDCl$_3$*/CD$_3$OD, 1:1): δ 5.40 (t, *J* = 0.8 Hz, 1H, H-4), 4.32 (d, *J* = 19.4 Hz, 1H, H$_a$-21), 3.96 (d, *J* = 19.4 Hz, 1H, H$_b$-21), 2.35 (ddd, *J* = 14.5, 11.5, 2.8 Hz, 1H, H$_a$-2), 0.89 (s, 3H, H-19), 0.34 (s, 3H, H-18). ^{13}C NMR (126 MHz, CDCl$_3$*/CD$_3$OD, 1:1): δ 212.1 (C20), 200.9 (C3), 173.2 (C4), 122.9 (C5), 88.7 (C17), 66.5 (C21), 53.0,

93

49.9, 47.5, 38.3, 35.3, 35.1, 33.5, 33.2, 32.5, 31.6, 29.9, 23.2, 20.3, 16.6 (C19), 14.2 (C18). The NMR analysis is consistent with the previous report.[283] LRMS (ESI pos): *m/z* 347.3 (100%, [M+H]$^+$). Purity 96.7% (*HPLC method B*, t_R = 10.03 min).

*Chemical shift reference solvent.

17α,21-Dihydroxypregn-4-en-3,11,20-trione (29), (Cortisone)

Compound **29** was taken from the group deposit, with the appearance of fine white powder. Selected ^{1}H NMR (500 MHz, CDCl$_3$*/CD$_3$OD, 1:1): δ 5.41 (s, 1H, H-4), 4.30 (d, *J* = 19.6 Hz, 1H, H$_a$-21), 3.90 (d, *J* = 19.6 Hz, 1H, H$_b$-21), 2.62 (d, *J* = 12.3 Hz, 1H, H$_a$-12), 1.76 (d, *J* = 12.3 Hz, 1H, H$_b$-12), 1.10 (s, 3H, H-19), 0.29 (s, 3H, H-18). ^{13}C NMR (126 MHz, CDCl$_3$*/CD$_3$OD, 1:1): δ 211.4 (C20), 210.4 (C11), 200.9 (C3), 170.7 (C5), 123.6 (C4), 87.6 (C17), 66.5 (C21), 62.0, 50.8, 49.9, 49.3, 37.9, 36.3, 34.1, 34.0, 33.8, 33.0, 31.8, 31.8, 22.7, 16.5 (C19), 15.0 (C18). The NMR analysis is consistent with the previous report.[284] LRMS (ESI pos): *m/z* 361.3 (100%, [M+H]$^+$). Purity 97.2% (*HPLC Method B*, t_R = 6.47 min).

*Chemical shift reference solvent.

11β,21-Dihydroxypregn-4-en-3,20-dione (30), (Corticosterone)
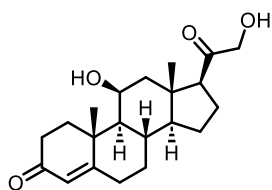
Compound **30** was taken from the group deposit, with the appearance of fine white powder. Selected ^{1}H NMR (401 MHz, CDCl$_3$*/CD$_3$OD, 9:1): δ 5.68 (s, 1H, H-4), 4.44–4.37 (m, 1H, H-11), 4.27–4.09 (m, 2H, H-21), 1.44 (s, 3H, H-19), 0.93 (s, 3H, H-18). ^{13}C NMR (101 MHz, CDCl$_3$*/CD$_3$OD, 9:1): δ 210.1 (C20), 199.6 (C3), 171.9 (C5), 122.6 (C4), 69.3 (C21), 68.1 (C11), 59.6, 57.6, 56.4, 48.1, 43.9, 39.3, 35.1, 33.9, 32.7, 32.1, 31.5, 24.6, 22.6, 21.1 (C19), 16.1 (C18). The NMR analysis is consistent with the previous report.[285] LRMS (ESI pos): *m/z* 347.2 (100%, [M+H]$^+$). Purity 95.9% (*HPLC Method B*, t_R = 9.30 min).

*Chemical shift reference solvent.

### 11β,17α-Dihydroxy-6α,9α-difluoro-3,20-dioxo-16α-methylpregna-1,4-dien-21-yl Pivalate (31), (Flumethasone Pivalate)
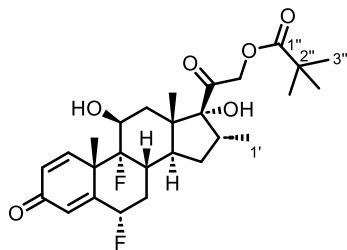
Compound **31** was taken from the group deposit, with the appearance of fine white powder. Selected ^{1}H NMR (500 MHz, DMSO-D_6): δ 7.27 (dd, *J* = 10.1, 1.5 Hz, 1H, H-1), 6.29 (dd, *J* = 10.2, 1.9 Hz, 1H, H-2), 6.10 (q, *J* = 1.5 Hz, 1H, H-4), 5.62 (dddd, *J* = 48.6, 11.5, 6.7, 1.9 Hz, 1H, H-6), 5.50 (dd, *J* = 5.1, 1.5 Hz, 1H, C11-O<u>H</u>), 5.19 (s, 1H, C17-O<u>H</u>), 5.00 (d, *J* = 17.6 Hz, 1H, H$_a$-21), 4.80 (d, *J* = 17.5 Hz, 1H, H$_b$-21), 4.19 – 4.11 (m, 1H, H-11), 2.89 (ddd, *J* = 11.2, 7.3, 4.1 Hz, 1H, H-16), 1.48 (s, 3H, H-19), 1.19 (s, 9H, H-3"), 0.88 (s, 3H, H-18), 0.79 (d, *J* = 7.3 Hz, 3H, H-1'). ^{13}C NMR (126 MHz, DMSO-D_6): δ 204.80 (C3), 184.54 (C20), 177.02 (C1"), 163.18 (d, *J* = 13.3 Hz, C5), 152.03 (C1), 129.11 (C2), 119.42 (d, *J* = 12.8 Hz, C4), 100.24 (d, *J* = 176.9 Hz, C9), 90.43 (C17), 86.93 (d, *J* = 179.9 Hz, C6), 70.32 (d, *J* = 35.8 Hz, C11), 67.92 (C21), 48.15 (d, *J* = 26.1 Hz), 48.01, 43.09, 39.69, 35.46, 35.37, 33.93 (d, *J* = 18.5 Hz), 32.18 (dd, *J* = 18.8, 11.2 Hz), 31.78, 27.02

(3 × C3"), 22.89 (d, J = 5.3 Hz, C19), 16.19 (C18), 15.17 (C1'). The NMR analysis is consistent with the previous report.[286] LRMS (ESI pos): *m/z* 495.4 (100%, [M+H]$^+$). Purity 99.9% (*HPLC Method B*, t_R = 14.20 min).

3-Oxoandrost-4-en-17-yl Cypionate (32), (Testosterone Cypionate)
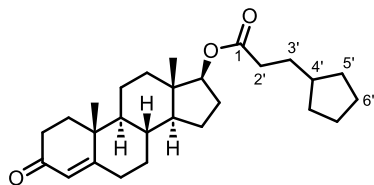
Compound **32** was taken from the group deposit, with the appearance of fine white powder. Selected ^{1}H NMR (500 MHz, DMSO-D_6): δ 5.65–5.61 (m, 1H, H-4), 4.52 (dd, J = 9.3, 7.7 Hz, 1H, H-17), 1.14 (s, 3H, H-19), 0.79 (s, 3H, H-18). ^{13}C NMR (126 MHz, (CD$_3$)$_2$SO): δ 198.1 (C3), 172.9 (C1'), 170.9 (C5), 123.2 (C4), 81.6 (C17), 53.1, 49.5, 42.1, 39.1, 38.2, 36.2, 35.2, 34.7, 33.6, 33.2, 31.96, 31.89, 31.2, 30.8, 27.2, 24.7, 23.1, 20.1, 16.9 (C19), 11.9 (C18). The NMR analysis is consistent with the previous report.[287] LRMS (APCI pos): *m/z* 413.3 (100%, [M+H]$^+$). Purity 98.7% (*HPLC Method B*, t_R = 23.85 min).

(20*R*)-20-Hydroxypregn-5-en-3-yl Acetate (33)

Compound **33** was taken from the group deposit, with the appearance of fine white powder. Selected ^{1}H NMR (401 MHz, CDCl$_3$): δ 5.37 (dd, J = 5.1, 2.2 Hz, 1H, H-5), 4.67–4.54 (m, 1H, H-3), 3.73 (dt, J = 10.5, 5.5 Hz, 1H, H-21), 2.03 (s, 3H, H-2'), 1.14 (d, J = 6.1 Hz, 3H, H-21), 1.03 (s, 3H, H-19), 0.77 (s, 3H, H-18). ^{13}C NMR (101 MHz, CDCl$_3$): δ 170.7 (C1'), 139.9 (C5), 122.6 (C6), 74.1 (C3), 70.7 (C21), 58.6, 56.3, 50.2, 42.4, 40.0, 38.3, 37.1, 36.8, 32.1, 31.8, 27.9, 25.8, 24.7, 23.8, 21.6, 21.0, 19.5 (C19), 12.5 (C18). The NMR analysis is consistent with the previous report.[288] LRMS (APCI pos): *m/z* 283.1 (100%, [M-AcOH-H$_2$O+H]$^+$), 300.1 (60%, [M-AcOH+H]$^+$). Purity 99.9% (*HPLC Method B*, t_R = 25.44 min).

3β-Hydroxypregn-5-en-20-one (34), (Pregnenolone)
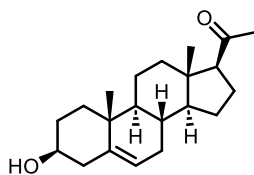
Compound **34** was taken from the group deposit, with the appearance of fish scale crystals. Selected ^{1}H NMR (401 MHz, CDCl$_3$): δ 5.35 (dt, J = 5.5, 1.9 Hz, 1H, H-6), 3.53 (s, 1H, H-3), 2.53 (t, J = 9.0 Hz, 1H, H-17), 2.12 (s, 3H, H-21), 1.01 (s, 3H, H-19), 0.63 (s, 3H, H-18). ^{13}C NMR (101 MHz, CDCl$_3$): δ 209.7 (C20), 140.9 (C5), 121.5 (C6), 71.9 (C3), 63.9, 57.1, 50.1, 44.2, 42.4, 39.0, 37.4, 36.7, 32.0, 31.9, 31.8, 31.7, 24.6, 23.0, 21.2, 19.5 (C19), 13.4 (C18). The NMR analysis is consistent with the previous report.[289] LRMS (APCI pos): *m/z* 299.0 (100%, [M-H$_2$O+H]$^+$), 317.0 (10%, [M+H]$^+$). Purity 99.3% (*HPLC Method B*, t_R = 17.85 min).

### (20S)-Pregn-5-en-3β,20-diol (35)
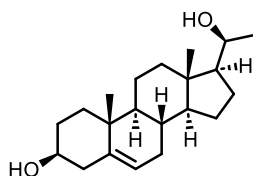
Compound **35** as purchased from Steraloids (Newport, RI, USA, cat. Q4460-000, Batch L1039). LRMS (DUIS pos): *m/z* 283.2 (98%, [M-2H$_2$O+H]$^+$), 301.3 (100%, [M-H$_2$O+H]$^+$). Purity 99.9% (*HPLC Method C*, t_R = 2.02 min).

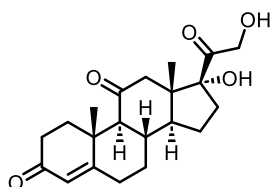### 3β,17α,21-Trihydroxypregn-5-en-20-one (36)

Compound **36** was taken from the group deposit, with the appearance of fine white powder. Selected ^{1}H NMR (500 MHz, CDCl$_3$*/CD$_3$OD, 1:1): δ 5.01 (dt, J = 5.4, 1.9 Hz, 1H, H-6), 4.33 (d, J = 19.4 Hz, 1H, H$_a$-21), 3.97 (d, J = 19.3 Hz, 1H, H$_b$-21), 3.17–3.07 (m, 1H, H-3), 0.69 (s, 3H, H-18), 0.31 (s, 3H, H-19). ^{13}C NMR (126 MHz, CDCl$_3$*/CD$_3$OD, 1:1): δ 212.6 (C20), 140.9 (C5), 121.2 (C6), 89.4 (C17), 71.1 (C3), 66.9 (C21), 51.2, 49.8, 47.9, 41.7, 37.3, 36.5, 34.0, 32.1, 31.9, 31.0, 30.5, 23.8, 20.7, 19.1 (C19), 14.5 (C18). LRMS (APCI pos): m/z 313.1 (50%, [M-2H$_2$O+H]$^+$), 330.9 (30%, [M-H$_2$O+H]$^+$). Purity 96.3% (*HPLC Method B*, t$_R$ = 7.45 min).

*Chemical shift reference solvent.

3β-(Methoxymethoxy)-pregn-5-en-20-one (37)
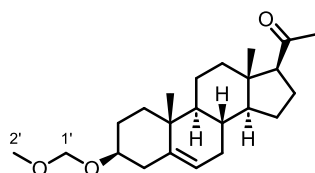
Compound **37** was taken from the group deposit, with the appearance of fine white powder. Selected ^{1}H NMR (401 MHz, CDCl$_3$): δ 5.35 (dt, J = 5.5, 2.0 Hz, 1H, H-6), 4.69 (s, 2H, H-1'), 3.43 (tt, J = 11.4, 4.7 Hz, 1H, H-3), 3.37 (s, 3H, H-2'), 2.12 (s, 3H, H-21), 1.01 (s, 3H, H-19), 0.63 (s, 3H, H-18). ^{13}C NMR (101 MHz, CDCl$_3$): δ 209.6 (C20), 140.7 (C5), 121.4 (C6), 94.7 (C1'), 77.3, 77.0, 76.8, 76.7, 63.7, 56.9, 55.2, 50.0, 44.0, 39.5, 38.9, 37.3, 36.8, 31.9, 31.8, 31.6, 29.7, 28.9, 24.5, 22.8, 21.1, 19.4 (C19), 13.2 (C18). The NMR analysis is consistent with the previous report.[290] LRMS (APCI pos): m/z 299.0 (100%, [M-CH$_3$OCH$_2$OH+H]$^+$), 360.9 (5%, [M+H]$^+$). Purity 98.1% (*HPLC Method B*, t$_R$ = 26.33 min).

(20S)-Pregn-5-en-3β,20-diyl 3-Acetate 20-Benzoate (38)
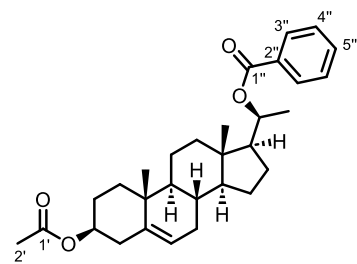
Compound **38** was taken from the group deposit, with the appearance of fine white powder. Selected ^{1}H NMR (401 MHz, CDCl$_3$): δ 8.06 (dd, J = 8.4, 1.3 Hz, 2H, H, H-3"), 7.55 (dd, J = 7.4, 1.4 Hz, 1H, H-5"), 7.44 (t, J = 7.6 Hz, 2H, H-4"), 5.40–5.33 (m, 1H, H-6), 5.13 (dq, J = 12.1, 6.1 Hz, 1H, H-20), 4.64–4.54 (m, 1H, H-3), 2.02 (s, 3H, H-2'), 1.27 (d, J = 6.1 Hz, 3H, H-20), 0.96 (s, 3H, H-19), 0.68 (s, 3H, H-18). ^{13}C NMR (101 MHz, CDCl$_3$): δ 170.7 (C1'), 165.9 (C1"), 139.9 (C5), 132.9 (C5"), 130.9 (C2"), 129.8 (C3"), 128.5 (C4"), 122.6 (C6), 74.1, 73.5, 56.2, 55.4, 50.2, 42.4, 39.2, 38.2, 37.1, 36.7, 32.0, 31.9, 27.9, 25.7, 24.5, 21.6, 21.1, 20.2, 19.4 (C19), 12.6 (C18). LRMS (APCI pos): m/z 283.1 (100%, [M-AcOH-BzOH+H]$^+$), 404.8 (95%, [M-AcOH+H]$^+$). Purity 98.4% (*HPLC Method B*, t$_R$ = 34.99 min).

20-Oxopregn-5-en-3β-yl Hemioxalate (39)
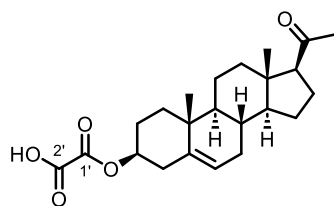
Compound **39** was taken from the group deposit, with the appearance of fine white powder. Selected ^{1}H NMR (400 MHz, CDCl$_3$): δ 5.45–5.38 (m, 1H, H-6), 4.81 (tt, J = 11.6, 4.9 Hz, 1H, H-3), 2.14 (s, 3H, H-21), 1.04 (s, 3H, H-19), 0.64 (s, 3H, H-18). ^{13}C NMR (101 MHz, CDCl$_3$): δ 210.5 (C20), 158.0, 157.7, 138.9 (C5), 123.4 (C6), 78.4 (C3), 63.8, 56.9, 50.0, 44.2, 38.9, 37.6, 37.0, 36.7, 2 × 31.9 (overlap), 31.7, 27.4,

96

24.6, 23.0, 21.2, 19.4 (C19), 13.4 (C18). The NMR analysis is consistent with the previous report.[291] LRMS (ESI neg): *m/z* 387.1 (100%, [M-H]⁻). Purity 99.9% (*HPLC Method B*, t_R = 9.55 min).

20-Oxopregn-5-en-3β-yl Hemimalonate (40)
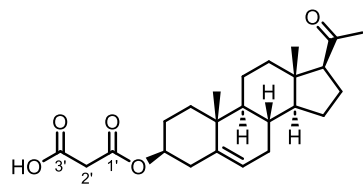
Compound **40** was taken from the group deposit, with the appearance of fine white powder. Selected ¹H NMR (400 MHz, CDCl₃): δ 5.43–5.34 (m, 1H, H-6), 4.73–5.68 (m, 1H, H-3), 3.42 (s, 2H, H-2'), 2.54 (t, *J* = 8.8, 1H, H-17), 2.13 (s, 3H, H-21), 1.02 (s, 3H, H-19), 0.63 (s, 3H, H-18). ¹³C NMR (101 MHz, CDCl₃): δ 209.9 (C20), 169.5 (C3'), 167.4 (C1'), 139.3 (C5), 122.9 (C6), 76.0 (C3), 63.8 (C17), 56.9, 49.9, 44.1, 40.4, 38.9, 37.9, 37.0, 36.7, 2 × 31.9 (overlap), 31.7, 27.6, 24.6, 22.9, 21.1, 19.4 (C19), 13.3 (C18). The NMR analysis is consistent with the previous report.[291] LRMS (ESI neg): *m/z* 357.1 (100%, [M-CO₂-H]⁻), 401.0 (90%, [M-H]⁻). Purity 99.9% (*HPLC Method B*, t_R = 8.26 min).

20-Oxopregn-5-en-3β-yl Hemiglutarate (41)
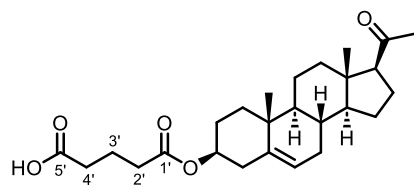
Compound **41** was taken from the group deposit, with the appearance of fine white powder. Selected ¹H NMR (400 MHz, CDCl₃): δ 5.42–5.32 (m, 1H, H-6), 4.67–4.60 (m, 1H, H-3), 2.54 (t, *J* = 8.9, 1H, H-17), 2.43 (t, *J* = 7.3, 2H, H-4'), 2.37 (t, *J* = 7.3, 2H, H-2'), 2.12 (s, 3H, H-21), 1.96 (p, J = 7.3, 2H, H-3'), 1.02 (s, 3H, H-19), 0.63 (s, 3H, H-18). ¹³C NMR (101 MHz, CDCl₃): δ 209.8 (C20), 177.9 (C5'), 172.4 (C1'), 139.7 (C5), 122.5 (C6), 74.1 (C3), 63.8 (C17), 56.9, 50.0, 44.1, 38.9, 38.2, 37.1, 36.7, 33.6, 32.9, 2 × 31.9 (overlap), 31.7, 27.8, 24.6, 22.9, 21.1, 20.0, 19.4 (C19), 13.3 (C18). The NMR analysis is consistent with the previous report.[291] LRMS (ESI neg): *m/z* 429.3 (100%, [M-H]⁻). Purity 99.9% (*HPLC Method B*, t_R = 14.40 min).
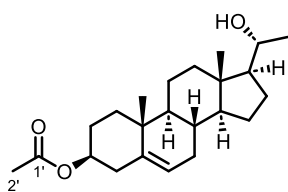
### 20-Oxopregn-5-en-3β-yl Hemiadipate (42)
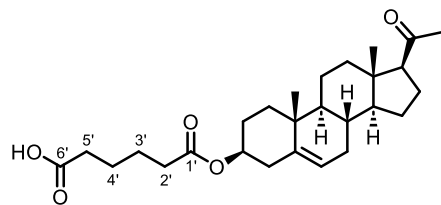
Compound **42** was taken from the group deposit, with the appearance of fine white powder. Selected ¹H NMR (400 MHz, CDCl₃): δ 5.40−5.32 (m, 1H, H-6), 4.67–4.58 (m, 1H, H-3), 2.53 (t, *J* = 9.0, 1H, H-17), 2.40−2.28 (m, 4H, H-2' and H-5'), 2.12 (s, 3H, H-21), 1.02 (s, 3H, H-19), 0.63 (s, 3H, H-18). ¹³C NMR (101 MHz, CDCl₃): δ 209.7 (C20), 178.0 (C6'), 172.8 (C1'), 139.8 (C5), 122.5 (C6), 73.9 (C3), 63.8 (C17), 56.9, 50.0, 44.1, 38.9, 38.2, 37.1, 36.7, 34.3, 33.5, 2 × 31.9 (overlap), 31.7, 27.9, 24.6, 24.5, 24.2, 22.9, 21.2, 19.4 (C19), 13.3 (C18). The NMR analysis is consistent with the previous report.[291] LRMS (ESI neg): *m/z* 443.4 (100%, [M-H]⁻). Purity 99.9% (*HPLC Method B*, t_R = 16.37 min).

20-Oxopregn-5-en-3β-yl Hemipimelate (43)
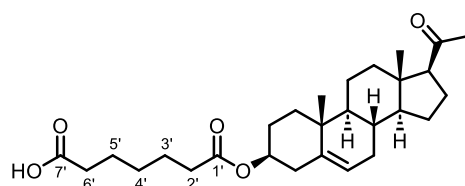
Compound **43** was taken from the group deposit, with the appearance of fine white powder. Selected ¹H NMR (400 MHz, CDCl₃): δ 5.40−5.31 (m, 1H, H-6), 4.69–4.58 (m, 1H, H-3), 2.53 (t, *J* = 8.9, 1H, H-17), 2.26−2.39 (m, 4H, H-2' and H-6'), 2.12 (s, 3H, H-21), 1.02 (s, 3H, H-19), 0.63

(s, 3H, H-18). ^{13}C NMR (101 MHz, CDCl$_3$): δ 209.7 (C20), 178.5 (C7'), 173.1 (C1'), 139.8 (C5), 122.4 (C6), 73.8 (C3), 63.8 (C17), 56.9, 50.0, 44.1, 38.9, 38.2, 37.1, 36.7, 34.5, 33.7, 2 × 31.9 (overlap), 31.7, 28.6, 27.9, 24.7, 24.6, 24.4, 22.9, 21.1, 19.4 (C19), 13.3 (C18). The NMR analysis is consistent with the previous report.[291] LRMS (ESI neg): *m/z* 457.3 (100%, [M-H]$^-$). Purity 99.9% (*HPLC Method B*, t$_R$ = 18.07 min).

20-Oxopregn-5-en-3β-yl Hemisuberate (44)
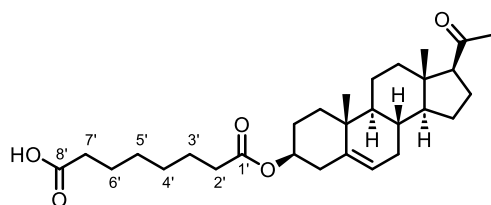
Compound **44** was taken from the group deposit, with the appearance of fine white powder. Selected ^{1}H NMR (400 MHz, CDCl$_3$): δ 5.80−5.72 (m, 1H, H-6), 4.66–4.51 (m, 1H, H-3), 2.53 (t, *J* = 9.0, 1H, H-17), 2.37−2.22 (4H, m, H-2' and H-7'), 2.12 (s, 3H, H-21), 1.02 (s, 3H, H-19), 0.63 (s, 3H, H-18). ^{13}C NMR (101 MHz, CDCl$_3$): δ 209.7 (C20), 178.6 (C8'), 173.3 (C1'), 139.8 (C5), 122.4 (C6), 73.7 (C3), 63.8 (C17), 56.9, 50.0, 44.1, 38.9, 38.2, 37.1, 36.7, 34.7, 33.9, 2 × 31.9 (overlap), 31.7, 28.89, 28.83, 27.9, 24.9, 24.6, 24.6, 22.9, 21.1, 19.4 (C19), 13.3 (C18). The NMR analysis is consistent with the previous report.[291] LRMS (ESI neg): *m/z* 471.3 (100%, [M-H]$^-$). Purity 99.9% (*HPLC Method B*, t$_R$ = 19.38 min).

17α-Methylandrost-5-en-3β,17β-diol (45)
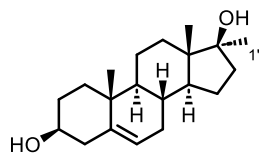
Compound **45** was taken from the group deposit, with the appearance of fine white powder. Selected ^{1}H NMR (401 MHz, CDCl$_3$): δ 5.35 (dt, *J* = 5.3, 1.9 Hz, 1H, H-6), 3.57–3.43 (m, 1H, H-3), 1.21 (d, *J* = 0.9 Hz, 3H, H-1'), 1.03 (s, 3H, H-19), 0.87 (s, 3H, H-18). ^{13}C NMR (101 MHz, CDCl$_3$): δ 141.0 (C5), 121.6 (C6), 81.9 (C17), 71.9 (C3), 51.2, 50.3, 45.4, 42.4, 39.1, 37.4, 36.7, 33.0, 31.8, 31.8, 31.7, 25.9 (C1'), 23.5, 20.9, 19.6 (C19), 14.0 (C18). The NMR analysis is consistent with the previous report.[292] LRMS (APCI pos): *m/z* 269.2 (100%, [M-2H$_2$O+H]$^+$), 287.0 (60%, [M-H$_2$O+H]$^+$). Purity 95.0% (*HPLC Method B*, t$_R$ = 12.87 min).
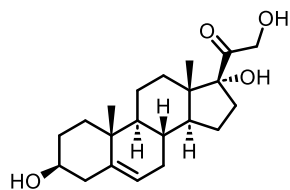
19-Hydroxy-17-oxoandrost-5-en-3β-yl Acetate (46)
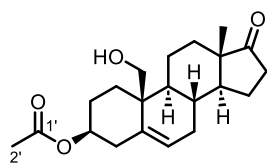
Compound **46** was taken from the group deposit, with the appearance of fine white powder. Selected ^{1}H NMR (401 MHz, CDCl$_3$): δ 5.81 (dt, *J* = 5.3, 2.0 Hz, 1H, H-6), 4.64 (tt, *J* = 11.5, 4.8 Hz, 1H, H-3), 3.88 (d, *J* = 11.5 Hz, 1H, H$_a$-19), 3.63 (dd, *J* = 11.2, 5.9 Hz, 1H, H$_b$-19), 2.51–2.39 (m, 2H, H-16), 2.03 (s, 3H, H-2'), 0.93 (s, 3H, H-18). ^{13}C NMR (101 MHz, CDCl$_3$): δ 221.2 (C17), 170.6 (C1'), 135.0 (C5), 127.7 (C6), 73.4 (C3), 62.9 (C19), 52.6, 50.5, 47.9, 41.8, 38.3, 35.9, 33.4, 33.1, 31.8, 30.3, 28.2, 21.8, 21.5 (C2'), 21.1, 14.1 (C18). The NMR analysis is consistent with the previous report.[293] LRMS (APCI pos): *m/z* 287.0 (100%, [M-AcOH+H]$^+$), 495.4 (25%, [M+H]$^+$). Purity 96.3% (*HPLC Method B*, t$_R$ = 10.47 min).

Methyl 3α,7α-Dihydroxy-5β-cholan-24-oate (57), (Methyl Chenodeoxycholate)
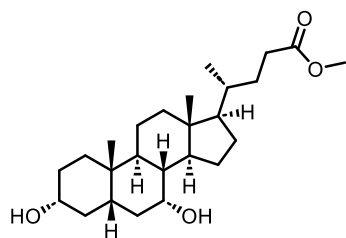
Chenodeoxycholic acid (10.0 g, 25.47 mmol) and concentrated H_2SO_4 (98%, 1 mL) were dissolved in MeOH (150 mL), and the mixture was refluxed for 8 hours. Reaction was then quenched by adding saturated aqueous solution of $NaHCO_3$ until approximately pH 7 was achieved. The solvent was partially evaporated, reducing the volume to approximately half of the original solution, and extracted with $CHCl_3$ (3 × 150 mL). Combined organic fractions were washed with a saturated solution of $NaHCO_3$ (2 × 150 mL), water (100 mL), brine (100 mL), and dried over anhydrous Na_2SO_4. After filtration and solvent evaporation, yellow oil was obtained (10.5 g). Column chromatography on silica gel (acetone/hexanes, 1:3) gave **57** as gum material (10.3 g, 99%). TLC: R_f 0.28 (EtOAc/hexanes, 1:1). $[\alpha]_D$: +11.0 (c 0.23, $CHCl_3$), lit.[294] +12.4 (c 0.5, $CHCl_3$). ^{1}H NMR (400 MHz, $CDCl_3$): δ 3.87–3.82 (m, 1H, H-7), 3.66 (s, 3H, H-25), 3.51–3.39 (m, 1H, H-3), 2.39–2.29 (m, 1H, H-8), 2.27–2.16 (m, 2H, H-23), 0.92 (d, J = 6.5 Hz, 3H, H-21), 0.85 (s, 3H, H-19), 0.65 (s, 3H, H-18). ^{13}C NMR (101 MHz, $CDCl_3$): δ 174.9 (C24), 72.2 (C3), 68.7 (C7), 55.9, 51.6 (C25), 50.6, 42.8, 41.6, 40.0, 39.8, 39.6, 35.5, 35.5, 35.2, 35.7, 33.0, 31.2, 31.1, 30.8, 28.3, 23.9, 22.9, 20.7 (C19), 18.4 (C21), 11.9 (C18). IR: ($CHCl_3$) 3613 (O-H), 1731 (C=O), 1234 (C-O), 1076 (C-OH). LRMS (ESI pos): m/z 371.2 (100%, $[M-2H_2O+H]^+$), 389.1 (10%, $[M-H_2O+H]^+$), 407.1 (5%, $[M+H]^+$), 424.1 (10%, $[M+NH_4]^+$). HRMS (ESI pos): m/z calcd for $C_{25}H_{42}O_4Na$ $[M+Na]^+$: 429.2975, found: 429.2976. Calcd for $C_{25}H_{42}O_4$: 73.85% C, 10.41% H, found: 73.83% C, 10.43% H. Purity 99.9% (*HPLC Method B*, t_R = 16.34 min).

Methyl 7α-Hydroxy-3-oxo-5β-cholan-24-oate (58), Methyl 3α-Hydroxy-7-oxo-5β-cholan-24-oate (59), and Methyl 3,7-Dioxo-5β-cholan-24-oate (60)

3α-Hydroxy-7-oxo-5β-cholan-24-oic acid (**57**, 6.80 g, 16.72 mmol) was dissolved in acetone (200 mL) and the solution was cooled to 0 °C in the ice bath. Next, the Jones reagent was slowly added dropwise (2.67 M, 0.75 equiv., 4.7 mL, 12.54 mmol). The reaction mixture was stirred at 0 °C for 30 min. Then, it was quenched with isopropanol (5 mL). Organic solvents were partially evaporated in vacuo to half the original volume. The products were extracted with $CHCl_3$ (3 × 100 mL). Combined organic fractions were washed with a saturated solution of $NaHCO_3$ (2 × 100 mL), water (100 mL), brine (100 mL), and dried over anhydrous Na_2SO_4. After filtration and solvent evaporation, thick yellow oil (6.95 g) was obtained. The purification of the crude material by column chromatography on silica gel (acetone/PE, 17:83) afforded **58** (0.40 g, 6%), **59** (3.75 g, 55%), and **60** (1.70 g, 25%) as oils:
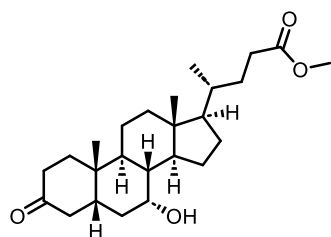
58: The material (0.40 g) was crystallized from hot EtOAc (60 °C, 1 mL) to afford tiny flakes (290 mg). Crystals were further recrystallized from HPLC grade acetone (1 mL), washed with dry pentane (3 × 10 mL), and dried to constant weight, affording small prism-shaped crystals of **58** (210 mg, 3%). TLC: R_f 0.48 (EtOAc/PE, 1:1). Mp: 110–114 °C (acetone), lit.[295] 123–126 °C (Et₂O). $[\alpha]_D$: +2.7 (c 0.400, $CHCl_3$), lit.[295] +20.7 (c 1.46, $CHCl_3$). Selected ^{1}H NMR (400 MHz, $CDCl_3$): δ 3.92 (ddd, $J_{1,2,3}$ = 3.0 Hz, 1H, H-7), 3.66 (s, 3H, H-25), 3.39 (t, J = 15.2 Hz, 1H, H_a-4), 1.00 (s, 3H, H-19), 0.93 (d, J = 6.4 Hz, 3H, H-21), 0.70 (s, 3H, H-18). ^{13}C NMR (100 MHz,

CDCl$_3$): δ 213.3 (C3), 174.9 (C24), 68.6 (C7), 55.9 (C17), 51.7 (C25), 50.5, 45.8, 43.3, 42.9 (C13), 39.7, 39.5, 37.1, 37.0, 35.53, 35.48 (C10), 34.0, 33.4, 31.14, 31.09, 28.3, 23.8, 22.1 (C19), 21.1, 18.4 (C21), 11.9 (C18). LRMS (ESI pos): *m/z* 387.2 (100%, [M-H$_2$O+H]$^+$), 405.2 (10%, [M+H]$^+$), 422.1 (85%, [M+NH$_4$]$^+$). HRMS (ESI pos): *m/z* calcd for C$_{25}$H$_{40}$O$_4$Na [M+Na]$^+$: 427.2819, found: 427.2819. Calcd for C$_{25}$H$_{40}$O$_4$: 74.22% C, 9.97% H, found: 74.44% C, 9.78% H. Purity 99.9% (*HPLC Method B*, t$_R$ = 17.47 min).
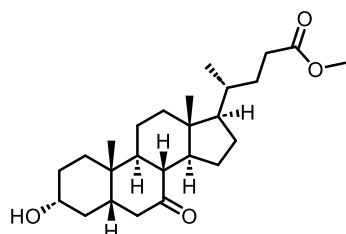
59: The material (3.75 g) was crystallized from boiling EtOAc (40 mL). Crystals were washed with dry pentane (3 × 10 mL) and dried to constant weight to obtain prism-shaped crystals of **59** (3.26 g, 48%). TLC: R$_f$ 0.27 (EtOAc/PE, 1:1). Mp: 108–110 °C (EtOAc), lit.[295] 107–109 °C, (Et$_2$O/pentane). [α]$_D$: -33.8 (c 0.20, CHCl$_3$), lit.[295] -38.0 (c 1.63, CHCl$_3$). Selected ^{1}H NMR (400 MHz, CDCl$_3$): δ 3.66 (s, 3H, H-25), 3.60 (tt, *J* = 10.6, 4.6 Hz, 1H, H-3), 2.85 (dd, *J* = 12.5, 6.0 Hz, 1H, H$_a$-6), 1.19 (s, 3H, H-19), 0.91 (d, *J* = 6.4 Hz, 3H, H-21), 0.65 (s, 3H, H-18). ^{13}C NMR (101 MHz, CDCl$_3$): δ 212.1 (C7), 174.8 (C24), 71.1 (C3), 54.9, 51.6 (C25), 49.7, 49.0, 46.2, 45.5, 42.9, 42.8, 39.1, 37.6, 35.4, 35.3, 34.3, 31.2, 31.1, 30.0, 28.4, 25.0, 23.2 (C19), 21.8, 18.5 (C21), 12.2 (C18). LRMS (ESI pos): *m/z* 387.1 (55%, [M-H$_2$O+H]$^+$), 405.1 (80%, [M+H]$^+$), 422.1 (100%, [M+NH$_4$]$^+$). HRMS (ESI pos): *m/z* calcd for C$_{25}$H$_{40}$O$_4$Na [M+Na]$^+$: 427.2819, found: 427.2808. Calcd for C$_{25}$H$_{40}$O$_4$: 74.22% C, 9.97% H, found: 74.20% C, 9.98% H. Purity 99.9% (*HPLC Method B*, t$_R$ = 14.75 min).
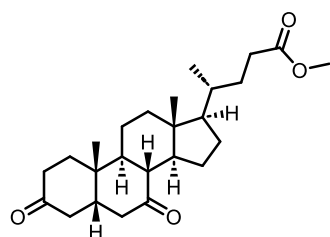
60: The material (1.70 g) was crystallized from warm MeOH (10 mL). The obtained needle crystals (1.25 g) were further recrystallized from HPLC grade acetone (5 mL), washed with dry pentane (3 × 10 mL), and dried to constant weight to obtain colorless needle crystals of compound **60** (1.08 g, 16%). TLC: R$_f$ 0.55 (EtOAc/PE, 1:1). Mp: 160–164 °C (acetone), lit.[295] 163–166 °C, (acetone/Et$_2$O). [α]$_D$: -32.1 (c 0.296, CHCl$_3$), lit.[294] -38.9 (c 0.55, CHCl$_3$). Selected ^{1}H NMR (401 MHz, CDCl$_3$): δ 3.66 (s, 3H, H-25), 2.87 (dd, *J* = 12.9, 5.5 Hz, 1H, H$_a$-6), 2.49 (t, *J* = 11.3 Hz, 1H, H-8), 1.30 (s, 3H, H-19), 0.92 (d, *J* = 6.5 Hz, 3H, H-21), 0.69 (s, 3H, H-18). ^{13}C NMR (101 MHz, CDCl$_3$): δ 211.3 (C7), 210.4 (C3), 174.8 (C24), 54.9 (C17), 51.7 (C25), 49.7 (C8), 49.0 (C14), 47.9 (C5), 45.1 (C6), 43.1, 43.0 (C9), 42.8 (C13), 39.0 (C12), 36.9, 35.6 (C1), 35.6 (C10), 35.3 (C20), 31.2 (C23), 31.1 (C22), 28.4, 24.9, 22.6 (C19), 22.3, 18.5 (C21), 12.2 (C18). LRMS (ESI pos): *m/z* 403.3 (100%, [M+H]$^+$). HRMS (ESI pos): *m/z* calcd for C$_{25}$H$_{38}$O$_4$Na [M+Na]$^+$: 425.2662, found: 425.2664. Calcd for C$_{25}$H$_{38}$O$_4$: 74.59% C, 9.51% H, found: 74.43% C, 9.31% H. Purity 99.9% (*HPLC Method B*, t$_R$ = 15.61 min).

3α-Hydroxy-7-oxo-5β-cholan-24-oic Acid (61)
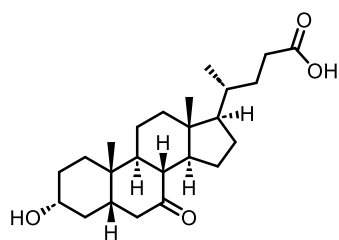
Methyl 3α-hydroxy-7-oxo-5β-cholan-24-oate (59, 8.2 g, 20.27 mmol) was dissolved in 300 mL of 5% NaOH in MeOH/H_2O (1:1) and heated to 50 °C. After 2 h, HCl (aqueous 1M solution) was added dropwise to pH 3. The product was extracted with EtOAc (3 × 200 mL), combined organic extracts were washed with brine (300 mL) and dried over anhydrous Na_2SO_4. After solvent evaporation, the oily residue (8.2 g) was purified by flash chromatography (EtOAc/hexanes/AcOH, 30:70:1) and further crystallized from boiling EtOAc to afford 61 (7.6 g, 96%). TLC: R_f 0.43 (acetone/hexanes/AcOH, 40:60:1). Mp: 202–203 °C (EtOAc), lit.[224] 202–203 °C (no solvent given). [α]$_D$: -29.6 (c 0.28, MeOH). ^{1}H NMR (401 MHz, CD_3OD): δ 3.53 (tt, J = 10.5, 4.7 Hz, 1H, H-3), 2.99 (ddd, J = 12.5, 6.0, 1.1 Hz, 1H, H-6$_a$), 2.54 (t, J = 11.3 Hz, 1H, H-8), 1.23 (s, 3H, H-19), 0.96 (d, J = 6.5 Hz, 3H, H-21), 0.71 (s, 3H, H-18). ^{13}C NMR (101 MHz, CD_3OD): δ 215.1 (C7), 178.1 (C24), 71.5 (C3), 56.3, 50.7, 50.4, 47.5, 46.4, 44.4, 43.8, 40.3, 38.2, 36.6, 36.3, 35.2, 32.3, 32.0, 30.6, 29.3, 25.8, 23.5, 22.8, 18.8, 12.5. LRMS (ESI neg): m/z 389.3 (100%, [M-H]⁻), 435.3 (5%, [M+FA-H]⁻), 779.5 (3%, [2M-H]⁻). HRMS (ESI neg): m/z calcd for $C_{24}H_{37}O_3$ [M-H]⁻: 389.26938, found: 389.26973. Calcd for $C_{24}H_{38}O_4$: 73.81% C, 9.81% H, found: 73.72% C, 9.57% H. Purity 99.9% (*HPLC Method B*, t_R = 9.46 min).

3α,7α-Dihydroxy-7β-methyl-5β-cholan-24-oic Acid (62)
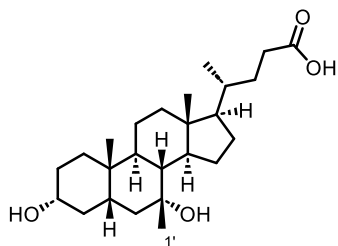
Compound 62 was prepared from 3α-hydroxy-7-oxo-5β-cholan-24-oic acid (61, 500 mg, 1.28 mmol), as described in *General Procedure for Grignard Reaction, section 6.1*. Compound 62 was obtained as a white solid (153 mg, 29%). TLC: R_f 0.28 (MeOH/DCM/AcOH, 5:95:1). Mp: 85–88 °C (DCM/MeOH, 200:1), lit.[216] 96–99 °C (no solvent given). [α]$_D$: +29.9 (c 0.15, MeOH). Selected ^{1}H NMR (401 MHz, $CDCl_3$): δ 3.49 (tt, J = 11.0, 4.5 Hz, 1H, H-3), 1.22 (s, 3H, H-1'), 0.95 (d, J = 6.4 Hz, 3H, H-21), 0.87 (s, 3H, H-19), 0.68 (s, 3H, H-18). ^{13}C NMR (101 MHz, $CDCl_3$): δ 179.0 (C24), 73.2 (C7), 72.1 (C3), 54.9, 51.5, 44.4, 44.2, 43.3, 42.1, 40.2, 38.5, 36.2, 35.7, 35.5, 34.7, 33.7, 31.0, 30.9, 30.5, 28.6, 28.2, 23.0, 21.4, 18.6, 12.4. LRMS (ESI neg): m/z 405.3 (100%, [M-H]⁻), 451.3 (11%, [2M-H]⁻). HRMS (ESI neg): m/z calcd for $C_{25}H_{41}O_4$ [M-H]⁻: 405.30103, found: 405.30043. Calcd for $C_{25}H_{42}O_4$: 73.85% C, 10.41% H, found: 73.56% C, 10.52% H. *HPLC Method B* (ESI neg, t_R = 12.66 min). Purity 95.6% (*HPLC method A*, t_R = 6.53 min).

3α,7α-Dihydroxy-7β-ethyl-5β-cholan-24-oic Acid (63)
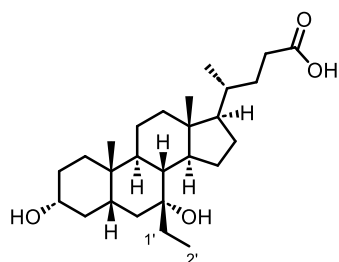
Compound 63 was prepared from 3α-hydroxy-7-oxo-5β-cholan-24-oic acid (61, 500 mg, 1.28 mmol), as described in *General Procedure for Grignard Reaction, section 6.1*. Compound 63 was obtained as a white solid (254 mg, 47%). TLC: R_f 0.21 (EtOAc/hexanes/AcOH, 50:50:1). Mp: 112–114 °C (EtOAc), lit.[216] 102–103 °C (no solvent given). [α]$_D$: +32.8 (c 0.27, MeOH). ^{1}H NMR (401 MHz, CD_3OD): δ 3.41 (tt, J = 11.2, 4.5 Hz, 1H, H-3), 0.97 (d, J = 6.5 Hz, 3H, H-21), 0.91–0.83 (m, 6H, H-19 and H-2'), 0.74 (s, 3H, H-18). ^{13}C NMR (101 MHz, CD_3OD): δ 178.3 (C24), 76.1 (C7), 72.8 (C3), 56.4, 52.6, 45.3, 43.3, 41.6, 40.7, 39.8, 39.4, 37.8, 37.3, 36.9, 36.7, 35.6, 32.3, 32.1, 31.2,

29.3, 27.8, 23.4, 22.6, 19.0, 12.6, 9.9. LRMS (ESI neg): *m/z* 419.3 (100%, [M-H]⁻), 465.3 (60%, [M+FA-H]⁻), 479.3 (44%, [M+AcOH-H]⁻), 839.6 (75%, [2M-H]⁻). HRMS (ESI neg): *m/z* calcd for $C_{26}H_{43}O_4$ [M-H]⁻: 419.31668, found: 419.31647. Calcd for $C_{26}H_{44}O_4$: 74.24% C, 10.54% H, found: 74.01% C, 10.38% H. *HPLC Method B* (ESI neg, t_R = 14.36 min). Purity 95.6% (*HPLC method A*, t_R = 6.44 min).

3α,7α-Dihydroxy-7β-vinyl-5β-cholan-24-oic Acid (64)
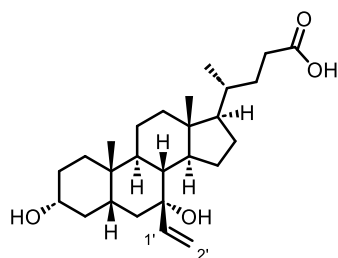
Compound **64** was prepared from 3α-hydroxy-7-oxo-5β-cholan-24-oic acid (**61**, 500 mg, 1.28 mmol), as described in *General Procedure for Grignard Reaction, section 6.1*. Compound **64** was obtained as a white solid. (273 mg, 51%). TLC: R_f 0.24 (EtOAc/hexanes/AcOH, 50:50:1). Mp: 90–95 °C (DCM/MeOH, 200:1). [α]$_D$: +9.3 (c 0.10, CHCl₃). Selected ¹H NMR (401 MHz, CDCl₃): δ 5.92 (dd, *J* = 17.3, 10.7 Hz, 1H, H-1'), 5.15 (dd, *J* = 17.3, 1.1 Hz, 1H, H$_{(Z)}$-2'), 4.91 (dd, *J* = 10.8, 1.0

Hz, 1H, H$_{(E)}$-2'), 3.55–3.45 (m, 1H, H-3), 0.96–0.87 (m, 6H, H-19 and H-21), 0.67 (s, 3H, H-18). ¹³C NMR (101 MHz, CDCl₃): δ 179.3 (C24), 150.3 (C1'), 110.2 (C2'), 75.8 (C7), 72.1 (C3), 55.1, 51.2, 43.8, 43.7, 41.8, 41.3, 40.0, 38.7, 35.6, 35.5, 35.2, 34.6, 31.0, 30.9, 30.5, 28.5, 27.9, 22.9, 21.1, 18.5, 12.3. LRMS (ESI neg): *m/z* 417.3 (80%, [M-H]⁻), 463.3 (100%, [M+FA-H]⁻), 477.3 (50%, [M+AcOH-H]⁻), 835.6 (35%, [2M-H]⁻). HRMS (ESI neg): *m/z* calcd for $C_{26}H_{41}O_4$ [M-H]⁻: 417.30103, found: 417.30066. Calcd for $C_{26}H_{42}O_4$: 74.60% C, 10.11% H, found: 74.21% C, 10.21% H. *HPLC Method B* (ESI neg, t_R = 13.22 min). Purity 96.5% (*HPLC method A*, t_R = 6.00 min).

7β-Ethynyl-3α,7α-dihydroxy-5β-cholan-24-oic Acid (65)
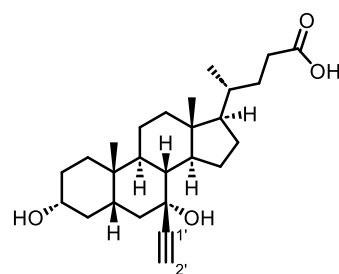
Compound **65** was prepared from 3α-hydroxy-7-oxo-5β-cholan-24-oic acid (**61**, 500 mg, 1.28 mmol), as described in *General Procedure for Grignard Reaction, section 6.1*. Compound **65** (370 mg) was obtained as a white solid that was re-dissolved in DCM (7 mL). After gentle evaporation with nitrogen blow-down, the precipitate formed. The solid material was filtered, washed with HPLC grade pentane (3 × 5 mL), and dried by high vacuum to obtain **65** as a fine white powder (337 mg,

63%). TLC: R_f 0.35 (MeOH/DCM/AcOH, 5:95:1). Mp: 122–125 °C (DCM/MeOH, 200:1). [α]$_D$: +48.6 (c 0.15, MeOH). Selected ¹H NMR (401 MHz, CDCl₃): δ 3.50–3.37 (m, 1H, H-3), 2.40 (s, 1H, H-2'), 0.92 (d, *J* = 6.6 Hz, 3H, H-21), 0.91 (s, 3H, H-19), 0.69 (s, 3H, H-18). ¹³C NMR (101 MHz, CDCl₃): δ 177.4 (C24), 90.7 (C1'), 71.73 (C2'), 71.68 (C7), 69.2 (C3), 55.2, 50.9, 43.7, 43.5, 42.8, 41.6, 39.8, 38.2, 35.4, 35.3, 34.9, 34.4, 30.9, 30.9, 30.3, 28.4, 26.2, 22.8, 20.9, 18.4, 12.1. LRMS (ESI neg): *m/z* 415.3 (100%, [M-H]⁻), 461.3 (10%, [M+FA-H]⁻). HRMS (ESI neg): *m/z* calcd for $C_{26}H_{39}O_4$ [M-H]⁻: 415.28538, found: 415.28490. Calcd for $C_{26}H_{40}O_4$: 74.96% C, 9.68% H, found: 74.59% C, 9.95% H. *HPLC Method B* (ESI neg, t_R = 12.27 min). Purity 95.4% (*HPLC method A*, t_R = 5.78 min).

3α,7α-Dihydroxy-7β-propyl-5β-cholan-24-oic Acid (66)
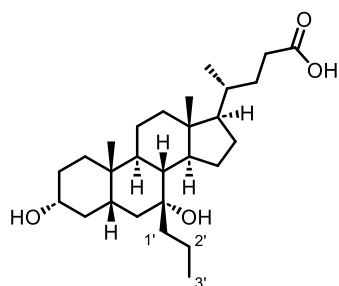
Compound **66** was prepared from 3α-hydroxy-7-oxo-5β-cholan-24-oic acid (**61**, 500 mg, 1.28 mmol), as described in *General Procedure for Grignard Reaction, section 6.1*. Compound **66** was obtained as a white solid (203 mg, 36%). TLC: R_f 0.26 (MeOH/DCM/AcOH, 5:95:1). Mp: 100–105 °C (DCM/MeOH, 200:1), lit.[216] 102–103 °C (no solvent given). $[α]_D$: +30.1 (c 0.13, CHCl$_3$). Selected ^{1}H NMR (401 MHz, CDCl$_3$): δ 3.49 (tt, J = 11.0, 4.5 Hz, 1H, H-3), 0.94 (d, J = 6.4 Hz, 3H, H-21), 0.88 (t, J = 6.9 Hz, 3H, H-3'), 0.84 (s, 3H, H-19), 0.70 (s, 3H, H-18). ^{13}C NMR (101 MHz, CDCl$_3$): δ 179.2 (C24), 75.4 (C7), 72.1 (C3), 54.9, 51.6, 47.6, 44.4, 41.8, 40.5, 40.3, 39.7, 38.8, 36.3, 35.7, 35.5, 34.5, 31.1, 30.9, 30.5, 28.5, 27.1, 22.9, 21.6, 18.6, 18.5, 14.7, 12.4. LRMS (ESI neg): m/z 433.3 (100%, [M-H]$^-$), 479.3 (6%, [M+FA-H]$^-$). HRMS (ESI neg): m/z calcd for C$_{27}$H$_{45}$O$_4$ [M-H]$^-$: 433.33233, found: 433.33180. Calcd for C$_{27}$H$_{46}$O$_4$: 74.61% C, 10.67% H, found: 74.32% C, 10.69% H. *HPLC Method B* (ESI neg, t_R = 16.63 min). Purity 97.8% (*HPLC method A*, t_R = 6.27 min).

7β-Allyl-3α,7α-dihydroxy-5β-cholan-24-oic Acid (67)
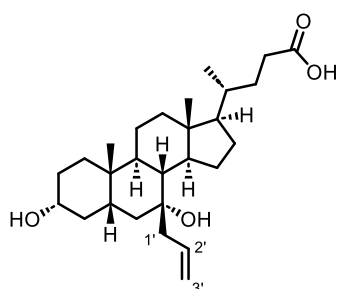
Compound **67** was prepared from 3α-hydroxy-7-oxo-5β-cholan-24-oic acid (**61**, 500 mg, 1.28 mmol), as described in *General Procedure for Grignard Reaction, section 6.1*. Compound **67** was obtained as a white solid (220 mg, 40%). TLC: R_f 0.29 (EtOAc/hexanes/AcOH, 50:50:1). Mp: 90–93 °C (DCM/MeOH, 200:1). $[α]_D$: +42.9 (c 0.11, CHCl$_3$). Selected ^{1}H NMR (401 MHz, CDCl$_3$): δ 5.82 (ddt, J = 17.3, 10.1, 7.4 Hz, 1H, H-2'), 5.10 (dd, J = 10.2, 2.2 Hz, 1H, H$_{(E)}$-3'), 5.04 (dd, J = 17.1, 2.1 Hz, 1H, H$_{(Z)}$-3'), 3.50 (tt, J = 11.1, 4.5 Hz, 1H, H-3), 0.95 (d, J = 6.4 Hz, 3H, H-21), 0.82 (s, 3H, H-19), 0.70 (s, 3H, H-18). ^{13}C NMR (101 MHz, CDCl$_3$): δ 179.0 (C24), 134.8 (C2'), 118.6 (C3'), 74.8 (C7), 72.1 (C3), 54.9, 51.7, 48.9, 44.4, 41.7, 41.2, 40.4, 39.8, 38.6, 36.6, 35.7, 35.5, 34.5, 31.0, 30.9, 30.5, 28.5, 27.7, 22.9, 21.6, 18.6, 12.4. LRMS (ESI neg): m/z 431.3 (100%, [M-H]$^-$), 477.3 (50%, [M+FA-H]$^-$), 491.3 (35%, [M+AcOH-H]$^-$), 863.6 (45%, [2M-H]$^-$). HRMS (ESI neg): m/z calcd for C$_{27}$H$_{43}$O$_4$ [M-H]$^-$: 431.31668, found: 431.31629. Calcd for C$_{27}$H$_{44}$O$_4$: 74.96% C, 10.25% H, found: 74.68% C, 10.35% H. *HPLC Method B* (ESI neg, t_R = 14.92 min). Purity 96.0% (*HPLC method A*, t_R = 8.45 min).

3α,7α-Dihydroxy-7β-isopropyl-5β-cholan-24-oic Acid (68)
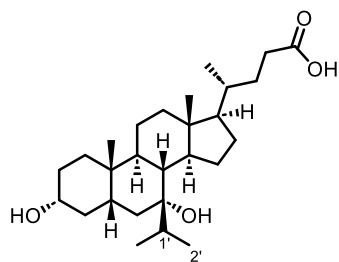
Compound **68** was prepared from 3α-hydroxy-7-oxo-5β-cholan-24-oic acid (**61**, 500 mg, 1.28 mmol), as described in *General Procedure for Grignard Reaction, section 6.1*. Compound **68** was obtained as a white solid (200 mg, 36%). Crystallization from DCM/MeOH (2 mL/1 drop) afforded cubic tiny crystals of **68** (40 mg). TLC: R_f 0.56 (MeOH/DCM/AcOH, 5:95:1). Mp: 95–100 °C (DCM/MeOH, 200:1). $[α]_D$: +34.0, c 0.19, CHCl$_3$. Selected ^{1}H NMR (401 MHz, CDCl$_3$): δ 3.50 (tt, J = 11.1, 4.6 Hz, 1H, H-3), 0.95 (d, J = 6.4 Hz, 3H, H-21), 0.89 (d, J = 5.5 Hz, 3H, H-2'), 0.87 (d, J = 5.5 Hz, 3H, H-2'), 0.83 (s, 3H, H-19), 0.72 (s, 3H, H-18). ^{13}C NMR (101 MHz, CDCl$_3$): δ 179.3 (C24), 77.48 (C7, CDCl$_3$ overlap), 72.1 (C3), 54.8, 51.6, 44.6, 41.2, 40.4, 39.1, 39.1, 36.9,

36.6, 35.8, 35.5, 34.4, 31.8, 31.1, 30.9, 30.5, 28.4, 27.3, 22.9, 21.7, 18.8, 18.6, 16.7, 12.4. LRMS (ESI neg): m/z 433.3 (100%, [M-H]$^+$), 479.3 (4%, [M+FA-H]$^+$). HRMS (ESI neg): m/z calcd for $C_{27}H_{45}O_4$ [M-H]$^+$: 433.33233, found: 433.33195. Calcd for $C_{27}H_{46}O_4$: 74.61% C, 10.67% H, found: 74.59% C, 10.70% H. *HPLC Method B* (ESI neg, t_R = 15.70 min). Purity 99.1% (*HPLC method A*, t_R = 7.97 min).

7β-Cyclopropyl-3α,7α-dihydroxy-5β-cholan-24-oic Acid (69)
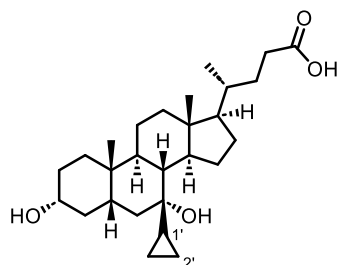
Compound **69** was prepared from 3α-hydroxy-7-oxo-5β-cholan-24-oic acid (**61**, 500 mg, 1.28 mmol), as described in *General Procedure for Grignard Reaction, section 6.1*. Compound **69** was obtained as a white solid (185 mg, 33%). TLC: R_f 0.38 (MeOH/DCM/AcOH, 10:90:1). Mp: 78–82 °C (DCM/MeOH, 200:1). [α]$_D$: +28.3 (c 0.37, CHCl$_3$). Selected ^{1}H NMR (401 MHz, CDCl$_3$): δ 3.54–3.42 (m, 1H, H-3), 0.95 (d, J = 6.4 Hz, 3H, H-21), 0.88 (s, 3H, H-19), 0.69 (s, 3H, H-18), 0.58–0.12 (m, 4H, H-2'). ^{13}C NMR (101 MHz, CDCl$_3$): δ 179.4 (C24), 72.6 (C7), 72.1 (C3), 54.9, 50.8, 45.5, 44.4, 41.8, 40.0, 39.1, 38.8, 35.9, 35.7, 35.4, 34.7, 31.2, 30.9, 30.4, 28.6, 27.5, 24.8, 23.0, 21.3, 18.6, 12.3, 4.5, 2.7. LRMS (ESI neg): m/z 431.3 (65%, [M-H]$^-$), 477.3 (100%, [M+FA-H]$^-$), 491.3 (56%, [M+AcOH-H]$^+$), 863.6 (37%, [2M-H]$^-$). HRMS (ESI neg): m/z calcd for $C_{27}H_{43}O_4$ [M-H]$^-$: 431.31668, found: 431.31619. Calcd for $C_{27}H_{44}O_4$: 74.96% C, 10.25% H, found: 74.35% C, 10.64% H. *HPLC Method B* (ESI neg, t_R = 15.15 min). Purity 96.2% (*HPLC method A*, t_R = 5.74 min).

3α,7α-Dihydroxy-7β-(pent-4-en-1-yl)-5β-cholan-24-oic Acid (70)
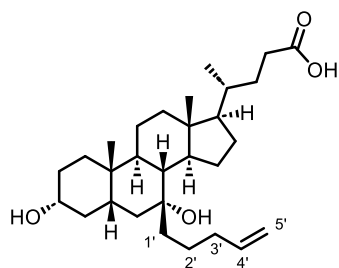
Compound **70** was prepared from 3α-hydroxy-7-oxo-5β-cholan-24-oic acid (**61**, 500 mg, 1.28 mmol), as described in *General Procedure for Grignard Reaction, section 6.1*. Compound **70** was obtained as white solids (198 mg, 34%). TLC: R_f 0.26 (MeOH/DCM/AcOH, 5:95:1), 87–90 °C (DCM/MeOH, 200:1), [α]$_D$: +34.9 (c 0.34, CHCl$_3$). Selected ^{1}H NMR (401 MHz, CDCl$_3$): δ 5.78 (ddt, J = 16.9, 10.1, 6.7 Hz, 1H, H-4'), 5.00 (dq, J = 17.2, 1.7 Hz, 1H, H$_{(Z)}$-5'), 4.97–4.93 (m, 1H, H$_{(E)}$-5'), 3.55–3.43 (m, 1H, H-3), 0.94 (d, J = 6.4 Hz, 3H, H-21), 0.84 (s, 3H, H-19), 0.70 (s, 3H, H-18). ^{13}C NMR (101 MHz, CDCl$_3$): δ 179.5 (C24), 138.8 (C4'), 114.9 (C5'), 75.3 (C7), 72.1 (C3), 54.9, 51.6, 44.5, 44.4, 41.7, 40.7, 40.4, 39.6, 38.8, 36.4, 35.7, 35.5, 34.5, 34.4, 31.2, 30.9, 30.5, 28.5, 27.3, 24.6, 23.0, 21.6, 18.6, 12.5. LRMS (ESI neg): m/z 459.3 (60%, [M-H]$^-$), 505.4 (100%, [M+FA-H]$^-$), 519.4 (47%, [M+AcOH-H]$^-$), 919.7 (45%, [2M-H]$^-$). HRMS (ESI neg): m/z calcd for $C_{29}H_{47}O_4$ [M-H]$^-$: 459.34798, found: 459.34770. Calcd for $C_{29}H_{48}O_4$: 75.61% C, 10.50% H, found: 75.56% C, 10.52% H. *HPLC Method B* (ESI neg, t_R = 17.73 min). Purity 99.4% (*HPLC method A*, t_R = 4.31 min).

3α,7α-Dihydroxy-7β-nonyl-5β-cholan-24-oic Acid (71)
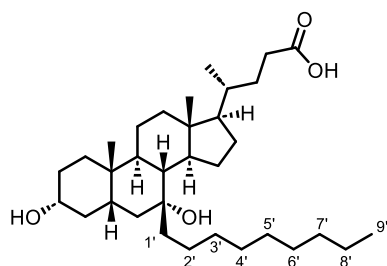
Compound **71** was prepared from 3α-hydroxy-7-oxo-5β-cholan-24-oic acid (**61**, 500 mg, 1.28 mmol), as described in *General Procedure for Grignard Reaction, section 6.1*. Compound **71** was obtained as a white solid (235 mg, 35%). TLC: R_f 0.27 (MeOH/DCM/AcOH, 5:95:1). Mp: 78–80 °C (DCM/MeOH, 200:1). [α]$_D$: +30.6 (c 0.36, CHCl$_3$). Selected ^{1}H NMR (401 MHz, CDCl$_3$): δ 3.49 (tt, J = 11.0, 6.2 Hz, 1H, H-3), 0.94 (d, J = 6.4 Hz, 3H, H-21), 0.87 (t, J = 6.5 Hz, 3H, H-9'), 0.84 (s, 3H, H-19), 0.70 (s, 3H, H-18). ^{13}C NMR (101 MHz, CDCl$_3$): δ 179.2 (C24), 75.4 (C7), 72.1 (C3), 54.9, 51.6, 45.1, 44.4, 41.8, 40.5, 40.4, 39.7, 38.8, 36.4, 35.7, 35.5, 34.5, 32.1, 31.1, 31.0, 30.9, 30.5, 30.3, 29.7, 29.4, 28.5, 27.2, 25.2, 23.0, 22.8, 21.6, 18.6, 14.2, 12.4. LRMS (ESI neg): m/z 517.4 (58%, [M-H]$^-$), 563.4 (100%, [M+FA-H]$^-$), 577.4 (60%, [M+AcOH-H]$^-$), 1035.9 (69%, [2M-H]$^-$). HRMS (ESI neg): m/z calcd for C$_{33}$H$_{57}$O$_4$ [M-H]$^-$: 517.4262, found: 517.4258. Calcd for C$_{33}$H$_{58}$O$_4$: 76.40% C, 11.27% H, found: 75.96% C, 11.15% H. *HPLC Method B* (ESI neg, t_R = 25.75 min). Purity 97.9% (*HPLC method A*, t_R = 4.36 min).

(*E*)-7-Ethylidene-3α-hydroxy-5β-cholan-24-oic Acid (75)
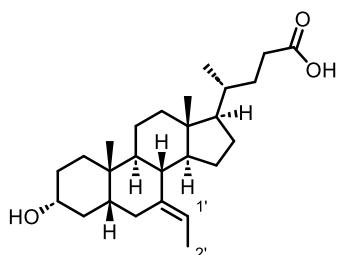
Sodium hydride (3.0 equiv., 60% in mineral oil, 59 mg, 1.48 mmol) was added to a solution of ethyltriphenylphosphonium bromide (3.0 equiv., 550 mg, 1.50 mmol) in dry THF (15 mL) under an inert atmosphere. The reaction mixture was refluxed until a deep orange color formed. Then, the solution was cooled to 50 °C, and a solution of 3α-hydroxy-7-oxo-5β-cholan-24-oic acid (**61**, 200 mg, 0.50 mmol) in dry THF (10 mL) was slowly added dropwise. After overnight reflux, the reaction mixture was poured into a beaker with crushed ice and extracted with EtOAc (3 × 50 mL). The combined organic extracts were washed with water (20 mL), brine (20 mL), dried over Na$_2$SO$_4$, and solvents evaporated. The crude product was purified by column chromatography on silica gel (MeOH/DCM, 2:98 to 5:95, both solvents with 0.01% formic acid), followed by purification on semi-preparative HPLC (column: Luna$^®$ 5 μm bare-silica 250 × 21.2 mm, isocratic: MeOH/DCM, 3:97, 15 mL/min, injected: in DCM) afforded compound **75** as a slightly yellowish powder (6 mg, 3%). TLC: R_f 0.69 (EtOAc/hexanes/AcOH, 50:50:1). Mp: 67–72 °C (DCM/MeOH, 200:1). ^{1}H NMR (500 MHz, CD$_3$OD): δ 5.30 (q, J = 6.7 Hz, 1H, H-1'), 3.58–3.50 (m, 1H, H-3), 1.59–1.56 (m, 3H, H-2'), 1.08 (s, 3H, H-19), 0.96 (d, J = 6.5 Hz, 3H, H-21), 0.71 (s, 3H, H-18). ^{13}C NMR (126 MHz, CD$_3$OD): δ 176.5 (C24), 140.9 (C6), 115.6 (C1'), 72.0 (C3), 56.4, 51.4, 46.5, 44.3, 44.12, 44.09, 40.5, 37.1, 37.1, 36.6, 36.1, 32.6, 32.3, 31.8, 31.0, 29.1, 26.5, 24.3, 22.1, 18.9, 13.3, 12.7. LRMS (ESI neg): m/z 401.3 (76%, [M-H]$^-$), 447.3 (100%, [M+FA-H]$^-$), 803.6 (10%, [2M-H]$^-$). HRMS (ESI neg): m/z calcd for C$_{26}$H$_{41}$O$_3$ [M-H]$^-$: 401.3061, found: 401.3062. *HPLC Method B* (ESI neg, t_R = 17.45 min). Purity 97.5% (*HPLC method A*, t_R = 5.26 min).

105

3α,7α-Dihydroxy-7β-(phenylethynyl)-5β-cholan-24-oic Acid (76)
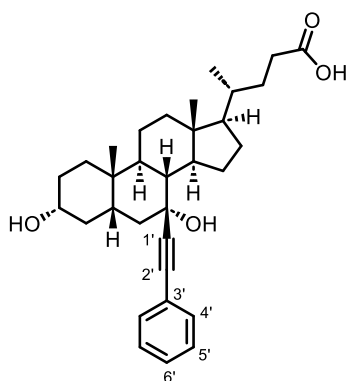
In round bottom flask (100 mL), under nitrogen and at rt, 3α,7α-dihydroxy-7β-ethynyl-5β-cholan-24-oic acid (65, 150 mg, 0.37 mmol), Pd(PPh$_3$)$_4$ (0.1 equiv., 43 mg, 0.04 mmol), CuI (0.2 equiv., 13 mg, 0.07 mmol), iodobenzene (1.0 equiv., 41 µL, 0.37 mmol) and TEA (2.4 equiv., 124 µL, 0.9 mmol) were dissolved in dry DMF (10 mL) and reaction was stirred 2 hours at 70 °C under nitrogen atmosphere. After 18 hours, silica (1.5 g) was added into the reaction mixture. After solvent evaporation, the resulting brown powder was subjected to flash column chromatography on silica gel (MeOH/DCM, 0:100 to 8:92, both solvents with 0.01% formic acid), followed by purification on semi-preparative HPLC (Column, Luna® 5 µm bare-silica 250 × 21.2 mm, Isocratic MeOH/DCM, 3:97, 20 mL/min, injected in THF) affording compound 76 as a white powder (30 mg, 16%). TLC: R$_f$ 0.31 (MeOH/DCM/AcOH, 10:100:1). [α]$_D$: +61.1 (c 0.244, MeOH). ^{1}H NMR (401 MHz, CD$_3$OD): δ 7.37–7.08 (m, 5H, 2 × H-4' + 2 × H-5' + H-6'), 3.40 (tt, J = 11.2, 4.5 Hz, 1H, H-3), 0.98 (s, 3H, H-19), 0.98 (d, J = 6.5 Hz, 3H, H-21), 0.75 (s, 3H, H-18). ^{13}C NMR (101 MHz, CD$_3$OD): δ 179.4 (C24), 132.1 (2 × C4'), 129.4 (2 × C5'), 128.9 (C6'), 125.1 (C3'), 97.9 (C1'), 83.8 (C2'), 72.7 (C3), 70.2 (C7), 56.8 (C17), 52.2 (C14), 45.4, 44.7 (C13), 43.7, 43.3, 41.4 (C12), 39.4, 36.8 (C20), 36.6, 36.2, 35.7 (C10), 32.4 (C22 + C23), 31.2, 29.5, 27.5 (C15), 23.5 (C19), 22.1, 19.0 (C21), 12.5 (C18). IR: (KBr) 3081 (O-H, dimer), 1709 (C=O, COOH, dimer), 2221 (C≡C). LRMS (ESI pos): m/z 515.3 (100%, [M+Na]$^+$), 457.3 (33%, [M-2H$_2$O+H]$^+$), 475.3 (30%, [M-H$_2$O+H]$^+$). HRMS (ESI pos): m/z calcd for C$_{32}$H$_{44}$O$_4$Na [M+Na]$^+$): 515.31318, found: 515.31263. Calcd for C$_{32}$H$_{44}$O$_4$ 78.01% C, 9.00% H, found: 77.81% C, 8.96% H. Purity 99.9% (*HPLC Method C*, t$_R$ = 6.13 min).

1-Azido-1,1,2,2,2-pentafluoroethane (79)

The molecule was synthesized with the help of Lukáš Janecký in Dr. Beier's lab.
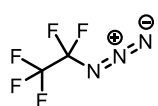
A tree neck round bottom flask was oven-dried overnight (100 °C) and flushed with nitrogen/vacuum 3 times. The vessel was closed with rubber septa and wrapped with parafilm. Under the backstream of the nitrogen, the vessel was charged with dry THF (40 mL). The needle with nitrogen backstream was removed, and through septa, C$_2$F$_5$H (1.0 equiv., 3.0 g, 25 mmol) was bubbled into THF. Then, the solution was cooled with ethanol/dry ice bath (-78°C), and *n*-BuLi was added slowly dropwise (2.5 M in hexanes, 1.0 equiv., 10.0 mL, 25 mmol, addition over 30 minutes). The reaction changed color to deep brown and stirring continued for 30 minutes at -78 °C. A solution of TsN$_3$ (80, 1.0 equiv., 25 mmol, 3.8 mL dissolved in 10 mL THF) was slowly added, which turned the reaction color to pinky-brownish. After 30 minutes at -78 °C, the reaction content was distilled (gentle flow of nitrogen, 40–67 °C, 760 torr) and collected as one fraction into a cryo-trap (-78 °C). This afforded a clear THF solution of 79 (40 mL, 0.15 M, 30%). The concentration and yield of azide were determined by ^{19}F NMR with PhCF$_3$ as an internal standard: airtight NMR cuvette was filled with THF solution of unknown azide concentration (100 µL), internal standard PhCF$_3$ (10 µL), and CDCl$_3$ (400 µL). The concentration is calculated as a ratio of

$N_3CF_2C\underline{F}_3$/PhC$\underline{F}_3$ in ^{19}F NMR experiment. ^{19}F NMR (376 MHz, CDCl$_3$): δ -86.3 (s, 2F, CF$_2$), -94.1 (s, 3F, CF$_3$). The NMR analysis is consistent with the previous report.[220]

The THF solution of **79** was stored in a tightly closed screw-cap vial in a freezer (-20 °C) overnight without a noticeable concentration decline.

4-Methylbenzene-1-sulfonyl Azide (**80**)

CAUTION: Sodium azide (NaN$_3$) can decompose explosively above its melting point. It forms explosive azides with metals such as Cu, Pb, Hg, Ag, and Au and reacts with acids to form hydrazoic acid (HN$_3$), which is a toxic, spontaneously explosive gas. Chlorinated solvents should be avoided. All work with NaN$_3$ should be conducted behind a shield and in a fume hood. Excess NaN$_3$ is extracted to the water phase and destroyed in a fume hood by oxidation with cerium(IV) ammonium nitrate.[296]
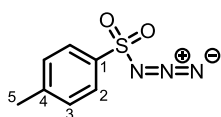
The round bottom flask (500 mL) was charged with tosyl chloride (15 g, 78.7 mmol), acetone (150 mL), magnetic stirring bar and cooled down to 0 °C. Then, a solution of sodium azide (1.5 equiv., 7.67 g, 118 mmol, in 50 mL of water) was added dropwise through a drip funnel, resulting in a milky white solution. The reaction was loosely closed with a cap and left stirring at rt overnight. After 18 hours the acetone was evaporated (rotavap, 30 °C). The resulting biphasic system was extracted with Et$_2$O (2 × 50 mL), combined organic extracts were washed with water (2 × 50 mL), 10% NaHCO$_3$ (50 mL), brine (50 mL) and dried over MgSO$_4$. The mixture was stripped of solvents, and the material was further dried on a central vacuum line (20 mbar, overnight, rt) to obtain **80** as a sweet-smelling colorless liquid (12.5 g, 81%). The material was used immediately without further purification. ^{1}H NMR (401 MHz, CDCl$_3$): δ 7.84 (d, J = 8.4 Hz, 2H, H-2), 7.41 (d, J = 8.7, 2H, H-3), 2.48 (s, 3H, H-5). The NMR analysis is consistent with the previous report.[297]

CAUTION: While Tosyl azide is considered a relatively safe azide, it thermally decomposes above 120 °C and should be handled at room temperature.[298-300]

3α-Hydroxy-7β-(1-(perfluoroethyl)-1*H*-1,2,3-triazol-4-yl)-5β-cholan-24-oic Acid (**81**)
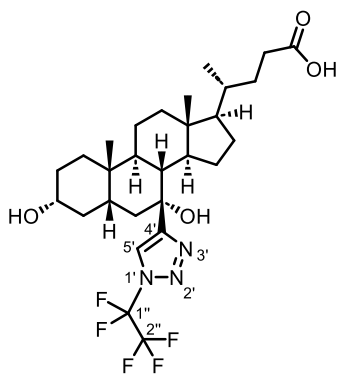
Tear flask (50 mL) was charged with magnetic stirring bar, 3α,7α-dihydroxy-7β-ethynyl-5β-cholan-24-oic acid (**65**, 215 mg, 0.53 mmol), copper(I) 3-methylsalicylate (2 mol%, 2 mg, 0.01 mmol), and freshly prepared solution of 1-azido-1,1,2,2,2-pentafluoroethane (**79**, 0.15 M in THF, 4 equiv., 14.1 mL, 2.12 mmol). The reaction turned slightly blue, flask was closed with septa and stirred at rt overnight. After 18 hours, silica (1.5 g) was added, and the mixture was stripped of solvents. The resulting blue powder was subjected to flash column chromatography on silica gel (MeOH/DCM, 0:100 to 8:92, both solvents with 0.01% formic acid), followed by purification on semi-preparative HPLC (column: Luna® 5 µm bare-silica 250 × 21.2 mm, isocratic: MeOH/DCM, 3:97, 20 mL/min, injected: in THF) affording compound **81** as a slightly yellowish powder (130 mg, 41%). TLC: R$_f$ 0.34 (MeOH/DCM/AcOH, 10:100:1). Mp: 198–203 °C (CHCl$_3$/MeOH, 2 mL:1 drop). [α]$_D$: +11.7 (c 0.205, MeOH). Selected ^{1}H NMR (401 MHz, CD$_3$OD): δ 8.18 (s, 1H, H-5'), 3.44 (tt, J = 11.1, 4.5 Hz, 1H, H-3), 2.45 (dd, J = 11.0, 11.0 Hz, 1H, H-8), 0.94 (d, J = 6.8 Hz, 3H, H-21), 0.19–0.04 (m, 1H, H$_a$-15).

^{13}C NMR (101 MHz, CD$_3$OD): δ 178.2 (C24), 161.9 (C4'), 121.7 (C5'), 74.2 (C-7), 72.6 (C3), 56.4 (C-17), 51.9 (C14), 44.7 (C13), 44.0, 43.9 (C8), 43.4, 41.3 (C12), 39.3, 36.7, 36.6, 36.4, 35.8 (C10), 32.2 (C22), 31.9 (C23), 31.3, 29.2, 26.8 (C15), 23.5 (C19), 22.2, 18.9 (C21), 12.4 (C18). ^{19}F NMR (376 MHz, CD$_3$OD): δ -84.04 (s, 3F, F-2''), -98.52 (d, J = 2.9 Hz, 2F, F-1''). IR (KBr): 3436 (O-H), 1713, 1696 (C=O, COOH, dimer), 1344, 1321 (CF$_3$), 1196 (CF$_2$), 3139, 1445, 1235 (=C-H). LRMS (ESI pos): m/z 578.3 (100%, [M+H]$^+$, 600.3 (35%, [M+Na]$^+$). HRMS (ESI pos): m/z calcd for C$_{28}$H$_{40}$O$_4$N$_3$F$_5$ [M+H]$^+$: 578.30317, found: 518.30086. Calcd for C$_{28}$H$_{42}$O$_4$N$_3$F$_5$: 58.22% C, 6.98% H, 7.27% N, found: 57.22% C, 7.14% H, 5.88% N. Purity 98.9% (*HPLC Method C*, t$_R$ = 5.22 min).

Methyl 3α,7-Bis[(trimethylsilyl)oxy]-5β-chol-6-en-24-oate (82)
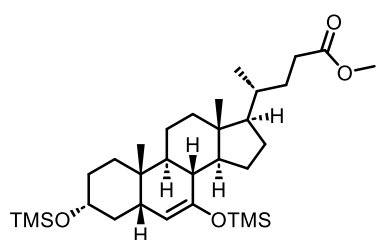
A solution of n-buthyllithium in hexanes (2.5 M, 6 equiv., 31.6 mL, 79 mmol) was added to the solution of diisopropylamine (6 equiv., 10.4 mL, 79 mmol) in dry THF (25 mL) at -78 °C under argon atmosphere. After 30 minutes, a solution of trimethylsilyl chloride was added dropwise (8 equiv., 18.0 mL, 97 mmol), and the reaction mixture was stirred at -78 °C another 10 minutes. Then, a solution of methyl 3α-hydroxy-7-oxo-5β-cholan-24-oate in dry THF (59, 5.01 g, 12 mmol, dissolved in 18 mL of dry THF) was added dropwise. The reaction mixture was then stirred at -78 °C for 30 minutes. Triethylamine was added (15 equiv., 24.1 mL, 180 mmol), and the reaction was allowed to warm to -20 °C and quenched by adding a saturated aqueous solution of NaHCO$_3$ (30 mL). After warming to rt, the water phase was extracted with EtOAc (3 × 50 mL). Combined organic fractions were washed with a saturated solution of NaHCO$_3$ (50 mL), water (50 mL), brine (50 mL), dried over anhydrous Na$_2$SO$_4$, and the solvent was evaporated to obtain thick yellow oil (6.85 g). Fast column chromatography on silica gel (EtOAc/hexanes, 3:97) gave compound 82 (6.62 g, 97%) as yellow oil, which was used immediately for the next reaction without further purification. Selected ^{1}H NMR (401 MHz, CDCl$_3$): δ 4.72 (dd, J = 5.9, 1.9 Hz, 1H, H-6), 3.65 (s, 3H, H-25), 3.50 (tt, J = 11.0, 4.5 Hz, 1H, H-3), 2.34 (ddd, J = 15.1, 10.0, 5.0 Hz, 1H, H$_a$-23), 2.21 (ddd, J = 15.5, 9.4, 6.6 Hz, 1H, H$_b$-23), 0.91 (d, J = 6.3 Hz, 3H, H-21), 0.81 (s, 3H, H-19), 0.67 (s, 3H, H-18), 0.15 (s, 6H, OTMS), 0.10 (s, 6H, OTMS). ^{13}C NMR (101 MHz, CDCl$_3$): δ 174.9 (C24), 151.8 (C6), 109.0 (C7), 71.7 (C3), 55.0 (C17), 54.2, 51.6 (C25), 44.5, 42.8, 41.1, 41.1, 40.5, 40.3, 35.4, 34.8, 33.1, 31.23, 31.17, 30.8, 28.8, 27.2, 22.7 (C19), 21.1, 18.6 (C21), 12.4 (C18), 0.5 (OTMS), 0.4 (OTMS).

Methyl (*E/Z*)-6-Ethylidene-3α-hydroxy-7-oxo-5β-cholan-24-oate (83)
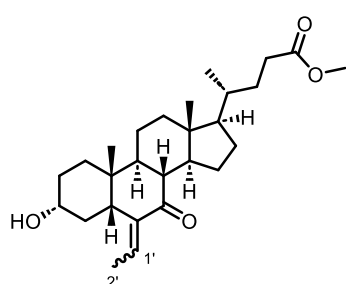
Methyl 3α,7-bis[(trimethylsilyl)oxy]-5β-chol-6-en-24-oate (82, 6.60 g, 12.02 mmol) was dissolved in dry DCM (20 mL) under argon. The mixture was cooled down to -78 °C. Then, a solution of acetaldehyde in dry DCM (1:9, 20.3 mL, 36.07 mmol) was added dropwise, and the mixture was stirred for 10 min. A solution of BF$_3$·Et$_2$O (13.4 mL, 48.09 mmol) was added dropwise over the course of 1 hour, and the reaction was stirred at -78 °C for an additional 2 hours and then allowed to warm to rt. The reaction was quenched by adding a saturated aqueous solution of NaHCO$_3$ (50 mL). The water phase was then extracted with DCM (3 × 50 mL). Combined organic fractions

were washed with a saturated solution of $NaHCO_3$ (50 mL), water (50 mL), brine (50 mL), dried over anhydrous Na_2SO_4, and the solvent was evaporated to obtain thick yellow oil (4.90 g). Column chromatography on silica gel (EtOAc/hexanes, 1:3) gave compound **83** (4.3 g, 83%), slightly yellowish powder as a mixture of *E/Z*-isomers (*E/Z*, 2:1 from ^{1}H NMR). TLC: R_f 0.52 (EtOAc/hexanes, 1:1). Selected ^{1}H NMR (400 MHz, $CDCl_3$): δ 6.18 (q, *J* = 7.1 Hz, 1H, H-1'), 3.69–3.62 (m, 4H, H-3 and H-25), 2.58 (dd, *J* = 13.0, 4.2 Hz, 1H, H-5), 1.69 (d, *J* = 7.1 Hz, 3H, H-2'), 1.00 (s, 3H, H-19), 0.93 (d, *J* = 6.4 Hz, 3H, H-21), 0.64 (s, 3H, H-18). ^{13}C NMR (101 MHz, $CDCl_3$): δ 207.4 (C7), 176.3 (C24), 145.3 (C6), 130.4 (C1'), 70.9 (C3), 55.9, 52.0 (C25), 52.0, 50.1, 46.8, 44.7, 40.7, 40.2, 38.4, 36.5, 35.8, 35.4, 32.2, 31.8, 30.5, 29.4, 27.0, 23.3 (C19), 22.4, 18.9 (C21), 12.7 (C2'), 12.5 (C18). IR ($CHCl_3$): 3608 (O-H), 1731 (C=O, COOMe), 1685 (C=O), 1632 (C=C), 1220 (C-O, COOMe), 1060 (C-OH). HRMS (EI pos): *m/z* calcd for $C_{27}H_{42}O_4$ [M+H]$^{+•}$: 430.3083, found: 430.3080. Calcd for $C_{27}H_{42}O_4$: 75.31% C, 9.83% H, found: 75.18% C, 9.99% H.

(*E/Z*)-6-Ethylidene-3α-hydroxy-7-oxo-5β-cholan-24-oic Acid (84)
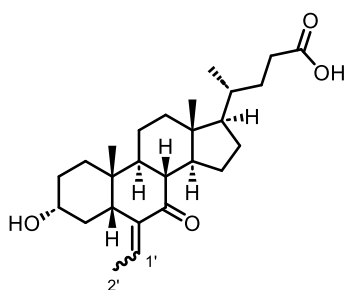
Methyl (*E/Z*)-6-ethylidene-3α-hydroxy-7-oxo-5β-cholan-24-oate (**83**, 700 mg, 1.62 mmol) was dissolved in 50 mL of 5% NaOH in MeOH/H_2O (1:1) and heated to 50 °C. After 2 hours, HCl (aq. 1M) was added dropwise to achieve acidic pH. The product was extracted with EtOAc (3 × 40 mL), combined organic extracts were washed with water, (30 mL), brine (30 mL), and dried over anhydrous Na_2SO_4. Column chromatography on silica gel (EtOAc/hexanes/AcOH, 20:80:1) gave off-white powder of **84** (670 mg, 99%) as a mixture of

E/Z-isomers. (*E/Z*, 2:1 from ^{1}H NMR). TLC: R_f 0.53 (acetone/hexanes/AcOH, 30:70:1). Selected ^{1}H NMR (400 MHz, CD_3OD): δ 6.08 (q, *J* = 7.1 Hz, 1H, H-1'), 3.60 (tt, *J* = 11.1, 4.7 Hz, 1H, H-3), 2.68 (dd, *J* = 13.0, 4.3 Hz, 1H, H-5), 1.71 (d, *J* = 7.1 Hz, 3H, H-2'), 1.04 (s, 3H, H-19), 0.98 (d, *J* = 6.5 Hz, 3H, H-21), 0.69 (s, 3H, H-18). ^{13}C NMR (101 MHz, CD_3OD): δ 207.6 (C7), 178.1 (C24), 145.4 (C6), 130.4 (C1′), 71.0 (C3), 56.0, 52.0, 50.2, 46.9 (C5), 44.7, 40.7, 40.3, 38.4, 36.6, 35.8, 35.4, 32.3, 32.0, 30.5, 29.4, 27.0, 23.2 (C19), 22.4, 18.9 (C21), 12.7 (C2′), 12.4 (C18). IR ($CHCl_3$): 3419 (O-H), 1707 (C=O, COOH), 1690 (C=O), 1624 (C=C), 1290 (C-O, COOH), 1064 (C-OH). HRMS (ESI neg): *m/z* calcd for $C_{26}H_{39}O_4$ [M-H]$^-$: 415.2854, found: 415.2849. Calcd for $C_{26}H_{39}O_4$: 74.96% C, 9.68% H, found: 74.81% C, 9.71% H.

6α-Ethyl-3α-hydroxy-7-oxo-5β-cholan-24-oic Acid (85)
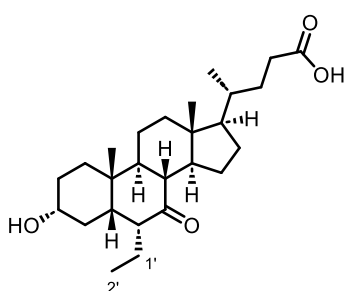
(*E/Z*)-6-Ethylidene-3α-hydroxy-7-oxo-5β-cholan-24-oic acid (**84**, 500 mg; 1.16 mmol) was dissolved in EtOH (96%, 20 mL), and Pd/C (10%, 1 wt.%, 50 mg) was added. The mixture was hydrogenated at 1 atm. while being vigorously stirred overnight. The catalyst was filtered through diatomaceous earth, and the solvent evaporated. Column chromatography on silica gel (EtOAc/hexanes/AcOH, 30:70:1) yielded compound **85** (473 mg, 95%) as a white powder. For crystallization, the material (450 mg) was placed in a 4 mL screw-cap vial and dissolved in an acetone/MeOH mixture (2 mL, 100:1). The vial was then placed in a 250 mL jar, which was partially filled with water (5 mL). The jar was sealed, and the vial was left to stand in the saturated water vapor

for two weeks. The obtained prism-shaped crystals (100 mg) were washed with redistilled HPLC-grade pentane (2 × 1 mL) and used for analysis after drying. The mother liquors were evaporated to dryness, and the residue was dried in a vacuum oven (1 week, 50 °C, 0.25 kPa) and used for further synthesis as such. TLC: R_F 0.40 (EtOAc/hexanes/AcOH, 50:50:1) $[α]_D$: -54.5 (c 0.08, CHCl$_3$). Mp: 182–184 °C (acetone/MeOH/water). Selected ^{1}H NMR (401 MHz, CD$_3$OD): δ 3.55–3.37 (m, 1H, H-3), 2.85 (dt, J = 7.7, 5.5 Hz, 1H, H-6), 2.52 (t, J = 11.2 Hz, 1H, H-8), 1.28 (s, 3H, H-19), 0.98 (d, J = 6.5 Hz, 3H, H-21), 0.84 (t, J = 7.4 Hz, 3H, H-2'), 0.73 (s, 3H, H-18). ^{13}C NMR (101 MHz, CD$_3$OD): δ 215.4 (C7), 178.0 (C24), 71.6 (C3), 56.3, 53.2, 52.1, 51.1, 50.4, 45.3, 43.8, 40.3, 36.8, 36.5, 35.2, 32.5, 32.3, 31.9, 30.5, 29.2, 25.6, 23.9 (C19), 22.9, 20.0, 18.8 (C21), 12.5 (C18), 12.2 (C2'). IR (KBr): 3439 (O-H), 1729 (C=O, COOMe), 1687 (C=O), 1294 (C-O, COOMe), 1061 (C-OH). LRMS (ESI neg): m/z 417.5 (100%, [M-H]$^-$). HRMS (ESI pos): m/z calcd for C$_{26}$H$_{42}$O$_4$Na [M+Na]$^+$: 441.2975, found: 441.2976. Calcd for C$_{26}$H$_{42}$O$_4$: 74.60% C, 10.11% H, found: 74.37% C, 10.09% H. Purity 98.1% (*HPLC Method B*, t_R = 13.35 min).

6α-Ethyl-3α-hydroxy-7-oxo-5β-cholan-24-oic Acid (86)
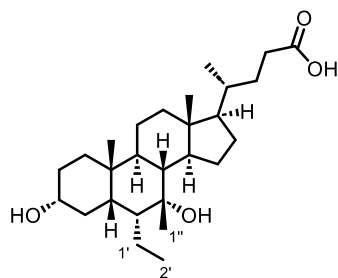
A three-neck round bottom flask (100 mL), equipped with a magnetic stirring bar, was heat gun dried, evacuated, backfilled with nitrogen, and charged with methylmagnesium bromide (5 equiv., 1.7 mL, 2.4 mmol, 1.4 M in THF/toluene 1:3) and dry THF (20 mL). A solution of 6α-ethyl-3α-hydroxy-7-oxo-5β-cholan-24-oic acid (85, 200 mg, 0.48 mmol in 5 mL dry THF) was added dropwise at room temperature through septa under counterflow of nitrogen. Upon steroid addition, a cloud-like precipitate formed. The solution was then vigorously stirred and heated to reflux. The progress of the reaction was monitored by TLC. After 2 hours, the reaction mixture was acidified to pH 2 (aq. 1 M HCl) and extracted with EtOAc (3 × 15 mL). The combined organic extracts were washed with water (20 mL), brine (20 mL), dried over Na$_2$SO$_4$, and the solvents were evaporated. The crude product was purified by column chromatography on silica gel (MeOH/DCM, 2:98 to 5:95), followed by purification on semi-preparative HPLC (column: Luna$^®$ 5 µm bare-silica 250 × 21.2 mm, isocratic: MeOH/DCM, 3:97, 15 mL/min, injected: in DCM). This afforded compound 86 as a white powder (40 mg, 32%). TLC: R_f 0.31 (MeOH/DCM/AcOH, 100:900:1). $[α]_D$: +9.9 (c 0.131, CHCl$_3$). Selected ^{1}H NMR (401 MHz, CDCl$_3$): δ 3.45 (tt, J = 10.5, 5.0 Hz, 1H, H-3), 2.45–2.33 (m, 1H, H$_a$-23), 2.31–2.19 (m, 1H, H$_b$-23), 1.25 (s, 3H, H-1'), 0.95 (d, J = 6.3 Hz, 3H, H-21), 0.87 (t, J = 6.5 Hz, 3H, H-2'), 0.84 (s, 3H, H-19), 0.70 (s, 3H, H-18). ^{13}C NMR (101 MHz, CDCl$_3$): δ 179.1 (C24), 75.3 (C7), 72.5 (C3), 55.0 (C17), 52.1 (C14), 46.2 (C6), 45.4 (C8), 44.5 (C13), 42.5 (C5), 40.6 (C12), 37.3 (C9), 36.1 (C1), 35.6 (C20), 34.7 (C10), 32.0 (C4), 31.0 (C23), 30.9 (C22), 30.5 (C2), 29.6 (C1''), 28.7 (C16), 28.6 (C15), 23.4 (C19), 21.8 (C11), 18.6 (C21), 17.5 (C1'), 12.7 (C18), 12.2 (C2'). IR (CHCl$_3$): 3611 (O-H), 1708 (C=O, COOH), 3517 (O-H, COOH). LRMS (ESI neg): m/z 433.3 (100%, [M-H]$^-$), 479.3 (70%, [M+FA-H]$^-$), 867.7 (65%, [2M-H]$^-$). HRMS (ESI neg): m/z calcd for C$_{27}$H$_{45}$O$_4$ [M-H]$^-$: 417.30103, found: 417.30072. Calcd for C$_{27}$H$_{46}$O$_4$: 76.61% C, 10.67% H, found: 74.15% C, 10.31% H. Purity 98.5% (*HPLC Method C*, t_R = 7.64 min).

cis-4-tert-Butylcyclohexanol (87) and trans-4-tert-Butylcyclohexanol (88)

Purification of a commercially available mixture of *cis*- and *trans*-4-*tert*-butylcyclohexanol (Merck, 10 g, 64 mmol) with flash chromatography (gradient 5% to 50% over 30 column volumes of Et_2O in PE) gave **87** (2.6 g, 26%) and **88** (7.1 g, 71%). Both crystallized directly from the eluting solvent as small needles.
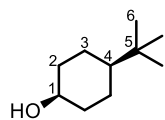
87: TLC: R_f 0.36 (Et_2O/PE, 1:1). Mp: 72–75 °C (Et_2O/PE), lit.[301] 78 °C (no solvent given). $[\alpha]_D$: 0 (c 0.367, $CHCl_3$). ^1H NMR (401 MHz, $CDCl_3$): δ 4.09–3.97 (m, 1H, H-1), 1.89–1.77 (m, 2H, H_a-2), 1.59–1.26 (m, 6H, H_b-2 and H-3), 0.99 (tt, J = 11.6, 3.1 Hz, 1H, H-4), 0.85 (s, 9H, H-6). ^{13}C NMR (101 MHz, $CDCl_3$): δ 66.0 (C1), 48.2 (C4), 33.5 (C3), 32.7 (C5), 27.6 (C6), 21.0 (C2). The NMR analysis is consistent with the previous report.[301] Calcd for $C_{10}H_{20}O$: 76.86% C, 12.90% H, found: 76.77% C, 12.74% H.
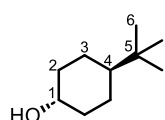
88: TLC: R_f 0.24 (Et_2O/PE, 1:1). Mp: 74–79 °C (Et_2O/PE), lit.[301] 79 °C (no solvent given). $[\alpha]_D$: 0 (c 0.333, $CHCl_3$). ^1H NMR (401 MHz, $CDCl_3$): δ 3.51 (tt, J = 10.9, 4.4 Hz, 1H, H-1), 2.05–1.94 (m, 2H, H_a-2), 1.84–1.73 (m, 2H, H_a-3), 1.30–1.14 (m, 2H, H_b-3), 1.12–1.00 (m, 2H, H_b-3), 0.99–0.92 (m, 1H, H-4), 0.84 (s, 9H, H-6). ^{13}C NMR (101 MHz, $CDCl_3$): δ 71.4 (C1), 47.3 (C4), 36.2 (C2), 32.4 (C5), 27.8 (C6), 25.7 (C3). The NMR analysis is consistent with the previous report.[301] Calcd for $C_{10}H_{20}O$: 76.86% C, 12.90% H, found: 76.66% C, 12.75% H.

4-tert-Butylcyclohexanone (89)
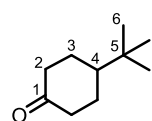
A commercially available mixture of *cis*- and *trans*-4-*tert*-butylcyclohexanol (Merck, 390 mg, 2.5 mmol) was dissolved in acetone (25 mL), and a solution was cooled to 0 °C with an ice bath. Jones reagent was added dropwise (2.67 M solution, 1.0 equiv., 2.5 mmol, 0.94 mL). After 30 minutes of stirring, the reaction mixture was neutralized with a saturated solution of aqueous $NaHCO_3$. Then, water was added (25 mL), and the product was extracted with DCM (3 × 25 mL). The organic solvent was dried with $MgSO_4$ and evaporated with silica gel (2.5 g). The dry load of crude material was purified by flash chromatography on a silica gel (gradient 5% to 50% over 30 column volumes of Et_2O in PE) to afford **89** as a white powder (238 mg, 62%). TLC: R_f 0.57 (Et_2O/PE, 1:1). Mp: 48–51 °C (Et_2O/PE), lit.[302] 48 °C (no solvent given). $[\alpha]_D$: 0 (c 0.285, $CHCl_3$). ^1H NMR (401 MHz, $CDCl_3$): δ 2.46–2.21 (m, 4H, H-2), 2.17–1.98 (m, 2H, H_a-3), 1.54–1.34 (m, 3H, H_b-3 and H-4), 0.91 (s, 9H, H-6). ^{13}C NMR (101 MHz, $CDCl_3$): δ 212.8 (C1), 46.8 (C4), 41.5 (C2), 32.6 (C5), 27.7 (C6), 27.7 (C3). The NMR analysis is consistent with the previous report.[303] Calcd for $C_{10}H_{18}O$: 77.87% C, 11.76% H, found: 77.67% C, 11.50% H.

Methyl 3α,12α-dihydroxy-5β-cholan-24-oate (90), (Methyl Deoxycholate)
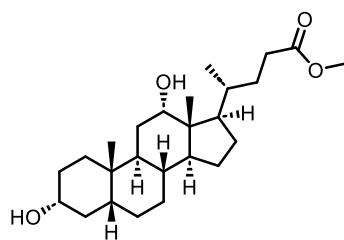
To a solution of 3α,12α-dihydroxy-5β-cholan-24-oic acid (10.0 g, 25.47 mmol) in MeOH (200 mL), was dropwise added concentrated H_2SO_4 (98%, 1 mL). The mixture was refluxed for 6 hours. The reaction was quenched with a saturated aqueous solution of $NaHCO_3$ until approximately pH 7 was achieved. The solvent was partially evaporated, reducing the volume to approximately half of the original volume, and extracted with $CHCl_3$ (3 × 150 mL). Combined organic

fractions were washed with saturated solution of $NaHCO_3$ (2 × 150 mL), water (100 mL), brine (100 mL), dried over anhydrous Na_2SO_4, and the solvent was evaporated to obtain yellow oil (10.0 g). The crude product was purified by column chromatography on silica gel (gradient 50% to 100% over 20 column volumes of EtOAc in PE) to obtain **90** as oily material (9.4 g, 94%) that solidified upon drying with the oil pump. TLC: R_f 0.28 (EtOAc/hexanes, 1:1). [α]$_D$: +42.2, (c 0.332, CHCl$_3$), lit.[304] +41.3 (c 2, CHCl$_3$). ^{1}H NMR (400 MHz, CDCl$_3$): δ 3.87–3.81 (m, 1H, H-12), 3.65 (s, 3H, H-25), 3.51–3.40 (m, 1H, H-3), 2.34 (ddd, J = 15.4, 10.1, 5.2 Hz, 1H, H$_a$-23), 2.26–2.20 (m, 1H, H$_b$-23), 0.91 (d, J = 6.5 Hz, 3H, H-21), 0.89 (s, 3H, H-19), 0.65 (s, 3H, H-18). ^{13}C NMR (101 MHz, CDCl$_3$): δ 174.9 (C24), 72.2 (C3), 68.6 (C12), 55.9 (C17), 51.6 (C25), 50.6, 42.8 (C13), 41.6, 39.9, 39.8, 39.5, 35.5 (C20), 35.5, 35.2 (C10), 34.7, 33.0, 31.1 (C23), 31.1, 30.7, 28.3, 23.8, 22.9 (C19), 20.7, 18.4 (C21), 11.9 (C18). IR (CHCl$_3$): COOMe, 1730 (C=O), 1234 (C-O); 3612 (O-H), 1062 and 1039 (C-OH). HRMS (ESI pos): m/z calcd for $C_{25}H_{43}O_4$ [M+H]$^+$: 407.31559, found: 407.31548. Calcd for $C_{25}H_{42}O_4$: 73.85% C, 10.41% H, found: 72.26% C, 10.27% H.

Methyl 12α-Hydroxy-3-oxo-5β-cholan-24-oate (91), Methyl 3α-Hydroxy-12-oxo-5β-cholan-24-oate (92), and Methyl 3,12-Dioxo-5β-cholan-24-oate (93)

The round bottom flask (100 mL) was charged with methyl 3α,12α-dihydroxy-5β-cholan-24-oate (**90**, 1.0 g, 2.5 mmol), DCM (25 mL), and a stirring bar. The mixture was stirred for 30 minutes, and then Dess–Martin periodinane (1.0 equiv., 1.06 g, 2.5 mmol) was added in one portion. The mixture was left open, stirred at rt for 24 hours. Then, silica gel (2.5 g) was added to the reaction mixture, and solvents were evaporated. The dry load of crude material was purified by flash chromatography on a silica gel. Elution with a gradient of EtOAc in PE (5% to 50% over 35 column volumes) afforded recovery of **90** (42 mg, 4%), **91** (8 mg, 1%), **92** (853 mg, 85%), and **93** (91 mg, 9%).
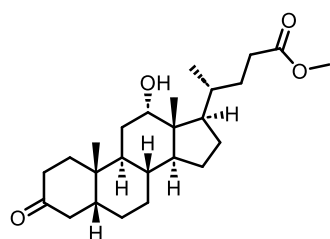
91: After solvent evaporation, the product solidified as a white powder (8 mg, 1%). TLC: R_f 0.25 (EtOAc/PE, 1:1). [α]$_D$: +56.9 (c 0.379, MeOH), lit.[305] +51.0 (c 0.5, EtOH). Selected ^{1}H NMR (401 MHz, CDCl$_3$): δ 3.92 (q, J = 3.1 Hz, 1H, H-12), 3.66 (s, 3H, H-25), 1.00 (s, 3H, H-19), 0.93 (d, J = 6.5 Hz, 3H, H-21), 0.69 (s, 3H, H-18). ^{13}C NMR (101 MHz, CDCl$_3$): δ 213.4 (C3), 174.9 (C24), 68.6 (C12), 56.0 (C17),

51.6 (C25), 50.5, 45.8, 43.3, 42.9, 39.7, 39.5, 37.1, 37.0, 35.49, 35.45, 34.0, 33.4, 31.12, 31.09, 28.3, 23.8, 22.1 (C19), 21.1, 18.4 (C21), 11.9 (C18). The NMR analysis is consistent with the previous report.[306] HRMS (ESI pos): m/z calcd for $C_{25}H_{40}O_4Na$ [M+Na]$^+$: 427.28188, found: 427.28163. Calcd for $C_{25}H_{40}O_4$: 74.22% C; 9.97% H, found: 73.88% C, 9.76% H.
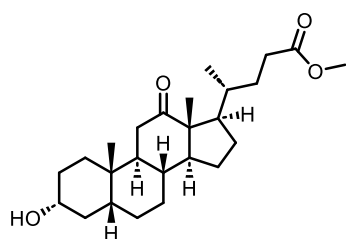
92: Product spontaneously crystalized after chromatography upon evaporation of solvents to afford white flakes (853 mg, 85%). TLC: R_f 0.18 (EtOAc/PE, 3:7). Mp: 115–118 °C (EtOAc/PE), lit.[304] 112–114 °C (acetone/H$_2$O). [α]$_D$: -16.5 (c 0.260, MeOH). Selected ^{1}H NMR (400 MHz, CDCl$_3$): δ 3.65 (s, 3H, H-25), 3.59 (tt, J = 10.8, 4.7 Hz, 1H, H-3), 2.84 (ddd, J = 12.6, 6.0, 1.1 Hz, 1H, H$_a$-11), 1.18 (s, 3H, H-19), 0.91 (d, J = 6.4 Hz, 3H, H-21), 0.64 (s, 3H, H-18). ^{13}C NMR (101 MHz, CDCl$_3$): δ 212.1 (C12), 174.8 (C24), 71.0 (C3), 54.9 (C17), 51.6 (C25), 49.6, 49.0, 46.2, 45.5, 42.9, 42.8, 39.1, 37.5, 35.4, 35.3, 34.3, 31.2, 31.1, 30.0, 28.4, 25.0, 23.2, 21.8 (C19), 18.5 (C21),

12.2 (C18). The NMR analysis is consistent with the previous report.[307] HRMS (ESI pos): *m/z* calcd for $C_{25}H_{40}O_4Na$ [M+Na]$^+$: 427.28188, found: 427.28167. Calcd for $C_{25}H_{40}O_4$: 74.22% C, 9.97% H, found: 73.91% C, 9.83% H.
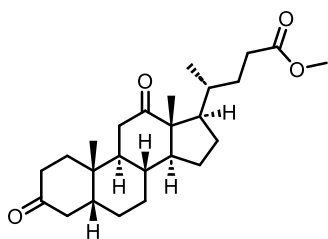
93: Product spontaneously crystalized after chromatography upon evaporation of solvents to afford colorless needles (91 mg, 9%). TLC: R$_f$ 0.34 (EtOAc/PE, 3:7). Mp: 133–135 °C (EtOAc/PE), lit.[308] 134–135 °C (aq. MeOH). [α]$_D$: +10.8 (c 0.258, MeOH), lit.[309] +12.2 (c 0.12, DCM). Selected ^{1}H NMR (400 MHz, CDCl$_3$): δ 3.65 (s, 3H, H-25), 2.87 (ddd, *J* = 12.9, 5.5, 1.0 Hz, 1H, H$_a$-11), 2.48 (ddd, *J* = 11.8, 10.7, 1.0 Hz, 1H, H$_a$-4), 1.29 (s, 3H, H-19), 0.92 (d, *J* = 6.5 Hz, 3H, H-21), 0.68 (s, 3H, H-18). ^{13}C NMR (101 MHz, CDCl$_3$): δ 211.3 (C3), 210.3 (C12), 174.7 (C24), 54.9 (C17), 51.6 (C25), 49.7, 49.0, 47.9, 45.1, 43.04, 42.98, 42.8, 39.0, 36.9, 35.6, 35.5, 35.3, 31.2, 31.1, 28.4, 24.9, 22.6 (C19), 22.2, 18.5 (C21), 12.2 (C18). The NMR analysis is consistent with the previous report.[310] HRMS (ESI pos): *m/z* calcd for $C_{25}H_{38}O_4Na$ [M+Na]$^+$: 425.26623, found: 425.26617. Calcd for $C_{25}H_{38}O_4$: 74.59% C, 9.51% H, found: C, 74.18% C, 9.47% H.

5α-Cholestan-2α,3α-diol (94)
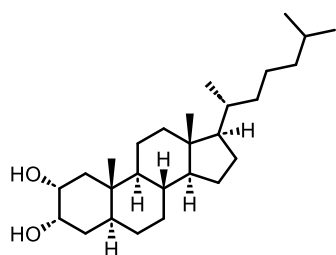
Compound **94** was taken from the group deposit, with the appearance of fine white powder. Selected ^{1}H NMR (400 MHz, CDCl$_3$): δ 3.96 (s, 1H, H-3), 3.76 (dt, *J* = 11.9, 4.3 Hz, 1H, H-2), 0.90 (d, *J* = 6.6 Hz, 3H, H-21), 0.86 (dd, *J* = 6.6, 1.9 Hz, 6H, H-26 and H-27), 0.80 (s, 3H, H-19), 0.65 (s, 3H, H-18). ^{13}C NMR (101 MHz, CDCl$_3$): δ 69.5 (C3), 69.3 (C2), 56.5, 56.4, 54.4, 42.7 (C14), 41.2, 40.1, 39.7, 38.3, 37.1 (C10), 36.3, 35.9, 35.0, 34.4, 32.0, 28.4, 28.2 (C25), 27.8, 24.4, 24.0, 23.0 (C26), 22.7 (C27), 21.1, 18.8 (C21), 12.6 (C19), 12.2 (C18).

3α-Hydroxy-5α-cholestan-2-one (95), 2α-Hydroxy-5α-cholestan-3-one (96)

Round bottom flask (100 mL) was charged with 5α-cholestan-2α,3α-diol (**94**, 1.0 g, 2.5 mmol), DCM (25 mL), and a stirring bar. The mixture was stirred for 30 minutes and then Dess–Martin periodinane (1.0 equiv., 1.06 g, 2.5 mmol) was added in one portion. The mixture was stirred at rt for 24 hours. Then, silica gel (2.5 g) was added to the reaction mixture, and solvents were evaporated. The dry load of crude material was purified by flash chromatography on a silica gel. Elution with a gradient of EtOAc in PE (5% to 50% over 35 column volumes) afforded recovery of **94** (30 mg, 30%), **95** (21 mg, 21%), **96** (23 mg, 23%), and an inseparable mixture of oily non-polar side products (21 mg).
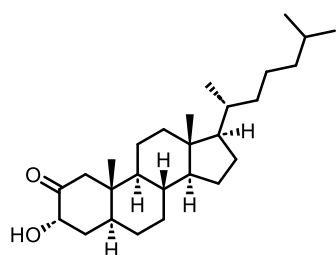
95: After solvent evaporation, the product solidified as a white powder (21 mg, 21%). TLC: R$_f$ 0.58 (EtOAc/PE, 3:7). Selected ^{1}H NMR (401 MHz, CDCl$_3$): δ 4.07 (dd, *J* = 5.0, 3.2, Hz, 1H, H-3), 2.47 (d, *J* = 14.3 Hz, 1H, H$_a$-1), 2.27 (d, *J* = 14.3 Hz, 1H, H$_b$-1), 0.90 (d, *J* = 6.5 Hz, 3H, H-21), 0.87 (d, *J* = 1.8 Hz, 3H, H-26), 0.85 (d, *J* = 1.8 Hz, 3H, H-27), 0.82 (s, 3H, H-19), 0.65 (s, 3H, H-18). ^{13}C NMR (101 MHz, CDCl$_3$): δ 212.9 (C2), 73.7 (C3), 56.4 (C17), 56.3, 54.5,

50.4, 42.7, 40.7, 39.9, 39.8, 39.7, 37.2, 36.3, 35.9, 35.0, 31.7, 28.4, 28.2, 28.0, 24.3, 24.0, 23.0, 22.7, 21.2, 18.8 (C21), 13.3 (C19), 12.2 (C18). HRMS (ESI pos): m/z calcd for $C_{27}H_{47}O_2$ [M+H]$^+$: 403.35706, found: 403.35673.
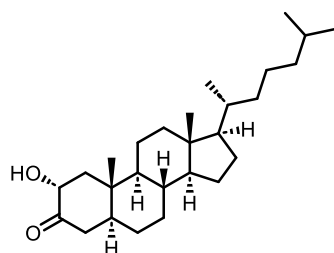
96: After solvent evaporation, product solidified as a white powder (23 mg, 23%). TLC: R_f 0.60 (EtOAc/PE, 3:7). Selected ^{1}H NMR (400 MHz, CDCl$_3$): δ 4.22 (ddd, J = 12.2, 7.0, 1.2 Hz, 1H, H$_a$-2), 1.09 (s, 3H, H-19), 0.90 (d, J = 6.6 Hz, 3H, H-21), 0.86 (dd, J = 6.6, 1.8 Hz, 6H, H-26 and H-27), 0.67 (s, 3H, H-18). ^{13}C NMR (101 MHz, CDCl$_3$): δ 211.3 (C3), 73.0 (C2), 56.4 (C17), 56.3, 53.9, 48.7, 48.6, 42.8, 42.6, 40.0, 39.7, 37.2, 36.3, 35.9, 34.8, 31.8, 29.9, 28.8, 28.4, 28.2, 24.4, 24.0, 23.0, 22.7, 21.8, 18.8 (C21), 13.0 (C19), 12.2 (C18). The NMR analysis is consistent with the previous report.[311] HRMS (ESI pos): m/z calcd for $C_{27}H_{46}O_2Na$ [M+Na]$^+$: 425.33900, found: 425.33858.

6.4 BIOLOGICAL EVALUATION

All experiments have been repeated at least three times, and each experiment was performed in biological triplicates (n = 3). Results are presented as fold change to control nontreated (NT) samples. Dimethyl sulfoxide (0.1%) was used as a vehicle in all samples, including a control sample. Results are presented as fold change to the control sample (positive control activity = 100%) with standard deviation calculated with the following equation (**eq. 3**).

$$\sigma = \sqrt{\frac{\sum_{i=1}^{n}|x_i - \bar{x}|^2}{n}}$$ (eq. 3)

Where n is the number of independent experiments, x is RLU (relative luminescence unit), and $\bar{x}$ is the arithmetic mean.

FXR LanthaScreen™ Assay

The assay was performed in collaboration with the group of Dr. Helena Mertlíková-Kaiserová by Dr. Jaroslav Kozák.

Commercially available LanthaScreen™ TR-FRET FXR Coactivator Assay Kit in 384 plate formats (Thermo Fischer Scientific, MA, USA, PV4833) was used according to the manufacturer, along with Bravo automated liquid handling platform (Agilent, CA, USA). Compounds were tested against DMSO and GW-4064 as negative and positive controls, respectively.

TGR5 Luciferase Assay

The assay was performed in collaboration with the Faculty of Pharmacy in Hradec Králové, Charles University, in the group of Prof. Petr Pávek by Dr. Alžběta Štefela.

Human hepatocellular carcinoma HepG2 cells (European Collection of Cell Cultures, ECACC, Salisbury, United Kingdom) were cultured in antibiotic-free Dulbecco's modified Eagle's medium (DMEM, Merck, Darmstadt, Germany) containing 10% fetal bovine serum, 1% L-glutamine, and 1% sodium pyruvate. For transfection, HepG2 cells were seeded at the density of 40,000 cells/cm^2. Cells were transfected using Lipofectamine 2000® (Thermo Fisher Scientific, MA, USA) with 200 ng CRE luciferase reporter vector (pGL4.29[luc2P/CRE/ Hygro], Promega, WI, United States), together with

150 ng TGR5 (GPBAR1-pcDNA3.1+/C-(K)-DYK) (Genscript, NJ, USA) or empty vector pcDNA3.1 and 50 ng pRL-TK Renilla luciferase vector (Promega, WI, USA). The next day, cells were challenged with tested ligands in indicated concentrations for 5 hours. Compounds were tested against DMSO and LCA as negative and positive controls, respectively.

FXR Luciferase Assay

The assay was performed in collaboration with the Faculty of Pharmacy in Hradec Králové, Charles University, in the group of Prof. Petr Pávek by Dr. Alžběta Štefela.

The above-described HepG2 cells were transfected using Lipofectamine 2000® (Thermo Fisher Scientific, MA, USA) with the luciferase FXRE-luc construct and with expression vectors. The next day, cells were challenged with tested ligands in indicated concentrations for 5 hours. Data were normalized to Renilla luciferase activity and are expressed relative to the activity of 10 μM CDCA (set as 100% activation).

7 APPENDIX

X-RAY Data

The experiment was performed and interpreted by Dr. Blanka Klepetářová.

The Xcalibur PX system, equipped with an Onyx CCD detector and a Cu Kα sealed tube (λ = 1.54178 Å) with an enhanced monochromator, using combined φ and ω scans at 180 K. CrysAlisProCCD[312] was used for data collection, cell refinement, and data reduction. The structure was solved by direct methods with SIR92,[313] and refined by full-matrix least-squares on F with CRYSTALS.[314] The positional and anisotropic thermal parameters of all non-hydrogen atoms were refined. All hydrogen atoms were found from a Fourier difference map. Hydrogen atoms attached to carbon atoms were recalculated into idealized positions and refined with riding constraints. Those attached to oxygen atoms were refined isotropically. The asymmetric unit contained two crystallographically independent molecules of **68** and a partially occupied (75%) molecule of dichloromethane solvent, which was found to be disordered over two positions with equal occupancy.

Table 14. The crystallographic data and experimental parameters for compound **68**.

Parameter	Value
Formula	$C_{27}H_{46}O_4 \cdot 0.375(CH_2Cl_2)$
Crystal size, mm^3	0.160 x 0.274 x 0.285
Crystal system	Orthorhombic
Space group	$P2_12_12_1$
Unit cell dimensions:	
a, Å	12.2954(4)
b, Å	18.8572(6)
c, Å	24.5090(7)
V, Å^3	5682.6(3)
Z	8
F(000)	2046
T, K	180
μ, mm^{-1}	1.181
D_{calc}, g/cm^3	1.091
$2\Theta_{max}$, deg.	133
Measured reflections	24766
Independent reflections	9978
R_{int}	0.025
Obs. Reflections $I > 2\sigma(I)$	8942
Parameters	623
R_1	0.0453
wR_2	0.0529
S	1.0914
Flack Parameter	0.09(3)
CCDC number	2012020

Molecular Docking

Table 15. Results of molecular docking for compounds presented in this study. AD – autodock v4.2.6 algorithm, Vina – AutoDock Vina v1.2.0 algorithm.

Compound	FXR		TGR5		Smiles
	AD	Vina	AD	Vina	
1	-10.4	-10.5	-7.4	-9.2	CC([C@H]1CC[C@@]2([H])[C@@]1(CC[C@]3([H])[C@@]4(C)CC[C@@H](O)C[C@]4([H])CC[C@]32[H])C)=O
2	-10.0	-10.1	-7.7	-9.0	C[C@@]12[C@]([C@@H](O)C)([H])CC[C@@]1([H])[C@]3([H])CC[C@@]4([H])C[C@@H](O)CC[C@@]4(C)[C@@]3([H])CC2
3	-9.3	-9.1	-7.5	-9.0	C[C@H](O)[C@@]1([H])CC[C@@]2([H])[C@]3([H])CC[C@@]4([H])C[C@@H](O)CC[C@]4(C)[C@@]3([H])CC[C@]12C
4	-9.1	-9.8	-7.3	-9.0	C[C@@H](O)[C@@]1([H])CC[C@@]2([H])[C@@]1(CC[C@]3([H])[C@@]4(C)CC[C@H](O)C[C@]4([H])[C@H](O)C[C@]32[H])C
5	-10.2	-9.9	-7.6	-9.3	CC[C@H]1CC[C@@]2([H])[C@@]1(CC[C@]3([H])[C@@]4(C)CCC(C)C[C@]4([H])CC[C@]32[H])=O)C=O
6	-9.7	-9.6	-7.2	-9.0	C[C@@]12[C@@H](C(CO)=O)CC[C@@]1([H])[C@]3([H])CC[C@]4([H])[C@@](CCC(C4)=O)(C)[C@@]3([H])CC2
7	-9.7	-10.2	-7.5	-8.8	O=C1CC[C@@]2([H])[C@]3([H])CC[C@@]4([H])CCC=C[C@]4(C)[C@@]3([H])CC[C@]12C
8	-11.1	-11.0	-8.2	-9.1	CC[C@H]1CC[C@@]2([H])[C@]3([H])CC[C@@]4([H])C[C@H](O)CC[C@@]4(C)[C@@]3([H])CC[C@]12C)=O
9	-10.3	-9.9	-7.3	-8.6	C[C@H](O)[C@@]1([H])CC[C@@]2([H])[C@]3([H])CC[C@]4([H])C[C@H](O)CC[C@]4(C)[C@@]3([H])CC[C@]12C
10	-10.3	-10.0	-7.9	-9.4	C[C@@H](O)[C@@]1([H])CC[C@@]2([H])[C@]3([H])CC[C@]4([H])C[C@@H](OC(C)=O)CC[C@]4(C)[C@@]3([H])CC[C@]12C
11	-10.6	-10.6	-7.9	-9.6	C[C@@]12[C@@H](C(C)=O)CC[C@@]1([H])[C@]3([H])[C@@H](OC(C)=O)[C@]4([H])C[C@@H](O)CC[C@@]4(C)[C@@]3([H])CC2
12	-11.1	-11.1	-7.7	-9.1	C[C@@]12[C@@H](C(C)=C)CC[C@@]1([H])[C@]3([H])CC[C@]4([H])C[C@@H](O)CC[C@@]4(C)[C@@]3([H])CC2
13	-9.3	-9.5	-7.4	-8.7	C[C@@H](O)[C@@]1([H])CC[C@@]2([H])[C@]3([H])CC[C@]4([H])C[C@@H](O)CC[C@@]4(C)[C@@]3([H])CC[C@]12C
14	-10.8	-10.0	-7.7	-8.9	C[C@@]12[C@]([C@@H](C)O)([H])CC[C@@]1([H])[C@]3([H])CC[C@]4([H])[C@@H](OC(C)=O)CC[C@]4(C)[C@@]3([H])CC2
15	-10.3	-9.9	-7.3	-8.7	C[C@H](O)[C@@]1([H])CC[C@@]2([H])[C@]3([H])CC[C@]4([H])C[C@@H](O)CC[C@@]4(C)[C@@]3([H])CC[C@]12C
16	-11.1	-11.2	-8.2	-9.5	CC([C@H]1CC[C@@]2([H])[C@]3([H])CC[C@]4([H])CC(CC[C@]4(C)[C@@]3([H])CC[C@]12C)=O)=O
17	-10.8	-10.9	-7.8	-9.3	C[C@@H](O)[C@@]1([H])CC[C@@]2([H])[C@]3([H])CC[C@]4([H])CC(CC[C@]4(C)[C@@]3([H])CC[C@]12C)=O
18	-10.3	-10.6	-7.3	-9.1	C[C@@]12[C@@]3([H])[C@@]4(C)[C@@H](O5)[C@@H]5C[C@@]4([H])[C@]3([H])CC[C@]1([H])C[C@@H](O)CC2
19	-10.9	-11.0	-7.7	-8.9	CC([C@H]1CC[C@@]2([H])[C@]3([H])CCC4=C[C@H](O)CC[C@]4(C)[C@@]3([H])CC[C@]12C)=O
20	-10.1	-10.0	-7.8	-8.9	CC[C@H]1CC[C@@]2([H])[C@]3([H])CCC4=C[C@@H](O)CC[C@]4(C)[C@@]3([H])CC[C@]12C)=O
21	-10.0	-10.1	-7.4	-8.7	C[C@@H](O)[C@@]1([H])CC[C@@]2([H])[C@]3([H])CCC4=C[C@@H](O)CC[C@]4(C)[C@@]3([H])CC[C@]12C
22	-10.2	-10.0	-7.8	-9.3	CC([C@H]1CC[C@@]2([H])[C@]3([H])CCC4=CC(CC[C@]4(C)[C@@]3([H])CC[C@]12C)=O)=O
23	-9.9	-9.3	-7.8	-9.1	C[C@@H](O)[C@@]1([H])CC[C@@]2([H])[C@]3([H])CCC4=CC(CC[C@]4(C)[C@@]3([H])CC[C@]12C)=O
24	-10.8	-11.1	-8.1	-9.2	C[C@@H](O)[C@@]1([H])CC[C@@]2([H])[C@]3([H])CCC4=CC(CC[C@]4(C)[C@@]3([H])CC[C@]12C)=O
25	-10.9	-9.4	-7.8	-9.1	C[C@@]12[C@@H](O)CC[C@@]1([H])[C@]3([H])CCC4=C/C(CC[C@]4(C)[C@@]3([H])CC2)=N/OCCC(O)=O
26	-10.2	-10.2	-7.7	-9.5	CC[C@H]1CC[C@@]2([H])[C@]3([H])C=CC4=CC(CC[C@]4(C)[C@@]3([H])CC[C@]12C)=O)=O
27	-9.9	-10.5	-7.4	-9.1	C[C@@]1(C2)[C@](C(CO)=O)(O)CC[C@@]1([H])[C@]3([H])CCC4=CC(C=C[C@]4(C)[C@@]3([H])C2=O)=O
28	-10.0	-9.9	-7.1	-8.9	C[C@@]12[C@](C(CO)=O)(O)CC[C@@]1([H])[C@]3([H])CCC4=CC(CC[C@]4(C)[C@@]3([H])CC2)=O
29	-10.2	-11.0	-7.6	-9.5	C[C@@]1(C2)[C@](C(CO)=O)(O)CC[C@@]1([H])[C@]3([H])CCC4=CC(CC[C@]4(C)[C@@]3([H])C2=O)=O
30	-9.3	-9.3	-6.8	-8.8	C[C@@]12[C@@H](C(CO)=O)CC[C@@]1([H])[C@]3([H])CCC4=CC(CC[C@]4(C)[C@@]3([H])[C@@H](O)C2)=O
31	-10.2	-10.6	-7.7	-10.4	C[C@@]12[C@](C(COC(C(C)C)C)=O)(O)(O)[C@@H](C)C[C@@]1([H])[C@]3([H])C[C@H](F)C4=CC(C=C[C@]4(C)[C@@]3(F)[C@@H](O)
32	-11.4	-10.7	-8.9	-10.0	C[C@@]12[C@@H](OC(CCC3CCCC3)=O)CC[C@@]1([H])[C@]4([H])CCC5=CC(CC[C@]5(C)[C@@]4([H])CC2)=O
33	-9.6	-9.8	-7.6	-9.3	C[C@@H](O)[C@@]1([H])CC[C@@]2([H])[C@]3([H])CC=C4C[C@@H](OC(C)=O)CC[C@]4(C)[C@@]3([H])CC[C@]12C
34	-9.5	-9.7	-7.8	-9.2	CC[C@H]1CC[C@@]2([H])[C@]3([H])CC=C4[C@@]((CC[C@H](O)C4)(C)[C@@]3([H])CC[C@]12C)=O
35	-8.8	-9.2	-7.6	-8.9	C[C@H](O)[C@@]1([H])CC[C@@]2([H])[C@]3([H])CC=C4[C@@](CC[C@@H](O)C4)(C)[C@@]3([H])CC[C@]12C
36	-9.1	-9.5	-7.1	-8.9	C[C@@]12[C@](C(CO)=O)(O)(O)CC[C@@]1([H])[C@]3([H])CC=C4[C@@]((CC[C@@H](O)C4)(C)[C@@]3([H])CC2
37	-10.0	-9.7	-7.4	-8.8	CC([C@H]1CC[C@@]2([H])[C@]3([H])CC=C4[C@@]((CC[C@H](OCOC)C4)(C)[C@@]3([H])CC[C@]12C)=O
38	-10.9	-9.9	-9.3	-10.4	C[C@H](OC(C1=CC=CC=C1)=O)[C@@]2([H])CC[C@@]3([H])[C@]4([H])CC=C5C[C@@H](OC(C)=O)CC[C@]5(C)[C@@]4([H])CC[C@]23C
39	-11.0	-9.9	-7.9	-9.4	C[C@@]([C@@]1([H])CC2)([C@C)C[C@]3([H])[C@@]4(C)CC[C@@H](OC(C(O)=O)=O)C4=CC[C@]31[H])[C@H]2C(C)=O
40	-11.8	-10.1	-8.3	-9.4	CC([C@H]1CC[C@@]2([H])[C@@]1(CC[C@]3([H])[C@@]4(C)CC[C@H](OC(CC(O)=O)=O)CC4=CC[C@]32[H])C)=O
41	-10.9	-9.9	-7.9	-9.6	C[C@@]12[C@@H](C(C)=O)CC[C@@]1([H])[C@]3([H])CC=C4[C@@]((CC[C@H](OC(CCCC(O)=O)=O)C4)(C)[C@@]3([H])CC2
42	-10.8	-10.1	-8.0	-9.5	CC([C@H]1CC[C@@]2([H])[C@@]1(CC[C@]3([H])[C@@]4(C)CC[C@H](OC(CCCCC(O)=O)=O)CC4=CC[C@]32[H])C)=O
43	-11.0	-10.3	-8.1	-10.0	C[C@@]12[C@@H](C(C)=O)CC[C@@]1([H])[C@]3([H])CC=C4[C@@]((CC[C@H](OC(CCCCCC(O)=O)=O)C4)(C)[C@@]3([H])CC2
44	-10.6	-10.2	-8.4	-9.8	C[C@@]12[C@@H](C(C)=O)CC[C@@]1([H])[C@]3([H])CC=C4[C@@]((CC[C@H](OCCCCCC(O)=O)=O)C4)(C)[C@@]3([H])CC2
45	-9.0	-10.2	-7.4	-8.8	C[C@@]12[C@](O)(C)CC[C@@]1([H])[C@]3([H])CC=C4[C@@]((CC[C@H](O)C4)(C)[C@@]3([H])CC2
46	-8.9	-9.1	-7.1	-8.7	O=C1CC[C@@]2([H])[C@]3([H])CC=C4C[C@@H](OC(C)=O)CC[C@]4(CO)[C@@]3([H])CC[C@]12C
61	-12.8	-11.3	-8.3	-9.4	C[C@H](CCC(O)=O)[C@H]1CC[C@@]2([H])[C@]3([H])C[C@H](O)[C@H]4[C@@]4(C)[C@@]((C)C[C@@]3([H])CC[C@]12C)=O
62	-11.9	-10.3	-8.0	-9.7	C[C@H](CCC(O)=O)[C@H]1CC[C@@]2([H])[C@]3([H])[C@@](O)(C)C[C@]4([H])C[C@@H](O)CC[C@]4(C)[C@@]3([H])CC[C@]12C
63	-11.3	-9.1	-8.3	-9.7	C[C@H](CCC(O)=O)[C@H]1CC[C@@]2([H])[C@]3([H])[C@@](O)(CC)C[C@]4([H])C[C@H](O)CC[C@]4(C)[C@@]3([H])CC[C@]12C
64	-11.4	-9.6	-7.9	-9.6	C[C@H](CCC(O)=O)[C@H]1CC[C@@]2([H])[C@]3([H])[C@@](O)(C=C)C[C@]4([H])C[C@H](O)CC[C@]4(C)[C@@]3([H])CC[C@]12C
65	-9.0	-8.0	-8.0	-9.3	C[C@H](CCC(O)=O)[C@H]1CC[C@@]2([H])[C@]3([H])[C@@](O)(C#C)C[C@]4([H])C[C@H](O)CC[C@]4(C)[C@@]3([H])CC[C@]12C
66	-10.1	-8.8	-8.0	-9.8	C[C@H](CCC(O)=O)[C@H]1CC[C@@]2([H])[C@]3([H])[C@@](O)C[C@]4([H])C[C@H](O)CC[C@]4(C)[C@@]3([H])CC[C@]12C
67	-9.5	-8.9	-8.0	-9.8	C[C@H](CCC(O)=O)[C@H]1CC[C@@]2([H])[C@]3([H])[C@@](O)(CC=C)C[C@]4([H])C[C@@H](O)CC[C@]4(C)[C@@]3([H])CC[C@]12C
68	-10.0	-7.7	-8.3	-9.6	C[C@H](CCC(O)=O)[C@H]1CC[C@@]2([H])[C@]3([H])[C@@](O)(C(C)C)C[C@]4([H])C[C@H](O)CC[C@]4(C)[C@@]3([H])CC[C@]12C
69	-9.2	-8.3	-8.2	-9.7	C[C@H](CCC(O)=O)[C@H]1CC[C@@]2([H])[C@]3([H])[C@@](O)(C4CC4)C[C@]5([H])C[C@H](O)CC[C@]5(C)[C@@]3([H])CC[C@]12C
70	-9.1	-8.9	-8.2	-9.5	C[C@H](CCC(O)=O)[C@H]1CC[C@@]2([H])[C@]3([H])[C@@](O)(CCCC=C)C[C@]4([H])C[C@H](O)CC[C@]4(C)[C@@]3([H])CC[C@]12C
71	-6.2	-7.5	-7.3	-8.6	C[C@H](CCC(O)=O)[C@H]1CC[C@@]2([H])[C@]3([H])[C@@](O)(CCCCCCCCCC)C[C@]4([H])C[C@H](O)CC[C@]4(C)[C@@]3([H])CC[C@]12C
75	-11.0	-8.6	-8.0	-9.6	C[C@H](CCC(O)=O)[C@H]1CC[C@@]2([H])[C@]3([H])C/C[C@]4([H])C[C@H](O)CC[C@]4(C)[C@@]3([H])CC[C@]12C=C/C
76	-0.5	-6.4	-8.1	-8.3	O[C@@H]1CC[C@]2(C)[C@@]3([H])CC[C@]4(C)[C@@H]([C@@H](CCC(O)=O)C)CC[C@@]4([H])[C@]3([H])[C@@](O)(C#CC5=CC=CC=C5)C[C@]2([H])C1
81	-3.1	-5.4	-7.0	-9.0	O[C@@H]1CC[C@]2(C)[C@@]3([H])CC[C@]4(C)[C@@H]([C@@H](CCC(O)=O)C)CC[C@@]4([H])[C@]3([H])[C@@](O)(C5=CN(C(F)(C(F)(F)F)F)N=N5)C[C@]2([H])C1
86	-12.9	-10.7	-8.3	-9.3	O[C@@H]1CC[C@]2(C)[C@@]3([H])CC[C@]4(C)[C@@H]([C@@H](CCC(O)=O)C)CC[C@@]4([H])[C@]3([H])[C@@](O)(C)C[C@]2([H])C1
LCA	-9.8	-10.5	-7.9	-9.3	O[C@@H]1CC[C@]2(C)[C@@]3([H])CC[C@]4(C)[C@@H]([C@@H](C)CCC(O)=O)CC[C@@]4([H])[C@]3([H])CCC2C1
CDCA	-12.9	-11.2	-7.9	-9.2	C[C@]12CC[C@]3([H])[C@@]4(C)CC[C@@H](O)C[C@@]4([H])C[C@@H](O)[C@]3([H])[C@]1([H])CC[C@@]2(C(CCC(O)=O)C)[H]
DCA	-12.0	-10.6	-7.7	-9.2	O[C@@H]1CC[C@]2(C)[C@@]3([H])C[C@@H](O)[C@]4(C)[C@@H]([C@@H](CCC(O)=O)C)CC[C@@]4([H])[C@]3([H])CC[C@@]([H])2C1

Toxicity Data

The assays were performed and interpreted by Dr. Alžběta Štefela.

The potential cytotoxicity of 7-alkylated chenodeoxycholic acid derivatives was assessed in different human (HepG2, HepaRG, and Huh7) and murine (AML12) hepatocyte-derived cell lines. For this purpose, hepatic cells were treated at increasing compound concentrations for 24 hours and analyzed by MTS viability assay.

Table 16. Cell viability was determined using the Cell Titer 96 Aqueous One Solution Cell Proliferation Assay (MTS assay) after treatment with test compounds for 24 hours in four different hepatic cell lines. Vehicle (0.1% DMSO) and background (10% SDS; v/v, toxic control) controls of cell viability was set to be 100% and 0%, respectively.

Compound	HepG2		HepaRG		Huh7		AML12	
	IC50 (μM)	Viability at 10 μM	IC50 (μM)	Viability at 10 μM	IC50 (μM)	Viability at 10 μM	IC50 (μM)	Viability at 10 μM
75	> 200	99.7±1.2	> 200	119.4±6.0	> 200	110.6±9.5	> 200	107.5±4.8
62	> 200	99.7±1.2	> 200	119.5±1.0	> 200	105.7±5.8	> 200	107.6±7.7
63	> 200	100.1±3.9	> 200	116.6±1.3	> 200	113.2±4.8	> 200	104.9±2.0
64	168.8±1.0	95.9±8.3	> 200	103.9±2.4	> 100	117.3±5.6	> 200	105.7±3.9
65	> 200	96.5±4.1	> 200	92.9±6.5	> 200	103.4±4.4	> 200	97.5±6.6
66	106.7±1.1	94.9±11.7	97.3	89.4±2.5	> 100	117.0±2.3	90.8	81.2±1.0
67	162.3±2.1	97.7±9.1	> 200	125.8±4.5	> 100	93.5±10.0	161.1	108.6±3.2
68	103.3±1.0	93.4±7.4	180.8	100.9±6.9	> 100	97.6±7.3	143.2	94.0±3.7
69	178.4±1.0	90.9±0.9	> 200	133.3±12.2	> 200	97.9±10.4	> 200	107.7±3.2
70	77.3±1.2	87.8±6.7	76.5	93.1±4.4	34.0±1.5	114.0±7.0	75.0	126.6±7.1
71	≈10.9	79.8±2.5	18.9	71.6±2.8	21.8	118.0±4.9	12.5	68.0±1.4
β-MCA	> 200	107.2±3.8	> 200	108.3±7.7	> 200	111.2±7.6	> 200	135.1±3.2

Dose Response Curves and Receptor Specifity Data

The assay was performed and interpreted by Dr. Alžběta Štefela.
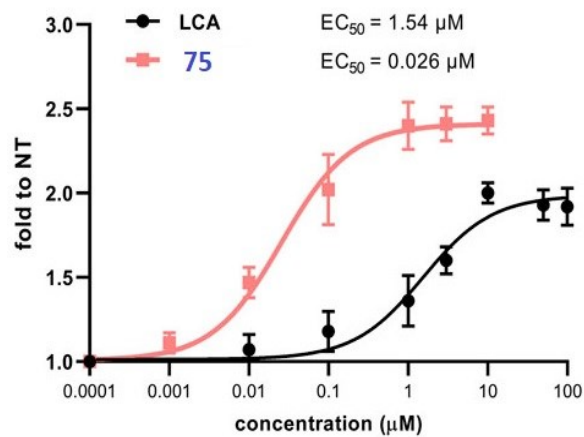
Figure 36. Concentration-response curves for activation of TGR5 by LCA and **75**. EC_{50} values were calculated using nonlinear fitting of concentration-response curves. Adopted and modified.[223]

119

Biological Specifity Data

The assay was performed and interpreted by Dr. Alžběta Štefela.
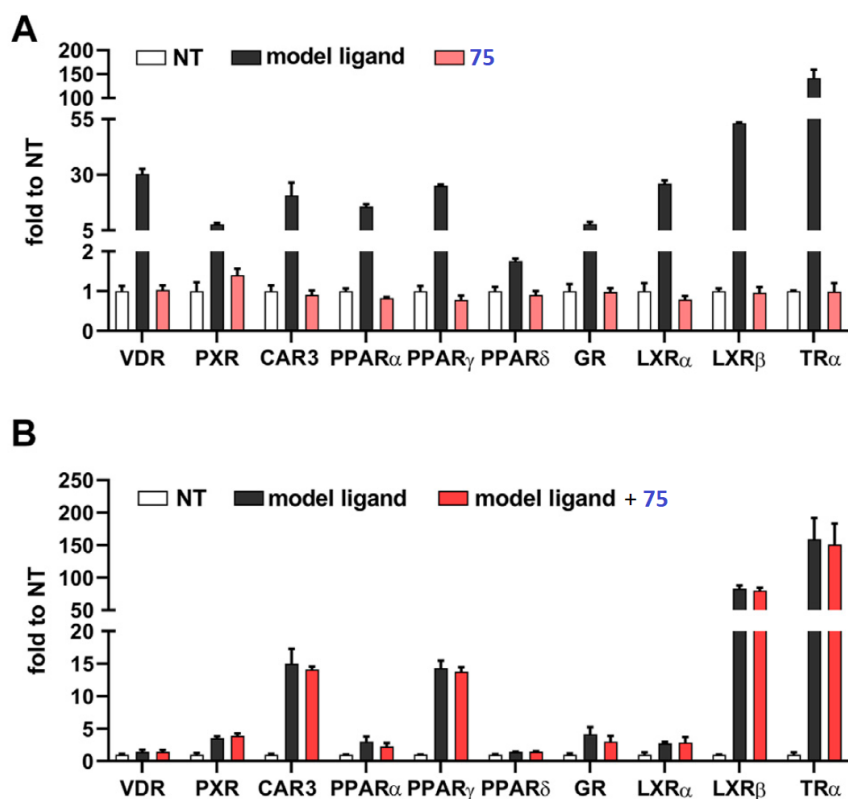
Figure 37. The efficacy of 75 in both agonistic (A) and antagonistic (B) mode. Activities were evaluated using HepG2 cells that were temporarily co-transfected with luciferase reporter genes and relevant expression vectors. In experiment (A), cells were exposed to 75 for 24 hours, and various standard ligands for nuclear receptors were employed: VDR (1α,25(OH)2vitaminD3 at 100 nM), PXR (rifampicin at 10 μM), human CAR (CITCO at 10 μM), PPARα (fenofibrate at 10 μM), PPARγ (rosiglitazone at 10 μM), PPARδ (GW501516 at 10 μM), GR (dexamethasone at 100 nM), LXRα and LXRβ (GW3964 at 10 μM), and TR (thyroxin at 10 μM). In experiment (B), the same nuclear receptor ligands were tested in conjunction with 75 using the same procedure, but at different concentrations: VDR (1α,25(OH)2vitaminD3 at 10 nM), PXR (rifampicin at 1 μM), human CAR (CITCO at 1 μM), PPARα (fenofibrate at 1 μM), PPARγ (rosiglitazone at 1 μM), PPARδ (GW501516 at 1 μM), GR (dexamethasone at 50 nM), LXRα and LXRβ (GW3965 at 1 μM), and TR (thyroxin at 1 μM). The results were standardized to Renilla luciferase activity and are expressed as a multiple of the activation compared to untreated control cells. The values represent the average ± standard deviation from three separate experiments. Adopted and modified.[223]

QSAR_TGR5

Compounds **1–46** were randomly clustered into training (70%, n = 34), validation (15%, n = 6), and test (15%, n = 6) sets. Subsequently, we trained 10 models for predicting TGR5 activity based on their structure. GPNEST performed best and was selected.

Table 17. Summary of training results.

Model	Training		Validation		Testing	
	Rsqr	**RMSE**	**Rsqr**	**RMSE**	**Rsqr**	**RMSE**
RBF Model	0.729	0.09586	-0.2972	0.1313	-1.119	0.1374
Random Forest Regression Model	0.79	0.08438	0.4445	0.08589	0.2157	0.08362
PLS Model	0.4517	0.1363	0.1797	0.1044	-0.5717	0.1184
GPFixed	0.6982	0.1012	0.5693	0.07563	-0.3283	0.1088
GP2DSearch	0.6684	0.106	0.5913	0.07367	-0.278	0.1067
GPRFVS	0.664	0.1067	0.2935	0.09687	-1.037	0.1348
GPFVS	0.6517	0.1087	0.5847	0.07426	-0.4547	0.1139
GPOPT	0.73	0.09568	0.5724	0.07536	0.2723	0.08054
GA-RBF Model	0.729	0.09585	-0.8089	0.155	-0.6758	0.1222
GPNEST	0.5754	0.12	0.602	0.0727	-0.5951	0.1192

Parameters used:

Threshold for minimum occurrence: 4%, threshold for minimum standard deviation: 0.0005, threshold for maximum correlation between descriptors: 0.95

Descriptors used: 55
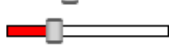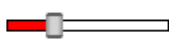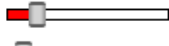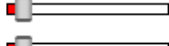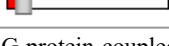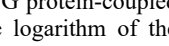
Training (34 compounds): **1**, **2**, **4**, **5**, **8**, **10**, **11**, **13**, **14**, **15**, **16**, **17**, **18**, **20**, **22**, **23**, **24**, **26**, **27**, **28**, **29**, **30**, **31**, **32**, **33**, **34**, **35**, **36**, **37**, **38**, **40**, **41**, **42**, **46**

Validation (6 compounds): **6**, **9**, **12**, **19**, **25**, **43**

Test (6 compounds): **3**, **7**, **21**, **39**, **44**
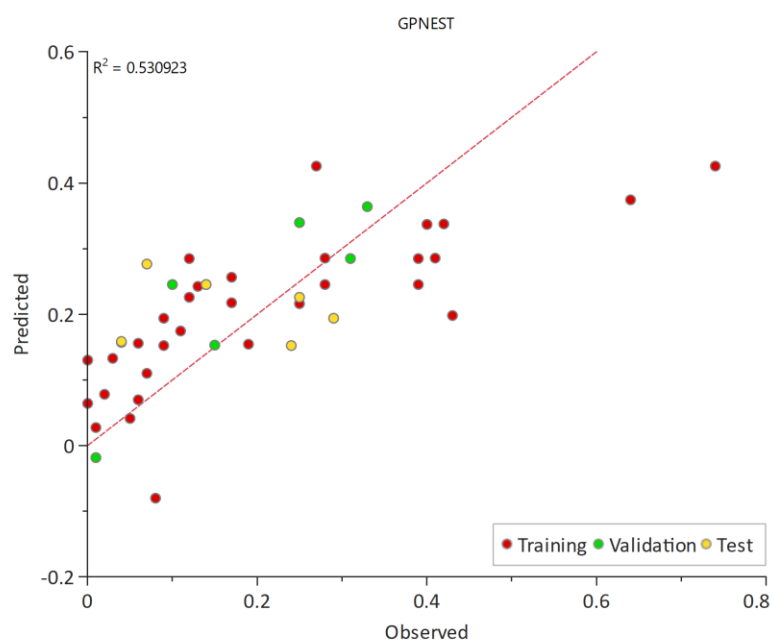
Figure 38. Performance of GPNEST, the model that was selected to predict compound activity on TGR5.

Non-Central Nervous System Orally Taken Drugs Scoring Function (NCNSOTD)

Property	Desired Value	Importance
▇ AMG_TGR5_activity_Model_GPNEST	0.6 -> inf ⊓	
▇ logS @ pH7.4	> 1	
▇ HIA category	+	
▇ Hyde pKi 7CFN FX0_R_403	7 -> inf ⊓	
▇ logP	0 -> 3.5 ⊓	
▇ P450	-inf -> 0 ⊓	
▇ hERG pIC50	⩽ 5	
▇ 2D6 affinity category	low medium ⊓	
▇ 2C9 pKi	⩽ 6	
▇ P-gp category	no	
▇ PPB90 category	low	
▇ BBB category	-	
▇ BBB log([brain]:[blood])	⩽ -0.5	

Figure 39. Non-central nervous system orally taken drugs scoring function (NCNSOTD). TGR5, Takeda G protein-coupled Receptor 5. FXR, Farnesoid X Receptor. RLU, Relative luminescence unit. logS pH 7.4 predicts the logarithm of the apparent solubility at pH 7.4 in μM. HIA category predicts a classification of '+' for compounds that are ≥30% absorbed and '-' for compounds that are < -0.5. logP predicts the logarithm of the octanol/water partition coefficient for neutral compounds. P450 predicts Composite Site Lability (CSL). The CSL is an estimate of the efficiency of metabolism for the entire molecule. hERG pIC50 predicts the pIC50 values for inhibition of hERG K+ channels expressed in mammalian cells. 2D6 affinity category predicts a classification of 'low' for compounds with a pKi7, 2C9 pKi – predicts the pKi values for affinity with CYP2C9. P-gp category predicts a classification of 'yes' for substrates and 'no' for non-substrates. PPB90 category predicts a classification of 'low' for compounds that are 90% bound. BBB category predicts a classification of '+' for compounds that have a log([brain]:[blood]) ≥ -0.5 and '-' for compounds that have a ratio < -0.5. BBB log([brain]:[blood]) predicts the logarithm of the brain/blood concentration ratio.

HPLC Data for Prepared Analytical Standards 57–60

Sample Name   : Diol
Sample ID   : 1
Data Filename   : Diol_001.lcd
Method Filename : Oxidations.lcm
Vial #   : 1-2
Injection Volume : 0.1 uL
Date Acquired   : 9/21/2020 5:18:06 PM
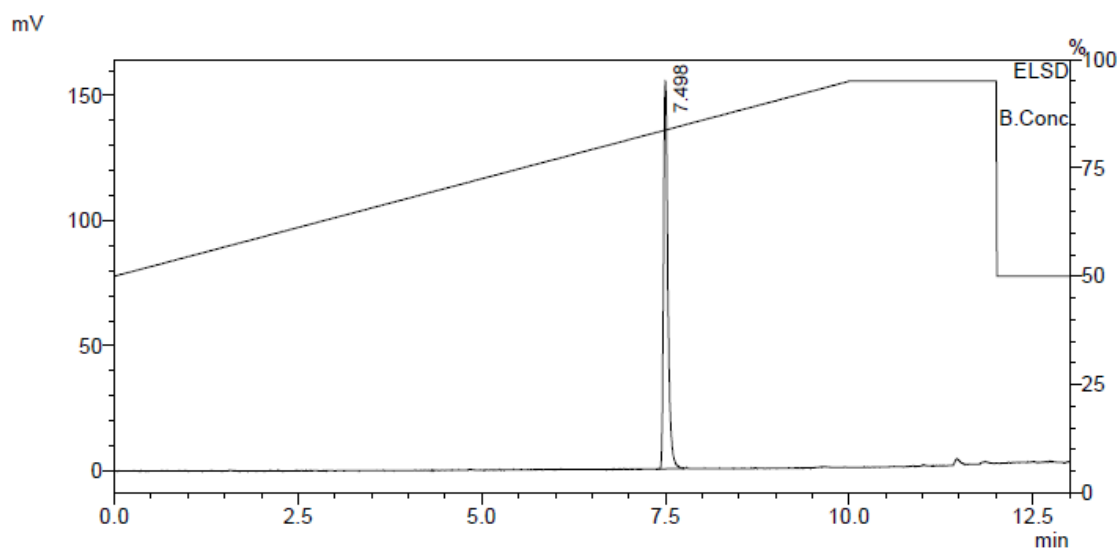
ELSD

Name	Ret. Time	Area	Area%
Diol	7.498	641910	100.000
		641910	100.000

Method

<<Pump>>
Pump A Mobile Phase Settings   : 0.45 /GPa
Pump B Mobile Phase Settings   : 1.25 /GPa
Gradient Program:
    Pump A + B
    # Time(min) / Flow(mL/min) / B.Conc(%) / B.Curve
    1 0.00/ 0.3500/ 50.0/ 0
    2 10.00/ 0.3500/ 95.0/ 0
    3 12.00/ 0.3500/ 95.0/ 0
    4 12.01/ 0.3500/ 50.0/ 0

<<Column Infomation>>
    Column Name   : XR-ODS III
    Column Length   : 150 mm
    Inner Diameter   : 2.0 mm
    ParticleSize   : 2.2 um
    VendorName   : SHIMADZU Corp.
    FunctionalGroup : C18 endcapped

Figure 40. HPLC trace, compound 57.

Sample Name   : 3-Oxo
Sample ID   : 1
Data Filename   : 3-Oxo.lcd
Method Filename : Oxidations.lcm
Vial #   : 1-1
Injection Volume : 0.1 uL
Date Acquired   : 9/21/2020 4:51:47 PM

ELSD

Name	Ret. Time	Area	Area%
3-Oxo	7.805	665971	100.000
		665971	100.000

Method

<<Pump>>
Pump A Mobile Phase Settings   : 0.45 /GPa
Pump B Mobile Phase Settings   : 1.25 /GPa
Gradient Program:
                    Pump A + B
                    #   Time(min) / Flow(mL/min) / B.Conc(%) / B.Curve
                    1   0.00/ 0.3500/ 50.0/ 0
                    2   10.00/ 0.3500/ 95.0/ 0
                    3   12.00/ 0.3500/ 95.0/ 0
                    4   12.01/ 0.3500/ 50.0/ 0

<<Column Infomation>>
Column Name   : XR-ODS III
Column Length   : 150 mm
Inner Diameter   : 2.0 mm
ParticleSize   : 2.2 um
VendorName   : SHIMADZU Corp.
FunctionalGroup   : C18 endcapped

Figure 41. HPLC trace, compound **58**.

Sample Name   : 7-oxo
Method Filename : Oxidations.lcm
Vial #   : 1-1
Injection Volume : 0.1 uL

ELSD

Name	Ret. Time	Area	Area%
7-Oxo	6.478	756910	100.000
		756910	100.000

Method
<<Pump>>
Pump A Mobile Phase Settings   : 0.45 /GPa
Pump B Mobile Phase Settings   : 1.25 /GPa
Gradient Program:
          Pump A + B
          #   Time(min) / Flow(mL/min) / B.Conc(%) / B.Curve
          1 0.00/ 0.3500/ 50.0/ 0
          2 10.00/ 0.3500/ 95.0/ 0
          3 12.00/ 0.3500/ 95.0/ 0
          4 12.01/ 0.3500/ 50.0/ 0

<<Column Infomation>>
Column Name   : XR-ODS III
Column Length   : 150 mm
Inner Diameter   : 2.0 mm
ParticleSize   : 2.2 um
VendorName   : SHIMADZU Corp.
FunctionalGroup   : C18 endcapped

Figure 42. HPLC trace, compound **59**.

Sample Name   : DiOxo
Sample ID   : 1
Data Filename   : DiOxo.lcd
Method Filename : Oxidations.lcm
Vial #   : 1-4
Injection Volume : 0.1 uL
Date Acquired   : 9/21/2020 4:33:35 PM
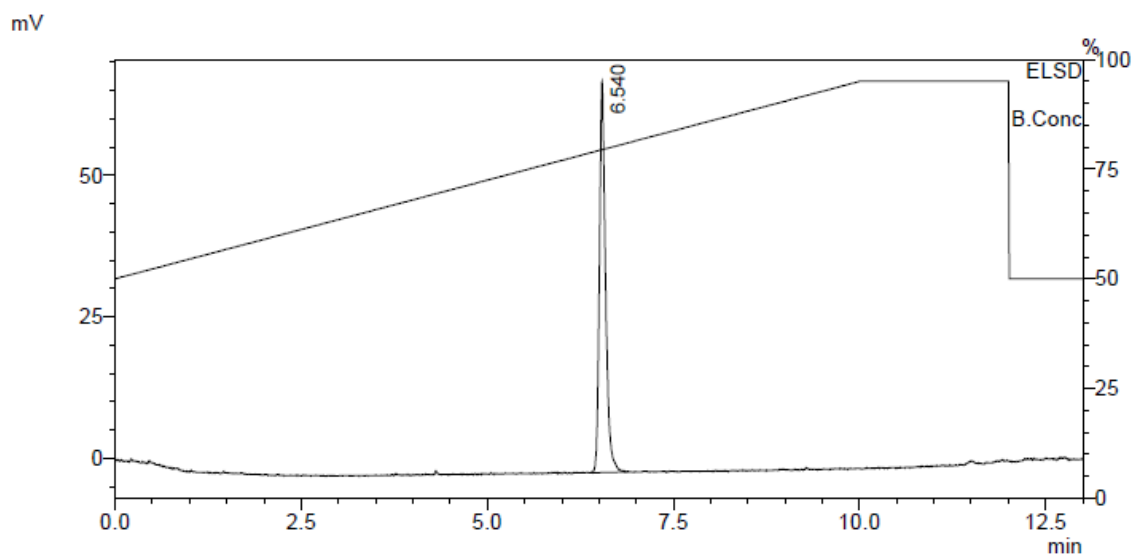
ELSD

Name	Ret. Time	Area	Area%
DiOxo	6.540	395518	100.000
		395518	100.000

Method

<<Pump>>
Pump A Mobile Phase Settings   : 0.45 /GPa
Pump B Mobile Phase Settings   : 1.25 /GPa
Gradient Program:
                  Pump A + B
                  # Time(min) / Flow(mL/min) / B.Conc(%) / B.Curve
                  1 0.00/ 0.3500/ 50.0/ 0
                  2 10.00/ 0.3500/ 95.0/ 0
                  3 12.00/ 0.3500/ 95.0/ 0
                  4 12.01/ 0.3500/ 50.0/ 0

<<Column Infomation>>
Column Name   : XR-ODS III
Column Length   : 150 mm
Inner Diameter   : 2.0 mm
ParticleSize   : 2.2 um
VendorName   : SHIMADZU Corp.
FunctionalGroup   : C18 endcapped

Figure 43. HPLC trace, compound 60.

126

Sample Name :
Method Filename : Oxidations.lcm
Vial # : 1-1
Injection Volume : 1 uL

ELSD

Name	Ret. Time	Area	Area%
7-Oxo	5.982	1945056	22.495
DiOxo	6.563	2079822	24.054
Diol	7.143	2274785	26.309
3-Oxo	7.498	2346867	27.142
		8646530	100.000

Method

<<Pump>>
Pump A Mobile Phase Settings   : 0.45 /GPa
Pump B Mobile Phase Settings   : 1.25 /GPa
Gradient Program:

Pump A + B
Time(min) / Flow(mL/min) / B.Conc(%) / B.Curve
1   0.00/ 0.3500/ 50.0/ 0
2   10.00/ 0.3500/ 95.0/ 0
3   12.00/ 0.3500/ 95.0/ 0
4   12.01/ 0.3500/ 50.0/ 0

<<Column Infomation>>
Column Name   : XR-ODS III
Column Length   : 150 mm
Inner Diameter   : 2.0 mm
ParticleSize   : 2.2 um
VendorName   : SHIMADZU Corp.
FunctionalGroup   : C18 endcapped

Figure 44. Representative HPLC trace, mixed standards, **57–60**, 500 µg · mL^{-1} each.

$$y = 9.8645x^{1.8016}$$
$$R^2 = 0.9972$$
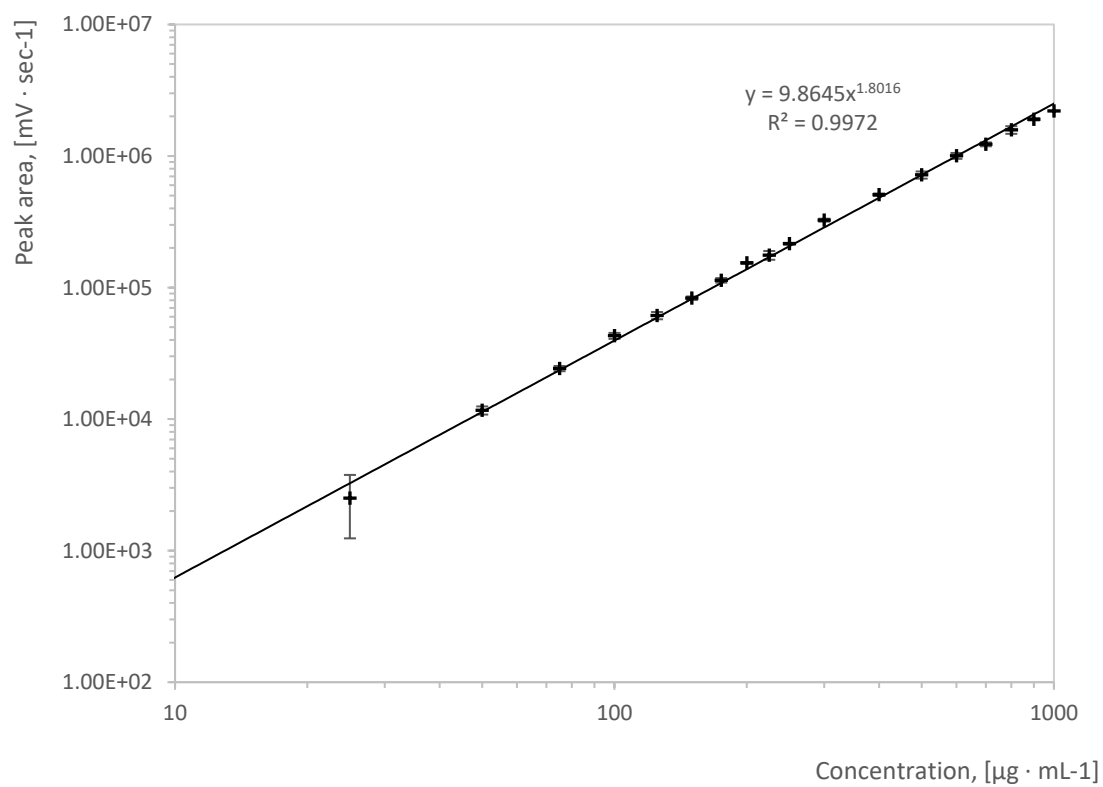
Figure 45. Calibration curve for compound **57**.

$$y = 10.388x^{1.806}$$
$$R^2 = 0.9934$$
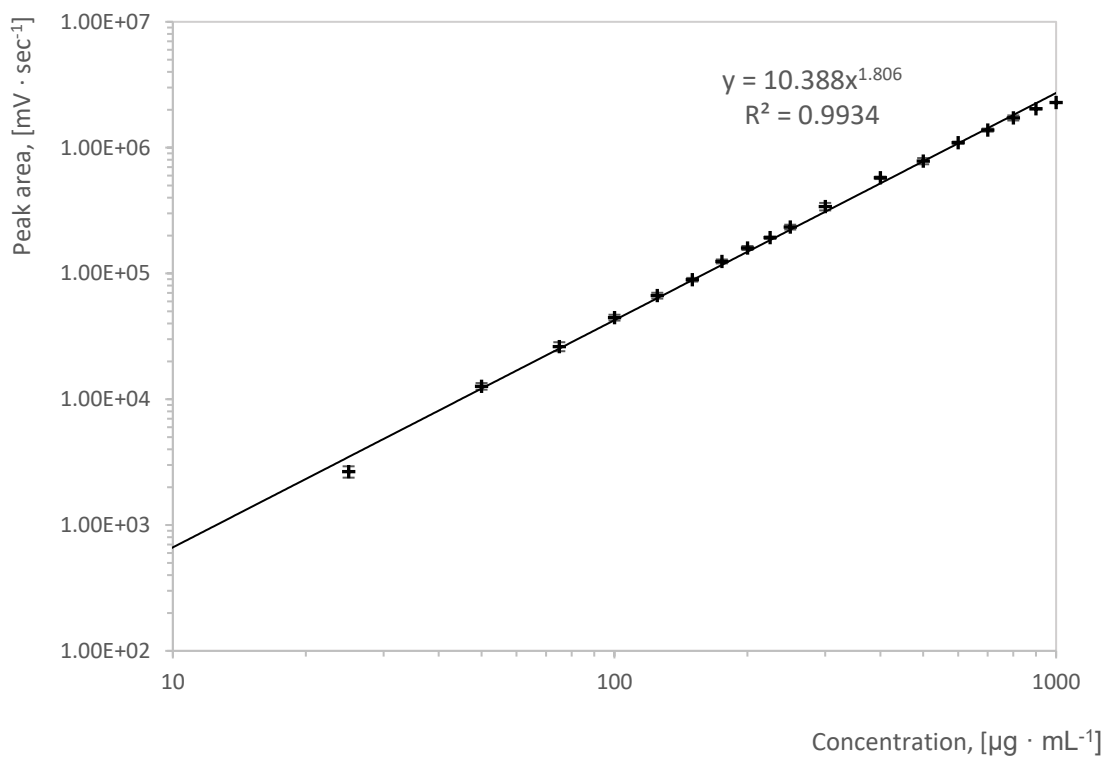
Figure 46. Calibration curve for compound **58**.

$$y = 6.3078x^{1.8397}$$
$$R^2 = 0.9984$$
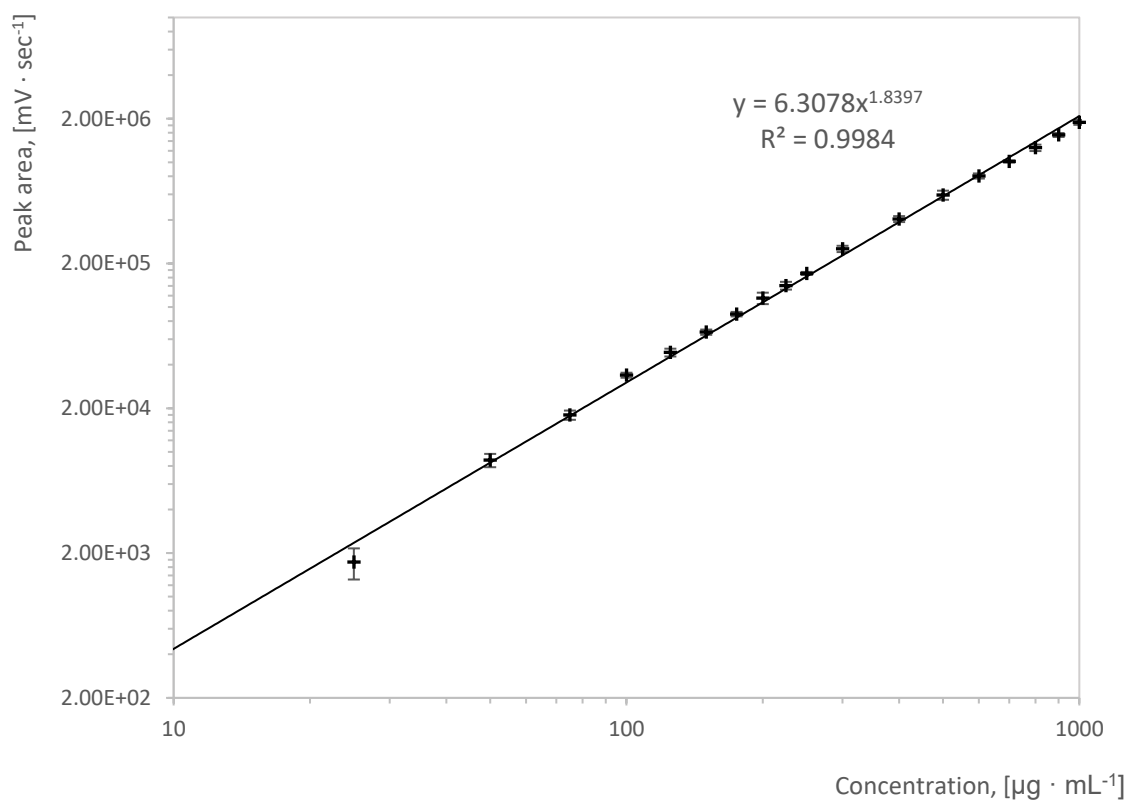
Figure 47. Calibration curve for compound **59**.

$$y = 6.2869x^{1.8489}$$
$$R^2 = 0.9983$$
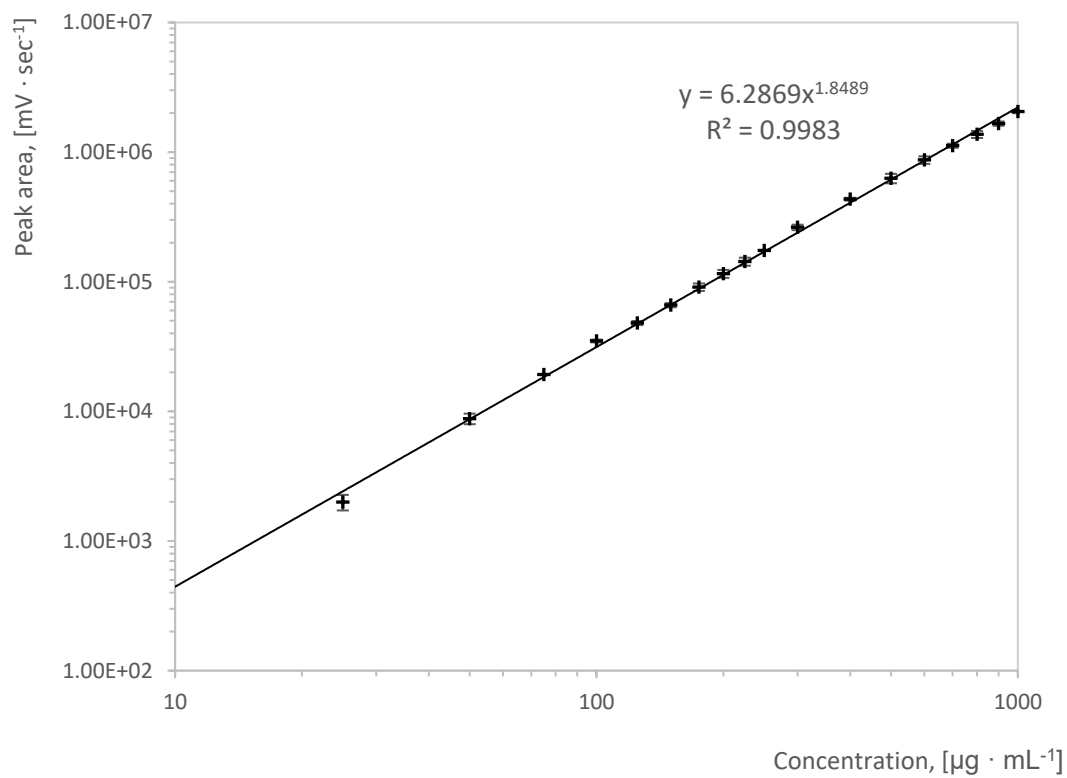
Figure 48. Calibration curve for compound **60**.

8 ABBREVIATIONS

Ac, Acetate

AI, Artificial Intelligence

APCI, Atmospheric Pressure Chemical Ionization

APT, Attached Proton Test

aq., aqueous

BA, Bile Acid

BARs, Bile Acid Receptors

CA, Cholic Acid

CAR, Constitutive Androstane Receptor

CDCA, Chenodeoxycholic Acid

COSY, Correlation Spectroscopy

Cryo-EM, Cryogenic Electron Microscopy

CuAAC, Cu(I)-catalyzed Azide-alkyne Cycloaddition

CuMeSal, Copper(I) 3-Methylsalicylate

DBD, DNA Binding Domain

DCM, Dichloromethane

DMP, Dess–Martin Periodinane

DMSO, Dimethyl Sulfoxide

DUIS, Dual Ion Source

EI, electron impact ionization

ELS, Evaporative Light Scattering

equiv., equivalent(s)

ESI, Electrospray Ionization

et al., et alii (Latin), and others

Et, ethyl

EtOAc, Ethyl Acetate

FA, Formic Acid

FBS, Fetal Bovine Serum

FDA, Food and Drug Administration

FXR, Farnesoid X Receptor

GPBAR1, G protein Coupled Bile Acid Receptor 1

GPCR19, G-protein Coupled Receptor 19

GPT, Generative Pre-trained Transformer

GUDCA, Glycoursodeoxycholic Acid

GβMCA, Glycine-β-Muricholic Acid

HCV, Hepatitis C Virus

HDL, High-density Lipoprotein

HMBC, Heteronuclear Multiple Bond Correlation

HPLC, High-Pressure Liquid Chromatography

HRMS, High-Resolution Mass Spectrometry

HSQC, Heteronuclear Single Quantum Coherence

IBX, *o*-Iodoxybenzoic Acid

IDE, Integrated Development Environment

LBD, Ligand-Binding Domain

LC, Liquid Chromatography

LCA, Lithocholic Acid

LDL, Low-density Lipoprotein

LRMS, Low-Resolution Mass Spectrometry

M3R, Muscarinic Acetylcholine Receptor M3

M-BAR, Membrane-type Bile Acid Receptor

Me, Methyl

MGL, Molecular Graphic Laboratory

Mp, Melting point

MS, Mass Spectrometry

NAFLD, Nonalcoholic Fatty Liver Disease

NASH, Non-Alcoholic Steatohepatitis

NCNSOTD, Non-Central Nervous System Orally Taken Drugs

NMO, *N*-Methylmorpholine *N*-oxide

NMR, Nuclear Magnetic Resonance

NOE, Nuclear Overhauser Effect

OCA, Obeticholic Acid

ORTEP, Oak Ridge Thermal Ellipsoid Plot

PBC, Primary Biliary Cholangitis

PDA, Photodiode Array Detector

PE, Petroleum Ether

Ph, Phenyl

pLDDT, predicted Local Distance Difference Test

Pr, Propyl

PXR, Pregnane X Receptor

RF, Retention Factor

RLU, Relative Luminescence Unit

ROESY, Rotating-Frame Overhauser Effect Spectroscopy

rt, room temperature

S1PR2, Sphingosine-1-phosphate Receptor 2

SMILES, Simplified Molecular Input Line Entry System

TEMPO, 2,2,6,6-Tetramethylpiperidine-1-oxyl

TFA, Trifluoroacetic Acid

TFAA, Trifluoroacetic Acid Anhydride

TGR5, Takeda G protein-coupled Receptor 5

TGR5, Takeda G-Protein Coupled Receptor

THF, Tetrahydrofuran

TLC, Thin Layer Chromatography

t_R, Retention Time

Ts, Toluene sulfonyl

UDCA, Ursodeoxycholic Acid

VDR, Vitamin D Receptor

9 REFERENCES

1. Berthold, A. A. Lehrbuch der Physiologie des Menschen und der Thiere. *Vandenhoeck und Ruprecht* **1839**.

2. Butenandt, A. Untersuchungen über das Weibliche Sexualhormon. *DMW-Deutsche Medizinische Wochenschrift* **1929,** *55* (52), 2171–2173.

3. Butenandt, A. Über die Chemische Untersuchung der Sexualhormone. *Angewandte Chemie* **1931,** *44* (46), 905–908.

4. Butenandt, A. Über „Progynon "ein Krystallisiertes Weibliches Sexualhormon. *Naturwissenschaften* **1929,** *17* (45), 879–879.

5. Shampo, M. A.; Kyle, R. A.; Steensma, D. P. In Leopold Ruzicka-1939 Nobel Prize in Chemistry, Mayo Clinic Proceedings, Elsevier Limited: 2007; 0_5.

6. Shampo, M. A.; Kyle, R. A.; Steensma, D. P. In Adolf Butenandt—Nobel Prize for Chemistry, Mayo Clinic Proceedings, Elsevier: 2012; e27.

7. Allen, W. M.; Wintersteiner, O. Crystalline Progestin. *Science* **1934,** *80* (2069), 190–191.

8. Butenandt, A.; Westphal, U. Zur Isolierung und Charakterisierung des Corpus-luteum-Hormons. *Berichte der Deutschen Chemischen Gesellschaft (A and B Series)* **1934,** *67* (8), 1440–1442.

9. Butenandt, A.; Westphal, U.; Hohlweg, W. Über das Hormon des Corpus luteum. *Hoppe-Seyler´s Zeitschrift für Physiologische Chemie* **1934,** *227* (1–4), 84−98.

10. Hartmann, M.; Wettstein, A. Ein Krystallisiertes Hormon aus Corpus luteum. (Vorläufige Mitteilung). *Helvetica Chimica Acta* **1934,** *17* (1), 878–882.

11. Hartmann, M.; Wettstein, A. Zur Kenntnis der Corpus luteum-Hormone (2. Mitteilung.). *Helvetica Chimica Acta* **1934,** *17* (1–4), 1365–1372.

12. Allen, W. M.; Butenandt, A.; Corner, G. W.; Slotta, K. H. Nomenclature of Corpus luteum Hormone. *Science* **1935,** *82* (2120), 153–153.

13. Slotta, K. H. The Isolation of Progesterone. *American Journal of Obstetrics & Gynecology* **1975,** *121* (3), 428.

14. Butenandt, A.; Hanisch, G. Über Testosteron. Umwandlung des Dehydro-androsterons in Androstendiol und Testosteron; ein Weg zur Darstellung des Testosterons aus Cholesterin. *Hoppe-Seyler´s Zeitschrift für Physiologische Chemie* **1935,** *237* (1–3), 89–97.

15. David, K.; Dingemanse, E.; Freud, J.; Laqueur, E. Über Krystallinisches Männliches Hormon aus Hoden (Testosteron), Wirksamer als aus Harn oder aus Cholesterin Bereitetes Androsteron. *Hoppe-Seyler´s Zeitschrift für Physiologische Chemie* **1935,** *233* (5–6), 281–283.

16. Ruzicka, L.; Wettstein, A. Uber die Krystallische Herstellung des Testikelhormons, Testosteron (Androsten-3-on-17-ol). *Helvetica Chimica Acta* **1935,** *18*, 1264–1275.

17. Mason, H. L.; Myers, C. S.; Kendall, E. C. The Chemistry of Crystalline Substances Isolated from the Suprarenal Gland. *Journal of Biological Chemistry* **1936,** *114* (3), 613–631.

18. Mason, H. L.; Myers, C. S.; Kendall, E. C. Chemical Studies of the Suprarenal Cortex: II. The Identification of a Substance Which Possesses the Qualitative Action of Cortin; Its Conversion Into a Diketone Closely Related to Androstenedione. *Journal of Biological Chemistry* **1936,** *116* (1), 267–276.

19. Reichstein, T. Constituents of the Adrenal Cortex. *Helvetica Chimica Acta* **1936,** *19*, 402.

20. Simpson, S. A. Physicochemical Methods of Detection of a Previously Unidentified Adrenal Hormone. *Memoirs of the Society for Endocrinology* **1953,** *2*, 9–24.

21. Simpson, S. A.; Tait, J. F.; Wettstein, A.; Neher, R.; Reichstein, T. Isolierung Eines Neuen Kristallisierten Hormons aus Nebennieren mit Besonders Hoher Wirksamkeit auf den Mineralstoffwechsel. *Experientia* **1953,** *9* (9), 333–335.

22. Simpson, S. A.; Tait, J. F.; Reichstein, T. The Correspondence of S.A. Simpson and J.F. Tait with T. Reichstein During Their Collaborative Work on the Isolation and Elucidation of the Structure of Electrocortin (Later Aldosterone). *Steroids* **1998,** *63*, 440–453.

23. Moss, G. P. Nomenclature of Steroids (Recommendations 1989). *Pure and Applied Chemistry* **1989,** *61* (10), 1783–1822.

24. Brecher, J. Graphical Representation of Stereochemical Configuration (IUPAC Recommendations 2006). *Pure and Applied Chemistry* **2006,** *78* (10), 1897-1970.

25. Moss, G. P. Basic Terminology of Stereochemistry (IUPAC Recommendations 1996). *Pure and Applied Chemistry* **1996,** *68* (12), 2193–2222.

26. Chiang, J. Y. L. Bile Acids: Regulation of Synthesis: Thematic Review Series: Bile Acids. *Journal of Lipid Research* **2009,** *50* (10), 1955-1966.

27. Chiang, J. Y. L. Bile Acid Metabolism and Signaling. In Comprehensive Physiology, **2013**; Vol. 3, pp 1191-1212.

28. Russell, D. W. The Enzymes, Regulation, and Genetics of Bile Acid Synthesis. *Annual Review of Biochemistry* **2003,** *72* (1), 137-174.

29. Bloch, K.; Berg, B. N.; Rittenberg, D. The Biological Conversion of Cholesterol to Cholic Acid. *Journal of Biological Chemistry* **1943,** *149* (2), 511–517.

30. Ishibashi, S.; Schwarz, M.; Frykman, P. K.; Herz, J.; Russell, D. W. Disruption of Cholesterol 7α-Hydroxylase Gene in Mice: I. POSTNATAL LETHALITY REVERSED BY BILE ACID

AND VITAMIN SUPPLEMENTATION *. *Journal of Biological Chemistry* **1996,** *271* (30), 18017-18023.

31. Erickson, S. K.; Lear, S. R.; Shefer, S.; Blanche, P. J.; Berkeley, L.; Batta, A. K.; Krauss, R. M.; Salen, G. Effect of Cholesterol 7alpha-Hydroxylase (cyp7A) Gene Knockout on Lipid Homeostasis. *Circulation* **1999,** *100* (18), 686–687.

32. Pullinger, C. R.; Eng, C.; Salen, G.; Shefer, S.; Batta, A. K.; Erickson, S. K.; Verhagen, A.; Rivera, C. R.; Mulvihill, S. J.; Malloy, M. J*., et al.* Human Cholesterol 7alpha-Hydroxylase (CYP7A1) Deficiency has a Hypercholesterolemic Phenotype. *The Journal of Clinical Investigation* **2002,** *110* (1), 109-17.

33. Setchell, K. D.; Schwarz, M.; O'Connell, N. C.; Lund, E. G.; Davis, D. L.; Lathe, R.; Thompson, H. R.; Tyson, W. R.; Sokol, R. J.; Russell, D. W. Identification of a New Inborn Error in Bile Acid Synthesis: Mutation of the Oxysterol 7alpha-Hydroxylase Gene Causes Severe Neonatal Liver Disease. *The Journal of Clinical Investigation* **1998,** *102* (9), 1690–1703.

34. Schwarz, M.; Lund, E. G.; Russell, D. W. Two 7α-Hydroxylase Enzymes in Bile Acid Biosynthesis. *Current Opinion in Lipidology* **1998,** *9* (2), 113–118.

35. Hofmann, A. F. The Function of Bile Salts in Fat Absorption. The Solvent Properties of Dilute Micellar Solutions of Conjugated Bile Salts. *Biochemical Journal* **1963,** *89*, 57–68.

36. Li, T.; Chiang, J. Y. L. Regulation of Bile Acid and Cholesterol Metabolism by PPARs. *PPAR Research* **2009,** *2009* (501739), 1–15.

37. Mertens, K. L.; Kalsbeek, A.; Soeters, M. R.; Eggink, H. M. Bile Acid Signaling Pathways from the Enterohepatic Circulation to the Central Nervous System. *Frontiers in Neuroscience* **2017,** *11*.

38. Fiorucci, S.; Biagioli, M.; Zampella, A.; Distrutti, E. Bile Acids Activated Receptors Regulate Innate Immunity. *Frontiers in Immunology* **2018,** *9*.

39. Stofan, M.; Guo, G. L. Bile Acids and FXR: Novel Targets for Liver Diseases. *Frontiers in Medicine* **2020,** *7*.

40. BioRenderApp. Subscription Student plan, Agreement number: EY24IFSI72, Computer Program; https://biorender.com, **2022**.

41. Guyton, A. C.; Hall, J. E. Textbook of Medical Physiology 14th, Editor. *Elsevier Inc.* **2021**.

42. Hylemon, P. B.; Zhou, H.; Pandak, W. M.; Ren, S.; Gil, G.; Dent, P. Bile Acids as Regulatory Molecules. *Journal of Lipid Research* **2009,** *50* (8), 1509-1520.

43. Trauner, M.; Claudel, T.; Fickert, P.; Moustafa, T.; Wagner, M. Bile Acids as Regulators of Hepatic Lipid and Glucose Metabolism. *Digestive Diseases* **2010,** *28* (1), 220-224.

44. Copple, B. L.; Li, T. Pharmacology of Bile Acid Receptors: Evolution of Bile Acids from Simple Detergents to Complex Signaling Molecules. *Pharmacological Research* **2016,** *104*, 9-21.

45. Di Ciaula, A.; Garruti, G.; Baccetto, R. L.; Molina-Molina, E.; Bonfrate, L.; Portincasa, P.; Wang, D. Q. H. Bile Acid Physiology. *Annals of Hepatology* **2018,** *16* (1), 4-14.

46. Attili, A. F.; Angelico, M.; Cantafora, A.; Alvaro, D.; Capocaccia, L. Bile Acid-Induced Liver Toxicity: Relation to the Hydrophobic-Hydrophilic Balance of Bile Acids. *Medical Hypotheses* **1986,** *19* (1), 57–69.

47. Lorenzo-Zuniga, V.; Bartoli, R.; Planas, R.; Hofmann, A. F.; Vinado, B.; Hagey, L. R.; Hernandez, J. M.; Mane, J.; Alvarez, M. A.; Ausina, V. Oral Bile Acids Reduce Bacterial Overgrowth, Bacterial Translocation, and Endotoxemia in Cirrhotic Rats. *Hepatology* **2003,** *37* (3), 551−557.

48. Islam, K. S.; Fukiya, S.; Hagio, M.; Fujii, N.; Ishizuka, S.; Ooka, T.; Ogura, Y.; Hayashi, T.; Yokota, A. Bile Acid is a Host Factor that Regulates the Composition of the Cecal Microbiota in Rats. *Gastroenterology* **2011,** *141* (5), 1773-1781.

49. Wang, H. B.; Chen, J.; Hollister, K.; Sowers, L. C.; Forman, B. M. Endogenous Bile Acids are Ligands for the Nuclear Receptor FXR BAR. *Molecular Cell* **1999,** *3* (5), 543–553.

50. Parks, D. J.; Blanchard, S. G.; Bledsoe, R. K.; Chandra, G.; Consler, T. G.; Kliewer, S. A.; Stimmel, J. B.; Willson, T. M.; Zavacki, A. M.; Moore, D. D*., et al.* Bile Acids: Natural Ligands for an Orphan Nuclear Receptor. *Science* **1999,** *284* (5418), 1365–1368.

51. Makishima, M.; Okamoto, A. Y.; Repa, J. J.; Tu, H.; Learned, R. M.; Luk, A.; Hull, M. V.; Lustig, K. D.; Mangelsdorf, D. J.; Shan, B. Identification of a Nuclear Receptor for Bile Acids. *Science* **1999,** *284* (5418), 1362–1365.

52. Mangelsdorf, D. J.; Evans, R. M. The RXR Heterodimers and Orphan Receptors. *Cell* **1995,** *83* (6), 841–850.

53. Forman, B. M.; Goode, E.; Chen, J.; Oro, A. E.; Bradley, D. J.; Perlmann, T.; Noonan, D. J.; Burka, L. T.; McMorris, T.; Lamph, W. W*., et al.* Identification of a Nuclear Receptor That is Activated by Farnesol Metabolites. *Cell* **1995,** *81* (5), 687–693.

54. O'Leary, N. A.; Wright, M. W.; Brister, J. R.; Ciufo, S.; Haddad, D.; McVeigh, R.; Rajput, B.; Robbertse, B.; Smith-White, B.; Ako-Adjei, D*., et al.* Reference Sequence (RefSeq) Database at NCBI: Current Status, Taxonomic Expansion, and Functional Annotation. *Nucleic Acids Research* **2016,** *44* (D1), D733-D745.

55. Akwabi-Ameyaw, A.; Bass, J. Y.; Caldwell, R. D.; Caravella, J. A.; Chen, L.; Creech, K. L.; Deaton, D. N.; Madauss, K. P.; Marr, H. B.; McFadyen, R. B*., et al.* FXR Agonist Activity of Conformationally Constrained Analogs of GW-4064. *Bioorganic & Medicinal Chemistry Letters* **2009,** *19* (16), 4733−4739.

56. Akwabi-Ameyaw, A.; Caravella, J. A.; Chen, L.; Creech, K. L.; Deaton, D. N.; Madauss, K. P.; Marr, H. B.; Miller, A. B.; Navas III, F.; Parks, D. J. Conformationally Constrained Farnesoid X Receptor (FXR) Agonists: Alternative Replacements of the Stilbene. *Bioorganic & Medicinal Chemistry Letters* **2011,** *21* (20), 6154-6160.

57. Bass, J. Y.; Caldwell, R. D.; Caravella, J. A.; Chen, L.; Creech, K. L.; Deaton, D. N.; Madauss, K. P.; Marr, H. B.; McFadyen, R. B.; Miller, A. B. Substituted Isoxazole Analogs of Farnesoid X Receptor (FXR) Agonist GW4064. *Bioorganic & Medicinal Chemistry Letters* **2009,** *19* (11), 2969-2973.

58. Bass, J. Y.; Caravella, J. A.; Chen, L.; Creech, K. L.; Deaton, D. N.; Madauss, K. P.; Marr, H. B.; McFadyen, R. B.; Miller, A. B.; Mills, W. Y. Conformationally Constrained Farnesoid X Receptor (FXR) Agonists: Heteroaryl Replacements of the Naphthalene. *Bioorganic & Medicinal Chemistry Letters* **2011,** *21* (4), 1206-1213.

59. Feng, S.; Yang, M.; Zhang, Z.; Wang, Z.; Hong, D.; Richter, H.; Benson, G. M.; Bleicher, K.; Grether, U.; Martin, R. E. Identification of an *N*-Oxide Pyridine GW4064 Analog as a Potent FXR Agonist. *Bioorganic & Medicinal Chemistry Letters* **2009,** *19* (9), 2595-2598.

60. Flatt, B.; Martin, R.; Wang, T.-L.; Mahaney, P.; Murphy, B.; Gu, X.-H.; Foster, P.; Li, J.; Pircher, P.; Petrowski, M*., et al.* Discovery of XL335 (WAY-362450), a Highly Potent, Selective, and Orally Active Agonist of the Farnesoid X Receptor (FXR). *Journal of Medicinal Chemistry* **2009,** *52* (4), 904-907.

61. Gaieb, Z.; Liu, S.; Gathiaka, S.; Chiu, M.; Yang, H.; Shao, C.; Feher, V. A.; Walters, W. P.; Kuhn, B.; Rudolph, M. G*., et al.* D3R Grand Challenge 2: Blind Prediction of Protein–Ligand Poses, Affinity Rankings, and Relative Binding Free Energies. *Journal of Computer-Aided Molecular Design* **2018,** *32* (1), 1-20.

62. Jiang, L.; Liu, X.; Wei, H.; Dai, S.; Qu, L.; Chen, X.; Guo, M.; Chen, Y. Structural Insight into the Molecular Mechanism of Cilofexor Binding to the Farnesoid X Receptor. *Biochemical and Biophysical Research Communications* **2022,** *595*, 1–6.

63. Jiang, L.; Xiao, D.; Li, Y.; Dai, S.; Qu, L.; Chen, X.; Guo, M.; Wei, H.; Chen, Y. Structural Basis of Tropifexor as a Potent and Selective Agonist of Farnesoid X Receptor. *Biochemical and Biophysical Research Communications* **2021,** *534*, 1047-1052.

64. Jin, L.; Feng, X.; Rong, H.; Pan, Z.; Inaba, Y.; Qiu, L.; Zheng, W.; Lin, S.; Wang, R.; Wang, Z. The Antiparasitic Drug Ivermectin is a Novel FXR Ligand that Regulates Metabolism. *Nature Communications* **2013,** *4* (1), 1-8.

65. Lu, Y.; Zheng, W.; Lin, S.; Guo, F.; Zhu, Y.; Wei, Y.; Liu, X.; Jin, S.; Jin, L.; Li, Y. Identification of an Oleanane-type Triterpene Hedragonic Acid as a Novel Farnesoid X Receptor Ligand with Liver Protective Effects and Anti-Inflammatory Activity. *Molecular Pharmacology* **2018,** *93* (2), 63-72.

66. Merk, D.; Sreeramulu, S.; Kudlinzki, D.; Saxena, K.; Linhard, V.; Gande, S. L.; Hiller, F.; Lamers, C.; Nilsson, E.; Aagaard, A. Molecular Tuning of Farnesoid X Receptor Partial Agonism. *Nature Communications* **2019,** *10* (1), 1-14.

67. Nara, S. J.; Jogi, S.; Cheruku, S.; Kandhasamy, S.; Jaipuri, F.; Kathi, P. K.; Reddy, S.; Sarodaya, S.; Cook, E. M.; Wang, T. Discovery of BMS-986339, a Pharmacologically Differentiated Farnesoid X Receptor Agonist for the Treatment of Nonalcoholic Steatohepatitis. *Journal of Medicinal Chemistry* **2022,** *65* (13), 8948-8960.

68. Richter, H. G. F.; Benson, G. M.; Bleicher, K. H.; Blum, D.; Chaput, E.; Clemann, N.; Feng, S.; Gardes, C.; Grether, U.; Hartman, P. Optimization of a Novel Class of Benzimidazole-Based Farnesoid X Receptor (FXR) Agonists to Improve Physicochemical and ADME Properties. *Bioorganic & Medicinal Chemistry Letters* **2011,** *21* (4), 1134-1140.

69. Richter, H. G. F.; Benson, G. M.; Blum, D.; Chaput, E.; Feng, S.; Gardes, C.; Grether, U.; Hartman, P.; Kuhn, B.; Martin, R. E. Discovery of Novel and Orally Active FXR Agonists for the Potential Treatment of Dyslipidemia & Diabetes. *Bioorganic & Medicinal Chemistry Letters* **2011,** *21* (1), 191-194.

70. Soisson, S. M.; Parthasarathy, G.; Adams, A. D.; Sahoo, S.; Sitlani, A.; Sparrow, C.; Cui, J.; Becker, J. W. Identification of a Potent Synthetic FXR Agonist with an Unexpected Mode of Binding and Activation. *Proceedings of the National Academy of Sciences* **2008,** *105* (14), 5337-5342.

71. Wang, N.; Zou, Q.; Xu, J.; Zhang, J.; Liu, J. Ligand Binding and Heterodimerization With Retinoid X Receptor α (RXRα) Induce Farnesoid X Receptor (FXR) Conformational Changes Affecting Coactivator Binding. *Journal of Biological Chemistry* **2018,** *293* (47), 18180-18191.

72. Xia, J.; Wang, Z.; Huan, Y.; Xue, W.; Wang, X.; Wang, Y.; Liu, Z.; Hsieh, J.-H.; Zhang, L.; Wu, S. Pose Filter-Based Ensemble Learning Enables Discovery of Orally Active, Nonsteroidal Farnesoid X Receptor Agonists. *Journal of Chemical Information and Modeling* **2020,** *60* (3), 1202–1214.

73. Xu, X.; Xu, X.; Liu, P.; Zhu, Z. Y.; Chen, J.; Fu, H. A.; Chen, L. L.; Hu, L. H.; Shen, X. Structural Basis for Small Molecule NDB (*N*-Benzyl-*N*-(3-(tert-butyl)-4-hydroxyphenyl)-2,6-dichloro-4-(dimethylamino) Benzamide) as a Selective Antagonist of Farnesoid X Receptor α (FXRα) in Stabilizing the Homodimerization of the Receptor. *Journal of Biological Chemistry* **2015,** *290* (32), 19888-19899.

74. Zheng, W.; Lu, Y.; Lin, S.; Wang, R.; Qiu, L.; Zhu, Y.; Yao, B.; Guo, F.; Jin, S.; Jin, L*., et al.* A Novel Class of Natural FXR Modulators with a Unique Mode of Selective Co-regulator Assembly. *ChemBioChem* **2017,** *18* (8), 721-725.

75. Zheng, W.; Lu, Y.; Tian, S.; Ma, F.; Wei, Y.; Xu, S.; Li, Y. Structural Insights Into the Heterodimeric Complex of the Nuclear Receptors FXR and RXR. *Journal of Biological Chemistry* **2018,** *293* (32), 12535-12541.

76. Benoit, G.; Cooney, A.; Giguere, V.; Ingraham, H.; Lazar, M.; Muscat, G.; Perlmann, T.; Renaud, J. P.; Schwabe, J.; Sladek, F*., et al.* International Union of Pharmacology. LXVI. Orphan Nuclear Receptors. *Pharmacological Reviews* **2006,** *58* (4), 798-836.

77. Giguere, V. Orphan Nuclear Receptors: From Gene to Function. *Endocrine Reviews* **1999,** *20* (5), 689–725.

78. Jumper, J.; Evans, R.; Pritzel, A.; Green, T.; Figurnov, M.; Ronneberger, O.; Tunyasuvunakool, K.; Bates, R.; Zidek, A.; Potapenko, A. Highly Accurate Protein Structure Prediction with AlphaFold. *Nature* **2021,** *596* (7873), 583-589.

79. Varadi, M.; Anyango, S.; Deshpande, M.; Nair, S.; Natassia, C.; Yordanova, G.; Yuan, D.; Stroe, O.; Wood, G.; Laydon, A. AlphaFold Protein Structure Database: Massively Expanding the Structural

Coverage of Protein-Sequence Space with High-Accuracy Models. *Nucleic Acids Research* **2022,** *50* (D1), D439-D444.

80. Goodwin, B.; Jones, S. A.; Price, R. R.; Watson, M. A.; McKee, D. D.; Moore, L. B.; Galardi, C.; Wilson, J. G.; Lewis, M. C.; Roth, M. E. A Regulatory Cascade of the Nuclear Receptors FXR, SHP-1, and LRH-1 Represses Bile Acid Biosynthesis. *Molecular Cell* **2000,** *6* (3), 517-526.

81. Ananthanarayanan, M.; Balasubramanian, N.; Makishima, M.; Mangelsdorf, D. J.; Suchy, F. J. Human Bile Salt Export Pump Promoter is Transactivated by the Farnesoid X Receptor/Bile acid Receptor. *Journal of Biological Chemistry* **2001,** *276* (31), 28857-28865.

82. Frankenberg, T.; Rao, A.; Chen, F.; Haywood, J.; Shneider, B. L.; Dawson, P. A. Regulation of the Mouse Organic Solute Transporter α-β, Ostα-Ostβ, by Bile Acids. *American Journal of Physiology-Gastrointestinal and Liver Physiology* **2006,** *290* (5), G912-G922.

83. Chen, F.; Ma, L.; Dawson, P. A.; Sinal, C. J.; Sehayek, E.; Gonzalez, F. J.; Breslow, J.; Ananthanarayanan, M.; Shneider, B. L. Liver Receptor Homologue-1 Mediates Species and Cell Line Specific Bile Acid Dependent Negative Feedback Regulation of the Apical Sodium Dependent Bile Acid Transporter. *Journal of Biological Chemistry* **2003,** *278* (22), 19909-19916.

84. Inagaki, T.; Choi, M.; Moschetta, A.; Peng, L.; Cummins, C. L.; McDonald, J. G.; Luo, G.; Jones, S. A.; Goodwin, B.; Richardson, J. A. Fibroblast growth Factor 15 Functions as an Enterohepatic Signal to Regulate Bile Acid Homeostasis. *Cell Metabolism* **2005,** *2* (4), 217-225.

85. Claudel, T.; Staels, B.; Kuipers, F. The Farnesoid X Receptor - a Molecular Link Between Bile Acid and Lipid and Glucose Metabolism. *Arteriosclerosis Thrombosis and Vascular Biology* **2005,** *25* (10), 2020-2031.

86. Peng, Z.; Chen, J.; Drachenberg, C. B.; Raufman, J.-P.; Xie, G. Farnesoid X Receptor Represses Matrix Metalloproteinase 7 Expression, Revealing this Regulatory Axis as a Promising Therapeutic Target in Colon Cancer. *Journal of Biological Chemistry* **2019,** *294* (21), 8529-8542.

87. Qiao, P.; Li, S.; Zhang, H.; Yao, L.; Wang, F. Farnesoid X Receptor Inhibits Proliferation of Human Colorectal Cancer Cells *via* the miR-135A1/CCNG2 Signaling Pathway. *Oncology Reports* **2018,** *40* (4), 2067-2078.

88. Vavassori, P.; Mencarelli, A.; Renga, B.; Distrutti, E.; Fiorucci, S. The Bile Acid Receptor FXR is a Modulator of Intestinal Innate Immunity. *The Journal of Immunology* **2009,** *183* (10), 6251-6261.

89. Deuschle, U.; Schüler, J.; Schulz, A.; Schlüter, T.; Kinzel, O.; Abel, U.; Kremoser, C. FXR Controls the Tumor Suppressor NDRG2 and FXR Agonists Reduce Liver Tumor Growth and Metastasis in an Orthotopic Mouse Xenograft Model. *PLoS One* **2012,** *7* (10), e43044.

90. Guo, F.; Xu, Z.; Zhang, Y.; Jiang, P.; Huang, G.; Chen, S.; Lyu, X.; Zheng, P.; Zhao, X.; Zeng, Y. FXR Induces SOCS3 and Suppresses Hepatocellular Carcinoma. *Oncotarget* **2015,** *6* (33), 34606.

91. He, J.; Zhao, K.; Zheng, L.; Xu, Z.; Gong, W.; Chen, S.; Shen, X.; Huang, G.; Gao, M.; Zeng, Y. Upregulation of microRNA-122 by Farnesoid X Receptor Suppresses the Growth of Hepatocellular Carcinoma Cells. *Molecular Cancer* **2015,** *14* (1), 1-11.

92. Fiorucci, S.; Mencarelli, A.; Distrutti, E.; Palladino, G.; Cipriani, S. Targeting Farnesoid X Receptor: From Medicinal Chemistry to Disease Treatment. *Current Medicinal Chemistry* **2010,** *17* (2), 139-159.

93. Fiorucci, S.; Cipriani, S.; Baldelli, F.; Mencarelli, A. Bile Acid-Activated Receptors in the Treatment of Dyslipidemia and Related Disorders. *Progress in Lipid Research* **2010,** *49* (2), 171-185.

94. Sun, L.; Cai, J.; Gonzalez, F. J. The Role of Farnesoid X Receptor in Metabolic Diseases, and Gastrointestinal and Liver Cancer. *Nature Reviews Gastroenterology & Hepatology* **2021,** *18* (5), 335–347.

95. Van Mil, S. W. C.; Milona, A.; Dixon, P. H.; Mullenbach, R.; Geenes, V. L.; Chambers, J.; Shevchuk, V.; Moore, G. E.; Lammert, F.; Glantz, A. G. Functional Variants of the Central Bile Acid Sensor FXR Identified in Intrahepatic Cholestasis of Pregnancy. *Gastroenterology* **2007,** *133* (2), 507-516.

96. Zollner, G.; Marschall, H.-U.; Wagner, M.; Trauner, M. Role of Nuclear Receptors in the Adaptive Response to Bile Acids and Cholestasis: Pathogenetic and Therapeutic Considerations. *Molecular Pharmaceutics* **2006,** *3* (3), 231-251.

97. Issa, D.; Wattacheril, J.; Sanyal, A. J. Treatment Options for Nonalcoholic Steatohepatitis a Safety Evaluation. *Expert Opinion on Drug Safety* **2017,** *16* (8), 903-913.

98. Neuschwander-Tetri, B. A.; Loomba, R.; Sanyal, A. J.; Lavine, J. E.; Van Natta, M. L.; Abdelmalek, M. F.; Chalasani, N.; Dasarathy, S.; Diehl, A. M.; Hameed, B. Farnesoid X Nuclear Receptor Ligand Obeticholic Acid for Non-Cirrhotic, Non-Alcoholic Steatohepatitis (FLINT): a Multicentre, Randomised, Placebo-Controlled Trial. *The Lancet* **2015,** *385* (9972), 956-965.

99. Yang, Z.-X.; Shen, W.; Sun, H. Effects of Nuclear Receptor FXR on the Regulation of Liver Lipid Metabolism in Patients with Non-Alcoholic Fatty Liver Disease. *Hepatology International* **2010,** *4* (4), 741-748.

100. Takahashi, S.; Tanaka, N.; Golla, S.; Fukami, T.; Krausz, K. W.; Polunas, M. A.; Weig, B. C.; Masuo, Y.; Xie, C.; Jiang, C. Editor's Highlight: Farnesoid X Receptor Protects Against Low-Dose Carbon Tetrachloride-Induced Liver Injury Through the Taurocholate-JNK Pathway. *Toxicological Sciences* **2017,** *158* (2), 334-346.

101. Fiorucci, S.; Antonelli, E.; Rizzo, G.; Renga, B.; Mencarelli, A.; Riccardi, L.; Orlandi, S.; Pellicciari, R.; Morelli, A. The Nuclear Receptor SHP Mediates Inhibition of Hepatic Stellate Cells by FXR and Protects Against Liver Fibrosis. *Gastroenterology* **2004,** *127* (5), 1497-1512.

102. Fiorucci, S.; Rizzo, G.; Antonelli, E.; Renga, B.; Mencarelli, A.; Riccardi, L.; Orlandi, S.; Pruzanski, M.; Morelli, A.; Pellicciari, R. A Farnesoid x Receptor-Small Heterodimer Partner Regulatory Cascade Modulates Tissue Metalloproteinase Inhibitor-1 and Matrix Metalloprotease Expression in Hepatic Stellate Cells and Promotes Resolution of Liver Fibrosis. *Journal of Pharmacology and Experimental Therapeutics* **2005,** *314* (2), 584-595.

103. Manley, S.; Ni, H.-M.; Williams, J. A.; Kong, B.; DiTacchio, L.; Guo, G.; Ding, W.-X. Farnesoid X Receptor Regulates Forkhead Box O3a Activation in Ethanol-Induced Autophagy and Hepatotoxicity. *Redox Biology* **2014,** *2*, 991-1002.

104. Wu, W.; Zhu, B.; Peng, X.; Zhou, M.; Jia, D.; Gu, J. Activation of Farnesoid X Receptor Attenuates Hepatic Injury in a Murine Model of Alcoholic Liver Disease. *Biochemical and Biophysical Research Communications* **2014,** *443* (1), 68-73.

105. Lu, W.; Cheng, F.; Jiang, J.; Zhang, C.; Deng, X.; Xu, Z.; Zou, S.; Shen, X.; Tang, Y.; Huang, J. FXR Antagonism of NSAIDs Contributes to Drug-Induced Liver Injury Identified by Systems Pharmacology Approach. *Scientific Reports* **2015,** *5* (1), 1-10.

106. Chen, W.-D.; Wang, Y.-D.; Meng, Z.; Zhang, L.; Huang, W. Nuclear Bile Acid Receptor FXR in the Hepatic Regeneration. *Biochimica et Biophysica Acta (BBA)-Molecular Basis of Disease* **2011,** *1812* (8), 888-892.

107. Gadaleta, R. M.; Van Erpecum, K. J.; Oldenburg, B.; Willemsen, E. C. L.; Renooij, W.; Murzilli, S.; Klomp, L. W. J.; Siersema, P. D.; Schipper, M. E. I.; Danese, S. Farnesoid X Receptor Activation Inhibits Inflammation and Preserves the Intestinal Barrier in Inflammatory Bowel Disease. *Gut* **2011,** *60* (4), 463-472.

108. Gonzalez, F. J.; Jiang, C.; Patterson, A. D. An Intestinal Microbiota–Farnesoid X Receptor Axis Modulates Metabolic Disease. *Gastroenterology* **2016,** *151* (5), 845-859.

109. Sun, L.; Xie, C.; Wang, G.; Wu, Y.; Wu, Q.; Wang, X.; Liu, J.; Deng, Y.; Xia, J.; Chen, B. Gut Microbiota and Intestinal FXR Mediate the Clinical Benefits of Metformin. *Nature Medicine* **2018,** *24* (12), 1919–1929.

110. Xie, C.; Jiang, C.; Shi, J.; Gao, X.; Sun, D.; Sun, L.; Wang, T.; Takahashi, S.; Anitha, M.; Krausz, K. W. An Intestinal Farnesoid X Receptor–Ceramide Signaling Axis Modulates Hepatic Gluconeogenesis in Mice. *Diabetes* **2017,** *66* (3), 613-626.

111. Jiang, C.; Xie, C.; Li, F.; Zhang, L.; Nichols, R. G.; Krausz, K. W.; Cai, J.; Qi, Y.; Fang, Z.-Z.; Takahashi, S. Intestinal Farnesoid X Receptor Signaling Promotes Nonalcoholic Fatty Liver Disease. *The Journal of Clinical Investigation* **2015,** *125* (1), 386-402.

112. Inagaki, T.; Moschetta, A.; Lee, Y.-K.; Peng, L.; Zhao, G.; Downes, M.; Yu, R. T.; Shelton, J. M.; Richardson, J. A.; Repa, J. J. Regulation of Antibacterial Defense in the Small Intestine by the Nuclear Bile Acid Receptor. *Proceedings of the National Academy of Sciences* **2006,** *103* (10), 3920-3925.

113. Jiang, T.; Wang, X. X.; Scherzer, P.; Wilson, P.; Tallman, J.; Takahashi, H.; Li, J.; Iwahashi, M.; Sutherland, E.; Arend, L. Farnesoid X Receptor Modulates Renal Lipid Metabolism, Fibrosis, and Diabetic Nephropathy. *Diabetes* **2007,** *56* (10), 2485-2493.

114. Gai, Z.; Chu, L.; Xu, Z.; Song, X.; Sun, D.; Kullak-Ublick, G. A. Farnesoid X Receptor Activation Protects the Kidney from Ischemia-Reperfusion Damage. *Scientific Reports* **2017,** *7* (1), 1-16.

115. Zhao, K.; He, J.; Zhang, Y.; Xu, Z.; Xiong, H.; Gong, R.; Li, S.; Chen, S.; He, F. Activation of FXR Protects Against Renal Fibrosis *via* Suppressing Smad3 Expression. *Scientific Reports* **2016,** *6* (1), 1-8.

116. Cariou, B.; van Harmelen, K.; Duran-Sandoval, D.; van Dijk, T. H.; Grefhorst, A.; Abdelkarim, M.; Caron, S.; Torpier, G.; Fruchart, J. C.; Gonzalez, F. J. The Farnesoid X Receptor Modulates Diposity and Peripheral Insulin Sensitivity in Mice. *Journal of Biological Chemistry* **2006,** *281* (16), 11039-11049.

117. Rizzo, G.; Disante, M.; Mencarelli, A.; Renga, B.; Gioiello, A.; Pellicciari, R.; Fiorucci, S. The Farnesoid X Receptor Promotes Adipocyte Differentiation and Regulates Adipose Cell Function in Vivo. *Molecular Pharmacology* **2006,** *70* (4), 1164-1173.

118. Nijmeijer, R. M.; Schaap, F. G.; Smits, A. J. J.; Kremer, A. E.; Akkermans, L. M. A.; Kroese, A. B. A.; Rijkers, G. T.; Schipper, M. E. I.; Verheem, A.; Wijmenga, C. Impact of Global FXR Deficiency on Experimental Acute Pancreatitis and Genetic Variation in the FXR Locus in Human Acute Pancreatitis. *PLoS One* **2014,** *9* (12), e114393.

119. Popescu, I. R.; Helleboid-Chapman, A.; Lucas, A.; Vandewalle, B.; Dumont, J.; Bouchaert, E.; Derudas, B.; Kerr-Conte, J.; Caron, S.; Pattou, F. The Nuclear Receptor FXR is Expressed in Pancreatic β-Cells and Protects Human Islets from Lipotoxicity. *FEBS Letters* **2010,** *584* (13), 2845-2851.

120. Moris, D.; Giaginis, C.; Tsourouflis, G.; Theocharis, S. Farnesoid X Receptor (FXR) as a Promising Pharmaceutical Target in Atherosclerosis. *Current Medicinal Chemistry* **2017,** *24* (11), 1147-1157.

121. Kim, S.; Chen, J.; Cheng, T.; Gindulyte, A.; He, J.; He, S.; Li, Q.; Shoemaker, B. A.; Thiessen, P. A.; Yu, B.*, et al.* PubChem in 2021: New Data Content and Improved Web Interfaces. *Nucleic Acids Research* **2021,** *49* (D1), D1388–D1395.

122. Kim, S.; Thiessen, P. A.; Bolton, E. E.; Bryant, S. H. PUG-SOAP and PUG-REST: Web Services for Programmatic Access to Chemical Information in PubChem. *Nucleic Acids Research* **2015,** *43* (W1), W605-11.

123. Kim, S.; Thiessen, P. A.; Cheng, T.; Zhang, J.; Gindulyte, A.; Bolton, E. E. PUG-View: Programmatic Access to Chemical Annotations Integrated in PubChem. *Journal of Cheminformatics* **2019,** *11* (1), 56.

124. Pellicciari, R.; Costantino, G.; Camaioni, E.; Sadeghpour, B. M.; Entrena, A.; Willson, T. M.; Fiorucci, S.; Clerici, C.; Gioiello, A. Bile Acid Derivatives as Ligands of the Farnesoid X Receptor. Synthesis, Evaluation, and Structure-Activity Relationship of a Series of Body and Side Chain Modified Analogues of Chenodeoxycholic Acid. *Journal of Medicinal Chemistry* **2004,** *47* (18), 4559-4569.

125. Xiao, H.; Li, P.; Li, X.; He, H.; Wang, J.; Guo, F.; Zhang, J.; Wei, L.; Zhang, H.; Shi, Y.*, et al.* Synthesis and Biological Evaluation of a Series of Bile Acid Derivatives as FXR Agonists for Treatment of NASH. *ACS Medicinal Chemistry Letters* **2017,** *8* (12), 1246-1251.

126. Mi, L.-Z.; Devarakonda, S.; Harp, J. M.; Han, Q.; Pellicciari, R.; Willson, T. M.; Khorasanizadeh, S.; Rastinejad, F. Structural Basis for Bile Acid binding and Activation of the Nuclear Receptor FXR. *Molecular Cell* **2003,** *11* (4), 1093−1100.

127. Pellicciari, R.; Costantino, G.; Fiorucci, S. Farnesoid X Receptor: From Structure to Potential Clinical Applications. *Journal of Medicinal Chemistry* **2005,** *48* (17), 5383-5403.

128. Merk, D.; Steinhilber, D.; Schubert-Zsilavecz, M. Medicinal Chemistry of Farnesoid X Receptor Ligands: From Agonists and Antagonists to Modulators. *Future Medicinal Chemistry* **2012,** *4* (8), 1015-1036.

129. Gioiello, A.; Macchiarulo, A.; Carotti, A.; Filipponi, P.; Costantino, G.; Rizzo, G.; Adorini, L.; Pellicciari, R. Extending SAR of Bile Acids as FXR Ligands: Discovery of 23-*N*-(Carbocinnamyloxy)-3alpha,7alpha-dihydroxy-6alpha-ethyl-24-nor-5beta-cholan-23-amine. *Bioorganic & Medicinal Chemistry* **2011,** *19* (8), 2650-2658.

130. Pellicciari, R.; Gioiello, A.; Costantino, G.; Sadeghpour, B. M.; Rizzo, G.; Meyer, U.; Parks, D. J.; Entrena-Guadix, A.; Fiorucci, S. Back Door Modulation of the Farnesoid X Receptor: Design, Synthesis, and Biological Evaluation of a Series of Side Chain Modified Chenodeoxycholic Acid Derivatives. *Journal of Medicinal Chemistry* **2006,** *49* (14), 4208-4215.

131. Pellicciari, R.; Fiorucci, S.; Camaioni, E.; Clerici, C.; Costantino, G.; Maloney, P. R.; Morelli, A.; Parks, D. J.; Willson, T. M. 6α-Ethyl-Chenodeoxycholic Acid (6-ECDCA), a Potent and Selective FXR Agonist Endowed with Anticholestatic Activity. *Journal of Medicinal Chemistry* **2002,** *45* (17), 3569-3572.

132. Release, F. N. FDA Approves Ocaliva for Rare, Chronic Liver Disease. https://www.fda.gov/news-events/press-announcements/fda-approves-ocaliva-rare-chronic-liver-disease.

133. Podcast, F. D. S. Due to risk of serious liver injury, FDA restricts use of obeticholic acid (Ocaliva) in primary biliary cholangitis (PBC) patients with advanced cirrhosis. https://www.fda.gov/drugs/fda-drug-safety-podcasts/due-risk-serious-liver-injury-fda-restricts-use-obeticholic-acid-ocaliva-primary-biliary-cholangitis (accessed 6.6.2022).

134. Rose, A. S.; Hildebrand, P. W. NGL Viewer: A Web Application for Molecular Visualization. *Nucleic Acids Research* **2015,** *43* (W1), 576-579.

135. Pan, L.; Aller, S. G. Tools and Procedures for Visualization of Proteins and Other Biomolecules. *Current Protocols in Molecular Biology* **2015,** *110*, 1-47.

136. Jiang, L.; Zhang, H.; Xiao, D.; Wei, H.; Chen, Y. Farnesoid X receptor (FXR): Structures and Ligands. *Computational and Structural Biotechnology Journal* **2021,** *19*, 2148-2159.

137. Travere Therapeutics Inc. Study to Evaluate Patients With Cerebrotendinous Xanthomatosis (RESTORE). https://ClinicalTrials.gov/show/NCT04270682 **2020**.

138. Fiorucci, S.; Clerici, C.; Antonelli, E.; Orlandi, S.; Goodwin, B.; Sadeghpour, B. M.; Sabatino, G.; Russo, G.; Castellani, D.; Willson, T. M.*, et al.* Protective Effects of 6-Ethyl Chenodeoxycholic

Acid, a Farnesoid X Receptor Ligand, in Estrogen-Induced Cholestasis. *Journal of Pharmacology and Experimental Therapeutics* **2005,** *313* (2), 604.

139. Younossi, Z. M.; Ratziu, V.; Loomba, R.; Rinella, M.; Anstee, Q. M.; Goodman, Z.; Bedossa, P.; Geier, A.; Beckebaum, S.; Newsome, P. N. Obeticholic Acid for the Treatment of Non-Alcoholic Steatohepatitis: Interim Analysis from a Multicentre, Randomised, Placebo-Controlled Phase 3 Trial. *The Lancet* **2019,** *394* (10215), 2184-2196.

140. Erstad, D. J.; Farrar, C. T.; Ghoshal, S.; Masia, R.; Ferreira, D. S.; Chen, Y.-C. I.; Choi, J.-K.; Wei, L.; Waghorn, P. A.; Rotile, N. J*., et al.* Molecular Magnetic Resonance Imaging Accurately Measures the Antifibrotic Effect of EDP-305, a Novel Farnesoid X Receptor Agonist. *Hepatology Communications* **2018,** *2* (7), 821-835.

141. Chau, M.; Li, Y.; Roqueta-Rivera, M.; Garlick, K.; Shen, R.; Wang, G.; Or, Y. S.; Jiang, L.-J. Characterization of EDP-305, a Highly Potent and Selective Farnesoid X Receptor Agonist, for the Treatment of Non-Alcoholic Steatohepatitis. *International Journal of Gastroenterology* **2019,** *3* (1), 4–16.

142. Ratziu, V.; Rinella, M. E.; Neuschwander-Tetri, B. A.; Lawitz, E.; Denham, D.; Kayali, Z.; Sheikh, A.; Kowdley, K. V.; Desta, T.; Elkhashab, M*., et al.* EDP-305 in Patients with NASH: A Phase II Double-Blind Placebo-Controlled Dose-Ranging Study. *Journal of Hepatology* **2022,** *76* (3), 506-517.

143. Akwabi-Ameyaw, A.; Bass, J. Y.; Caldwell, R. D.; Caravella, J. A.; Chen, L.; Creech, K. L.; Deaton, D. N.; Jones, S. A.; Kaldor, I.; Liu, Y*., et al.* Conformationally Constrained Farnesoid X Receptor (FXR) Agonists: Naphthoic Acid-Based Analogs of GW4064. *Bioorganic & Medicinal Chemistry Letters* **2008,** *18* (15), 4339-4343.

144. Liu, Y.; Binz, J.; Numerick, M. J.; Dennis, S.; Luo, G.; Desai, B.; MacKenzie, K. I.; Mansfield, T. A.; Kliewer, S. A.; Goodwin, B*., et al.* Hepatoprotection by the Farnesoid X Receptor Agonist GW4064 in Rat Models of Intra- and Extrahepatic Cholestasis. *The Journal of Clinical Investigation* **2003,** *112* (11), 1678−1687.

145. Ma, Y.; Huang, Y.; Yan, L.; Gao, M.; Liu, D. Synthetic FXR Agonist GW4064 Prevents Diet-Induced Hepatic Steatosis and Insulin Resistance. *Pharmaceutical Research* **2013,** *30* (5), 1447-1457.

146. Novartis Pharmaceuticals. Study of Safety and Efficacy of Tropifexor (LJN452) in Patients With Non-alcoholic Steatohepatitis (NASH). https://ClinicalTrials.gov/show/NCT02855164 **2016-2020**.

147. Tully, D. C.; Rucker, P. V.; Chianelli, D.; Williams, J.; Vidal, A.; Alper, P. B.; Mutnick, D.; Bursulaya, B.; Schmeits, J.; Wu, X*., et al.* Discovery of Tropifexor (LJN452), a Highly Potent Non-bile Acid FXR Agonist for the Treatment of Cholestatic Liver Diseases and Nonalcoholic Steatohepatitis (NASH). *Journal of Medicinal Chemistry* **2017,** *60* (24), 9960-9973.

148. Novartis Pharmaceuticals. A Multi-part, Double Blind Study to Assess Safety, Tolerability and Efficacy of Tropifexor (LJN452) in PBC Patients. https://ClinicalTrials.gov/show/NCT02516605 **2015-2018**.

149. Downes, M.; Verdecia, M. A.; Roecker, A. J.; Hughes, R.; Hogenesch, J. B.; Kast-Woelbern, H. R.; Bowman, M. E.; Ferrer, J.-L.; Anisfeld, A. M.; Edwards, P. A., *et al.* A Chemical, Genetic, and Structural Analysis of the Nuclear Bile Acid Receptor FXR. *Molecular Cell* **2003,** *11* (4), 1079-1092.

150. Fang, S.; Suh, J. M.; Reilly, S. M.; Yu, E.; Osborn, O.; Lackey, D.; Yoshihara, E.; Perino, A.; Jacinto, S.; Lukasheva, Y. Intestinal FXR Agonism Promotes Adipose Tissue Browning and Reduces Obesity and Insulin Resistance. *Nature Medicine* **2015,** *21* (2), 159-165.

151. Lam, I. P. Y.; Lee, L. T. O.; Choi, H.-S.; Alpini, G.; Chow, B. K. C. Bile Acids Inhibit Duodenal Secretin Expression *via* Orphan Nuclear Receptor Small Heterodimer Partner (SHP). *American Journal of Physiology-Gastrointestinal and Liver Physiology* **2009,** *297* (1), G90-G97.

152. Mark, J. E.; Paige, E. M.; Lisa, B.-M.; KehDih, L.; Shuguang, W.; Julie, A. K.; Stephen, J. G.; Christine, H.; Robert, M.; George, P. V., *et al.* A Synthetic Farnesoid X Receptor (FXR) Agonist Promotes Cholesterol Lowering in Models of Dyslipidemia. *American Journal of Physiology-Gastrointestinal and Liver Physiology* **2009,** *296* (3), G543-G552.

153. Chianelli, D.; Rucker, P. V.; Roland, J.; Tully, D. C.; Nelson, J.; Liu, X.; Bursulaya, B.; Hernandez, E. D.; Wu, J.; Prashad, M., *et al.* Nidufexor (LMB763), a Novel FXR Modulator for the Treatment of Nonalcoholic Steatohepatitis. *Journal of Medicinal Chemistry* **2020,** *63* (8), 3868-3880.

154. Novartis Pharmaceuticals. Safety, Tolerability, Pharmacokinetics and Efficacy of LMB763 in Patients With NASH. https://ClinicalTrials.gov/show/NCT02913105 **2016-2018**.

155. Novartis Pharmaceuticals. Safety, Tolerability and Efficacy of Nidufexor in Patients With Diabetic Nephropathy. https://ClinicalTrials.gov/show/NCT03804879 **2018-2021**.

156. Kinzel, O.; Steeneck, C.; Schlüter, T.; Schulz, A.; Gege, C.; Hahn, U.; Hambruch, E.; Hornberger, M.; Spalwisz, A.; Frick, K., *et al.* Novel Substituted Isoxazole FXR Agonists with Cyclopropyl, Hydroxycyclobutyl and Hydroxyazetidinyl Linkers: Understanding and Improving Key Determinants of Pharmacological Properties. *Bioorganic & Medicinal Chemistry Letters* **2016,** *26* (15), 3746-3753.

157. Al-Khaifi, A.; Rudling, M.; Angelin, B. An FXR Agonist Reduces Bile Acid Synthesis Independently of Increases in FGF19 in Healthy Volunteers. *Gastroenterology* **2018,** *155* (4), 1012-1016.

158. Patel, K.; Harrison, S. A.; Elkhashab, M.; Trotter, J. F.; Herring, R.; Rojter, S. E.; Kayali, Z.; Wong, V. W.-S.; Greenbloom, S.; Jayakumar, S., *et al.* Cilofexor, a Nonsteroidal FXR Agonist, in Patients With Noncirrhotic NASH: A Phase 2 Randomized Controlled Trial. *Hepatology* **2020,** *72* (1), 58-71.

159. Schwabl, P.; Budas, G.; Hambruch, E.; Supper, P.; Burnet, M.; Liles, J.; Sullivan, T.; Huntzicker, E.; Birkel, M.; French, D., *et al.* FRI-248 - The FXR Agonist GS-9674 Reduces Fibrosis and Portal Hypertension in a Rat Model of NASH. *Journal of Hepatology* **2018,** *68*, S471-S472.

160. Trauner, M.; Gulamhusein, A.; Hameed, B.; Caldwell, S.; Shiffman, M. L.; Landis, C.; Eksteen, B.; Agarwal, K.; Muir, A.; Rushbrook, S., *et al.* The Nonsteroidal Farnesoid X Receptor Agonist Cilofexor (GS-9674) Improves Markers of Cholestasis and Liver Injury in Patients With Primary Sclerosing Cholangitis. *Hepatology* **2019,** *70* (3), 788-801.

161. Jackson, H.; Solaymani-Dodaran, M.; Card, T. R.; Aithal, G. P.; Logan, R.; West, J. Influence of Ursodeoxycholic Acid on the Mortality and Malignancy Associated with Primary Biliary Cirrhosis: A Population-Based Cohort Study. *Hepatology* **2007,** *46* (4), 1131-1137.

162. Kumar, D.; Tandon, R. K. Use of Ursodeoxycholic Acid in Liver Diseases. *Journal of Gastroenterology and Hepatology* **2001,** *16* (1), 3-14.

163. Nie, B.; Park, H. M.; Kazantzis, M.; Lin, M.; Henkin, A.; Ng, S.; Song, S.; Chen, Y.; Tran, H.; Lai, R*., et al.* Specific Bile Acids Inhibit Hepatic Fatty Acid Uptake in Mice. *Hepatology* **2012,** *56* (4), 1300-1310.

164. Floreani, A.; Mangini, C. Primary Biliary Cholangitis: Old and Novel Therapy. *European Journal of Internal Medicine* **2018,** *47*, 1-5.

165. Jiang, C.; Xie, C.; Lv, Y.; Li, J.; Krausz, K. W.; Shi, J.; Brocker, C. N.; Desai, D.; Amin, S. G.; Bisson, W. H*., et al.* Intestine-Selective Farnesoid X Receptor Inhibition Improves Obesity-Related Metabolic Dysfunction. *Nature Communications* **2015,** *6* (1), 10166.

166. Palmela, I.; Correia, L.; Silva, R. F. M.; Sasaki, H.; Kim, K. S.; Brites, D.; Brito, M. A. Hydrophilic Bile Acids Protect Human Blood-Brain Barrier Endothelial Cells from Disruption by Unconjugated Bilirubin: An *in vitro* Study. *Frontiers in Neuroscience* **2015,** *9*, 80.

167. Vaz, A. R.; Cunha, C.; Gomes, C.; Schmucki, N.; Barbosa, M.; Brites, D. Glycoursodeoxycholic Acid Reduces Matrix Metalloproteinase-9 and Caspase-9 Activation in a Cellular Model of Superoxide Dismutase-1 Neurodegeneration. *Molecular Neurobiology* **2015,** *51* (3), 864-877.

168. Vaz, A. R.; Delgado-Esteban, M.; Brito, M. A.; Bolanos, J. P.; Brites, D.; Almeida, A. Bilirubin Selectively Inhibits Cytochrome c Oxidase Activity and Induces Apoptosis in Immature Cortical Neurons: Assessment of the Protective Effects of Glycoursodeoxycholic Acid. *Journal of Neurochemistry* **2010,** *112* (1), 56-65.

169. Lyon, H. C. d. Role of FXR in Hepatitis C Virus Replication. https://ClinicalTrials.gov/show/NCT01492998 **2010**-2010.

170. Maruyama, T.; Miyamoto, Y.; Nakamura, T.; Tamai, Y.; Okada, H.; Sugiyama, E.; Nakamura, T.; Itadani, H.; Tanaka, K. Identification of Membrane-Type Receptor for Bile Acids (M-BAR). *Biochemical and Biophysical Research Communications* **2002,** *298* (5), 714-719.

171. Kawamata, Y.; Fujii, R.; Hosoya, M.; Harada, M.; Yoshida, H.; Miwa, M.; Fukusumi, S.; Habata, Y.; Itoh, T.; Shintani, Y. A G protein-Coupled Receptor Responsive to Bile Acids. *Journal of Biological Chemistry* **2003,** *278* (11), 9435−9440.

172. Keitel, V.; Reinehr, R.; Gatsios, P.; Rupprecht, C.; Görg, B.; Selbach, O.; Häussinger, D.; Kubitz, R. The G-protein Coupled Bile Salt Receptor TGR5 is Expressed in Liver Sinusoidal Endothelial Cells. *Hepatology* **2007,** *45* (3), 695-704.

173. Tiwari, A.; Maiti, P. TGR5: An Emerging Bile Acid G-Protein-Coupled Receptor Target for the Potential Treatment of Metabolic Disorders. *Drug Discovery Today* **2009,** *14* (9-10), 523-530.

174. Yang, F.; Mao, C.; Guo, L.; Lin, J.; Ming, Q.; Xiao, P.; Wu, X.; Shen, Q.; Guo, S.; Shen, D.-D., *et al.* Structural Basis of GPBAR Activation and Bile Acid Recognition. *Nature* **2020,** *587* (7834), 499-504.

175. Rohrer, D. K.; Kobilka, B. K. G Protein-Coupled Receptors: Functional and Mechanistic Insights Through Altered Gene Expression. *Physiological Reviews* **1998,** *78* (1), 35–52.

176. Pastan, I. H. The 1971 Nobel Prize for Physiology or Medicine. *Science* **1971,** *174* (4007), 392–393.

177. Ali, E. S.; Hua, J.; Wilson, C. H.; Tallis, G. A.; Zhou, F. H.; Rychkov, G. Y.; Barritt, G. J. The Glucagon-Like Peptide-1 Analogue Exendin-4 Reverses Impaired Intracellular Ca^{2+} Signalling in Steatotic Hepatocytes. *Biochimica et Biophysica Acta (BBA) - Molecular Cell Research* **2016,** *1863* (9), 2135-2146.

178. Masyuk, A. I.; Masyuk, T. V.; LaRusso, N. F. Exosomes in the Pathogenesis, Diagnostics and Therapeutics of Liver Diseases. *Journal of hepatology* **2013,** *59* (3), 621-625.

179. Zhong, M. TGR5 as a Therapeutic Target for Treating Obesity. *Current Topics in Medicinal Chemistry* **2010,** *10* (4), 386-396.

180. Pols, T. W. H.; Noriega, L. G.; Nomura, M.; Auwerx, J.; Schoonjans, K. The Bile Acid Membrane Receptor TGR5 as an Emerging Target in Metabolism and Inflammation. *Journal of Hepatology* **2011,** *54* (6), 1263-1272.

181. Kumar, D. P.; Rajagopal, S.; Mahavadi, S.; Mirshahi, F.; Grider, J. R.; Murthy, K. S.; Sanyal, A. J. Activation of Transmembrane Bile Acid Receptor TGR5 Stimulates Insulin Secretion in Pancreatic β Cells. *Biochemical and Biophysical Research Communications* **2012,** *427* (3), 600-605.

182. Chen, X.; Lou, G.; Meng, Z.; Huang, W. TGR5: A Novel Target for Weight Maintenance and Glucose Metabolism. *Experimental Diabetes Research* **2011,** *2011*, 853501.

183. Broeders, Evie P. M.; Nascimento, Emmani B. M.; Havekes, B.; Brans, B.; Roumans, Kay H. M.; Tailleux, A.; Schaart, G.; Kouach, M.; Charton, J.; Deprez, B., *et al.* The Bile Acid Chenodeoxycholic Acid Increases Human Brown Adipose Tissue Activity. *Cell Metabolism* **2015,** *22* (3), 418-426.

184. Phillips, D. P.; Gao, W.; Yang, Y.; Zhang, G.; Lerario, I. K.; Lau, T. L.; Jiang, J.; Wang, X.; Nguyen, D. G.; Bhat, B. G. Discovery of Trifluoromethyl (Pyrimidin-2-yl) Azetidine-2-carboxamides as Potent, Orally Bioavailable TGR5 (GPBAR1) Agonists: Structure–Activity Relationships, Lead Optimization, and Chronic *in vivo* Efficacy. *Journal of Medicinal Chemistry* **2014,** *57* (8), 3263-3282.

185. Martin, R. E.; Bissantz, C.; Gavelle, O.; Kuratli, C.; Dehmlow, H.; Richter, H. G. F.; Obst Sander, U.; Erickson, S. D.; Kim, K.; Pietranico-Cole, S. L. 2-Phenoxy-nicotinamides are Potent Agonists at the Bile Acid Receptor GPBAR1 (TGR5). *ChemMedChem* **2013,** *8* (4), 569-576.

186. Fryer, R. M.; Ng, K. J.; Mazurek, S. G. N.; Patnaude, L.; Skow, D. J.; Muthukumarana, A.; Gilpin, K. E.; Dinallo, R. M.; Kuzmich, D.; Lord, J. G Protein–Coupled Bile Acid Receptor 1

Stimulation Mediates Arterial Vasodilation Through a KCa1. 1 (BKCa)–Dependent Mechanism. *Journal of Pharmacology and Experimental Therapeutics* **2014,** *348* (3), 421-431.

187. Evans, K. A.; Budzik, B. W.; Ross, S. A.; Wisnoski, D. D.; Jin, J.; Rivero, R. A.; Vimal, M.; Szewczyk, G. R.; Jayawickreme, C.; Moncol, D. L. Discovery of 3-Aryl-4-isoxazolecarboxamides as TGR5 Receptor Agonists. *Journal of Medicinal Chemistry* **2009,** *52* (24), 7962-7965.

188. Briere, D. A.; Ruan, X.; Cheng, C. C.; Siesky, A. M.; Fitch, T. E.; Dominguez, C.; Sanfeliciano, S. G.; Montero, C.; Suen, C. S.; Xu, Y. Novel Small Molecule Agonist of TGR5 Possesses Anti-Diabetic Effects but Causes Gallbladder Filling in Mice. *PLoS One* **2015,** *10* (8), e0136873.

189. Agarwal, S.; Patil, A.; Aware, U.; Deshmukh, P.; Darji, B.; Sasane, S.; Sairam, K. V. V. M.; Priyadarsiny, P.; Giri, P.; Patel, H. Discovery of a Potent and Orally Efficacious TGR5 Receptor Agonist. *ACS Medicinal Chemistry Letters* **2016,** *7* (1), 51-55.

190. Carino, A.; Graziosi, L.; D'Amore, C.; Cipriani, S.; Marchiano, S.; Marino, E.; Zampella, A.; Rende, M.; Mosci, P.; Distrutti, E. The Bile Acid Receptor GPBAR1 (TGR5) is Expressed in Human Gastric Cancers and Promotes Epithelial-Mesenchymal Transition in Gastric Cancer Cell Lines. *Oncotarget* **2016,** *7* (38), 61021.

191. Sato, H.; Macchiarulo, A.; Thomas, C.; Gioiello, A.; Une, M.; Hofmann, A. F.; Saladin, R.; Schoonjans, K.; Pellicciari, R.; Auwerx, J. Novel Potent and Selective Bile Acid Derivatives as TGR5 Agonists: Biological Screening, Structure-Activity Relationships, and Molecular Modeling Studies. *Journal of Medicinal Chemistry* **2008,** *51* (6), 1831-1841.

192. Nakhi, A.; McDermott, C. M.; Stoltz, K. L.; John, K.; Hawkinson, J. E.; Ambrose, E. A.; Khoruts, A.; Sadowsky, M. J.; Dosa, P. I. 7-Methylation of Chenodeoxycholic Acid Derivatives Yields a Substantial Increase in TGR5 Receptor Potency. *Journal of Medicinal Chemistry* **2019,** *62* (14), 6824-6830.

193. Macchiarulo, A.; Gioiello, A.; Thomas, C.; Pols, T. W. H.; Nuti, R.; Ferrari, C.; Giacchè, N.; De Franco, F.; Pruzanski, M.; Auwerx, J*., et al.* Probing the Binding Site of Bile Acids in TGR5. *ACS Medicinal Chemistry Letters* **2013,** *4* (12), 1158-1162.

194. Marino, S. D.; Finamore, C.; Biagioli, M.; Carino, A.; Marchianò, S.; Roselli, R.; Giorgio, C. D.; Bordoni, M.; Di Leva, F. S.; Novellino, E*., et al.* GPBAR1 Activation by C6-Substituted Hyodeoxycholane Analogues Protect against Colitis. *ACS Medicinal Chemistry Letters* **2020,** *11* (5), 818-824.

195. Festa, C.; Renga, B.; D'Amore, C.; Sepe, V.; Finamore, C.; De Marino, S.; Carino, A.; Cipriani, S.; Monti, M. C.; Zampella, A*., et al.* Exploitation of Cholane Scaffold for the Discovery of Potent and Selective Farnesoid X Receptor (FXR) and G-Protein Coupled Bile Acid Receptor 1 (GP-BAR1) Ligands. *Journal of Medicinal Chemistry* **2014,** *57* (20), 8477-8495.

196. Keitel, V.; Gorg, B.; Bidmon, H. J.; Zemtsova, I.; Spomer, L.; Zilles, K.; Haussinger, D. The Bile Acid Receptor TGR5 (Gpbar-1) Acts as a Neurosteroid Receptor in Brain. *Glia* **2010,** *58* (15), 1794-1805.

197. Thomas, C.; Gioiello, A.; Noriega, L.; Strehle, A.; Oury, J.; Rizzo, G.; Macchiarulo, A.; Yamamoto, H.; Mataki, C.; Pruzanski, M. TGR5-Mediated Bile Acid Sensing Controls Glucose Homeostasis. *Cell Metabolism* **2009,** *10* (3), 167-177.

198. Duan, H.; Ning, M.; Chen, X.; Zou, Q.; Zhang, L.; Feng, Y.; Zhang, L.; Leng, Y.; Shen, J. Design, Synthesis, and Antidiabetic Activity of 4-Phenoxynicotinamide and 4-Phenoxypyrimidine-5-carboxamide Derivatives as Potent and Orally Efficacious TGR5 Agonists. *Journal of Medicinal Chemistry* **2012,** *55* (23), 10475-10489.

199. Urso, A.; D'Ovidio, F.; Xu, D.; Emala Sr, C. W.; Bunnett, N. W.; Perez-Zoghbi, J. F. Bile Acids Inhibit Cholinergic Constriction in Proximal and Peripheral Airways from Humans and Rodents. *American Journal of Physiology-Lung Cellular and Molecular Physiology* **2020,** *318* (2), L264-L275.

200. Hodge, R. J.; Lin, J.; Vasist Johnson, L. S.; Gould, E. P.; Bowers, G. D.; Nunez, D. J. Safety, Pharmacokinetics, and Pharmacodynamic Effects of a Selective TGR5 Agonist, SB-756050, in Type 2 Diabetes. *Clinical Pharmacology in Drug Development* **2013,** *2* (3), 213-222.

201. GlaxoSmithKline. First-Time-in-Humans Study to Assess Safety, Pharmacokinetics & Pharmacodynamics of SB756050. https://ClinicalTrials.gov/show/NCT00607906 **2007-2008**.

202. GlaxoSmithKline. A Study to Test How SB756050 Affects Subjects With Type 2 Diabetes Mellitus After 6 Days of Dosing. https://ClinicalTrials.gov/show/NCT00733577 **2008-2009**.

203. Masyuk, T. V.; Masyuk, A. I.; Lorenzo Pisarello, M.; Howard, B. N.; Huang, B. Q.; Lee, P. Y.; Fung, X.; Sergienko, E.; Ardecky, R. J.; Chung, T. D. Y.*, et al.* TGR5 Contributes to Hepatic Cystogenesis in Rodents With Polycystic Liver Diseases Through Cyclic Adenosine Monophosphate/Gαs Signaling. *Hepatology* **2017,** *66* (4), 1197-1218.

204. Landrum, G. Rdkit Documentation, Computer Program; https://www.rdkit.org/docs, **2013**.

205. Landrum, G. RDKit: A Software Suite for Cheminformatics, Computational Chemistry, and Predictive Modeling, Computer Program; https://github.com/rdkit, **2013**.

206. Kover, K. E.; Szilagyi, L.; Batta, G.; Uhrin, D.; Jimenez-Barbero, J. Biomolecular Recognition by Oligosaccharides and Glycopeptides: The NMR Point of View. In Comprehensive Natural Products II, Liu H.-W.; Mander L., Eds. *Elsevier* Oxford, **2010**; pp 197-246.

207. Karplus, M. Vicinal Proton Coupling in Nuclear Magnetic Resonance. *Journal of the American Chemical Society* **1963,** *85* (18), 2870–2871.

208. OriginPro, v9.0 64Bit, Computer Program; *OriginLab Corporation* https://www.originlab.com/, **2016**.

209. StarDrop v7.4 Desktop, Computer Program; *Optibrium Ltd.* **2021**.

210. Artrith, N.; Butler, K. T.; Coudert, F.-X.; Han, S.; Isayev, O.; Jain, A.; Walsh, A. Best Practices in Machine Learning for Chemistry. *Nature Chemistry* **2021,** *13* (6), 505-508.

211. Trott, O.; Olson, A. J. AutoDock Vina: Improving the Speed and Accuracy of Docking with a New Scoring Function, Efficient Optimization, and Multithreading. *Journal of Computational Chemistry* **2010,** *31* (2), 455-461.

212. Discovery Studio Modeling Environment, Computer Program; *Biovia Dassault Systemes* **2021**.

213. CorelDRAW v20.0.0.593, Computer Program; *Corel Corporation* 1600 Carling Avenue, Ottawa, Ontario, K1Z 8R7, **2019**.

214. Blicke, F. F.; Powers, L. D. The Reducing Action of Aliphatic Grignard Reagents. *Journal of the American Chemical Society* **1929,** *51* (11), 3378–3383.

215. Gough, R. G.; Dixon, J. A. Radical Mechanisms in Reactions of Grignard Reagents. *The Journal of Organic Chemistry* **1968,** *33* (5), 2148–2149.

216. Une, M.; Yamanaga, K.; Mosbach, E. H.; Kuroki, S.; Hoshita, T. Synthesis of Bile Acid Analogs: 7-Alkylated Chenodeoxycholic Acids. *Steroids* **1989,** *53* (1), 97–105.

217. Farrugia, L. J. WinGX and ORTEP for Windows: an Update. *Journal of Applied Crystallography* **2012,** *45* (4), 849-854.

218. Posa, M.; Bjedov, S.; Sebenji, A.; Sakac, M. Wittig Reaction (with Ethylidene Triphenylphosphorane) of Oxo-hydroxy Derivatives of 5beta-Cholanic Acid: Hydrophobicity, Haemolytic Potential and Capacity of Derived Ethylidene Derivatives for Solubilisation of Cholesterol. *Steroids* **2014,** *86*, 16–25.

219. Bakhanovich, O.; Beier, P. Synthesis, Stability and Reactivity of α-Fluorinated Azidoalkanes. *Chemistry–A European Journal* **2020,** *26* (4), 773-782.

220. Blastik, Z. E.; Voltrova, S.; Matousek, V.; Jurasek, B.; Manley, D. W.; Klepetarová, B.; Beier, P. Azidoperfluoroalkanes: Synthesis and Application in Copper(I)-Catalyzed Azide–Alkyne Cycloaddition. *Angewandte Chemie International Edition* **2017,** *56* (1), 346-349.

221. D'Amore, C.; Di Leva, F. S.; Sepe, V.; Renga, B.; Del Gaudio, C.; D'Auria, M. V.; Zampella, A.; Fiorucci, S.; Limongelli, V. Design, Synthesis, and Biological Evaluation of Potent Dual Agonists of Nuclear and Membrane Bile Acid Receptors. *Journal of Medicinal Chemistry* **2014,** *57* (3), 937-954.

222. Kaspar, M. Synthesis of Ligands for Farnesoid X Receptor. Master Thesis, Charles University, Prague, **2018**.

223. Stefela, A.; Kaspar, M.; Drastik, M.; Kronenberger, T.; Micuda, S.; Dracinsky, M.; Klepetarova, B.; Kudova, E.; Pavek, P. (E)-7-Ethylidene-lithocholic Acid (7-ELCA) Is a Potent Dual Farnesoid X Receptor (FXR) Antagonist and GPBAR1 Agonist Inhibiting FXR-Induced Gene Expression in Hepatocytes and Stimulating Glucagon-like Peptide-1 Secretion From Enteroendocrine Cells. *Frontiers in Pharmacology* **2021**, 1980.

224. Fieser, L. F.; Rajagopalan, S. Oxidation of steroids. III. Selective Oxidations and Acylations in the Bile Acid Series. *Journal of the American Chemical Society* **1950,** *72* (12), 5530–5536.

225. Haslewood, G. A. D. Preparation of Deoxycholic Acid. *Nature* **1942,** *150*, 211.

226. Fieser, L. F.; Rajagopalan, S. Selective Oxidation with *N*-Bromosuccinimide. I. Cholic Acid. *Journal of the American Chemical Society* **1949,** *71* (12), 3935–3938.

227. Dauben, H. J.; McCoy, L. L. *N-B*romosuccinimide. I. Allylic Bromination, a General Survey of Reaction Variables. *Journal of the American Chemical Society* **1959,** *81* (18), 4863–4873.

228. Schreiber, J.; Eschenmoser, A. Über die Relative Geschwindigkeit der Chromosäureoxydation Sekundärer, alicyclischer Alkohole. Vorläufige Mitteilung. *Helvetica Chimica Acta* **1955,** *38* (6), 1529–1536.

229. Burstein, S. H.; Ringold, H. J. Chromic Acid Oxidation of Allyl Alcohols. *Journal of the American Chemical Society* **1967,** *89* (18), 4722–4725.

230. Huang, S. L.; Omura, K.; Swern, D. Oxidation of Sterically Hindered Alcohols to Carbonyls with Dimethyl Sulfoxide-trifluoracetic Anhydride. *The Journal of Organic Chemistry* **1976,** *41* (20), 3329–3331.

231. Omura, K.; Swern, D. Oxidation of Alcohols by "activated" Dimethyl Sulfoxide. A Preparative, Steric and Mechanistic Study. *Tetrahedron* **1978,** *34* (11), 1651–1660.

232. Mikhael, M.; Adler, S. A.; Wengryniuk, S. E. Chemoselective Oxidation of Equatorial Alcohols with *N*-Ligated λ^3-Iodanes. *Organic Letters* **2019,** *21* (15), 5889-5893.

233. Kurti, L.; Czako, B. Strategic Applications of Named Reactions in Organic Synthesis. *Elsevier* **2005**.

234. Tojo, G.; Fernandez, M. I. Oxidation of Alcohols to Aldehydes and Ketones: a Guide to Current Common Practice. *Springer Science & Business Media* **2006**.

235. Kakis, F. J.; Fetizon, M.; Douchkine, N.; Golfier, M.; Mourgues, P.; Prange, T. Mechanistic Studies Regarding the Oxidation of Alcohols by Silver Carbonate on Celite. *The Journal of Organic Chemistry* **1974,** *39* (4), 523–533.

236. Bowden, K.; Heilbron, I. M.; Jones, E. R. H.; Weedon, B. C. L. Researches on Acetylenic Compounds. Part I. The Preparation of Acetylenic Ketones by Oxidation of Acetylenic Carbinols and Glycols. *Journal of the Chemical Society* **1946**, 39–45.

237. Parikh, J. R.; Doering, W. E. Sulfur Trioxide in the Oxidation of Alcohols by Dimethyl Sulfoxide. *Journal of the American Chemical Society* **1967,** *89* (21), 5505–5507.

238. Anelli, P. L.; Biffi, C.; Montanari, F.; Quici, S. Fast and Selective Oxidation of Primary Alcohols to Aldehydes or to Carboxylic Acids and of Secondary Alcohols to Ketones Mediated by Oxoammonium Salts Under Two-Phase Conditions. *The Journal of Organic Chemistry* **1987,** *52* (12), 2559–2562.

239. Anelli, P. L.; Banfi, S.; Montanari, F.; Quici, S. Oxidation of Diols with Alkali Hypochlorites Catalyzed by Oxammonium Salts under Two-Phase Conditions. *The Journal of Organic Chemistry* **1989,** *54* (12), 2970–2972.

240. De Mico, A.; Margarita, R.; Parlanti, L.; Vescovi, A.; Piancatelli, G. A Versatile and Highly Selective Hypervalent Iodine (III)/2, 2, 6, 6-tetramethyl-1-piperidinyloxyl-Mediated Oxidation of Alcohols to Carbonyl Compounds. *The Journal of Organic Chemistry* **1997,** *62* (20), 6974–6977.

241. Holan, M.; Jahn, U. Anaerobic Nitroxide-Catalyzed Oxidation of Alcohols Using the NO^+/NO^- Redox Pair. *Organic Letters* **2014,** *16* (1), 58-61.

242. Hartmann, C.; Meyer, V. Ueber Jodobenzoësäure. *Berichte der Deutschen Chemischen Gesellschaft* **1893,** *26* (2), 1727–1732.

243. Dess, D. B.; Martin, J. C. Readily Accessible 12-I-5 Oxidant for the Conversion of Primary and Secondary Alcohols to Aldehydes and Ketones. *The Journal of Organic Chemistry* **1983,** *48* (22), 4155–4156.

244. Frigerio, M.; Santagostino, M. A Mild Oxidizing Reagent for Alcohols and 1,2-Diols: *o*-Iodoxybenzoic Acid (IBX) in DMSO. *Tetrahedron Letters* **1994,** *35* (43), 8019–8022.

245. Piccialli, V. Ruthenium Tetroxide and Perruthenate Chemistry. Recent Advances and Related Transformations Mediated by Other Transition Metal Oxo-Species. *Molecules* **2014,** *19* (5), 6534-6582.

246. Djerassi, C.; Engle, R. R. Oxidations with Ruthenium Tetroxide. *Journal of the American Chemical Society* **1953,** *75* (15), 3838–3840.

247. Reich, R.; Keana, J. F. W. Oppenauer Oxidations Using 1-Methyl-4-piperidone as the Hydride Acceptor. *Synthetic Communications* **1972,** *2* (5), 323–325.

248. Königsberger, K.; Chen, G.-P.; Vivelo, J.; Lee, G.; Fitt, J.; McKenna, J.; Jenson, T.; Prasad, K.; Repič, O. An Expedient Synthesis of 6α-Fluoroursodeoxycholic Acid. *Organic Process Research & Development* **2002,** *6* (5), 665-669.

249. Galvin, G. M. Methods for Preparation of Bile Acids and Derivatives Thereof, Patent WO2017027396A1. 16.2. **2017**.

250. William, J. M.; Kuriyama, M.; Onomura, O. Simple Method for Selective Oxidation of 1,2-diols in Water with $KBrO_3/KHSO_4$. *Tetrahedron Letters* **2014,** *55* (48), 6589-6592.

251. William, J. M.; Kuriyama, M.; Onomura, O. An Efficient Method for Selective Oxidation of 1,2-Diols in Water Catalyzed by Me_2SnCl_2. *RSC Advances* **2013,** *3* (42), 19247-19250.

252. Eliel, E. L.; Schroeter, S. H.; Brett, T. J.; Biros, F. J.; Richer, J.-C. Conformational Analysis. XI. Configurational Equilibria and Chromic Acid Oxidation Rates of Alkylcyclohexanols. Deformation Effects. *Journal of the American Chemical Society* **1966,** *88* (14), 3327–3334.

253. Kwart, H.; Nickle, J. H. Transition States in Chromium (VI) Oxidation of Alcohols. *Journal of the American Chemical Society* **1973,** *95* (10), 3394–3396.

254. De Munari, S.; Frigerio, M.; Santagostino, M. Hypervalent Iodine Oxidants: Structure and Kinetics of the Reactive Intermediates in the Oxidation of Alcohols and 1,2-Diols by *o*-Iodoxybenzoic Acid (IBX) and Dess− Martin Periodinane. A Comparative ^{1}H-NMR Study. *The Journal of Organic Chemistry* **1996,** *61* (26), 9272–9279.

255. Nadupalli, S.; Dasireddy, V. D. B. C.; Koorbanally, N. A.; Jonnalagadda, S. B. Kinetics and Mechanism of the Oxidation of Coomassie Brilliant Blue-R dye by Hypochlorite and Role of Acid Therein. *South African Journal of Chemistry* **2015,** *68*, 85-92.

256. Rajendran, P.; Nisha, K. J.; Bashpa, P.; Bijudas, K. Kinetic Studies on the Oxidation of Benzyl Alcohol by Hypochlorite in Aqueous Acetic Medium. *Journal of Chemical and Pharmaceutical Research* **2015,** *7* (10), 461-465.

257. Amin, G. C.; Wadekar, S. D.; Mehta, H. U. Kinetics and Mechanism of Hypochlorite Oxidation of Polyvinyl Alcohol. *Indian Journal of Textile Research* **1977,** *3*, 20–23.

258. Kaspar, M.; Kudova, E. Selectivity of Oxidizing Agents toward Axial and Equatorial Hydroxyl Groups. *The Journal of Organic Chemistry* **2022,** *87* (14), 9157-9170.

259. Patnaik, P. Handbook of Inorganic Chemicals. *McGraw-Hill New York* **2003**; p 529.

260. Frigerio, M.; Santagostino, M.; Sputore, S. A User-Friendly Entry to 2-Iodoxybenzoic Acid (IBX). *The Journal of Organic Chemistry* **1999,** *64* (12), 4537–4538.

261. Djerassi, C.; Engle, R. R.; Bowers, A. Notes - The Direct Conversion of Steroidal Δ^5-3β-Alcohols to Δ^5- and Δ^4-3-Ketones. *The Journal of Organic Chemistry* **1956,** *21* (12), 1547–1549.

262. Willcott, M. R. MestRe Nova. *Journal of the American Chemical Society* **2009,** *131* (36), 13180-13180.

263. Morris, G. M.; Huey, R.; Lindstrom, W.; Sanner, M. F.; Belew, R. K.; Goodsell, D. S.; Olson, A. J. AutoDock4 and AutoDockTools4: Automated Docking with Selective Receptor Flexibility. *Journal of Computational Chemistry* **2009,** *30* (16), 2785-2791.

264. O'Boyle, N. M.; Banck, M.; James, C. A.; Morley, C.; Vandermeersch, T.; Hutchison, G. R. Open Babel: An Open Chemical Toolbox. *Journal of Cheminformatics* **2011,** *3* (1), 1-14.

265. Forli, S.; Huey, R.; Pique, M. E.; Sanner, M. F.; Goodsell, D. S.; Olson, A. J. Computational Protein–Ligand Docking and Virtual Drug Screening with the AutoDock Suite. *Nature Protocols* **2016,** *11* (5), 905-919.

266. Opinion and Recommendations of the Dean's Advisory Board for the Use of Artificial Intelligence. https://www.natur.cuni.cz/eng/aktuality/opinion-and-recommendations-of-the-deans-advisory-board-for-the-use-of-artificial-intelligence?set_language=en (accessed 16. 06).

267. Sanderson, K. GPT-4 is Here: What Scientists Think. *Nature* **2023,** *615* (7954), 773.

268. Charles University Central Library. Grammarly Premium Licenses for Charles University Students. https://library.cuni.cz/grammarly-premium-licenses-for-cu-users/ (accessed 25. 07. 2023).

269. McMunn-Tetangco, E. ProQuest One Literature. *The Charleston Advisor* **2022,** *23* (4), 40-44.

270. EndNote v20 Desktop, Computer Program; *Clarivate* https://www.ncbi.nlm.nih.gov/pmc/articles/PMC8485940/pdf/jmla-109-3-520.pdf, **2021**.

271. Vogel, T.; Cardinal, S.; Butkovich, N.; Wrublewski, D.; Baysinger, G. Citation Elements. In The ACS Guide to Scholarly Communication, *American Chemical Society* **2019**.

272. Plumb, J. B.; Harper, D. J. 2-Iodoxybenzoic Acid. *ChemInform* **1990,** *21* (51).

273. Kapras, V.; Stastna, E.; Chodounska, H.; Pouzar, V.; Kristofikova, Z. Preparation of Steroid Sulfamates and Their Interaction With GABA A Aeceptor. *Collection of Czechoslovak Chemical Communications* **2009,** *74* (4), 643-650.

274. Chodounska, H.; Budesinsky, M.; Sidova, R.; Sisa, M.; Kasal, A.; Kohout, L. Simple NMR Determination of 5α/5β Configuration of 3-Oxosteroids. *Collection of Czechoslovak Chemical Communications* **2001,** *66* (10), 1529-1544.

275. Slavikova, B.; Kasal, A.; Budesinsky, M. Autoxidation vs Hydrolysis in 16α-acyloxy Steroids. *Collection of Czechoslovak Chemical Communications* **1999,** *64* (7), 1125–1134.

276. Varela, C.; Tavares da Silva, E. J.; Amaral, C.; Correia da Silva, G.; Baptista, T.; Alcaro, S.; Costa, G.; Carvalho, R. A.; Teixeira, N. A. A.; Roleira, F. M. F. New Structure–Activity Relationships of A- and D-Ring Modified Steroidal Aromatase Inhibitors: Design, Synthesis, and Biochemical Evaluation. *Journal of Medicinal Chemistry* **2012,** *55* (8), 3992-4002.

277. Singh, C.; Hassam, M.; Verma, V. P.; Singh, A. S.; Naikade, N. K.; Puri, S. K.; Maulik, P. R.; Kant, R. Bile Acid-Based 1,2,4-Trioxanes: Synthesis and Antimalarial Assessment. *Journal of Medicinal Chemistry* **2012,** *55* (23), 10662-10673.

278. Stastna, E.; Cerny, I.; Pouzar, V.; Chodounska, H. Stereoselectivity of Sodium Borohydride Reduction of Saturated Steroidal Ketones Utilizing Conditions of Luche Reduction. *Steroids* **2010,** *75* (10), 721-725.

279. Kudova, E.; Chodounska, H.; Slavikova, B.; Budesinsky, M.; Nekardova, M.; Vyklicky, V.; Krausova, B.; Svehla, P.; Vyklicky, L. A New Class of Potent *N*-Methyl-d-Aspartate Receptor Inhibitors: Sulfated Neuroactive Steroids with Lipophilic D-Ring Modifications. *Journal of Medicinal Chemistry* **2015,** *58* (15), 5950-5966.

280. Donslund, A. S.; Pedersen, S. S.; Gaardbo, C.; Neumann, K. T.; Kingston, L.; Elmore, C. S.; Skrydstrup, T. Direct Access to Isotopically Labeled Aliphatic Ketones Mediated by Nickel(I) Activation. *Angewandte Chemie International Edition* **2020,** *59* (21), 8099-8103.

281. Pouzar, V.; Cerny, I. Preparation and Properties of 3-(O-(2-Carboxyethyl)) Oxime Derivatives of Steroid Hormones. *Steroids* **1996,** *61* (2), 89–93.

282. Colebrook, L. D.; Qing, N. A Study of Computed Rotational Barriers of Methyl Groups and ^{1}H and [13]C Spin-Lattice Relaxation Rates in Some Steroids. *Canadian Journal of Chemistry* **1992,** *70* (8), 2154–2160.

283. Ferraboschi, P.; Legnani, L.; Celasco, G.; Moro, L.; Ragonesi, L.; Colombo, D. A Full Conformational Characterization of Antiandrogen Cortexolone-17α-propionate and Related Compounds Through Theoretical Calculations and Nuclear Magnetic Resonance Spectroscopy. *MedChemComm* **2014,** *5* (7), 904-914.

284. He, C.; Ma, F.; Zhang, W.; Tong, R. Reinvestigating $FeBr_3$-Catalyzed Alcohol Oxidation with H_2O_2: Is a High-Valent Iron Species (HIS) or a Reactive Brominating Species (RBS) Responsible for Alcohol Oxidation? *Organic Letters* **2022,** *24* (19), 3499–3503.

285. Kraan, G. P. B.; van Wee, K. T.; Wolthers, B. G.; van der Molen, J. C.; Nagel, G. T.; Drayer, N. M.; van Leusen, D. Synthesis and Characterization of the 6α- and 6β-Hydroxylated Derivatives of Corticosterone, 11-Dehydrocorticosterone, and 11-Deoxycortisol. *Steroids* **1993,** *58* (10), 495–503.

286. Kartashov, V. S.; Shorshnev, S. V.; Arzamastsev, A. P. Identification of Halcortigosteroid Drugs by ^{13}C NMR Spectroscopy. *Pharmaceutical Chemistry Journal* **1992,** *26* (4), 356–359.

287. Ribeiro, M. V. d. M.; Boralle, N.; Felippe, L. G.; Pezza, H. R.; Pezza, L. ^{1}H NMR Determination of Adulteration of Anabolic Steroids in Seized Drugs. *Steroids* **2018,** *138*, 47-56.

288. Yoshimoto, F. K.; Arman, H. D.; Griffith, W. P.; Yan, F.; Wherritt, D. J. Chemical Synthesis of 7α-Hydroxypregnenolone, a Neuroactive Steroid that Stimulates Locomotor Activity. *Steroids* **2017,** *128*, 50-57.

289. Cerny, I.; Pouzar, V.; Budesinsky, M.; Bicíkova, M.; Hill, M.; Hampl, R. Synthesis of [19-2H3]-Analogs of Dehydroepiandrosterone and Pregnenolone and Their Sulfates. *Steroids* **2004,** *69* (3), 161-171.

290. Cerny, I.; Pouzar, V.; Drasar, P.; Turecek, F.; Havel, M. Steroids with the β-Crotonate (2-Butenoate) Side Chain. *Collection of Czechoslovak Chemical Communications* **1986,** *51* (1), 128–140.

291. Krausova, B.; Slavikova, B.; Nekardova, M.; Hubalkova, P.; Vyklicky, V.; Chodounska, H.; Vyklicky, L.; Kudova, E. Positive Modulators of the *N*-Methyl-d-aspartate Receptor: Structure–Activity Relationship Study of Steroidal 3-Hemiesters. *Journal of Medicinal Chemistry* **2018,** *61* (10), 4505-4516.

292. Adachi, M.; Hashimoto, H.; Sakakibara, R.; Imazu, T.; Nishikawa, T. A New Deprotection Procedure of MTM Ether. *Synlett* **2014,** *25* (17), 2498-2502.

293. Wang, Y.; Ju, W.; Tian, H.; Sun, S.; Li, X.; Tian, W.; Gui, J. Facile Access to Bridged Ring Systems via Point-to-Planar Chirality Transfer: Unified Synthesis of Ten Cyclocitrinols. *Journal of the American Chemical Society* **2019,** *141* (12), 5021-5033.

294. Zhou, W.-S.; Wang, Z.-Q.; Jiang, B. Stereocontrolled Conversion of Hyodeoxycholic Acid Into Chenodeoxycholic Acid and Ursodeoxycholic Acid. *Journal of the Chemical Society, Perkin Transactions 1* **1990,** (1), 1–3.

295. Hauser, E.; Baumgartner, E.; Meyer, K. Zur Kenntnis der Chenodesoxycholasäure (3alpha,7alpha-Dihydroxy-5beta-cholansäure). *Helvetica Chimica Acta* **1960,** *43* (6), 1595–1600.

296. Turnbull, K.; Narsaiah, B.; Yadav, J. S.; Yakaiah, T.; Lingaiah, B. P. V. Sodium Azide. In Encyclopedia of Reagents for Organic Synthesis, **2008**.

297. Macleod, F.; Lang, S.; Murphy, J. A. The 2-(2-Azidoethyl) Cycloalkanone Strategy for Bridged Amides and Medium-Sized Cyclic Amine Derivatives in the Aubé-Schmidt Reaction. *Synlett* **2010,** *2010* (04), 529-534.

298. Urben, P. Bretherick's Handbook of Reactive Chemical Hazards. *Elsevier* **2017**.

299. Cardillo, P.; Gigante, L.; Lunghi, A.; Fraleoni-Morgera, A.; Zanirato, P. Hazardous N-Containing System: Thermochemical and Computational Evaluation of the Intrinsic Molecular Reactivity of Some Aryl Azides and Diazides. *New Journal of Chemistry* **2008,** *32* (1), 47-53.

300. Hazen, G. G.; Weinstock, L. M.; Connell, R.; Bollinger, F. W. A Safer Diazotransfer Reagent. *Synthetic Communications* **1981,** *11* (12), 947–956.

301. Andersen, C.; Ferey, V.; Daumas, M.; Bernardelli, P.; Guérinot, A.; Cossy, J. Introduction of Cyclopropyl and Cyclobutyl Ring on Alkyl Iodides through Cobalt-Catalyzed Cross-Coupling. *Organic Letters* **2019,** *21* (7), 2285-2289.

302. Corey, E. J.; Barrette, E.-P.; Magriotis, P. A. A New Cr(VI) Reagent for the Catalytic Oxidation of Secondary Alcohols to Ketones. *Tetrahedron Letters* **1985,** *26* (48), 5855–5858.

303. Shen, H.-J.; Duan, Y.-N.; Zheng, K.; Zhang, C. Redetermination of the Structure of a Water-Soluble Hypervalent Iodine(V) Reagent AIBX and Its Synthetic Utility in the Oxidation of Alcohols and Synthesis of Isoxazoline *N*-Oxides. *The Journal of Organic Chemistry* **2019,** *84* (22), 14381-14393.

304. Chang, F. C.; Wood, N. F.; Holton, W. G. 3β, 12β-Dihydroxycholanic Acid*. *The Journal of Organic Chemistry* **1965,** *30* (6), 1718–1723.

305. Jones, A. S.; Webb, M.; Smith, F. Basic Derivatives of Steroids. 3-Amino-7 : 12-Dihydroxy- and 3-Amino-12-hydroxy-cholanic acid. *Journal of the Chemical Society (Resumed)* **1949,** (0), 2164–2168.

306. Li, Q.; Tochtrop, G. P. A Stereoselective Synthesis of the Allo-Bile Acids from the 5β-Isomers. *Tetrahedron Letters* **2011,** *52* (32), 4137-4139.

307. Popadyuk, I. I.; Markov, A. V.; Morozova, E. A.; Babich, V. O.; Salomatina, O. V.; Logashenko, E. B.; Zenkova, M. A.; Tolstikova, T. G.; Salakhutdinov, N. F. Synthesis and Evaluation of Antitumor, Anti-Inflammatory and Analgesic Activity of Novel Deoxycholic Acid Derivatives Bearing Aryl- or Hetarylsulfanyl Moieties at the C-3 Position. *Steroids* **2017,** *127*, 1-12.

308. Reich, H.; Reichstein, T. Über Gallensäuren und Verwandte Stoffe. 22. Mitteilung. 11 α-Keto- und 11 α-Oxy-Cholansäure. *Helvetica Chimica Acta* **1943,** *26* (2), 562–585.

309. Shi, Z.; Zhao, Z.; Liu, X.; Wu, L. Synthesis of New Deoxycholic Acid bis Thiocarbazones under Solvent-Free Conditions Using Microwave Irradiation. *Journal of Chemical Research* **2011,** *35* (4), 198-201.

310. Popadyuk, I. I.; Markov, A. V.; Salomatina, O. V.; Logashenko, E. B.; Shernyukov, A. V.; Zenkova, M. A.; Salakhutdinov, N. F. Synthesis and Biological Activity of Novel Deoxycholic Acid Derivatives. *Bioorganic & Medicinal Chemistry* **2015,** *23* (15), 5022-5034.

311. Sica, D.; Musumeci, D. Secosteroids of Marine Origin. *Steroids* **2004,** *69* (11-12), 743-756.

312. CrysAlisPro. *Oxford Diffraction.* **2002**.

313. Altomare, A.; Cascarano, G.; Cascarano, G.; Guagliardi, A.; Burla, M. C.; Polidori, G.; Camalli, M. SIR92 - A Program for Automatic Solution of Crystal Structures by Direct Methods. *Journal of Applied Crystallography* **1994,** *27*, 435.

314. Betteridge, P. W.; Carruthers, R. J.; Cooper, R. I.; Prout, K.; Watkin, D. J. Crystals Version 12: Software for Guided Crystal Structure Analysis. *Journal of Applied Crystallography* **2003,** *36* (6).

10 PUBLICATIONS

This thesis

- <u>Kaspar, M.</u>[*]; Stefela, A.[*]; Drastik, M.; Kronenberger, T.; Micuda, S.; Dracinsky, M.; Klepetarova, B.; Kudova, E.; Pavek, P., (*E*)-7-Ethylidene-lithocholic Acid (7-ELCA) Is a Potent Dual Farnesoid X Receptor (FXR) Antagonist and GPBAR1 Agonist Inhibiting FXR-Induced Gene Expression in Hepatocytes and Stimulating Glucagon-like Peptide-1 Secretion from Enteroendocrine Cells. *Frontiers in Pharmacology* **2021**, 1980.

  (IF 5.988, Q1 in Pharmacology & Pharmacy, 2021 Clarivate analytics)

- <u>Kaspar, M.</u>; Kudova, E., Selectivity of Oxidizing Agents toward Axial and Equatorial Hydroxyl Groups. *The Journal of Organic Chemistry* **2022,** *87* (14), 9157-9170.

  (IF 3.600, Q1 in Organic Chemistry, 2022 Clarivate analytics)

Other

- Stefela, A.; <u>Kaspar, M.</u>; Drastik, M.; Holas, O.; Hroch, M.; Smutny, T.; Skoda, J.; Hutníková, M.; Pandey, A. V.; Micuda, S.; Kudova, E.; Pavek, P., 3β-Isoobeticholic Acid Efficiently Activates the Farnesoid X Receptor (FXR) due to Its Epimerization to 3α-Epimer by Hepatic Metabolism. *The Journal of Steroid Biochemistry and Molecular Biology* **2020,** *202*, 105702.

  (IF 4.294, Q2 in Biochemistry & Molecular Biology, 2020 Clarivate analytics)

- Díaz-Holguín, A.; Rashidian, A.; Pijnenburg, D.; Monteiro Ferreira, G.; Stefela, A.; <u>Kaspar, M.</u>; Kudova, E.; Poso, A.; van Beuningen, R.; Pavek, P.; Kronenberger, T., When Two Become One: Conformational Changes in FXR/RXR Heterodimers Bound to Steroidal Antagonists. *ChemMedChem* **2023,** *18* (4), e202200556.

  (IF 3.400, Q3 in Medicinal Chemistry, 2022 Clarivate analytics)

---

[*]These authors have contributed equally to the publication and share the first authorship.